

厚生労働行政推進調査事業費補助金

医薬品・医療機器等レギュラトリーサイエンス

政策研究事業

「専ら医薬品」たる成分本質の判断のための調査・分析
及びその判断基準・範囲の整備に関する研究

平成 30～令和 2 年度 総合研究報告書

(H30-医薬-指定-005)

研究代表者 袴塚 高志

令和 3 (2021) 年 3 月

目 次

I. 総合研究報告書

「専ら医薬品」たる成分本質の判断のための調査・分析及びその判断基準・範囲の整備に関する研究

袴塚 高志 1

(資料 1) Fluorescence coupled with macro and microscopic examinations of morphological phenotype give key characteristics for identification of crude drugs derived from scorpions. *Biol. Pharm. Bull.*, 41, 510-523(2018) (22)

(資料 2) Eight ent-kaurane diterpenoid glycosides named diosmariosides A-H from the leaves of *Diospyros maritima* and their cytotoxic activity. *Chem. Pharm. Bull.*, 66, 1057-1064 (2018). (36)

(資料 3) Preliminary quality evaluation and characterization of phenolic constituents in *Cynanchi Wilfordii Radix*. *Molecules*, 23, 656; doi:10.3390/molecules23030656 (2018). (44)

(資料 4) Rapid and efficient high-performance liquid chromatography analysis of N-nitrosodimethylamine impurity in valsartan drug substance and its medicines. *Sci. Rep.*, 9, 11852, doi: <https://doi.org/10.1038/s41598-019-48344-5> 1 (2019). (55)

(資料 5) Triterpene glucosides and megastigmanes from the leaves of *Diospyros maritime*. *Chem. Pharm. Bull.*, 67, 1337-1346 (2019). (61)

(資料 6) Temperature-dependent formation of N-nitrosodimethylamine during the storage of ranitidine reagent powders and tablets., *Chem. Pharm. Bull.* 68, 1008-12 (2020). (71)

(資料 7) A megastigmane glucoside from *Sambucus chinensis*. *J. Med. Plants Stud.*, 9, 29-32 (76)

(2021).		
(資料 8) 成分本質(原材料)の分類にかかる照会様式(植物・動物等由来)		(80)
(資料 9) 成分本質(原材料)の分類にかかる照会様式(その他(化学物質等))		(93)
II. 研究成果の刊行に関する一覧表	103

「専ら医薬品」たる成分本質の判断のための調査・分析及び その判断基準・範囲の整備に関する研究

研究代表者 袴塚高志 国立医薬品食品衛生研究所 生薬部長

研究要旨 無承認無許可医薬品は、医薬品としての承認や許可がないにもかかわらず、医薬品としての目的性を持たせた製品であり、これらの流通により、適正な医療機会の喪失等、様々な健康被害が予想されるため、医薬品医療機器等法により、その製造、販売、授与、広告が禁止されている。本研究は、専ら医薬品たる成分本質を適切に判断するための調査・分析を行い、また、量的概念を含む判断基準の社会実装について検討し、同時に、既存の例示リストの見直し・整備を行うことで、無承認無許可医薬品の流通を防止し、国民の健康と安全を確保する目的で行われる。

我が国の「専ら医薬品として使用される成分本質（原材料）リスト（専医リスト）」に例示される成分であるかどうか、平成30年度～令和2年度に依頼のあった植物由来16品目及び化学物質20品目の本質について文献調査等を行い、パスタカ、キバナオランダセンニチ等、医薬品の成分本質ワーキンググループでの議論が重要と考えられた品目について、その旨を調査結果と共に報告した。他方、ED治療薬類似化合物については、PDE5の活性発現部に結合し、また実際に阻害活性を持つことから、専ら医薬品に指定すべき成分本質と判断されるべきと考察された。

グレーズーンの植物体に関する研究では、カツアバ製品の有害性評価のため、ドラージェンドルフ試液陽性を指標に、成分分画を行い、クマリン誘導体の1つであるbraylinを単離した。

さらに、コウトウスギ（紅豆杉）は、食薬区分上、心材の食品利用は可能だが、樹皮及び葉は専ら医薬品として使用される成分本質に該当するため、商品の一部や断片等を対象として樹皮と材の明確な区別法を確立する目的で、同属植物の地上部の形態について検討し、組織形態学的手法が識別に活用できることを明らかにした。

また、健康食品市場に流通する紅豆杉製品の基原植物を同定するため、同製品及び*Taxus*属植物試料について、葉緑体DNAの

さらに、その使用部位が非医の材部であることを確認した「紅豆杉」製品について、paclitaxel (PTX)含量をUPLC-UV分析にて定量し、比較としてイチイ *T. cuspidata* の各部位においても、その含量を調査したところ、*T. cuspidata*における各部位のPTX含量は、樹皮>葉>種子>枝>心材>仮種皮の順であり、「紅豆杉」製品とイチイの心材の定量値は、ほぼ同程度であることが分かった。これらの結果から、イチイの種子及びコウトウスギの心材を、「非医薬品」から「専ら医薬品」に移行する改正案を作成した。

また、専ら医薬品であるカスカラサグラダ及びフラングラ皮を使用と表示された健康食品の流通が認められたことから、塩基配列解析による種同定とLC/MSによる成分組成解析を行ったところ、それぞれに特徴的なクロマトグラムが得られ、表示通りの原料を含むことが確認された。

さらに、沖縄に産するカキノキ科植物であるリュウキュウガキ(*Diospyros maritima*)について、その果実は毒とされているが、時として、「柿」という名称から、誤食の可能性もあるため、成分検討を行ったところ、カウレン誘導体、フラボン配糖体、トリテルペン配糖体とメガステイグマンを単離した。ただし、危害要因成分と予測していたナフトキノン誘導体の単離には至らなかった。さらに、沖縄に産するレンプクソウ科(スイカツラ科)植物であるソクズ(*Sambucus chinensis*)について、アシタバとソクズの若葉がよく似ており、近年、沖縄においてソクズの青汁がアシタバジュースとして販売され健康被害が報告されていることから、ソクズの化学成分について検討した。その結果、本植物の葉部より数種類の青酸配糖体が単離され、これを青汁ジュースとして飲用することは危険であると考察された。

また、韓国において誤用が問題となったハクシュウ及びイヨウイケマの市場品を用いて TLC 分析を行い、種々の分析条件で検討した結果、イヨウイケマにハクシュウと判別しうる明瞭なスポットを観察し、当該スポットの成分について単離構造決定した。

さらに、強壯用健康食品中に ED 治療薬類縁体が混入され、このものが原因と考えられる健康被害が発生していることや、近年では、インターネットを介して ED 治療薬を購入するケースもあることから、健康食品中からの単離が報告されている新規 ED 治療薬類縁体について文献調査を行った。その結果、2017 年以降、日本、韓国、台湾、シンガポールの 4 カ国から、計 9 化合物が報告されており、その内訳は、7 化合物が sildenafil 誘導体、残り 2 化合物は、tadalafil 誘導体であった。このうち、dithiopropylcarbodenafil, dimethyldithiodenafil 及び desmethylpiperazinyl propoxysildenafil の流通に備え、同化合物の標準品を購入し、各種機器分析データ及び LC-PDA-MS 分析法をまとめた。

食薬区分の量的規制に関する研究では、従前の研究で確立した Sennoside A, B の LC-MS による検出条件をセンナ茎およびハネセンナ含有健康食品に適用して、定量分析を行った結果、センナ茎含有健康食品においては全てのサンプルから Sennoside が検出され、ハネセンナ含有健康食品においては 42 製品中 37 製品から Sennoside が検出された。また、ハネセンナ含有健康食品のうち 4 製品について 1 日あたりの Sennoside 摂取量が通常医薬品として用いられる用量 (12 mg/日) を超過するものが見られた。また、日局センナおよびハネセンナ葉の識別に適した化学成分の探索を目的として LC-MS データによる多変量解析を行ったところ、センナを判別する指標成分として Sennoside A, B, C および D, Tinnevellin glucoside, Isorhamnetin 3-*O*-gentiobioside, Vicenin-II の 7 化合物、ハネセンナを判別する指標成分として Kaempferol, Kaempferol diglucoside の 2 化合物を見出した。

さらに、トウゲシバ (*Huperzia serrata*) (ヒゲノカズラ科) は、全草がセンソウトウの名称で、「医薬品的効能効果を標ぼうしない限り医薬品と判断しない成分本質 (原材料) リスト」(非医リスト) に掲載されており、トウゲシバエキス含有健康食品が市場に流通しているが、その含有成分であるアルカロイド Huperzine A によって吐き気や発汗に至った事例が報告されており、イタリアでトウゲシバエキス含有ダイエット用ハーブとの因果関係が疑われる薬物誘発性肝障害と診断された事例も報告されている。そこで、市販のトウゲシバエキスおよび Huperzine 含有健康食品について UHPLC-PDA-MS を用いて Huperzine A の分析を行い、1 日あたりの Huperzine A 摂取量を算出した。

食薬区分リストの整備に関する研究では、食品衛生法改正に伴う指定成分制度の構築と連動し

て、現行の非医リストの内容について、原材料の基原や使用部位、名称、別名等の項目と共に、含有成分の種類とその毒性、市場流通実態、健康被害情報、食経験等を調べ、エンベリア、カイコウズ、カンレンボク、クジチョウ、ケイコツソウ、コオウレン、ハナビシソウ、ヒヨドリジョウゴ、ヒルガオ、ビンロウジ、ルリヒエンソウについて、専医リストへの移行を提案する資料等について整備した。

また、セントウソウについて既報の薬理作用や毒性情報などを調査し、センソウトウの含有成分として報告のあった 119 化合物中 113 化合物がアルカロイドであり、そのうち 4 成分 (lycopodine, lycocotinine, huperzine A, huperzine B) の急性毒性を調査した結果、lycopodine 及び huperzine B は劇薬相当、huperzine A は毒薬相当であった。以上の調査結果から、センソウトウは、「非医リスト」から「専ら医リスト」に移行することが妥当であると考察した。

研究分担者

合田 幸広 国立医薬品食品衛生研究所
副所長
丸山 卓郎 国立医薬品食品衛生研究所
生薬部第一室長
内山 奈穂子 国立医薬品食品衛生研究所
生薬部第二室長
大塚 英昭 安田女子大学薬学部教授
西川 秋佳 国立医薬品食品衛生研究所
客員研究員
小川久美子 国立医薬品食品衛生研究所
病理部長
辻本 恭 東京農工大学工学部特任助教

A. 目的

人が経口的に服用する物について、医薬品に該当するか否かの判断は、「医薬品の範囲に関する基準」(平成 31 年 3 月 22 日付厚生労働省医薬・生活衛生局長通知(薬生発第 0322 第 2 号)の別紙)に基づいて行われ、その判断例が令和 3 年 5 月 12 日薬生監麻発 0512 第 1 号、厚生労働省医薬・生活衛生局監視指導・麻薬対策課長通知「食薬区分における成分本質(原材料)の取扱いの例示の一部改正について」の別添に、「専ら医薬品として使用される成分本質(原材料)リスト(専医リスト)」及び「医薬

品的効能効果を標ぼうしない限り医薬品と判断しない成分本質(原材料)リスト(非医リスト)」として示されている。

無承認無許可医薬品の流通は、適正な医療機会の喪失等による様々な健康被害の発生が予想されるため、厚生労働省医薬・生活衛生局監視指導・麻薬対策課(監麻課)と密接に連携し、専医リスト・非医リストに例示されていない成分本質(原材料)について、都道府県の薬務課を通じて事業者より厚生労働省へ照会された場合は、医薬品としての使用実態、麻薬様作用、薬理活性等を調査し、専ら医薬品に分類すべきであるか注意深く検討する必要がある。また、無承認無許可医薬品流通の監視を念頭に、グレーゾーンにある成分本質について予め調査・分析を進めることにより、迅速に監視・指導できる体制を整える必要がある。さらに、近年、原材料を高濃度に濃縮して製造する健康食品が見受けられることから、従前の研究において提案した量的規制案の社会実装について検討する必要がある。また、機能性表示食品の流通等により既存の例示リストの示す範囲の明確化が求められていることに対応し、既存リストの見直しを行う必要がある。

このような状況において本研究は、専ら医薬品たる成分本質を適切に判断するための調

査・分析を行い、また、量的概念を含む判断基準の社会実装について検討し、同時に、既存の例示リストの見直し・整備を行うことで、無承認無許可医薬品の流通を防止し、国民の健康と安全を確保する目的で行われる。

『食薬区分の判断に関する検討』では、無承認無許可医薬品の調査と分析、有害性評価に関する研究の他の分担研究と連携しながら、文献調査等を行い、医薬生活衛生局監視指導・麻薬対策課長が招集する「医薬品の成分本質に関するワーキンググループ」（食薬区分 WG）のための調査・検討を行った。

『グレーゾーンの植物体に関する研究』では、『カツアバ製品の含有成分について』の研究として、カツアバ製品中に含まれるアルカロイドの探索を目的に、ドラージェンドルフ試液陽性成分について単離、同定を行った。なお、カツアバはブラジルなどで使用される生薬であり、日本国内においては食薬区分上、非医薬品に分類され、強壯などを目的とする健康食品の原料として流通している。カツアバの基原植物は *Erythroxylum catuaba* とされているが、*Trichilia catigua* を基原植物とする場合もあり、これらが混同されている可能性もある。*Erythroxylum* 属にはココノキ (*E. coca*) をはじめとして、アルカロイドを含有する種が存在しており、これらがカツアバとして製品中に入っていた場合、摂取した人が健康被害を起こす恐れがある。

『イチイ属植物由来植物製品の鑑別に関する研究』として、市場に流通する『紅豆杉』の使用部位の鑑別法を確立するべく、『紅豆杉』の基原植物の1つである *T. wallichiana* s. l. 及び日本国内に流通するイチイ *T. cuspidata* の枝を用い、イチイ属植物の樹皮、皮部、材部の組織形態との比較検討を行った。なお、イチイ科 (*Taxaceae*) イチイ属 (*Taxus*) 植物は樹皮にジテルペンアルカロイド taxine や paclitaxel

(taxol) を含むとされ、日本では『いちい』、『あらざ』の名で民間的に枝、葉が用いられるほか、中国では『紫杉』の名で葉、小枝が通経、利尿の目的で糖尿病や腎疾患に、樹皮は古来糖尿病に用いるとされる。近年、これらの仲間である *T. wallichiana* や *T. media* の材が『紅豆杉茶』と称され、リウマチ痛の緩解や癌に良いなどとして茶剤として流通するものが市場で見いだされるようになった。コウトウスギ（紅豆杉）は、材の食品利用は可能なものの、ジテルペンアルカロイド類を含む樹皮は『専ら医薬品』として扱われる成分本質であるため、商品に混入されてはならない。

『遺伝子情報による「紅豆杉」製品の基原植物の同定について』の研究として、「紅豆杉」と称する健康食品製品の安全性評価のため、同製品に使用されている *Taxus* 属植物の遺伝子鑑別を行なった。なお、コウトウスギは、中国に分布するイチイ科イチイ属植物、*Taxus wallichiana* であり、原変種である var. *wallichiana* の他、var. *mairei* 及び var. *chinensis* の3変種が存在し、それぞれ、須弥紅豆杉、南方紅豆杉、紅豆杉と呼称される。コウトウスギも含めて、*Taxus* 属植物の多くには、抗腫瘍活性物質である paclitaxel (PTX) をはじめタキサン型ジテルペンアルカロイドが含まれている。

『「紅豆杉」製品及びイチイ (*Taxus cuspidata*) の各部位におけるパクリタキセル (PTX) 含量について』として、「紅豆杉」の同属植物であるイチイ (*Taxus cuspidata*) は、樹皮、葉、心材が専ら医薬品に区分され、果実が非医薬品に分類されているため、材のみからなると確認された「紅豆杉」製品についても、安全性確保の観点から、PTX の含量を UPLC-UV 分析により定量した。さらに、心材部の含量比較のため *T. cuspidata* を用いて、部位別（樹皮、葉、心材など）に定量分析を行い、イチイ属植物の食薬区分上の判断のためのデータを取得した。

「健康食品として流通するカスカラサグラダ及びフラングラ皮製品の基原種と成分について」の研究として、カスカラサグラダ及びフラングラ皮を原料と表記している健康食品について、これらの製品の実態把握を目的に、塩基配列解析による原料植物の鑑別及びLC/MS分析による、アントラキノン類の組成解析を行った。なお、カスカラサグラダ及びフラングラ皮は、それぞれ、*Frangula purshiana* (Syn.: *Rhamnus purshiana*) 及び *F. alnus* (Syn.: *Rhamnus frangula*; 和名 セイヨウイソノキ) の樹皮由来の生薬であり、カスカラサグラダは、日局7 (第二部) 及び日局8に収載されており、現在でも、European Pharmacopoeia 及び US Pharmacopoeia に収載されている。センナと同様に、瀉下目的で使用される西洋生薬としてカスカラサグラダ及びフラングラ皮が知られており、これらの生薬も、cascarosides や glucofrangulins などのアントラキノン類を含有しており、センナと同様の機序により瀉下作用を発揮すると考えられる。

「リュウキュウガキの化学成分に関する研究」として、リュウキュウガキの成分の検索を行った。なお、リュウキュウガキ (*D. maritima*) は沖縄本島から先島諸島にわたって自生しており、芳醇な果実を結ぶことが知られ、一般に毒といわれているが、一見喫食が可能であると見間違えられる可能性がある。この実にはナフトキノンであるが含まれ毒性を示す物質であるとされている。

「ソズクの化学成分に関する研究」として、ソズクの成分検索を行った。なお、ソズク (蒴藋 *Sambucus chinensis*) はレンプクソウ科 (以前はスイカズラ科とされていた) ニワトコ属の多年草で、本州から九州、沖縄まで分布し、東南アジア等でも普通に分布しているが、これらは近縁種と言われて、大変変種の多いことでも知られている。アシタバとよく似ており、近年、沖縄において本植物の青汁がアシタバジュースとして販売され健康被害が報告されている。

「ハクシュウの成分研究」として、ハクシュウについて成分精査を行い、イヨウイケマと判別可能な簡便法として紫外線 (UV) 照射による薄層クロマトグラフ (TLC) 法を検討した。なお、カシュウ (何首烏) はツルドクダミ (*Polygonum multiflorum* Thunberg) の塊根を基原とする第17改正日本薬局方収載の生薬であるが、韓国ではカシュウの代わりにハクシュウ (白首烏; *Cynanchum wilfordii* Hemsley の根) も使用されてきた。近年、ハクシュウ配合の健康食品が主に更年期障害を改善する目的で、韓国国内で流通している。一方で、2015年に韓国市場に流通するハクシュウ配合製品を調査した結果、65%の製品でハクシュウと形態が類似しているイヨウイケマ (異葉牛皮消) が使用されていることが明らかとなり、それらの誤用が社会問題となっている。イヨウイケマは、*Cynanchum auriculatum* Royle ex Wight の根を基原とし、体重減少などの毒性を有することが報告され、アメリカ食品医薬局 (FDA) のデータベースでは有毒植物とされている。また、従前の研究において、日本国外でカシュウ、ハクシュウ、イヨウイケマとして流通する生薬の基原種について、成分と遺伝子の両面から実態を調査した結果、カシュウとして販売されていたもののなかに誤った基原種由来のものが存在し、また、国外でハクシュウとして流通するもののなかには、イヨウイケマの基原種やその他の種由来のものが見られることを明らかとしている。日本においては、ハクシュウとイヨウイケマの誤用は報告されていないが、今後、日本でも流通する可能性も考えられる。

「健康食品中から見出された新規 ED 治療薬類縁体の文献調査について」として、国立衛研及び地方自治体における無承認無許可医薬品の分析業務への情報提供のため、学術誌上に新規流通が報告された ED 治療薬類縁体の文献検索を行った。なお、厚生労働省では、昭和46年の薬務局長通知、「無承認無許可医薬品の指導取り締まりについて」を順次、改定し、「医

薬品の範囲に関する基準」を提示するとともに、監視業務を強化している。近年、国内の市場品から新規の ED 治療薬類縁体が報告されるケースは無くなっていったが、2018年に再び、我が国からの報告がなされた。

「Dithiopropylcarbodenafil の LC-PDA-MS 分析について」として、海外において新規に流通事例が報告された化合物群を含有する健康食品が流通した場合に備え、それらの内、dithiopropylcarbodenafil の標準品を購入し、各種機器分析データと LC-PDA-MS 分析法をまとめた。なお、2017年から2018年までに、海外における ED 治療薬の新規類縁化合物は、11種類報告されており、いずれも強壮用健康食品中から発見された。過去に、海外での報告から数年後、日本国内の市場品から検出される例も認められており、今後も監視業務を継続する必要があると考えられる。

「dimethyldithiodenafil 及び desmethylpiperazinyl propoxysildenafil の LC-PDA-MS 分析について」として、海外において新規に流通事例が報告された化合物群を含有する健康食品が流通した場合に備え、それらの内、dimethyldithiodenafil 及び desmethylpiperazinyl propoxysildenafil の標準品を購入し、各種機器分析データと LC-PDA-MS 分析法をまとめた。

『食薬区分の量的規制に関する研究』では、「センナ茎およびハネセンナ含有健康食品における Sennoside の定量分析」として、従前の研究にて見出した UPLC-MS により Sennoside A および B を独立したピークとして得る条件について、市販のセンナ茎またはハネセンナ含有健康食品の分析に適用し、製品中に含まれる Sennoside の定量分析を行った。なお、ハネセンナ (*Cassia alata*) は「医薬品的効能効果を標ぼうしない限り医薬品と判断しない成分本質(原材料)リスト」(非医薬品リスト)に掲載されており、キャンドルブッシュ、ゴールデン

キャンドル等の名称で、痩身、便秘の解消などの目的で、健康食品として広く流通している。ハネセンナには瀉下作用を有する Sennoside 類が含まれているため、市販のハネセンナ(キャンドルブッシュ)を含む製品に関する健康被害事例も報告されている。

「LC-MS を用いた Cassia 属ハネセンナおよびセンナの分析に関する研究 (2)」として、従前の研究にて見出した UPLC-MS により Sennoside A および B を独立したピークとして得る分析条件を用いて、日局センナとハネセンナをサンプルとして、その両者を化学的に識別する成分の探索を LC-MS データの多変量解析によって行った。

「トウゲシバエキスおよび Huperzine 含有健康食品における Huperzine A の定量分析」として、市販のトウゲシバエキスおよび Huperzine 含有健康食品についてその安全性を確認するため UHPLC-PDA-MS を用いて定性分析を行うとともに、Huperzine A の定量分析を試みた。なお、ヒゲノカズラ科植物であるトウゲシバ (*Huperzia serrata*) は、全草がセンソウトウの名称で、非医リストに掲載されており、認知・記憶機能の改善や記憶・学習能力の向上の目的で、トウゲシバエキス含有健康食品として広く流通している。また、Huperzine A は *H. serrata* より 1986年に上海薬物研究所の Liu らによって単離・構造決定されたアルカロイドであり、強力なアセチルコリンエステラーゼ阻害作用を有している。さらに、NMDA 型グルタミン受容体拮抗作用が示され、アルツハイマー型認知症治療薬として期待が持たれ研究がすすめられていた。一方、マウスに対する比較的強い致死活性があることから、Huperzine A が含まれる健康食品を過剰摂取した際に健康被害を引き起こす可能性が考えられる。

『食薬区分リストの整備に関する研究』では、「非医リストの見直しに関する研究」として、食品衛生法改正に伴う指定成分制度の構築と

連動して改めて非医薬品リストの精査を行い、専ら医薬品リストへの移行の候補としての20品目とその理由等について報告した。また、これらを含む11品目について、食薬区分WGにて、非医リストより専医リストへの移行について審議を受けることとなり、その審議資料の整備を行った。

「センソウトウ(トウゲシバ)の成分本質(原材料)の分類変更に関する調査」として、現在非医リストに分類されているセンソウトウについて、既報の薬理作用や毒性情報などを精査し、非医リストから専ら医リストへの移行の可能性について検討するための基礎的調査を行った。

B. 研究方法

B-1. 食薬区分の判断に関する検討

「食薬区分の判断に関する検討」では、主に以下の①～⑩の調査項目について検討した。

- ①名称、他名等、部位等、備考
- ②学名、基原植物和名等、生薬名、英名等
- ③医薬品としての使用実態があるか
- ④毒性データ
- ⑤アルカロイド、毒性タンパク、毒薬劇薬指定成分等を含むか
- ⑥麻薬、向精神薬及び覚醒剤様作用があるもの(類似化合物も含む)及びその原料植物であるか
- ⑦主要な二次代謝産物等
- ⑧主要な生理活性
- ⑨その他注意すべき点
- ⑩指定医薬品または要指示医薬品に相当する成分を含むか

なお、本調査では、原著論文以外に、主に以下の参考文献を使用した。

- 1：日本薬局方(17局)
- 2：日本薬局方外生薬規格2018
- 3：(新訂)和漢薬，医歯薬出版(赤松金芳)
- 4：中薬大辞典，小学館
- 5：The Complete German Commission E

Monographs Therapeutic Guide to Herbal Medicines, The American Botanical Council (Com E)

6：Botanical Safety Handbook, American Herbal Products Association

7：Dictionary of Plant Toxins, Jeffery B. Harborne FRS, Herbert Baxter, Willey

8：WHO Monographs on Selected Medicinal Plants

9：ブラジル産 薬用植物事典(橋本梧郎)

10：和漢薬百科図鑑(難波恒雄)

11：原色牧野和漢薬草大図鑑，北隆館

12：(原色) 牧野植物大図鑑：北隆館

13：日本の野生植物，平凡社

14：園芸植物大辞典，小学館

15：世界の植物，朝日新聞社

16：中国薬典2015

B-2. グレーズーンの植物体に関する研究

「カツアバ製品の含有成分について」では、カツアバ製品中に含まれるアルカロイドの探索を目的に、ドラージェンドルフ試液陽性成分について単離、同定を行った。成分分画は、カツアバ製品粉末に CHCl_3 と NH_4OH を加えて振とうし、 CHCl_3 層を回収したものについて、Flash chromatographyに供して行った。構造解析には、高分解能LC-MS OrbiTrap LTQ XL (Thermo Fisher)及びNMR ECZ600又はECZ800 (Jeol)を用いた。

また、「イチイ属植物由来植物製品の鑑別に関する研究」では、試料として日本国内にて流通していた商品『紅豆杉』(ティーバッグ仕様)、及び比較植物の*Taxus wallichiana* Zucc. s.l. (中国名：南方紅豆杉)、イチイ *T. cuspidata* Siebold et Zucc. (中国名：北方紅豆杉)を用い、主として横切片を作成し、必要に応じて Sudan III 染色液やフロログルシン塩酸反応による呈色反応のほか、Eau de Javellを用いた漂白、透明化を施した後、光学顕微鏡(オリンパスBX51)下にて観察した。

「遺伝子情報による「紅豆杉」製品の基原植物の同定について」では、試料として前述の中国上海の植物園より譲渡された植物標本 (*Taxus wallichiana* var. *mairei* 及び *T. media*) 及び北海道帯広で採集したイチイ (*T. cuspidata*) 並びに日本国内にて流通していた商品『紅豆杉』(ティーバッグ仕様)を用い、ゲノム DNA を抽出、精製し、葉緑体 DNA の *trnS-trnQ* の遺伝子間領域を、PCR により増幅した。PCR 産物を精製した後、ダイレクトシーケンスにより塩基配列を決定し、塩基配列の整列は、ClustalW により行い、系統樹は、Kimura の 2 パラメーターモデルにより作成した距離行列に基づき、NJ 法により構築した。

「「紅豆杉」製品及びイチイ (*Taxus cuspidata*) の各部位におけるパクリタキセル (PTX) 含量について」では、試料として前述の国内流通品『紅豆杉』及び北海道帯広で採集したイチイ (*T. cuspidata*) を用いた。イチイを樹皮、葉、枝、心材、仮種皮、種子の 6 つの部位に分離し、それぞれを乾燥後に粉碎し、各部位ごとにメタノールで抽出し、固相抽出カラムにて前処理し、溶媒を留去後の残渣にメタノールを加え、メスフラスコに移して定容し、0.45 μm のメンブレンフィルターでろ過したものを分析試料とした。「紅豆杉」製品の茶剤エキスは、水にて煮沸抽出し、同様に前処理、定容、ろ過を施して調製した。分析は UPLC-PDA-MS にて行った。

「健康食品として流通するカスカラサグラダ及びフラングラ皮製品の基原種と成分について」では、医薬基盤・健康・栄養研究所・薬用植物資源研究センター・北海道研究部より譲り受けたカスカラサグラダ及びセイヨウイソノキ標準植物試料、及び、インターネット上の販売店より購入した健康食品製品、並びに、参考試料として、松浦薬業株式会社より譲り受けた生薬として使用されるカスカラサグラダを用い、ゲノム DNA を抽出し、ITS 領域及び葉緑体 DNA の *trnH-psbA* 領域を含む DNA を、PCR に

より増幅した。PCR 産物を精製した後、塩基配列を決定し、塩基配列の整列は、ClustalW により行った。また、各試料をミキサーミルで粉碎し、粉末にメタノールを加えて振とう抽出を行った。抽出液を遠心し、上清を試料溶液として LC/MS 分析に供した。

「リュウキュウガキの化学成分に関する研究」では、先島諸島八重山郡竹富町で採集したリュウキュウガキの葉を MeOH で抽出し、濃縮残渣を水に懸濁して、EtOAc で分配して EtOAc 可溶画分と水可溶画分を得た。水画分はさらに 1-BuOH と分配して 1-BuOH 画分を得た。1-BuOH 画分を Diaion HP-20, silica gel カラムクロマトグラフィーで精製し、得られた化合物は、核磁気共鳴スペクトルを中心とする、機器分析によってその構造を明らかとした。トリテルペンサポニン及びその加水分解物については A549 細胞におよび *Leishmania major* に対する生物活性を検討した。

「ソズクの化学成分に関する研究」では、沖縄県中頭郡本部町で採集したソズク (*S. chinensis*) の地上部 (5.45 kg) を MeOH で抽出し、濃縮残渣を水に懸濁して、EtOAc で分配して EtOAc 可溶画分と水可溶画分を得た。水画分はさらに 1-BuOH と分配して 1-BuOH 画分を得た。1-BuOH 画分を Diaion HP-20, silica gel カラムクロマトグラフィー、液滴向流クロマトグラフ (DCCC)、高速液体クロマトグラフ (HPLC) で精製して 8 種の化合物を得た。

「ハクシュウの成分研究」では、ハクシュウを 80% メタノール中でホモジナイズし、濾過後、濃縮し、*n*-ヘキサン、酢酸エチル (EtOAc)、*n*-ブタノール (BuOH) で順次分配し、*n*-ヘキサンエキス、EtOAc エキス、*n*-BuOH エキス、 H_2O エキスを得た。EtOAc エキスを Chromatorex ODS カラムクロマトグラフィー等で分取し、cynandionene A 等を得た。また、*n*-BuOH エキスを Diaion HP-20 カラムクロマトグラフィー等を繰り返し、2-*O*- β -laminaribiosyl-4-hydroxyacetophenone 等を得た。

一方、イヨウイケマを 80% MeOH 中でホモジナイズし、濾過後、濃縮し、n-ヘキサン、EtOAc、n-BuOH で順次分配し、n-ヘキサンエキス、EtOAc エキス、n-BuOH エキス、H₂O エキスを得た。EtOAc エキスを MeOH に溶解し、分取 TLC [n-ヘキサン：アセトン (1:1)] で分取し wilfoside C1N 等を得た。

得られた化合物については、NMR スペクトル等の各種機器分析データを文献値または標品データとの直接比較により同定した。

TLC による分析では、粉碎したハクシュウまたはイヨウイケマをそれぞれ MeOH で超音波処理 (5 分間) により抽出し、抽出液を遠心分離後、その上澄みを試料溶液とした。試料溶液をそれぞれ 5 μ L スポットし、展開溶媒 [EtOAc:H₂O:MeOH:酢酸 (200:10:10:3)] で約 8 cm 展開後、UV (254 nm) 照射下で検出した。

「健康食品中から見出された新規 ED 治療薬類縁体の文献調査について」では、Google Scholar を用い、"sildenafil" / "vardenafil" / "tadalafil" と "dietary supplement" でコンビネーション検索し、2017 年以降の報告を抽出した。

「Dithiopropylcarbodenafil の LC-PDA-MS 分析について」では、ED 治療薬及びその類縁化合物を含有する健康食品 2 製品、並びに Dithiopropylcarbodenafil の標準品について、LC-PDA-MS を用いて分析条件の検討を行った。

「dimethyldithiodenafil 及び desmethylpiperazinyl propoxysildenafil の LC-PDA-MS 分析について」では、ED 治療薬及びその類縁化合物を含有する健康食品 2 製品、並びに dimethyldithiodenafil 及び desmethylpiperazinyl propoxysildenafil の標準品について、LC-PDA-MS を用いて分析条件の検討を行った。

B-3 食薬区分の量的規制に関する研究

「センナ茎およびハネセンナ含有健康食品における Sennoside の定量分析」では、市販の日

局センナ、ハネセンナ葉、センナ茎含有健康食品およびハネセンナ含有健康食品を検体とし、ミキサーミル MM400 (Verder Scientific 社製) にて粉碎した後、得られた粉末試料を 70% MeOH にて抽出し、LC-MS 分析条件に附した。また、粉末試料を熱水に懸濁し、湯浴 (70 °C) 中マグネティックスターラーを用いて攪拌したものを 50% MeOH に溶かして試料溶液とし、同様に LC-MS 分析条件に附した。LC-MS 分析には UltiMate 3000 RS LC system および Q Exactive Quadrupole-Orbitrap ハイブリッド型質量分析計 (Thermo Fisher Scientific 社製) を用いた。

「LC-MS を用いた Cassia 属ハネセンナおよびセンナの分析に関する研究 (2)」では、市販の日局センナ及び栽培品のハネセンナ葉を検体とし、ミキサーミルにて粉碎した後、得られた粉末試料を 70% MeOH にて抽出し、LC-MS 分析条件に附した。測定データをメタボローム解析ソフトウェア Progenesis QI ver. 2.0 (Waters) で処理し、ピークの検出、アライメントを行い、EzInfo (Waters) でデータマトリクスを作成し、SIMCA Ver. 14 (Umetrics) を用いて判別分析を行った。

「トウゲシバエキスおよび Huperzine 含有健康食品における Huperzine A の定量分析」では、インターネットで販売されているトウゲシバエキスまたは Huperzine 含有健康食品を検体とし、ミキサーミルにて粉碎した後、得られた粉末試料を MeOH にて抽出し、LC-PDA-MS 分析に附した。

B-4 食薬区分リストの整備に関する研究

「非医リストの見直しに関する研究」では、非リストの植物由来の品目について、原材料の基原や使用部位、名称、別名等の項目と共に、含有成分の種類とその毒性、市場流通実態、健康被害情報、食経験等を調べ、「非医リスト」に収載されることの妥当性について検討した。このうち、11 品目について、専医リストへの移行

を提案する根拠となる資料を集めた。

「センソウトウ(トウゲシバ)の成分本質(原材料)の分類変更に関する調査」では、センソウトウ(トウゲシバ)の1)成分本質(原材料)の概要:植物・動物等由来,2)含有成分等に関する情報,3)成分本質の医薬品としての使用実態に関する情報,4)含有成分等の医薬品としての使用実態に関する情報,5)食経験に関する情報,6)成分本質の安全性に関する情報,7)含有成分等の安全性に関する情報,8)諸外国における評価と規制に関する情報について、文献、各種公定書やデータベースなどを参考とし、調査を行った。

(倫理面への配慮)

ヒト由来サンプル及び実験動物を使用しておらず、該当する事由はない。

C. 結果・考察

C-1. 食薬区分の判断に関する検討

新規に調査以来のあった天然物は以下の16品目であった。

パスチャカは、ペルーの中央アンデス山系に自生するゼラニウム属ハーブであり、抗糖尿病作用を持つことが知られている。本品については、成分的な研究は、殆どないものの、生理活性についての論文において、成分構成の表があり、カテキンや、エピガロカテキン、クエルセチン等ポリフェノールを含むとの記載があるのみである。一方で、特許関係には、男性ホルモン様作用、testosterone 5- α -reductase 阻害作用(ノギリヤシ油相当)、 α -グルコシダーゼ阻害作用等の報告があるものの、RTECSには、評価に役に立つデータは存在しなかった。このうち、特開2007-230988では、本品エキスに男性ホルモン様作用があると報告しており、最低活性量として、一日量10mg/kgで効くとされている。従って、ヒト体重50kgとして、500mg投与すると男性ホルモン作用があるとすれば、医薬品としての活性レベルである物と考え

ることも可能と推定された。他方、専ら医薬品としてしての使用実態があるわけではないので、この点で、WGでの議論が重要と考えられた。ただし、動物実験の結果を見ると(パウダー1%)、この量では安全性に問題無く、またヒト試験で1.2g/day(Glycactive Stress Research 22015: 2(4), 208-216)でも問題ないとのデータも報告されており、基本的に量の問題であるとも考えられた。

コウキクサは、学名が不適切で、*Lemna minor* L.であるべきである。また、この学名は、The plant listでウキクサ(浮草、*Spirodela polyrhiza*)のシノニムとなっているが、*S. polyrhiza*の抽出物については、ipでmouseに対してLD50が150mg/kgとなっている。ただし、通常、LD50値が出ているときは、Effect欄は空欄であるべきだが、M10(尿量増加)となっており、その原因は不明である。もし、LD50が150mg/kgとすると、WGでの議論が重要と考えられる。また、コウキクサの同属の*Lemna paucicostata* Hegelmだと、さらにip mouseでLD50が100mg/kgで劇薬基準となる。ただし、これにもEffectがあり、H30血管その他の変化、M10となっているおり注意深い議論が必要である。

インド月桂樹は、クスノキ科で、精油が豊富な植物で、抗糖尿病、抗高脂血症等に関する生理活性が報告されているが、これはケイヒでも同様である。精油からは、cinnamyl acetate, cinnamaldehyde, linalool, eugenol等が主成分として同定され、これらのうち、eugenolのLD50値は、iv mouse 112mg/kg, oral rat 810mg/kgとやや強いが、通常の用途で特に問題はないと考えられる。また、アルカロイドは同定されておらず、食経験とケイヒの類縁植物であることを考え合わせると、非医薬品であるものとする。ただし、名称は、世界有用植物事典での記載のタマラニッケイを推奨する。

肝臓エキスは、その名称では、医療用医薬品原料であるが、カツオ肝臓の場合は、一般用医

薬品（第二類）の原料(レバコール)で、医療用医薬品原料についての精査が重要と考える。

霊芝は、子実体とすれば、食経験より非医と考えられるが、菌糸体の場合、菌糸体による固形培地の分解物や菌糸体の自己消化成分なども含まれ、その主な物質として多糖類、蛋白質、核酸、微量元素、リグニン、リグニンの分解産物であるポリフェノール類などについても考慮する必要がある。従って、菌糸体については、培地も含めて製造方法を考慮して食薬区分を議論する必要があるかもしれない。

*Polygonum tinctorium*は、その構成成分が、主にフラボノイド系のポリフェノール類の配糖体で、さらに一応の食経験と、ラットの急性経口毒性試験の結果を考え合わせると、非医と推定するが、タデであるため、生薬、青黛を製造する原料にもなり得るので、その点について議論が必要と考える。

ソリザヤノキは、oral, mouse で LD50 が 487mg/kg の lapachol を含有することについて、議論が必要と思われる。

キバナオランダセンニチの葉・花・茎葉、ガルシニア・インディカの果皮、ソリザヤノキの樹皮及びエフエドリンアルカロイド除去麻黄エキス (EFE) については、成分本質自体あるいは含有成分の毒性、医薬品としての使用実態、食経験等に関する調査結果より、医薬品に該当しないと判断して差し支えないと考察した。ただし、同属植物のガルシニア・カンボジアについて、平成 14 年 3 月 7 日に「ガルシニア抽出物を継続的に摂取する健康食品に関する情報提供について」(食発第 0307001 号通知) が発出され、「過剰摂取を控える旨の注意喚起を表示や説明書等により、当該食品を利用する消費者に見易く且つわかりやすく行うこと。」等が通知されている。幸い我が国ではガルシニアパウダーによる健康被害情報を報告されていないが、近年、海外においては多くの健康被害情報が報告されており、ガルシニア・インディカの主な含有成分（ヒドロキシクエン酸, Garcinol

等のベンゾフェノン類、アントシアニン類）はガルシニア・カンボジアと共通していることを鑑み、ガルシニア・カンボジアと同様の注意喚起を実施する必要があるか検討する必要があるものと思われる。

EFEの原料であるマオウは専医リストに掲載され、海外においても注意を要する素材として扱われている。今回申請のあった製品を、申請者以外の事業者が製造した場合、今回と同等の安全性が保証されるとは限らないため、EFE を独立の品目として一般化して非医リストに掲載することは妥当ではないと考察した。

キュウリ抽出物については、個別の製品（加工食品、中間加工品）であるため、食薬区分 WG における議論の対象ではないと考察した。

ゴマについて、種子、種子油、根は既に非医リストに掲載されているが、新たに葉及び地上部の食薬区分判断の申請があった。ゴマの葉及び地上部に関する毒性、医薬品としての使用実態、食経験等に関する調査結果より、医薬品に該当しないと判断して差し支えないと考察した。

専医リストに既掲載のブクリョウについては、食薬区分見直しに関する申請があったが、我が国においてほとんど食品として利用されず、専ら医薬品目的に使用されており、専医に留め置くことが妥当と考察した。

次に、調査依頼のあった化学物質等のうち、ジオスゲニン、酸化亜鉛、エルゴチオネイン、ベータヒドロキシ酪酸及びピテアクリンについては、成分本質自体あるいは含有成分の毒性、医薬品としての使用実態、食経験等に関する調査結果より、安全性に特段の問題はなく、医薬品に該当しないと判断して差し支えないと考察した。

ホスファチジルイノシトールについては、提出されたデータが、大豆より抽出精製したレシチンに酵素処理を行い、ホスファチジルイノシトールを濃縮精製したものについて検討されたものであり、ホスファチジルイノシトールそ

のものに関するデータではないため、この点の扱いについて WG における議論が必要であると思われた。

還元型グルタチオンについては、日本薬局方収載のグルタチオンと同一のものであり、グルタチオンは国内で医療用医薬品としての使用実態があり、既に専医リストに収載されているため、還元型グルタチオンも医薬品に該当すると判断することが妥当と考察した。

この他に、専医リストに既収載のグルタチオン、1-デオキシノジリマイシン、タウリン、γ-オリザノール、S-アデノシル-L-メチオニンについて、食薬区分見直しに関する申請があった。グルタチオン、タウリン、γ-オリザノール、S-アデノシル-L-メチオニンについては、日本あるいは海外にて医療用医薬品成分として使用実績があり、食薬区分の見直しを行うべき新たな知見が生じたわけではなかったため、いずれも専医リストに留め置くことが妥当と考察した。1-デオキシノジリマイシンについては、血糖降下作用、脂肪蓄積抑制作用が報告されており、これらは医薬品として規制する必要があるものと考えられるため、専医リストに留め置くことが妥当と考察した。

新規に調査以来のあった化学物質等は以下の20品目であった。

ノルタダラフィル、ノルカルボデナフィル、プロポキシフェニルノルアセチルデナフィルは ED 治療薬類似物質であり、PDE5 の活性発現部に結合し、また実際に阻害活性を持つこと、さらに処方箋薬であるシルデナフィル、タダラフィル様の作用を意図して合成されたものと考えられることから、専ら医薬品に指定すべき成分本質と判断されると考察した。

ジメチルジチオノルカルボデナフィルについて、その構造からシルデナフィル様の作用を期待して合成された物質と推測され、その構造から容易に Phosphodiesterase 5 阻害活性を持つことが予測できる化合物であり、処方箋薬であるシルデナフィルに相当する成分であると

考えられ、保健衛生上の観点から医薬品成分として規制を行う必要があるものと考察した。

ピリミデナフィルは、その構造からシルデナフィル様の作用を期待して合成された物質と推測され、その構造から容易に Phosphodiesterase 5 阻害活性を持つことが予測され、実際にシルデナフィルの約 3.2 倍のホスホジエステラーゼ 5 阻害活性があることが報告されていた。従って、本物質は、処方箋薬であるシルデナフィルに相当する成分であると考えられ、保健衛生上の観点から医薬品成分として規制を行う必要があるものと考察した。

これらの情報は、平成 31 年 3 月 15 日、令和元年 7 月 9 日、同 9 月 13 日、同 12 月 9 日、令和 2 年 2 月 18 日、同 2 年 6 月 16 日、同 7 月 14 日、同 9 月 25 日、同 12 月 15 日、令和 3 年 3 月 5 日に開催された食薬 WG における基礎資料となった。

また別に、ホコウエイ、マツホド菌核、イリス、ニコチンアミドモノヌクレオチド、ウンカロアポ、スマック、ウシの血漿由来免疫グロブリン、エゾウコギ、ニコチンアミドリボシドクロライド、杭白菊、ワスレグサ、サナギタケ、セージ、HMB-Ca、ゴミシ、ゲンチアナ等、スペイン産ベルモット等、イリスやロクジョウ等、担当部局からの問い合わせに、科学的見地から対応した。

C-2. グレーゾーンの植物体に関する研究

「カッアバ製品の含有成分について」では、全 15 検体について TLC 分析を行った結果、6 検体で UV 254 nm に吸収を持ち、365 nm 照射により青色の蛍光を発するスポットを認めた。これらのスポットは、いずれもドラーゲンドルフ試液陽性であった。また、2 検体で、上記のスポットと Rf 値の異なるドラーゲンドルフ試液陽性のスポットを検出したが、このものは、UV 照射による吸収/蛍光を認めなかった。ドラーゲンドルフ試液陽性スポットが検出された検体のうちの前者のグループの 1 つについ

て、当該スポットの分離精製を行った。CHCl₃画分について、Flash chromatography 分取を行い、6つの画分を得た。このうち、最も精製度が高いと思われた画分について、高分解能 LC-MS 分析を行った結果、このものはほぼ単一の成分で構成されており、構造解析を進めた結果、イソプレニル化されたクマリン化合物の braylin と同定された。

「イチイ属植物由来植物製品の鑑別に関する研究」では、イチイ *Taxus* 属植物の *T. wallichiana* s.l. 及びイチイ *T. cuspidata* の枝における一般的形態を観察した後、商品『紅豆杉』の形態と比較検討したところ、『紅豆杉』商品は *T. wallichiana* s.l. の材の組織形態学的特徴とよく一致し、イチイ属植物の材が用いられていることが分かった。

『紅豆杉』商品は、中国国内の法規制を理由に、雲南省の栽培品を主に利用するとの情報がある。一方、イチイ属は大型材から茶器を製するとの情報もある。今回入手した『紅豆杉』商品からは、比較植物の髓に多く認められた石細胞がまったく認められなかったことから、『紅豆杉』の商品は、大型のイチイ属樹木の材の端材や切削くずなどを粉碎して用いた可能性も示唆される。

「遺伝子情報による「紅豆杉」製品の基原植物の同定について」において、中国の植物園より譲り受けた2つの標本（試料1, 2）は、どちらも同一の配列を示し、全長1684 bpであった。一方、イチイ *T. cuspidata*（試料3）は、全長1682 bp、紅豆杉製品は、1687 bpであった。特に、スパーサー領域の後半部に、塩基の挿入／欠失が多く認められた。それぞれの配列に対して blast search program による相同性検索を行った結果、試料1, 2の配列は、Haoらが *T. wallichiana* var. *mairei* の配列として登録しているものと一致したほか、その他の *T. wallichiana* var. *mairei* のものとして登録されている7つの配列と99.7%以上の相同性を示した。一方、試料3の配列は、Haoら、Wuらが

T. cuspidata の配列として登録しているものと完全に一致し、さらに、その他の *T. cuspidata* の配列5種と99.76%以上の相同性を示した。紅豆杉製品の配列は、Haoらが *T. wallichiana* の配列として登録しているものと完全に一致し、その他の *T. wallichiana* (var. *wallichiana*) の配列5種と99.82%以上の相同性を示した。

ここで明らかにした *Taxus* 属植物の *trnS-trnQ* IGS 配列に、Haoらが、国際塩基配列データベース (DDBJ/EMBL/GenBank; INSD) に登録している *Taxus* 属植物の配列を加えて作成した系統樹では、試料1, 2の配列は、それぞれ、データベース上の *T. wallichiana* var. *mairei* からなるクラスターに配置された。同様に、紅豆杉製品の配列も、*T. wallichiana* var. *wallichiana* の配列からなるクラスターに配置された。

以上のことから、試料2は、*T. media* として譲渡されたが、試料1と同じ、*T. wallichiana* var. *mairei*（南方紅豆杉）であった。また、今回、解析に用いた紅豆杉製品の基原植物は、相同性検索の結果からも予想された通り、*T. wallichiana* var. *wallichiana* であると同定された。

「「紅豆杉」製品及びイチイ (*Taxus cuspidata*) の各部位におけるパクリタキセル (PTX) 含量について」では、まず、PTX の LC 条件の検討を行った。PTX は3つの芳香環を含む6/8/6員環からなるタキサン型ジテルペンであり、非常に疎水性の高い化合物であることから、最初の移動相 B 比率を43%に設定し、溶出時間の短縮を図るとともに、UPLC 用カラムを使用し、Sep-Pak による前処理により調製した試料溶液について、PTX と各試料中の夾雑成分との分離を試みたところ、PTX と夾雑成分は、ベースライン分離した。続いて、PTX 抽出条件の検討を行った。抽出は、イチイ全体の粉碎試料100 mg に対し、メタノール1 mL を加え30分間、振とう抽出することにより行った。遠心分離後、上

澄み液を 2 mL メスフラスコに回収し、メタノールで定容したものを分析試料とした。残渣を同様の方法で抽出後、再度分析し、残存率を算出し、最終的に、抽出回数は 4 回と決定した。さらに、分析法のバリデーションを行い、標準品と試料の両面から評価し、検量線の直線性、併行精度、分離度、特異性、回収率いずれも良好な結果が確認された。その上で、*T. cuspidata* の各部位における定量値を求めたところ、その含量は樹皮>葉>種子>枝>心材>仮種皮の順に高いことが明らかになった。タキサン骨格を有するアルカロイドはイチイ属植物の各部位から報告されているが、種子を覆う仮種皮部分には含まれていないとされていたが、今回の測定では微量含まれていることが分かった。ただし、イチイの仮種皮部は古くから食経験があることから、食薬区分上の扱いは、現行通り、非医薬品で良いと考える。一方、種子における含量は、樹皮や葉と同程度含まれていることが確認されたことから、専ら医薬品へ移行するのが適切と考えられた。また、現在の食薬区分リストでは、種子及び仮種皮に相当する部分を「果実」と表記していると思われるが、イチイは裸子植物であり、子房を持たないことから、真正果実は存在しない。このため、現在の「果実」の表現は、「仮種皮」と「種子」に改める必要がある。以上のことから、イチイの食薬区分上の扱いは、種子を専ら医薬品に移行し、仮種皮を非医薬品に留めるべきと考える。

次に、「紅豆杉」製品とイチイの各部位における PTX の定量値を比較した。その結果、イチイの心材部分と「紅豆杉」製品は、ほぼ同程度の定量値を示し、両者に大きな差は確認されなかった。今回、我々は一連の分析において、「紅豆杉」製品の使用部位を材部と特定し、遺伝子鑑別から、基原種を *T. wallichiana* var. *wallichiana* と同定した。従って、イチイの材部と「紅豆杉」製品の定量値が同程度なのは妥当な結果と考えられた。

「紅豆杉」製品との定量値の比較では、心材

とほぼ同じ定量値を示した。また、「紅豆杉」製品は茶用飲料として用いられることから、茶剤の PTX 含量も調査した。その結果、PTX は極微量ながら含まれていることが確認された。

今回分析した「紅豆杉」製品は茶用飲料として用いられることから、茶剤中の PTX 含量も調査したところ、PTX は極微量ながら含まれていることが確認された。PTX の毒性は、LD50 が 12 mg/kg (mouse, 静脈投与) であることなどを考慮すると、本製品の摂取により、直ちに健康被害が発生する可能性は低いと考えられるが、PTX は毒薬であり、濃縮エキス製品の販売の可能性や多量摂取の危険性、イチイの食薬区分上の扱いとの整合性を考えると、材部も専ら医薬品に移行すべきものとする。ただし、茶剤については、トウシンソウの例に倣い、除外処置を検討する余地はあるものと思われる。

なお、現行の食薬区分リストでは、「ハクトウスギ」の別名が「ウンナンコウトウスギ」とされているが、ハクトウスギは、*Pseudotaxus chienii* を指し、コウトウスギとは、属レベルで異なる植物であることから、両者は、別品目として記載されるべきである。以上のことから、コウトウスギ、ハクトウスギの食薬区分上の扱いは、以下の通り改正することを提案する。専ら医薬品リストは、ハクトウスギとコウトウスギに分けた上で、コウトウスギの別名に、ウンナンコウトウスギを記載し、部位に心材を含める。一方、非医薬品リストは、ハクトウスギの別名からウンナンコウトウスギを削除し、さらに備考欄にコウトウスギの樹皮、葉、心材は、医薬品相当であることを記載し、ハクトウスギとコウトウスギが別の区分であることを明確にする。

「健康食品として流通するカスカラサグラダ及びフラングラ皮製品の基原種と成分について」では、食薬区分上、医薬品相当と判断されているカスカラサグラダ及びフラングラ皮を原料に用いたと表記されている製品が多数見受けられたことから、当該製品を購入し、遺

伝子解析及び LC/MS 分析を行った。その結果、生薬の規格外品の中に、別種基原のものが存在したものの、健康食品製品は、表示通りカスカラサグラダ及びセイヨウイソノキを原料としていることが確認された。LC/MS 分析の結果からは、それぞれの植物から報告されているアントラキノン類と推定されるピークが複数確認された。

カスカラサグラダとセイヨウイソノキは、遺伝子解析を行った2つの領域における配列の違いはわずかであったが、メタノールエキスの成分組成は、大きく異なっており、両者の区別には、遺伝子解析よりも成分化学的手法の方が有効であると思われた。これらの植物は、伝統的に下剤として使用されてきたものであり、これらを原料とする健康食品の摂取した場合、センナ及びハネセンナと同様に、様々な健康被害が発生する恐れがあり、注意が必要である。

「リュウキュウガキの化学成分に関する研究」では、リュウキュウガキより単離された化合物について構造解析を進めた結果、カウラン型ジテルペンである diosmarioside E と diosmarioside H が同定された。さらに、ebenamrioides A-D と命名した新規トリテルペンサポニン4種と、2種のメガスティグマンが同定された。得られたトリテルペンの配糖体、及びそれらの部分加水分解物の A549 細胞に対する毒性を検討したところ、一部化合物に弱い活性が見られた。

「ソズクの化学成分に関する研究」では、ソズクより単離された化合物について核磁気共鳴スペクトルを中心とする機器分析を行い、文献未報告の (3*S*, 5*R*, 6*S*, 9*R*)-megastigman-5, 6-epoxy-3, 9-diol 9-*O*- β -D-glucopyranoside に加えて、(6*R*, 7*E*, 9*R*)-megastigma-4, 7-dien-9-ol *O*- β -D-glucopyranoside, (6*R*, 7*E*, 9*R*)-megastigman-3-on-9-ol *O*- α -L-arabinopyranosyl(1'' \rightarrow 6')- β -D-glucopyranoside, citroside B,

actindioionoside, prunasin, lucumin 及び demethylalangiside と同定した。このうち prunasin 及び lucumin は青酸配糖体であり、加熱などの適切な処理を施さない限り食用に供することは問題があると思われた。

「「ハクシュウの成分研究」」では、80%メタノールで抽出したハクシュウの EtOAc エキス及び n-BuOH エキスより単離した成分から、それぞれ cynandionene A 及び 2-*O*- β -laminaribiosyl- 4-hydroxyacetophenone 等が同定された。ハクシュウ 4 品、イヨウイケマ 9 品を用いて TLC 分析を行い、種々の分析条件で検討した結果、EtOAc/H₂O/MeOH/酢酸(200:10:10:3)で展開したところ、UV 照射(254 nm) 検出のみで比較的分離のよいデータが得られた。本条件で各試料溶液について検討したところ、イヨウイケマにハクシュウと判別しうる明瞭なスポットが観察された。当該スポットについてイヨウイケマより単離構造決定したところ、スポットには2つの化合物が重複しており、それぞれ wilfoside C1N 及び wilfoside K1N と同定された。

「健康食品中から見出された新規 ED 治療薬類縁体の文献調査について」では、Google Scholar による検索を行った結果、2017 年以降に新規に報告された ED 治療薬類縁体は、9 化合物であり、その内訳は、sildenafil タイプが、7 種、残りの 2 種は、tadalafil タイプであり、vardenafil タイプのものは、認められなかった。国別では、日本が 3 化合物、韓国と台湾が 2 化合物、シンガポールが 1 化合物であった。

「Dithiopropylcarbodenafil の LC-PDA-MS 分析について」では、Dithiopropylcarbodenafil の標準溶液について厚生労働省の通知の条件により分析を行った結果、当該化合物は十分に担体へ保持され、他の成分との分離も良好であることが分かった。また、in-source collision-induced dissociation (IS-CID) 法によるイオン化を利

用した MS による構造情報の確認を検討した結果、ED 治療薬とその類縁化合物の構造情報が得られることを確認した。フラグメントを起こすイオンを選択できないデメリットはあるものの、比較的安価なシングル型四重極質量分析計でもフラグメントイオンを検出できるため、構造推定などに有効であると考えられた。

さらに、「dimethyldithiodenafil 及び desmethyloxypropoxy sildenafil の LC-PDA-MS 分析について」では、海外の健康食品市場に流通する製品から、検出事例が報告された dimethyldithiodenafil 及び desmethyloxypropoxy sildenafil の標準品を購入し、各種機器分析データ及び分析法をまとめた。ウデナフィルの分析方法として厚生労働省通知された分析条件において、担体に十分に保持され、分析が可能であることが確認された。

C-3 食薬区分の量的規制に関する研究

「センナ茎およびハネセンナ含有健康食品における Sennoside の定量分析」では、センナ茎含有健康食品とハネセンナ含有健康食品から 1 種ずつ選択し、それらの LC-MS 分析を行い Sennoside A, B が含まれている事を確認した。選択した健康食品は、センナ茎含有健康食品においては、原材料の先頭にセンナ茎が記載されているものを選択した。ハネセンナ含有健康食品においては、原材料がキャンドルブッシュとのみ記載されているものを選択した。次に、日局センナ (5 種)、ハネセンナ葉 (2 種)、センナ茎含有健康食品 (18 種) およびハネセンナ含有健康食品 (42 種) について分析を行った。センナ茎含有健康食品については、全ての検体から Sennoside A, B が検出され、製品記載の用法を参照し、1 日当たりの最大摂取量を算出したところ、Sennoside 摂取量が医療用医薬品の最低服用量で摂取される量 (12 mg/日) を上回るものが無かったものの、>10 mg/日と算出されたものが 2 検体存在した。次に、ハネセン

ナ含有健康食品においては、分析に供した 42 検体中 37 検体から Sennoside A, B が検出され、製品記載の用法を参照し、1 日当たりの最大摂取量を算出したところ、Sennoside 摂取量が医療用医薬品の最低服用量で摂取される量を上回るものが 4 検体存在した。

一方、センナ茎およびハネセンナ含有健康食品について各 2 検体を選択し、日局センナ 1 検体とハネセンナ葉 1 検体を追加した計 6 検体について熱水抽出を行い、LC-MS 分析と定量分析を行った。その結果を 70% MeOH で抽出した場合と比較すると、全ての検体において Sennoside の抽出量は低下した。

「LC-MS を用いた Cassia 属ハネセンナおよびセンナの分析に関する研究 (2)」では、従前の研究にて見出した LC-MS により Sennoside 類を良好に分離し得る分析条件を用いて、市販の日局センナ 5 種と種子島産及び東京産のハネセンナを対象として、ポジティブモード (LC-ESI (+) -MS クロマトグラム) 及びネガティブモード (LC-ESI (-) -MS クロマトグラム) の分析を行い、取得した LC-MS データを多変量解析に供した。

得られた LCMS データについてセンナ及びハネセンナのグループで判別分析を行ったところ、LC-ESI- (+) -MS のスコアプロット上でセンナ、ハネセンナの 2 つのグループに分かれ、さらに、ハネセンナのグループにおいては、種子島産のサンプルと東京産のグループが分離されていた。また、LC-ESI (+) -MS の S-Plot より、センナの指標成分として Sennoside C, Isorhamnetin 3-O-gentiobioside, Tinnevellin glucoside および Vicenin- II が見出され、ハネセンナの指標成分としては、Kaempferol が見出された。

一方、LC-ESI (-) -MS の OPLS-DA スコアプロット上でもセンナ、ハネセンナの 2 つのグループに分かれる事が確認され、ここでも、ハネセンナのグループにおいては、種子島産のサンプルと東京産のグループが分離されていた。LC-ESI (-) -MS の S-Plot からは、さらにセンナの判別に Sennoside A, B, C, Isorhamnetin 3-O-

gentiobioside, Tinnevellin glucoside および Vicenin-II が寄与しているものと考えられ、ハネセンナの判別には、Kaempferol diglucoside が寄与しているものと考えられた。

「トウゲシバエキスおよび Huperzine 含有健康食品における Huperzine A の定量分析」では、定性分析として、トウゲシバエキスまたは Huperzine 含有健康食品 13 種の UHPLC-PDA-MS のクロマトグラムを確認した。このうち 12 サンプルより Huperzine A が検出された。

定量分析においては、UV 310 nm でのクロマトグラムにおいてピーク分離は十分であったので、このクロマトグラムを用いてピーク面積を算出し定量分析を行ったところ、. 一日の最大摂取量が 5~691 μ g/day の範囲に相当することが明らかになった。今回の分析に供した検体の中では、Huperzine A の一日最大摂取量が中華人民共和国薬典において設定されている上限値を上回るものが 1 検体存在した。

C-4 食薬区分リストの整備に関する研究

「非医リストの見直しに関する研究」では、非医薬品リスト（植物由来）の精査を行い、専ら医薬品リストへの移行が望ましいと思われる品目として 20 品目（イボツヅラフジ、ウンナンコウトウスギ、エンベリア、カイコウズ、カンレンボク、クジチョウ、ケイコツソウ、ゲットウ、コンフリー、シンキンソウ、セイヨウアカネ、センソウトウ、ノゲイトウ、ハクトウスギ、ハナビシソウ、ヒメツルニチニチソウ、ヒヨドリジョウゴ、ヒルガオ、ビンロウジ、ルリヒエンソウ）が候補に挙げられた。現行の非医薬品リストにおいて、ウンナンコウトウスギとハクトウスギは同じ植物の扱いであるが、ここでは別の植物として挙げた。このうち、エンベリア、カイコウズ、カンレンボク、クジチョウ、ケイコツソウ、ハナビシソウ、ヒヨドリジョウゴ、ヒルガオ、ビンロウジ、ルリヒエンソウにコオウレンを加えた 11 品目について、専医リストへの移行を提案する理由等とその根拠となる文献等

が見出され、いずれも、エキス及び含有化合物に強い毒性が報告されており、専医への移行が妥当と判断された。

「センソウトウ(トウゲシバ)の成分本質(原材料)の分類変更に関する調査」では、センソウトウ(トウゲシバ)に多くのアルカロイドが含まれていることを確認し、そのうち、4 成分の急性毒性を調査した結果、lycopodine 及び huperzine B は劇薬相当、huperzine A は毒薬相当であった。また、lycopodine, huperzine A 及び huperzine B は痙攣や呼吸抑制等、lycoctonine は運動失調など中枢神経作用が観察されており、センソウトウは、「毒劇薬指定成分に相当する成分を含む物」に該当するものとして、専ら医リストに移行することが妥当であると考察された。

D. 結論

新規に「専ら医薬品」であるかどうか判断が求められた品目について、医薬食品局監視指導・麻薬対策課長が招集する「医薬品の成分本質に関するワーキンググループ」のための調査を遂行するとともに、既存の専医リスト並びに、非医リストの様々な項目について、同課の依頼に基づき検討を行った。なお、本研究の成果は、厚生労働省において食薬区分の見直しを検討するための厚生労働行政上重要な基礎資料となるものであり、平成 13 年 3 月 27 日付医薬発第 243 号厚生労働省医薬局長通知で、「リストについては、科学的な検証に基づき定期的に見直しを行うこととし、概ね一年程度の期間毎に追加、訂正、削除等を行うこととする」とした、現行の「専医リスト」の見直し作業に貢献するものである。

カツアバ製品の有害性評価を目的に、昨年度の遺伝子解析に引き続き、1 製品のアルカリ画分について、ドラーゲンドルフ試液陽性を指標に、成分分画を行い、クマリン誘導体の 1 つである braylin を単離した。

『紅豆杉』商品について、組織形態学的手法

を用いて商品の使用部位を特定し得た。このような生薬の基原同定法は、分子生物学的手法では解明困難な、商品の利用部位を明らかでることから、いわゆる『専ら医薬品』扱いとなる薬用植物や『無承認無認可医薬品』における、利用部位がグレーゾーンな商品の明確な鑑別に貢献しうるものと思われる。

健康食品市場に流通する紅豆杉製品の基原植物を同定するため、同製品及び *Taxus* 属植物試料について、葉緑体 DNA の *trnS-trnQ* IGS 領域の塩基配列解析を行い、同製品の基原植物を *Taxus wallichiana* var. *wallichiana* と同定した。一方、イチイ *T. cuspidata* の各部位について、PTX の定量を行ったところ、含量は樹皮 > 葉 > 種子 > 枝 > 心材 > 仮種皮の順であることが明らかとなった。また、「紅豆杉」製品とイチイの心材の定量値は、ほぼ同程度であった。これらの結果から、イチイの種子及びコウトウスギの心材を、「非医薬品」から「専ら医薬品」に移行するとともに、植物分類学及び植物形態学上の誤りを修正する以下の改正案を作成した。

専ら医薬品であるカスカラサグラダ及びフラングラ皮を使用と表示した健康食品の流通が認められたことから、実態調査のため、塩基配列解析による種同定と LC/MS による成分組成解析を行ったところ、表示通りカスカラサグラダ及びフラングラ皮を原料としていることが分かった。

沖縄で採集したリュウキュウガキの葉の成分検索を行い、10 種のカウレン誘導体、4 種のトリテルペン配糖体と 2 のメガスティグマンを単離した。リュウキュウガキに魚毒活性があることが知られており、両親媒性であるサポニンが得られたことは、言い伝えと符合するものであった。ただし、毒性成分と目されるナフトキノ誘導体の単離には至らなかった。

沖縄において、その青汁がアシタバジュースとして販売され、健康被害が報告されているソズクについて成分検索を行ったところ、本植物

葉部 5.45 Kg より 2 g と大量の青酸配糖体 prunasin が単離され、本植物若葉を青汁ジュースとして飲用するのは甚だ危険であると考えられた。

ハクシュウの 80%MeOH 抽出物について各種クロマトグラフィーを繰り返して成分精査した結果、文献未記載の化合物 2-O- β -laminaribiosyl-4-hydroxyacetophenone の単離構造決定に成功した。さらに、ハクシュウとイヨウイケマを TLC により比較検討した結果、EtOAc/水/MeOH/酢酸 (200:10:10:3) を展開溶媒として分析したところ、イヨウイケマにのみ明瞭に観察されるスポットが認められ、wilfoside C1N と wilfoside K1N の 2 化合物が同定された。

検索エンジンを用い、2017 年以降に健康食品中からの単離が報告された ED 治療薬類縁体を調査した結果、4 カ国から、計 9 化合物が報告されており、その内、7 化合物は、sildenafil 誘導体、残りは tadalafil の類縁体であり、tadalafil 誘導体が主流だった 2 年前の調査結果とは反転していた。

強壯用製品への添加が危惧される ED 治療薬類縁化合物の内、dithiopropylcarbodenafil、dimethyldithiodenafil 及び desmethylpiperazinyl propoxysildenafil への対応に備え、同化合物の標準品を購入し、各種機器分析データ及びその分析法をまとめた。

これまでの検討で確立した Sennoside A, B の LC-MS による検出条件をセンナ茎およびハネセンナ含有健康食品に適用し、定量分析を行った結果、ハネセンナ含有健康食品のうち 4 検体から 1 日あたりの摂取量が医療用医薬品の最低服用量で摂取される量を上回る量の Sennoside が検出された。しかしながら、Sennoside の抽出量は抽出溶媒、抽出操作により大きく左右される可能性が考えられるため、試料調製操作について検討する必要があるものと考えられた。

日局センナとハネセンナ葉を試料として

LCMS データを用いた判別分析を行い、寄与成分として 9 種の化合物を同定した。センナについて 7 種、ハネセンナについて 2 種の化合物が寄与成分として見出されたが、その中でも Vicenin-II がセンナ・ハネセンナ間においてセンナ特有の指標成分となる可能性が考えられた。

トウゲシバエキスおよび Huperzine A 含有と表示した健康食品について定量分析したところ、中華人民共和国薬典収載の一日摂取量の上限値を上回るものが 1 検体存在した。また、今回分析に供したものの以外にも多くのトウゲシバエキスおよび Huperzine A 含有健康食品は現在流通していることから、今後さらにサンプルを増やし、定量分析を行う必要があるものと考えられた。

非医薬品リスト（植物由来等）について見直しを行い、専ら医薬品リストへの移行が望ましいと思われる品目を見出し、食薬区分 WG での議論に必要な根拠資料等を整備した。

非医リストに分類されているセンソウトウ（トウゲシバ）について、既報の薬理作用や毒性情報などを調査し、センソウトウには多くのアルカロイドが含まれており、中には劇薬相当あるいは毒薬相当のものも存在することにより、センソウトウは、「非医リスト」から「専ら医リスト」に移行することが妥当であると考察した。

E. 研究発表

論文発表等

1) Tokumoto, H., Shimomura, H., Hakamatsuka, T., Ozeki, Y. and Goda, Y.: Fluorescence coupled with macro and microscopic examinations of morphological phenotype give key characteristics for identification of crude drugs derived from scorpions. *Biol. Pharm. Bull.*, 41(4): 510-523 (2018)

- 2) Kawakami, S., Nishida, S., Nobe, A., Inagaki, M., Nishimura, M., Matsunami, K., Otsuka, H., Aramoto, M., Hyodo, T., Yamaguchi, K.: Eight ent-kaurane diterpenoid glycosides named diosmariosides A-H from the leaves of *Diospyros maritima* and their cytotoxic activity. *Chem. Pharm. Bull.*, 66, 1057-1064 (2018).
- 3) Uchikura, T., Tanaka, H., Sugiwaki, H., Yoshimura, M., Sato-Masumoto, N., Tsujimoto, T., Uchiyama, N., Hakamatsuka, T., Amakura, Y.: Preliminary quality evaluation and characterization of phenolic constituents in *Cynanchi Wilfordii Radix*. *Molecules*, 23, 656; doi:10.3390/molecules23030656 (2018).
- 4) Masada, S., Tuji, G., Arai, R., Uchiyama, N., Demizu, Y., Tsutsumi, T., Abe, Y., Akiyama, H., Hakamatsuka, T., Izutsu, K.-i., Goda, Y. & Okuda, H.: Rapid and efficient high-performance liquid chromatography analysis of N-nitrosodimethylamine impurity in valsartan drug substance and its medicines. *Sci. Rep.*, 9, 11852, doi: <https://doi.org/10.1038/s41598-019-48344-5> 1 (2019).
- 5) Kawakami, S., Miura, E., Nobe, A., Inagaki, M., Nishimura, M., Matsunami, K., Otsuka, H., Aramoto, M.: Ebenamariosides A-D: Triterpene glucosides and megastigmanes from the leaves of *Diospyros maritime*. *Chem. Pharm. Bull.*, 67, 1337-1346 (2019).
- 6) Abe Y, Yamamoto E, Yoshida H, Usui A, Tomita N, Kanno H, Masada S, Yokoo H, Tsuji G, Uchiyama N, Hakamatsuka T,

Demizu Y, Izutsu KI, Goda Y, Okuda H: Temperature-dependent formation of N-nitrosodimethylamine during the storage of ranitidine reagent powders and tablets., Chem. Pharm. Bull. 2020;68(10):1008-12.

- 7) Otsuka, H., Shitamoto, J., Sueyoshi, E., Matsunami, K., Takeda, Y.: A megastigmane glucoside from *Sambucus chinensis*. J. Med. Plants Stud., 9, 29-32 (2021).

学会発表等

- 1) 合田幸広, 生活に即した薬学「レギュラトリーサイエンス」の実践 健康食品の品質とニセ薬の話を中心に, 昭和薬科大学講義, 東京 (2018. 9).
- 2) 合田幸広, アントシアニンを機能性関与成分とする上で考えるべきことは, 日本アントシアニン研究会第 7 回研究会, 東京 (2018. 11) .
- 3) 合田幸広, 食薬区分と生薬, 東京農工大学工学部講義, 東京 (2018. 11) .
- 4) 合田幸広, 天然物医薬品及び機能性表示食品の品質保証, 第55回植物化学シンポジウム(2018. 11).
- 5) 山路誠一, 高橋直熙, 丸山卓郎, 徳本廣子, 袴塚高志, イチイ属植物由来生薬の鑑別に関する研究, 日本薬学会第 139 年会, 千葉 (2019. 3).
- 6) 川上 晋, 野辺彩香, 西村基弘, 稲垣昌宣, 大塚英昭, 松浪勝義 リュウキュウガキ葉部の成分研究(5) 日本薬学会第 138 年会, 金沢(2018. 03.)
- 7) 野辺彩香, 西田祥子, 川上 晋, 西村基弘, 稲垣昌宣, 松浪勝義, 大塚英昭, 兵頭直, 山口健太郎 リュウキュウガキ葉部より得られた *ent*-カウランジテルペンと細胞毒性 日本生薬学会第 65 回年会, 広島 (2018. 09.)
- 8) 内倉 崇, 杉脇秀美, 好村守生, 増本直子, 内山奈穂子, 袴塚高志, 天倉吉章, TLC による白首烏と異葉牛皮消の比較検討, 日本生薬学会第 65 回年会, 広島 (2018. 9)
- 9) 合田幸広, 天然物由来, 錠剤, カプセル形状食品の品質保証, 名古屋市立大学薬友会関西支部講演会, 大阪 (2019. 7).
- 10) 合田幸広, 天然物由来, 医薬品, 医薬部外品, 機能性表示食品の品質保証, 岐阜薬科大学第 6 回化粧品健康学セミナー, 岐阜 (2019. 10) .
- 11) 合田幸広, 食薬区分と生薬, 東京農工大学工学部講義, 東京 (2019. 11) .
- 12) 合田幸広, 天然物製品の品質とメタボロミクス, 大阪大学/島津分析イノベーション協働研究所開所記念式記念講演会, 大阪 (2019. 12).
- 13) 合田幸広, 生活に即した薬学[レギュラトリーサイエンス]の実践 健康食品の品質とニセ薬の話を中心に, 大阪大学講義, 大阪 (2019. 12).
- 14) 吉富太一, 山路誠一, 徳本廣子, 袴塚高志, 丸山卓郎, 健康食品として販売されるコウトウスギ製品の基原植物, 使用部位, paclitaxel 含量について, 第5回 次世代を担う若手のためのレギュラトリーサイエンスフォーラム, 東京 (2019. 9).
- 15) 吉富太一, 山路誠一, 徳本廣子, 袴塚高志, 丸山卓郎, イチイ *Taxus cuspidata* の部位別パクリタキセル含量と健康食品として販売されるコウトウスギ製品中の含量比較について, 日本薬学会第 140 年会, 京都 (2020. 3).
- 16) 川上晋, 稲垣昌宣, 西村基弘, 松浪勝義, 大塚英昭, リュウキュウガキ葉部より得られた新規メガスティグマン 2 種およびトリテルペン配糖体の酵素加水分解誘導体, 日本生薬学会第 66 回年会, 東京 (2019. 9).
- 17) 辻本 恭, 内山奈穂子, 丸山卓郎, 徳本廣子, 安食菜穂子, 林 茂樹, 三宅克典, 川原信夫,

- 袴塚高志, 高分解能 LC-MS を用いた Cassia 属ハネセンナ及びセンナの分析に関する研究, 日本生薬学会 第 65 回年会, 広島 (2018.9 月)
- 18) 辻本 恭, 徳本廣子, 細江潤子, 丸山卓郎, 川原信夫, 林 茂樹, 安食菜穂子, 小関良宏, 袴塚高志, 内山奈穂子, センナ及びハネセンナ含有健康食品に関する Sennoside の定量分析, 日本薬学会 第 140 年会, 京都 (2020.3)
- 19) Hakamatsuka T., Adulteration of Health Food Products with Unapproved Drugs in Japan, Western Pacific Regional Forum for the Harmonization of Herbal Medicines (FHH) Sub-Committee 2 Meeting, Korea (2019.6)
- 20) 袴塚高志, 医薬品と食品の境界について, 日本生薬学会第 66 回年会シンポジウム I 「健康食品と生薬に共通する植物素材—有効性と安全性を考える」, 東京 (2019.9)
- 21) 袴塚高志, 天然物医薬品の品質管理方法に関する国際調和, 第 48 回生薬分析シンポジウム, 京都 (2019.11)
- 22) Hakamatsuka T., Herbal Good Manufacturing Practice for Assurance of Quality and Safety of Raw Herbal Materials in Japan, The 11th annual meeting of International Regulatory Cooperation for Herbal Medicines (IRCH), Hungary (2019.12)
- 23) 政田さやか, 内山奈穂子, 袴塚高志, 合田幸広: 食薬区分照会に係る申請様式の整備について. 第 57 回全国衛生化学技術協議会年会 (2020.11.9, 誌上発表) 宮崎
- 24) Abe Y, Yamamoto E, Yoshida H, Masada S, Yokoo H, Tsuji G, Uchiyama N, Hakamatsuka T, Demizu Y, Izutsu KI, Goda Y, Okuda H: Temperature-dependent formation of N-nitrosodimehtylamine (NDMA) during the storage of ranitidine reagent powders and tablets. AAPS 2020 PharmSci 360 (2020.10.26-11.5, online)
- 25) 辻本 恭, 小関良宏, 袴塚高志, 内山奈穂子: トウゲシバエキス含有健康食品中に含まれる Huperzine A の分析. 日本食品化学学会 第 26 総会・学術大会 (2020 年 8 月. 誌上開催)
- F. 知的財産権の出願・登録状況
なし

Regular Article

Fluorescence Coupled with Macro and Microscopic Examinations of Morphological Phenotype Give Key Characteristics for Identification of Crude Drugs Derived from Scorpions

Hiroko Tokumoto,^{a,b} Hiroko Shimomura,^a Takashi Hakamatsuka,^a Yoshihiro Ozeki,^c and Yukihiro Goda^{*d}

^aDivision of Pharmacognosy, Phytochemistry, and Narcotics, National Institute of Health Sciences; 3–25–26 Tonomachi, Kawasaki-ku, Kawasaki 210–9501, Japan; ^bGraduate School of Engineering, Tokyo University of Agriculture and Technology; 2–24–16 Naka-cho, Koganei, Tokyo 184–8588, Japan; ^cDepartment of Biotechnology and Life Science, Faculty of Engineering, Tokyo University of Agriculture and Technology; 2–24–16 Naka-cho, Koganei, Tokyo 184–8588, Japan; and ^dDivision of Drugs, National Institute of Health Sciences; 3–25–26 Tonomachi, Kawasaki-ku, Kawasaki 210–9501, Japan.

Received October 4, 2017; accepted January 8, 2018

Microscopic examination of crude drug components has been the traditional method to identify the origin of biological materials. For the identification of components in a given mixture *via* microscopy, standard reference photographs of fragments derived from different organs and tissues of individual species are required. In addition to these reference photographs, a highly observant eye is needed to compare the morphological characteristics observed under the microscope with those of the references and to then identify the origin of the materials. Therefore, if other indexes are available to be coupled with microscope examination, the accuracy of identification would be significantly improved. Here, we prepared standard reference photographs for microscopic examination to identify powdered and fragmented materials in the crude drug “Quanxie” derived from individual organs of dried scorpion (*Buthus martensii* KARSCH). Since a remarkable characteristic of scorpion bodies is that they fluoresce under UV light, two methods to identify “Quanxie” were established, including fluorescence fingerprint analysis and microscopic fluorescent luminance imaging analysis. In the former, at least 0.1 g of powdered materials was used, which could be recovered after the measurement, and in the latter, only small amounts of powders were used for microscopic examinations. Both methods could distinguish powders of “Quanxie” from those of other micro-morphologically similar crude drugs, namely, “Chantui,” “Sangpiaoxiao,” and “Jianggan.” The combination of these methods should improve the swiftness and accuracy of “Quanxie” identification.

Key words *Buthus martensii*; fluorescence fingerprint; microscopic morphology; microscopic fluorescent luminance imaging analysis; powdered preparation; Quanxie

The origin of crude drugs should be clearly identified to ensure their effectiveness as suitable medicines. Currently, in order to ensure the efficacy of medicines, active components in crude drugs are extracted followed by their identification and quantification by chromatographic techniques such as TLC, HPLC, and gas chromatography coupled with MS.^{1,2)} Recent progress in molecular biology has allowed for the use of DNA profiling to extract DNA from dried and powdered crude drugs followed by PCR amplification to obtain nucleotide sequences, and real-time PCR technologies such as TaqMan and SYBR green have allowed for the possibility of species-specific quantification in mixtures prepared from many biological sources.^{3,4)} Although the recent progress in chromatographic and PCR micro analysis has provided us with the means to identify the origin of biological materials in trace amounts, these methods are tedious, expensive, and time-consuming. Compared to these instrumental analytical methods, traditional microscopic examination has economic advantages for the identification of ingredients in cut and powdered crude drugs,^{5–7)} because only a microscope is required. Particularly, fine-powdered materials, which do not need slicing into sections with a microtome, are needed to be placed on slides, fixed with mounting reagents, stained if necessary, and covered with a coverslip, before being placed under a micro-

scope for identification. This makes microscopic examination significantly less expensive than instrumental methods, as well as convenient, *in situ*, and instantaneous. The major difficulty of microscopic examination is the requirement of high-proficiency microscopic observation and the prerequisite of detailed and accurate comparative standard reference photographs. Other indices or profiles coupled with microscopic examination are expected to significantly improve the accuracy in crude drug identification over the sole use of microscopes.

The crude drug “Quanxie” (Scorpion, 全蝎) is made from dried whole *Buthus martensii* KARSCH (Buthidae, Scorpions, Arachnida, Arthropoda)⁸⁾ and has been used in China as an antispasmodic in pediatric epilepsy, an analgesic for headache and joint aches, and to treat stroke, bronchitis, and parotitis.^{9–11)} “Quanxie” is one of the crude drugs in “Usaien,” the ancient crude drug formulation described in “Korean Wazai-kyokuho (Taioing Huimin Heji Jufang Zochuhon version)”¹²⁾ as being one of the valuable possessions found in the Kunozan Toshogu shrine, Japan. Microscopic examination of a trace amount of the dry black preparation remaining at the bottom of the gallipot for Ieyasu Tokugawa, the first shogun of the Edo shogunate in Japan approximately 400 years ago revealed that the medicine contained in the gallipot was “Usaien.”¹³⁾

Buthidae belongs to the largest family of scorpions; in

*To whom correspondence should be addressed. e-mail: goda@nihs.go.jp

total, 1101 species in 90 families have been identified worldwide.¹⁴⁾ Studies on scorpions for taxonomical purposes were conducted long ago and were focused on external macro-morphological features.^{14–16)} These did not include any studies on *B. martensii*. The studies on Buthidae by Pavlovsky^{17–19)} provided useful morphological information regarding each organ system, such as gastrointestinal organs and respiratory organs, from an anatomical viewpoint, but no description of *B. martensii*, specifically, was included.

Scorpion research has been conducted in Japan for many years and Takashima^{20–22)} and Isshiki and Yonezawa²³⁾ have both described *B. martensii*. They reported that *B. martensii* lacks a subaculear tubercle beneath the aculeus, that the number of teeth on the pectene ranges from 16 to 25, and that it has tibial spur at the top of the tibia of the third and fourth legs. These characteristics differentiate it from the other Japanese domestic scorpions, *Isometrus europaeus* and *Liocheles australasiae*.

In the pharmacognosy field, the identification of the dried and powdered scorpion as a crude drug using morphological features, especially with microscopic observation, has rarely been reported other than by Xu²⁴⁾ and Zhang *et al.*^{25,26)} Animal-based crude drugs, especially those derived from insects, are complex and diversified compared to plant-based crude drugs. Many plant-based crude drugs are prepared from specific and limited organs and tissues, such as leaves, stems, roots, and seeds in which the medicinal components are accumulated. The powdered contents of these drugs become homogenous fragmented tissues and organs that can be identified easily with a microscope. In crude drugs derived from insects such as scorpions, the whole body including whole organs and tissues are crushed and fragmented. The resultant powder includes a complex mixture of tissues and organs, which constitute one drug, making it difficult to identify its origin. Confusion in the identification of scorpion has also been caused by inaccurate identification of the origins of the Buthidae species and by the inconsistent nomenclature of tissues and organs in the literature. For example, some literature concerning scorpions have reported seven segments in the prosoma,^{9,27)} but other sources have reported six segments,^{27,28)} and nomenclatures of the legs vary with the author.^{27–30)} In order to give an accurate name to the tissue fragments observed in powdered crude drugs, it is a pre-requisite to possess true and correct original materials along with correct names for fragmented and powdered tissues and organs found in the drug.

In the case of the identification of elements present in powdered “Quanxie,” while some characteristics of the muscles and exoskeleton were already indicated in the old literature,^{10,24)} a complete accounting of the characteristics of all individual parts of organs and tissues that make up the whole *B. martensii* body is unavailable. Identification of the characteristics of many *B. martensii* parts such as the book-lung and the pectenes, which are organs specific to the scorpions, remains to be performed. Furthermore, standard reference microphotographs of all *B. martensii* parts including whole tissues and organs still need to be produced.

The accuracy of crude drug identification by microscopic examination would be much greater if it was coupled to other evidence. It has been reported that scorpions fluoresce when illuminated with UV light.^{31–34)} Studies on scorpion fluorescence have revealed that this fluorescence is due to the

presence of β -carbolines (norharman)³⁵⁾ and hymecromone,³⁶⁾ which are generally thought to be contained in the epicuticle and hyaline layers.^{37,38)} β -Carbolines, a physiologically active class of molecules, act on the central nervous system to inhibit monoamine oxidase activity and may alter the level of brain neurotransmitters. They exist in natural materials such as baked meat, spices, coffee, and tobacco smoke and recent reports have indicated that they might be mutagenic in humans.^{39,40)} Hymecromone has been chemically synthesized and widely used as a fluorescent marker in enzyme assays and also as a medicine for seizures and biliary tract diseases, and has been detected in cuticle of arthropods.³⁶⁾ Since both β -carbolines and hymecromone are reported to be naturally contained in the epicuticle and hyaline layers of scorpions, the existence of these compounds in the fragmented tissues and organs being observed should help to improve the identification of “Quanxie.”

In this study, first, a detailed observation of mesoscopic morphology was performed in order to identify the correct origins of tissues and organs in commercially available scorpions. Later, powders were prepared from each tissue and organ and observed with a microscope to create standard reference photographs for the identification of fragmented scorpion parts contained in drug preparations. In order to improve identification of the powders, two fluorescence analyses were used. One was the fluorescence fingerprint method^{41,42)} where the fluorescence spectrum was measured after irradiation with a continuous spectrum, while the other was a microscopic fluorescent luminance imaging analysis in which the distribution of luminance at different wavelengths was observed using microscopic fluorescence filters at pin-points in the observation fields and the results were shown as histograms. These two methods coupled with microscopic examination may improve and support the identification of the crude drug powders obtained from scorpions.

MATERIALS AND METHODS

Materials The crude drug “Quanxie” (Uchida Wakanyaku Ltd., Tokyo, Japan, NIHS-DPP-20010-92-27), preserved in the Division of Pharmacognosy, Phytochemistry and Narcotics, National Institute of Health Sciences, was used as the main observation material. Commercially available, Japanese commercial brand “Quanxie” was gifted by Tochimoto Tenkaido Co., Ltd., Osaka, Japan (Lot 064014001, NIHS-DPP-20011), and Takasago Yakugyo Co., Ltd., Osaka, Japan (Lot 022916, NIHS-DPP-20012) (Fig. 1). Vietnam commercial brand “Toàn yết⁴³⁾” (NIHS-DPP-20013, NIHS-DPP-20014) was obtained for comparative observation. Other crude drugs derived from insect origins, “Chantui” (Cicada Slough, 蝉退) (Uchida Wakanyaku Ltd., NIHS-DPP-92-06) and “Sangpiaoxiao” (Mantis Egg-case, 桑螺蛸) (Uchida Wakanyaku Ltd., NIHS-DPP-92-52) were preserved in the Division of Pharmacognosy Phytochemistry and Narcotics, National Institute of Health Sciences. Cut “Jiangcan” (Stiff Silkworm, 白僵蚕) was purchased from Daikoshoyaku Co., Ltd., Aichi, Japan (Lot. 6127, NIHS-DPP-20030).

Observation of Morphological and Microscopic Characteristics under Visible Light The surfaces of crude drugs were observed using a digital microscope (VH-8000C; Keyence Co., Osaka, Japan) with a VH-Z25 zoom lens (Keyence)

and Olympus SZ stereomicroscope (Olympus Co., Tokyo, Japan). Microscopic morphology was observed using normal and polarized light with a BH-2 (Olympus) attached to a VH-8000C and Axio Scope A1 (Carl Zeiss AG, Oberkochen, Germany). For microphotography, a Micrograph Imager Olympus PM-10AK (Olympus), VH-8000C, and DP-21 digital camera (Olympus) were used.

The fine structure of each material was observed by preparing sectioned specimens. Rough sections of whole "Quanxie" were cut approximately 3 to 5 mm wide using a razor blade. These sections were then wetted with water for 20 to 30 min at room temperature until they were swollen, frozen, and sliced 30 to 60 μm thick using a freezing microtome (Kelk Ltd., Kanagawa, Japan). The sections were placed on glass slides and mounted with a mixture of glycerol and water (1:1), as mentioned in the "Microscopic examination" section of the Japanese Pharmacopoeia 17th edition (JP17)⁷⁾ and covered with a coverslip. A surface view was used in order to prepare sequential sections that were parallel at the surface (paradermal sections). Transverse (cross) and longitudinal (vertical) sections were prepared by slicing the body in midline and parallel directions, respectively. For the observation of oils, Sudan III staining was performed according to the literature.⁴⁴⁾

For the observation of powdered samples, dried whole "Quanxie" or individual organ sections cut using a razor blade were pulverized with a mortar and pestle. Since some "Quanxie" drugs were obtained from the hard scorpion external skeleton or accumulated high amounts of oil, pulverized materials were sieved through a #50 (300 μm) stainless-steel sieve to isolate the particles categorized as "moderately fine powder" to "very fine powder." In accordance with the procedure described in the "Microscopic examination" section of JP17, approximately 1 mg of powder was mixed with a drop of mounting agent on a glass slide using a small glass rod to prevent the formation of air bubbles, and allowed to stand until rehydrated. An additional drop of mounting agent was then added and a coverslip was placed on the slide. Under an optical microscope, pictures of the microscopic characteristics of each sample were taken in order to prepare standard microscopic reference photographs of powdered "Quanxie" for identification.

In this report, tissues and organs are referred to with the names used in previously published books.^{28, 45–50)}

Fluorescence Fingerprint Analysis Fluorescence of crude drugs was observed after irradiation with UV light at 365 nm using a ChromaDoc-It Imaging System (Ultra-Violet Products Ltd., Cambridge, U.K.). A fluorescence spectrophotometer (F-7100, Hitachi High-Tech Science Co., Tokyo, Japan) was used. Measurement conditions were as follows: slit width of 5 nm for both excitation and fluorescence; excitation and fluorescence wavelengths of 200–600 and 200–750 nm, respectively; sampling intervals of 10 and 5 nm for excitation and fluorescence, respectively; photomultiplier tube voltage of 400 V; scan speed of 60000 nm/min; response set to the automatic mode. The powders were placed into a solid cell prior to analysis with the spectrophotometer and three-dimensional measurements were taken. Each measurement took approximately 2 min, and three repetitive measurements were taken. Whole of "Chantui," parts of "Chantui" eyes and thorax, and surface layers of "Sangpiaoxiao" and "Jiangcan" were simi-

larly treated and the fluorescence fingerprints were measured under the same conditions as above.

Microscopic Fluorescent Luminance Analysis at Pixel Level "Quanxie" and its fine powder, excluding the very fine powder, were observed under an inverted fluorescence phase contrast microscope BZ-X700 (Keyence). The excitation/emission wavelengths and dichroic mirror wavelength of the filters were 4',6-diamidino-2-phenylindole (DAPI): 340–380/435–485, 400 nm, green fluorescent protein (GFP): 450–490/500–550, 495 nm, and tetramethyl-rhodamine (TRITC): 522.5–557.5/570–640, 565 nm, respectively. Data in the range of 0–255 stepwise gradients for each pixel were monitored with a CCD 8-bit camera and the luminance brightness distribution within the designated region of the tissue fragments was shown as a histogram. "Chantui" powder, surface layers of "Sangpiaoxiao" and "Jiangcan," and a mixture of powdered "Quanxie" and "Chantui" (1:1) were observed in the same manner.

RESULTS

Morphological Characteristics of Commercially Available "Quanxie" and Other Drugs Derived from Insects Observed under Fluorescent Light "Quanxie" is commercially available as dried whole body and as broken pieces (Figs. 1A–E). A unique characteristic of scorpions is that they emit fluorescence under illumination with UV light (Figs. 1A–(2) and E). Such fluorescence could also be observed in parts of the cicada slough "Chantui," mantis egg-case "Sangpiaoxiao," and stiff silkworm "Jiangcan" (Figs. 1F–H). Crushed and powdered "Quanxie" can be difficult to distinguish from crushed and powdered "Chantui," "Sangpiaoxiao," or "Jiangcan." Since parts of all these dried insects fluoresce under UV light illumination, the superficial observation of fluorescence could not be used to distinguish between them. Detailed morphological and fluorescent observations were therefore required to identify "Quanxie" from other insect materials.

Mesoscopic Morphological Characteristics of "Quanxie" as Seen by Microscopic Observation (Fig. 2) The nomenclature of scorpion organs, especially the legs, has been used with contradictory meanings by differing authors, as mentioned before. Here, we adopted the nomenclature of the legs described as the opinion of Couzijn in the literature.³⁰⁾

Prosoma (Figs. 2A–G) As shown in Fig. 2, the carapace (a) is accompanied by one pair of shiny reddish-brown ocelli (median eyes (b)) at the center and three pairs of ocelli (lateral eyes (c)) on either side. Many reddish-brown tubercular processes (d) are scattered on the surface and concentrated around the eyes. The appendages of the first segment are chelicerae (e) followed by pedipalps and legs. On the ventral-side surface of the prosoma, coxa (f) and coxal endites (gnathobase (g),²⁸⁾ Figs. 2B and C), which are important tissues in the feeding process, were observed at the bottom of the first two pairs of legs with numerous colorless short hair (h1). Chelicera (e) are accompanied by dark-reddish teeth (i) and densely brown long hair (h2) (Fig. 2D).

Pedipal chela (j) (Fig. 2E), accompanied by a regularly-arranged reddish denticle row (k), brown bristle hair assumed to be seta (h3), colorless or grayish-white short hair (h4), and long brown hair assumed to be trichobothrium (h5),^{29,51)} were observed.

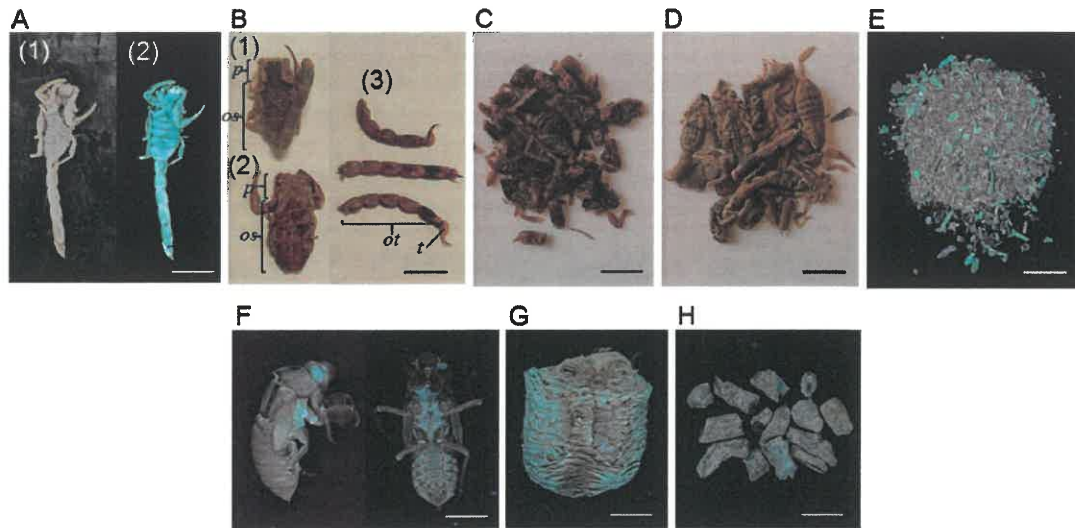


Fig. 1. Photographs of Commercial Crude Drug Derived from Scorpions (A–E) or from Insects (F, G) Observed under Visual and UV Light

“Toàn yết” acquired from Vietnam (A) photographed under visual light (1) and UV light at 365 nm (2). “Quanxie” from Uchida Wakanyaku Ltd. (B): ventral side (1) and dorsal side (2) metasoma and telson (3). Cut “Quanxie” from Tochimoto Tenkaido Co., Ltd. (C). “Quanxie” from Takasago Yakugyo Co., Ltd. (D). Coarse “Quanxie” powder from Uchida Wakanyaku Ltd. (E). “Chantui” (F), “Sangpiaoxiao” (G) and cut “Jiangcan” (H) photographed under UV light at 365 nm. Bar length: 1 cm. *p*: prosoma, *os*: mesosoma, *ot*: metasoma, *t*: telson.

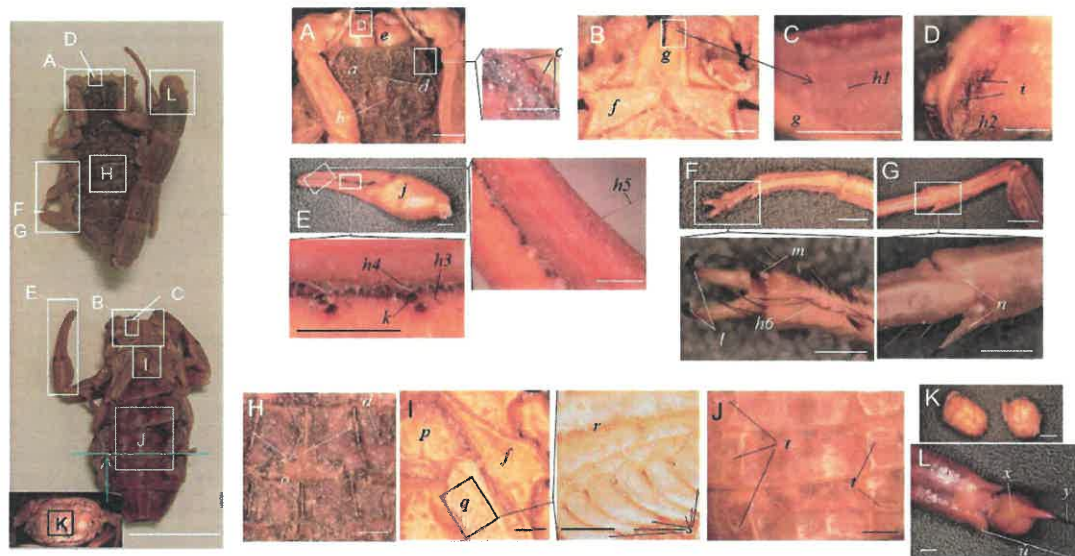


Fig. 2. Photographs of “Quanxie” Morphological Characteristics

The left panel shows the macro-morphology of the “Quanxie” body with particular areas notes by the letters (A) to (L). Bar length: 1 cm. Dorsal side of the prosoma (A)-the right hand photograph shows an enlarged observation of the squared area; Ventral side of the prosoma (B); Backside surface of the coxal endite (gnathobase) (C); Chelicera (D); Pedipalp chela (E)-right and lower hand photographs are enlarged observation of the squared areas; Tip and middle of leg (F and G)-lower hand photographs correspond to the squared areas; Tergite (H). Genital opercula and pecten (I)-the right hand photograph shows an enlargement of the squared area; Sternite (J); Intraperitoneal contents (K); Metasoma and telson (L). Bar length: (A), (B), (E), (F), (G), (I), (K) and (L), 1 mm, high magnification photographs of (C), (D), (H), (J) and those of right and lower sides of (A), (E), (F), (G) and (I), 0.5 mm. *a*: carapace, *b*: median eye, *c*: lateral eye, *d*: tubercular process, *e*: chelicera, *f*: coxa of leg, *g*: coxal endite (gnathobase), *h1*: fine and silky hair of gnathobase backside surface, *h2*: brown long hair on the chelicera, *h3*: brown short seta on the pedipalp, *h4*: colorless short seta on the pedipalp, *h5*: trichobothrium on the pedipalp, *h6*: brown trichobothrium on the leg, *i*: teeth on the chelicera, *j*: pedipalp chela, *k*: denticle row, *l*: unguis on the leg telotarsus, *m*: dactyl on the apotele, *n*: tibial spur on the leg tibia, *o*: keel, *p*: genital opercula, *q*: pecten, *r*: marginal lamella and median lamella on the pecten, *s*: pectinal tooth (comb-like structures of pecten), *t*: spiracle, *u*: telson, *x*: vesicle, *y*: aculeus.

In each leg segment (Figs. 2F and G), brown bristle hair (seta) (*h6*) was observed. The top of the seventh segment (telotarsus) was accompanied by one or two unguis (*l*) and an apotele with a dactyl (*m*).²⁸ Between one and three spurs (pedal spur, tibial spur (*n*)) could be observed at the end of the fifth and sixth segments.

Opisthosoma and Telson (Figs. 2H–2L) The dorsal side of the mesosoma was covered with blackish-brown tergites

(Fig. 2H). Remarkably, three lines of keel (*o*) were observed and reddish-brown tubercular processes (*d*) were scattered on the surface. The ventral side was yellowish brown and covered with sternites (Figs. 2I and 2J), which were accompanied by genital opercula (*p*), pecten (*q*), and spiracles (*t*). The pecten consisted of marginal and median lamellae (*r*), fulcra, and pectinal tooth (comb-like structure) (*s*). There were approximately twenty teeth in total. Pleural membranes

were observed at the boundary of the tergites and sternites (no image). In domestic market products, some scorpions producing “Quanxie” contained tissues in the peritoneal cavity. Peritoneal tissues were yellowish-white globular substances (Fig. 2K), in some of which embryos initiated cell division, and/or blackish to whitish-gray fragile tissues. In samples from Vietnam, one of “Toàn yết” were almost empty, while the other was filled with whitish-gray fragile and sand-like materials in their peritoneal cavity.

The metasoma (Fig. 2L) consisted of five segments shaped like a barrel, the inside of which was almost vacant except for long black tissues thought to be muscles. The telson (Fig. 2L (z)), followed by the metasoma, was a small, round, brownish vesicle (x) to which a reddish brown hooked aculeus (y) was attached. Under the aculeus, no subaculear tubercle was found.

The following characteristics were determined by Takashima to be key to the identification of *B. martensii*: 16–25 pectinal teeth, tibial spurs on the third and fourth legs, and a lack of subaculear tubercle.^{20–22} Based on these criteria, it was concluded that the origin of the “Quanxie” drug samples used here was *B. martensii*.

Microscopic Characteristics of “Quanxie” (Fig. 3) Microscopic examination to determine the origin of crude drugs involves determining if the powdered materials are “fine powder” tissues and organs, and studying the microscopic morphology of the surface and cross-sectioned sides of each tissue and organ. Microscopic characteristics observed from every orientation are given below for the preparation of “Quanxie” standard reference photographs.

Although the microscopic morphology of the “Quanxie” has been already reported,^{10,24,25} the names for each tissue in different reports are not the same. The appropriate names are given below in the descriptions of our observations.

Prosoma (Figs. 3A–3E) In the surface view of the outermost carapace layer (Fig. 3A-(1)), clear characteristic pentagonal or hexagonal border patterns were observed. Major and minor diameters of cuticle patterns were 11 to 16 μm and 5 to 8 μm , respectively. Yellow shining tubercular processes (a) were scattered and many pore canals (b) were found on the surface. At different depths of focus on the outermost layer, fine pores and a sinuous pattern emerged (Figs. 3A-(2), -(3) and -(4)). Most trichobothria had been removed and the double ring-shaped structure of socket cells was found at the base of the vestigial trichobothria (Figs. 3D-(1) and -(2)). In the transverse carapace section (Figs. 3A-(5) and -(6)), the outermost layer was an epicuticle (c) with a brown exocuticle (d), and an almost colorless longitudinal fibrous endocuticle (e) appeared underneath. Numerous parallel pore canals (b) penetrated through this layer. The outside tissues around the median eyes (f) and lateral eyes (g) were notable characteristics and the inside tissues were highly concave (Fig. 3A-(7)). Eyeballs were shiny yellow with orbicular elements (Fig. 3A-(8)).

The inner surface of the leg coxal endite (gnathobase) (Figs. 3B-(1) and -(2)) consisted of thinner tissue than the carapace cuticle. The gnathobase cuticle pattern was fuzzy and its surface was covered with numerous colorless hair (Fig. 3B-(1) (h1)). The diameters of the hair were 0.8 to 1.8 μm and their length was approximately 60 μm , which was obviously finer than the hair on other parts.²⁵ The base of the hair was circular and the vestige after the hair was removed was a small

pore (Fig. 3B-(2)).

In the surface view of the chelicera coxa (Fig. 3C-(1)), the pattern of the epicuticle was slightly unclear. Pore canals (b) and curved hair (h2) were scattered on the surface. Under a polarization field, the pore canals (Fig. 3C-(2)) shined in a cross pattern (Fig. 3C-(3)). The diameters and lengths of the hair were 6 to 10 μm and 300 to 500 μm , respectively. Most hair were removed and the vestiges looked more like slightly larger circular pores than like pore canals. Chelicera chela (Figs. 3C-(4) and -(5)), accompanied by seta (h3) and reddish and round papillary processes (i), were arranged in lines.

On the surface of the pedipalp cuticle (Fig. 3D), a clear border pattern consisting of numerous pore canals was observed. Trichobothria (h4) were scattered on the surface and the double ring structures derived from the socket cells were clear. In a surface view of the procuticle (paradermal section), a volute pattern was observed around the pores. In longitudinal sections of the chela and movable and fixed fingers of the sixth and fifth segments, large and small dark reddish-brown denticle processes, respectively, were lined up on the ventral sides (Fig. 3D-(3) (j)). Clear pore canals that passed through the cuticle and muscles (k1) were observed (Fig. 3D-(4)). Muscles were colorless or slightly light brown with clear striations. Individual fibers had a diameter of 17 to 50 μm and formed bundles with diameters thicker than 100 μm .

In the surface view of the legs (Fig. 3E), the surface pattern on the cuticle was unclear in the first, second, sixth and seventh segments, but was clear from the third, fourth and fifth segments to the coxa. Trichobothria were densely distributed and arranged in lines (h5) on the sixth and seventh segments. In the transverse leg section, muscles were clearly observed. Larger muscles were found in the segments nearer the coxa (k2). In the interspace between the muscles and the cuticle, some tissues stained with Sudan III reagent (Fig. 3E-(3)). Ungues derived from the seventh segment and dactyls or spurs derived from other segments showed reddish spire-like and falciform shapes, and the tibial spurs of the third and fourth legs had the characteristic morphology of *B. martensii*.

Opisthosoma–Mesosoma (Figs. 3F and 3G) The surface view of the outermost layer of the tergite, sternite, and pleural membrane (Figs. 3F-(1), -(2) and -(3)) showed almost the same characteristics as the prosoma epicuticle. The cuticle pattern seen in the surface view of the sternites (Fig. 3F-(2)) was slightly unclear although it could be seen that the density of the tubercular processes was less than that of the tergites. In the transverse sections of tergites and sternites (Figs. 3F-(4), -(5) and -(6)), circular muscle arranged circularly along the cuticle (kc) and longitudinal muscle arranged vertically towards the cuticle (kl) were observed. Sternites (Fig. 3F-(6)) had some spiracles and book-lungs (o) consisting of many thin tissue layers.

The pleural membrane that connected to the tergites and sternites was constructed of a soft cuticle⁴⁸ and the surface view showed an irregular circular floral pattern (Fig. 3F-(3)). In the transverse section (Fig. 3F-(7)), the outmost layer was grayish green followed by a colorless, curved, wavy, longitudinal layer underneath. Adjacent to the pleural membrane, muscle was observed (Fig. 3F-(7) (k3)). Soft cuticle was observed not only in the pleural membrane but also in the genital opercula and in other tissues. In a longitudinal section of sternites (Fig. 3F-(8)), book-lungs were seen as stacks of

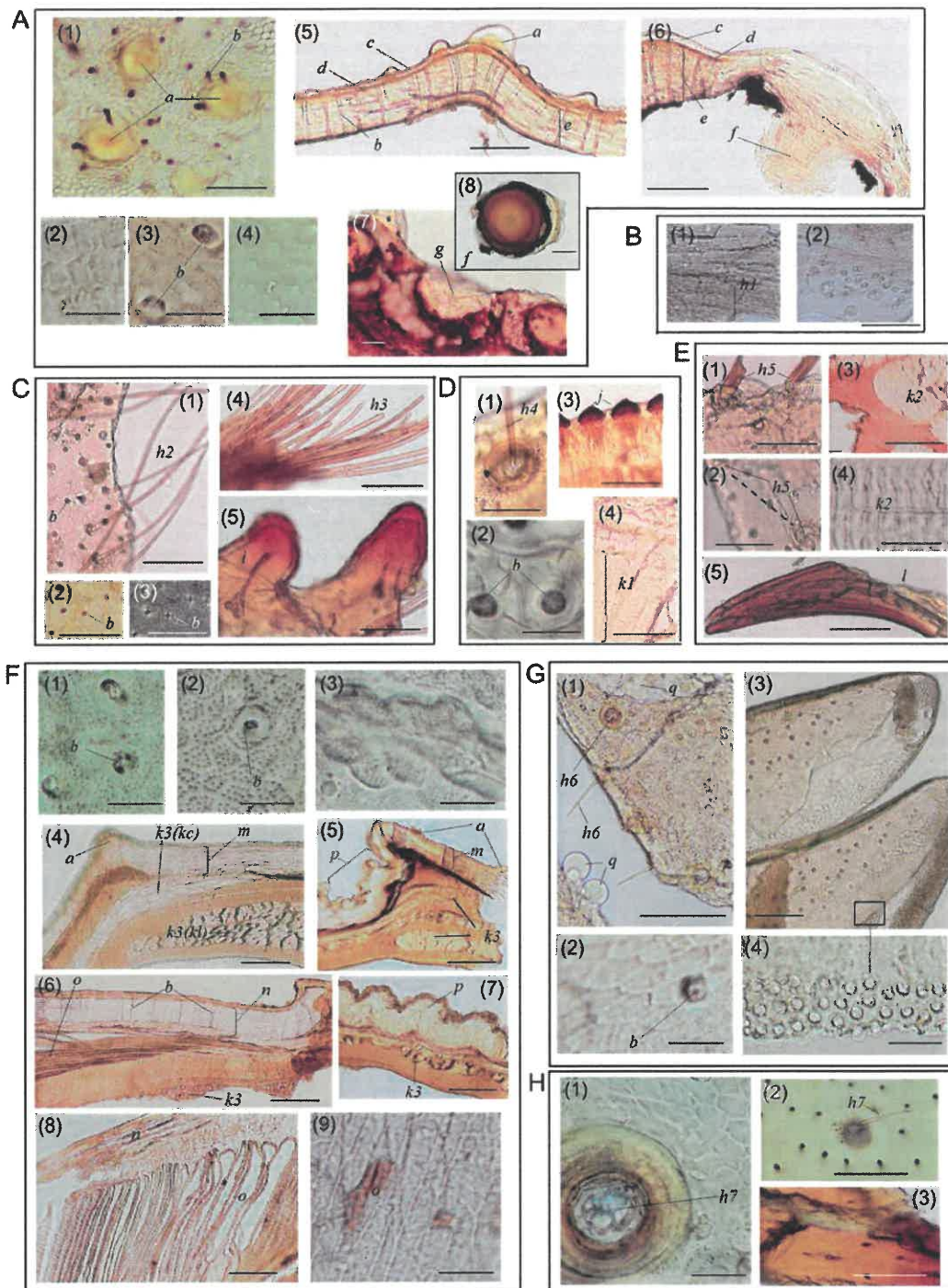


Fig. 3. Microscopic "Quanxie" Morphology

Carapace (A): (1) Surface view of the outermost cuticle layer; (2), (3), and (4) microscopic observations at different depths of the outermost layer; (5) and (6) transverse sections; (7) longitudinal sections of the lateral eyes; (8) surface view of the median eye. Bar lengths: (1), (5), (6), (7) and (8): 100 μm ; (2-4): 20 μm . Coxal endite (gnathobase) (B): (1) and (2) Surface views of the coxal endite backside. Numerous colorless short hair (*hl*) and vestiges (2) were observed. Bar length: 100 μm . Chelicera (C): (1) Surface view of chelicerae coxa; (2) and (3) surface views of pore canals under normal and polarized condition, respectively; (4) and (5) longitudinal chela sections. Anterior segment had numerous brown bristle hair (assumed to be seta). Bar length: 100 μm . Pedipalp (D): (1) and (2) Surface view of cuticle and procuticle, respectively; (3) and (4), longitudinal sections of chela, denticle row (*j*) and muscle (*kl*). Bar lengths: (1), (3) and (4): 100 μm ; (2): 20 μm . Leg (E): (1) and (2) Surface views of the sternite and book-lung; (3) transverse section of the leg. Numerous muscles were observed and brownish regions were stained with Sudan III; (4) longitudinal section of the leg muscle; (5), unguis or dactyls on the leg telotarsus. Bar lengths: (1), (2) and (3) and (5): 100 μm ; (4): 20 μm . Mesosoma (F): (1), (2) and (3) Surfaces view of the tergite, sternite and pleural membrane, respectively; (4), (5) and (6), transverse sections of a pleural membrane section; (7) longitudinal section of the sternite and book-lung; (9), surface view of the book-lung. Bar length: (1), (2) and (3) and (9): 20 μm ; (4), (5), (6), (7) and (8): 100 μm . Pecten (G): (1) and (2) Surface view of marginal lamella on the pecten; (3) and (4) section of pecten piece. Bar lengths: (1) and (3): 100 μm ; (2) and (4) 20 μm . Metasoma and telson (H): (1) Surface view of the metasoma cuticle; (2) surface view of vesicle cuticle on the telson; (3) surface view of the aculeus cuticle. Bar lengths: (1): 20 μm ; (2) and (3): 100 μm . *a*: tubercular process, *b*: pore canal, *c*: epicuticle, *d*: exocuticle, *e*: endocuticle, *f*: median eye, *g*: lateral eye, *hl*: fine and silky hair on the gnathobase, *h2*: brown long hair on the chelicera coxa, *h3*: brown seta on the chelicera, *h4*: trichobothrium on the pedipalp, *h5*: trichobothrium on the leg, *h6*: seta on the pecten marginal lamella, *h7*: socket cell in the trichobothrium on the metasoma, *i*: teeth on the chelicera, *j*: denticle row of pedipalp chela, *kl*: pedipalp muscle, *k2*: leg muscle, *k3*: mesosoma muscle, *kc*: circular muscle, *l*: pedipalp muscle, *m*: tergite, *n*: sternite, *o*: book-lung, *p*: pleural membrane, *q*: oil drop.

many thin tissue layer and the book-lung surface showed a flat rhomboid reticulate pattern (Fig. 3F-(9)).

On the marginal and median lamella of the pecten (Fig. 3G-(1)), bristle hair (*h6*), pore canals (Fig. 3G-(2) (*b*)) and cuticle patterns were observed. In some regions of these lamellae, film-like and flat pentagonal or hexagonal reticulate patterns (Fig. 3G-(2)) were observed with scattered oil drops (*g*). In a transverse section of pecten pieces showing comb-like structures (Fig. 3G-(3)), the top shape was loosely curved and a series of circular pores along the marginal region were observed. Teeth had neither hair nor muscles. Since the tissues in the abdominal cavity were easily broken, it was hard to prepare slice sections for observation. The tissues from the abdominal cavity were therefore powdered and their morphology was observed later.

Metasoma and Telson (Fig. 3H) In the surface view of the metasoma (Fig. 3H-(1)), a clear cuticle pattern, shiny reddish-brown tubercular processes, trichobothrium with socket cells (*h7*), and pore canals were observed. Inside the metasomal cuticle, muscles were observed. Trichobothrium and pore canals were observed in the telson vesicle (Fig. 3H-(2)). The vesicle was vacant and had only a few muscles in it. The surface of the aculeus tip (Fig. 3H-(3)) was dark reddish-brown, spire-like, and falciform.

Microscopic Characteristics and Standard Reference

Microphotographs of Powdered Quanxie (Fig. 4) In order to prepare standard reference photographs for the identification of powdered crude drugs *via* microscopic observation, the whole dried body of “Quanxie” (Fig. 1A) was pulverized using a motor and pestle followed by sieving through stainless mesh (No. 50⁷¹) and the resulting powders were mounted on slide glasses to be observed with a light microscope. The observed parts were grouped into appropriate tissues by comparison with the characteristic microscopic photographs of tissue sections shown in Fig. 3. The photographs of representative powder characteristics were arranged and summarized in Fig. 4 as tissue fragments mainly derived from cuticle or epidermal system (Fig. 4A), seta and trichobothrium (Fig. 4B), muscles (Fig. 4C), and other parts (Fig. 4D). The parts with morphologies useful for identification of the origin of the tissue as *B. martensii* were observed at high magnification, as shown in Fig. 4E.

Carapace cuticle and its enlarged view are shown in Figs. 4A-a and 4E-a. Observation at high magnification showed the cuticle pattern (Fig. 4E-a-1), socket cells (Fig. 4E-a-2), pore canals (Fig. 4E-a-3), tubercular process (Fig. 4E-a-4), and a fine cuticle pattern (Fig. 4E-a-5). Cuticles derived from gnathobase (leg coxal endites) were observed as fragments covered with colorless, fine, straight hair (Figs. 4A-b, 4E-b-1 and 4E-b-2). Cuticles derived from the chelicera were reddish-

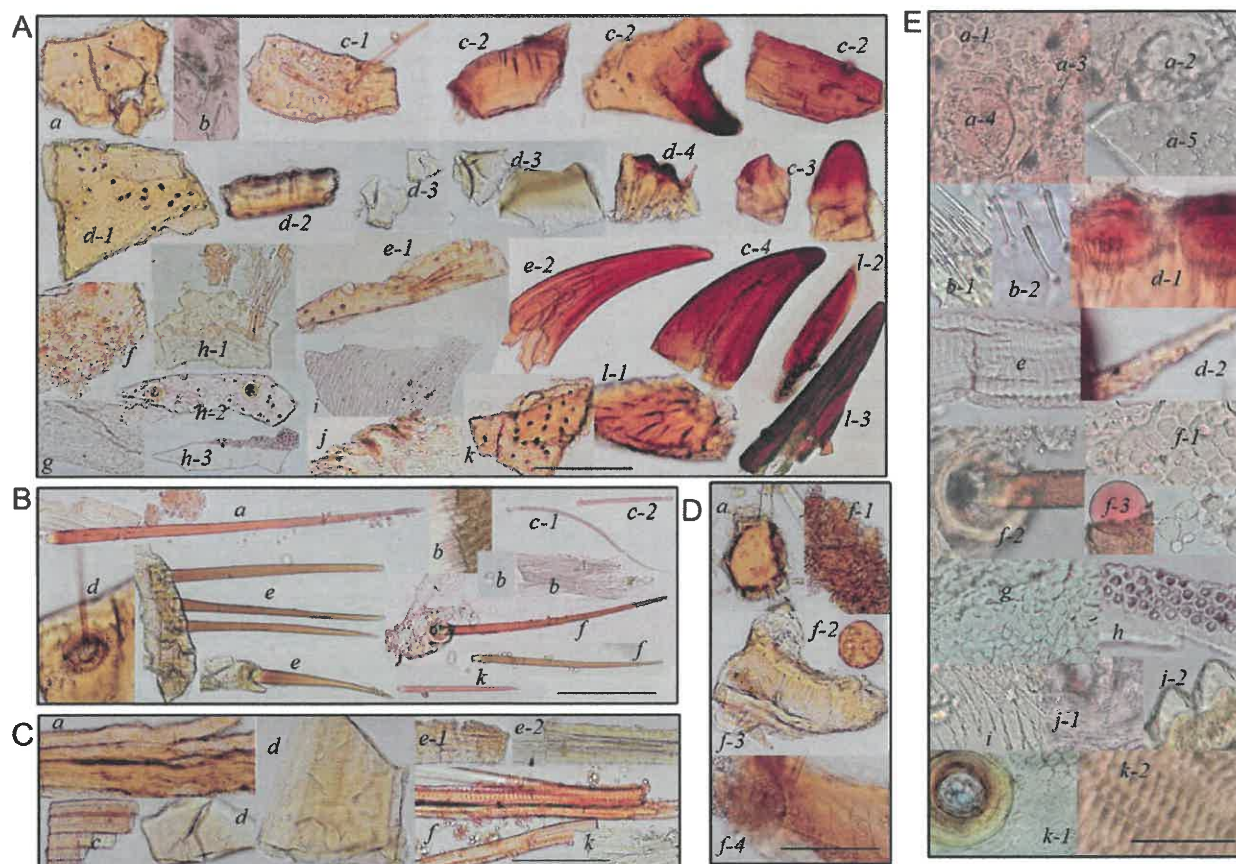


Fig. 4. Standard Reference Microphotographs of Powdered “Quanxie”

Fragments derived from cuticle or epidermal systems (A). Hairs (seta and trichobothrium) (B). Fragments derived from muscle (C). Fragments derived from other tissues (D). High magnified photographs of characteristic and important morphologies useful for identifying the origin of *B. martensii*-derived tissues (E). Small italicized letters refer to the tissue origin and hyphenated numbers represent different micro-morphology characteristics in samples derived from the same origin of tissues. Bar lengths: (A–D): 200 μ m; (E): 50 μ m. Fragments derived from *a*: carapace, *b*: gnathobase, *c*: chelicera, *d*: pedipalp, *e*: leg, *f*: mososoma, *g*: genital opercula, *h*: pecten, *i*: book-lung, *j*: pleural membrane, *k*: metasoma, *l*: telson.

brown and had numerous slightly curved hair (Figs. 4A-c-1 and 4A-c-2). Papillary processes accompanied by a reddish-brown tip (Fig. 4A-c-3) were characteristic of chelicera, which were observed as single and multiple rows and were derived from two anterior chela-forming segments. Fragments derived from the chela tip were dark reddish-brown and appeared in a falciform shape (Fig. 4A-c-4). Most pedipalp cuticles appeared in the surface view under microscopic observation (Fig. 4A-d-1) and some fragments were observed in the cross-section (Fig. 4A-d-2). Some procuticle fragments were observed as shiny plate-like layers (Fig. 4A-d-3). Reddish brown processes derived from denticle rows of the sixth (tarsus, movable finger) and the fifth (tibia, fixed finger) segments appeared as single and multiple rows of processes (Figs. 4A-d-4 and 4E-d-1). Fibrous connections from these processes to other tissues through the cuticle might be sensory tissue (Fig. 4E-d-1). Cuticle derived from the legs (Fig. 4A-e-1) had trichobothria arrayed on a straight line. Ungues and dactyls were observed as reddish spire-like and falciform fragments (Fig. 4A-e-2). Although the shape of unguis and dactyls were similar to each other and the powder preparations were difficult to distinguish, in the external morphology dactyls are less curved than unguis. The width of the unguis and dactyls (Fig. 4A-e-2) was generally narrower than that of the chela tip (Fig. 4A-c-4). Cuticles derived from tergites and sternites (Figs. 4A-f and 4E-f-1) had trichobothria with clear socket cells (Fig. 4E-f-2) and some of them included oil drops stained with Sudan III reagent (Fig. 4E-f-3). Characteristics of the tergite cuticles were similar to those of the sternites, but they were distinguishable by the slightly unclear cuticle pattern found in the sternites, a higher density of tubercular process found in the tergites, and the fact that some sternite fragments were accompanied by book-lungs. Genital operculum was a tiny tissue associated with soft cuticle with particular pattern (Figs. 4A-g and 4E-g). Some cuticle fragments derived from basal pecten pieces showed a slightly flat pentagonal or hexagonal reticulate pattern, the socket cells derived from which were smaller than those derived from other tissues (Fig. 4A-h-1). In the cuticle fragments of cuticle derived from pectinal teeth (comb-like structure), many circular pores were densely arranged along the marginal region (Figs. 4A-h-3 and 4E-h). Epidermal cells in the book-lung, which is an organ specific to arachnida, were film-like structures with a flat rhomboid reticulate pattern (Figs. 4A-i and 4E-i). The pleural membrane was made up of amorphous fragments of soft cuticle with irregular circular and floral patterns (Figs. 4A-j, 4E-j-1 and 4E-j-2). The genital operculum, pleural membrane, and the intersegmental membrane consisted of soft cuticles and showed similar characteristics to each other. Fragments derived from cuticles of the metasoma and telson were darker red than those derived from other tissues (Fig. 4A-k) and the large socket cells were found on the surface (Fig. 4E-k-1). The cuticle derived from vesicle was dark reddish brown (Figs. 4A-l-1 and 4A-l-2). The tip of the aculeus was also colored dark reddish brown and was not curved but sharp (Fig. 4A-l-3).

Most tissue fragments identified as hair were derived from the seta and trichobothrium (Figs. 4B and 4E). Some hair (trichobothrium) accompanied a cuticle attached to a socket cell with a double ring-like shape. Hair (trichobothrium) of the carapace was reddish brown and had vertical lines on the surface (Fig. 4B-a). Two types of hair on the gnathobase

(Fig. 4B-b) were observed; one was very fine with a sharp top (Fig. 4E-b-1) and the other was not (Fig. 4E-b-2). Chelicera hair showed two types of shapes, one soft curved and the other rectilinear with a difficult-to-see lumen (Figs. 4B-c-1 and 4B-c-2). Pedipalp trichobothrium also showed two types of shapes, where one was similar to those of the carapace and the other was a fine seta with a socket cell (Figs. 4B-d and 4E-d-2). Multiple trichobothria of legs arranged in a line could be observed (Fig. 4B-e). Most hair on the mesosoma was brownish with vertical stripes (Figs. 4B-f and 4E-f-2), but some of them were colorless and short. Hair from metasoma was similar to those of mesosoma but their lumen was clear (Fig. 4B-k).

Muscles were derived from almost all tissues and were observed in large amounts of pulverized fragments (Fig. 4C). They were colorless to yellowish brown with clear striations and appeared separately or as bundles. Some muscles derived from the carapace appeared to be attached to the eye ball or other tissues (Figs. 4C-a and 4D-a). Pedipalp muscles were composed of bundles larger than 100 μm in diameter (Fig. 4C-d). In the legs, some muscles had striations (Figs. 4C-e-1 and 4E-e) and some did not (Fig. 4C-e-2). Muscles derived from the mesosoma developed better in the ventral side than in the dorsal side and appeared as elongated fragments (Fig. 4C-f). Some muscles derived from metasoma were almost colorless (Figs. 4C-k and 4E-k-2).

Other sections appeared as major observed objects (Fig. 4D) and may have been the tissues in the peritoneal cavity, which seen to be colorless or yellowish-brown granules with single or spherical lumps (Fig. 4D-f-1) containing oil drops stained with Sudan III (Fig. 4D-f-2). Other tubular tissue fragments (Figs. 4D-f-3 and 4D-f-4) were thought to be derived from other gastrointestinal organs.

Fluorescence Fingerprint Analysis of “Quanxie” and of Other Crude Drugs Derived from Insect Origins The fluorescence fingerprint method involves scanning a sample for a continuous wavelength of emission light and recording the luminescence intensity of the fluorescence at a continuous excitation wavelength. The results are presented as three-dimensional graphs of luminescence intensity at varied emission wavelengths and excitation fluorescence (Fig. 5 x- and y-axes, respectively). The samples for the fluorescence spectrometer were mounted as solid materials irrespective of shape such as fragmented cut bodies and powders. “Quanxie” gave strong fluorescence upon UV light illumination (Fig. 1A(2)) and its coarse powders showed remarkable fluorescence (Fig. 1E). In order to prepare crude drugs for medication, whole or cut bodies of “Quanxie” are pulverized into powders. The representative fluorescence fingerprint profile of “Quanxie” powders prepared from a whole body is shown in Fig. 5A. The graphs on the left-hand side of Fig. 5 show the contour lines of luminescence intensity, while the upper and lower right-hand graphs show two-dimensional spectrograms at the peak luminescence intensities for fixed excitation and emission wavelengths, respectively. The data given are the maximum luminescence intensities derived from the fluorescence spectrophotometer at peak excitation/emission light wavelengths. Powders of whole bodies of “Quanxie” showed remarkably high emission peaks at approximately 490 nm when irradiated with 400 nm (Fig. 5A). Almost identical fingerprint profiles showed a peak at 480–490 nm emission light against 400 nm excitation light in

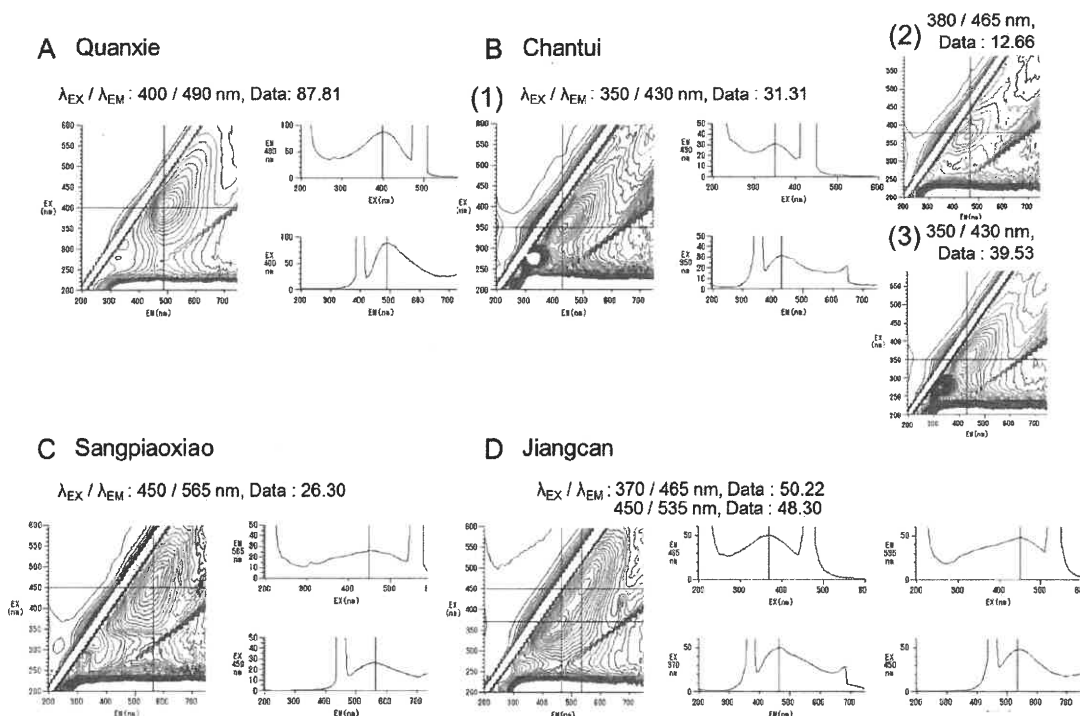


Fig. 5. Fluorescent Fingerprint of “Quanxie” and Other Crude Drugs Derived from Arthropods

Powder of whole bodies of “Quanxie” (Uchida-Wakanyaku Ltd.) (A). Powder of whole bodies “Chantui” (B): (1) Powder of whole slough; (2) Powder of eye part; (3) Powder of thorax part. Powder of “Sangpiaoxiao” surface layer (C). Powder of “Jiangcan” surface layer (D). The left-hand diagrams (A–D) show contour lines of luminescence intensity *versus* emission and excitation wavelengths of *x*- and *y*-axes, respectively. The right upper diagrams show the luminescence intensity of excitation spectra and the lower diagrams show emission spectra at the peak excitation wavelengths. Data represent the value of luminescence intensity output from the fluorescence spectrophotometer at the peak excitation and emission wavelengths. Contour line interval: (A), 5; (B)(1), (B)(2) and (C), 1; (B)(3) and (D), 2.

powders of different “Quanxie” products obtained from Japanese wholesalers of crude drugs (Supplementary Fig. 1). These profiles might be reflected by the fluorescence observed for “Quanxie” (Fig. 1A(2)) and the powders of surface cuticles of each part of mesosoma or metasoma showed remarkably high emission peaks at 480–490nm when irradiated with 400nm (Supplementary Figs. 2A and 2B). Compared to surface side of outer tissues visible in the outside, we found that the tissues inside the peritoneal cavity in “Quanxie” purchased from Japanese wholesalers exhibited fluorescence at approximately 550nm after irradiation at 450nm (Supplementary Figs. 2C-(1), -(2) and -(3)). “Toàn yết” acquired from Vietnam exhibited strong fluorescence image at outside (Fig. 1A) and similar fingerprint profiles for powders of mesosoma and metasoma parts to those obtained from Japanese wholesalers; the powder of sand-like materials in the peritoneal cavity of “Toàn yết” did not exhibit a remarkable fluorescence fingerprint profile (Supplementary Fig. 2C-(4)), indicating that these materials might be different from intraperitoneal tissues inside the peritoneal cavity of “Quanxie” obtained from Japanese wholesalers.

Since other insect crude drugs, “Chantui,” “Sangpiaoxiao” and “Jiangcan” showed fluorescence upon illumination with UV-light (Fig. 1), powders of these crude drugs prepared by pulverization of whole bodies were mounted in the fluorescence spectrometer. We succeeded in observation of the fingerprint profile of the powders of “Chantui” whole bodies (Fig. 5B), but failed in that of “Sangpiaoxiao” and “Jiangcan” (data not shown). This might be because “Chantui” consists of molten skins of cicada without any tissues inside and the

powders are composed of parts of cicada slough with less contamination from materials interfering with fluorescence as observed in Fig. 1F. “Sangpiaoxiao” and “Jiangcan” are egg cases of mantis and bodies of sick silkworm, respectively, in which large amounts of internal tissues contaminate the powder preparation of whole bodies of crude drugs and interfere and/or quench fluorescence derived from surface parts as observed in Figs. 1G and H, respectively. The fingerprint profile of whole “Chantui” slough showed an emission peak at 430nm after irradiation at 350nm, but the luminescence intensities, 31.31, were smaller than those of “Quanxie,” 87.81 (Figs. 5A and B-(1)). In the body, remarkable fluorescence was observed at eye and thorax part (Fig. 1F). Characteristic emission peaks were found in the eye and thorax of “Chantui” at 465nm emission after irradiation at 380 and at 430nm emission after irradiation at 350nm (Figs. 5B(2) and 5B(3), respectively), indicating that the fingerprint profiles observed for the powders of “Chantui” whole bodies might be majorly caused by the fluorescence exhibited by the powder of these parts. Although remarkable fingerprint profiles could not be obtained for the whole bodies of “Sangpiaoxiao” and “Jiangcan,” the parts of surface layer shaved and collected from these bodies, for which the fluorescence could be observed as shown in Figs. 1G and H, exhibited a typical fingerprint profile of fluorescence; “Sangpiaoxiao” had an emission peak at approximately 565nm after excitation at 450nm and “Jiangcan” had emission peaks at approximately 465 and 535nm after excitation at 370 and 450nm, respectively, both of which showed different patterns compared from “Quanxie” and “Chantui” and lower luminescence intensities than “Quanxie.”

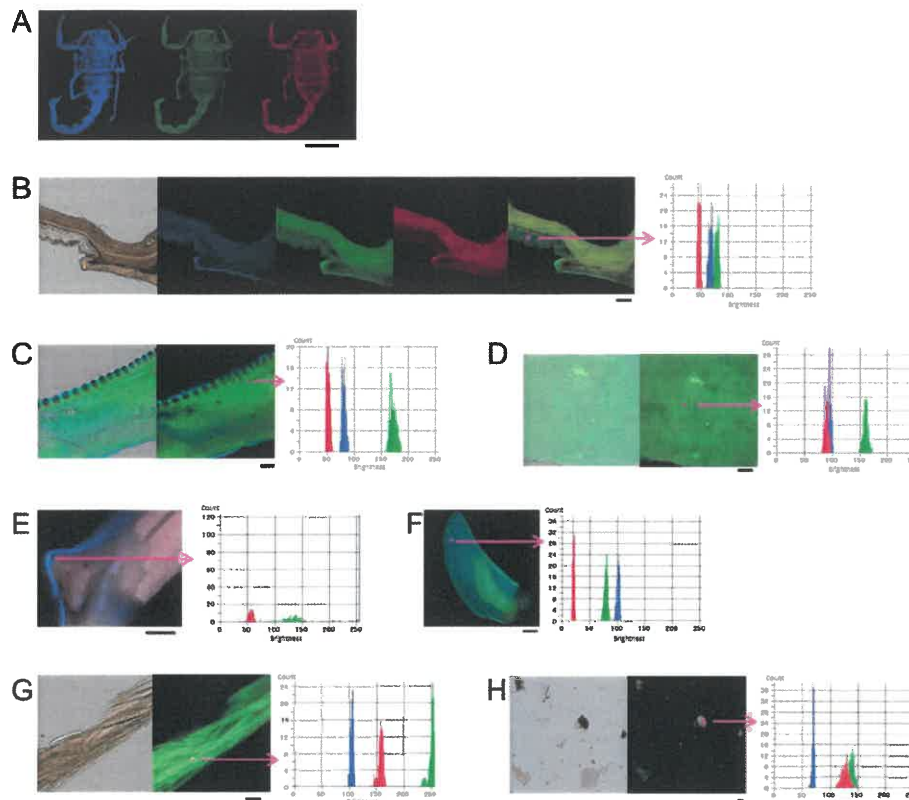


Fig. 6. “Quanxie” Observed with a Fluorescence Microscope and Fluorescent Luminance Imaging Analysis for Brightness at Pixel Level

Composite fluorescence images (sum of sixty scans) of a whole “Quanxie” body with excitation at 340–380, 450–490, and 532.5–557.5 nm then observed through DAPI, GFP, and TRITC filters (A, left, center, and right, respectively). Cross-section of the tergite area (B): images under visual light (left) observed through DAPI, GFP and TRITC filters (second, third, and fourth photographs, respectively), and a merged photograph (the right end of photographs). Fluorescence brightness was independently derived from three filters at the point indicated by the pink square ($13 \times 13 \text{ pix}^2$ = B, C, D, F, G, $20 \times 20 \mu\text{m}^2$, E, $10 \times 10 \mu\text{m}^2$, H, $50 \times 50 \mu\text{m}^2$). Fluorescence was observed using a CCD camera attached to the fluorescence microscope and the number of counts observed through each filter was plotted to obtain the brightness (DAPI, GFP, and TRITC filters for blue, green, and red histograms, respectively). Surface view of the pedipalp and sternite (C and D): overlay image of fluorescence with the three filtered lights (right) and further merged with visible light image (left). Merged image of three fluorescent images of tergite and pectinal tooth cross sections (E and F). Longitudinal section of muscle and fragmented intraperitoneal contents (G and H): images under visible light (left) and overlay of three fluorescent images (right). Bar lengths: (A): 1 cm; (B) to (H): $100 \mu\text{m}$.

Microscopic Fluorescent Luminance Imaging Analyses of “Quanxie” Powdered Fragments Distinguishable from Other Insect Derived Materials Since scorpion bodies fluoresce after irradiation with approximately 380 nm light (Fig. 1A), the emitted light gave characteristic fluorescence images when viewed through DAPI, GFP, and TRITC filters (Fig. 6A). In the slice preparation, we could observe that the epicuticle fluoresced blue and the procuticle fluoresced green. These properties were used to characterize “Quanxie” using a fluorescence microscope attached to a 2.38-million-pixel monochrome CCD camera and analyzed using BZ-X Analyzer software (Keyence). Figure 6B shows a representative resultant photograph and histogram of the pleural membrane section. Observation by visual light (Fig. 6B, photograph furthest to the left) was used for the identification of micro-morphological characters and, in the same view field, observation through fluorescent light through individual DAPI, GFP, and TRITC filters (Fig. 6B, the second, third and fourth of photographs from the left, respectively, and the fifth was overlay of these three photographs) gave characteristic information about the tissues. The individual images were taken with a CCD camera and the fluorescence brightness of specific pixels (shown as the pink squares in the following figures) was analyzed and overlaid into a histogram (Fig. 6B right) by the software with

blue, green, and red bars corresponding to images derived from DAPI, GFP, and TRITC filters, respectively. In the tergite area, the pleural membrane was more transparent under visual light on the lower left side of the specimen (Fig. 6B). In the observation of these images by individual filters to the view field, any point of objective area of $20 \times 20 \mu\text{m}^2$, which corresponded to $13 \times 13 \text{ pix}^2$ in CCD camera image, could be selected. Several pixel square points of different areas in an identical view field were designated to measure fluorescence brightness. Our detailed histogram-based observations that surveyed several points of the tergite area revealed that similar histogram profiles could be observed in separate, individual areas of homogenous cells (Supplementary Fig. 3).

The visual and fluorescence overlay photographs for surface views of the pedipalp and sternite samples are shown in Figs. 6C and 6D. In these regions, the green color was very brightness and the histograms at the pixel point showed higher quantified results for the green brightness than for blue or red. For the cross-section view of the sternite, the epicuticle in particular shined bright blue with remarkable fluorescence (Fig. 6E). The histogram, therefore, showed a high value for the brightness of the blue color. The surface of pectinal tooth was also observed to fluoresce blue (Fig. 6F). Muscle (Fig. 6G) and intraperitoneal tissues (Fig. 6H) had high values for brightness

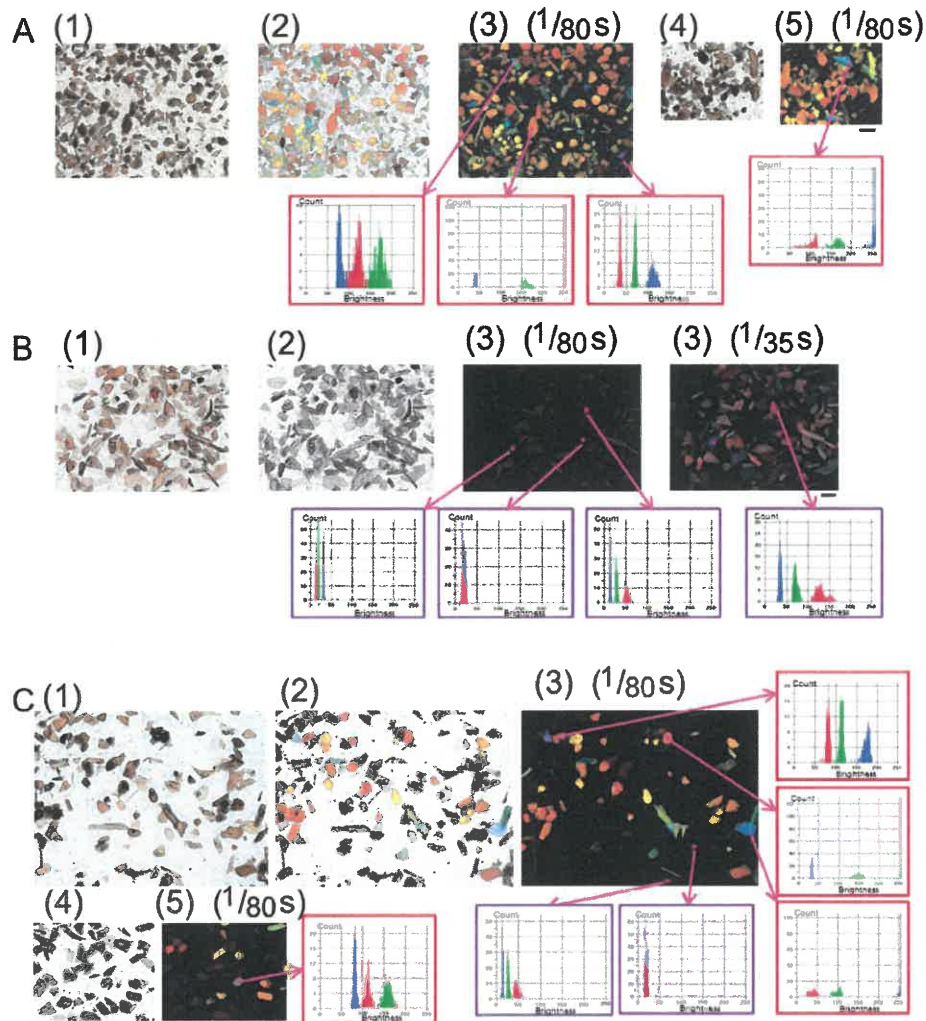


Fig. 7. Powdered “Quanxie” and “Chantui” Observed with a Fluorescence Microscope and Fluorescent Luminance Imaging Analysis

Powdered “Quanxie” (Uchida-Wakanyaku Ltd.) (A); Powdered “Chantui” (B); Mixture of “Quanxie” and “Chantui” powders (1:1, w/w) (C). A-(1), A-(4), B-(1), C-(1), and C-(4) show powders observed with visible light; A-(2), B-(2), and C-(2) show overlays of merged visible light images with three fluorescence images observed through DAPI, GFP, and TRITC filters (Excitation: 340–380, 450–490, and 532.5–557.5 nm, respectively); A-(3), A-(5), B-(3), C-(3), and C-(5) show merged images of three fluorescence images. Exposure times were 1/80 and 1/35 s. Histograms show the distribution of the brightness for the fluorescence observed through DAPI (blue bars), GFP (green bars), and TRITC (red bars) filters in the areas indicated by the pink squares ($13 \times 13 \text{ pix}^2 = 50 \times 50 \mu\text{m}^2$). Red and purple framed histograms were determined to be fragments derived from “Quanxie” and “Chantui,” respectively. Bar length: $200 \mu\text{m}$.

of green and red and some were observed as yellow to brown. In the preparation of the standard reference photographs from the powdered materials mentioned in the previous section, intraperitoneal contents were frequently observed, suggesting that this particle-like material might be a good marker to identify “Quanxie” using microscopic fluorescent luminance imaging analysis.

In the “Quanxie”-derived powders (Fig. 7A), fragments shined blue and yellow under the fluorescence microscope. In particular, many yellowish fragments were observed in “Quanxie” from Uchida-Wakanyaku Ltd. which contained a lot of intraperitoneal contents (Fig. 7A). In contrast, there were many fragments that shone blue in the Vietnam commercial brand “Toàn yết” powder (Supplementary Figs. 4A and B). In the bluish fluorescent fragments found in the powders, the distribution of brightness of each color depended on which tissues each fragment derived from; the fragments showing strong blue brightness were likely derived from the epicuticle and those showing strong green brightness could be from the

pedipalp, sternite or muscle.

The powders derived from “Chantui” fluoresced only weakly under irradiation with light that generated a strong response from “Quanxie.” In order to strengthen the weak fluorescent brightness of “Chantui” fragments, a long exposure time, 1/35 s, was required, as compared to an exposure time of 1/80 s for “Quanxie” (Fig. 7B). The brightness histogram after 1/80 s exposure showed that the weak fluorescence distributed at lower range in “Chantui” than that in “Quanxie” (compare Figs. 7A-(3) and B-(3)). A few fragments fluoresced blue and other major fragments fluoresced almost red in “Chantui” powder after 1/35 s exposure (Fig. 7B-(3)(1/35 s)); an abundance of blue-fluorescing fragments was observed in the thorax sample (Supplementary Fig. 4C). Since “Sangpiaoxiao” and “Jiangcan” powders fluoresced less brightly, exposure times of 1/25 and 1/35 s, respectively, were necessary to take photographs with enough quantifiable data to produce histograms. Many fragments that showed strong brightness values for red and green in the histograms looked as though they

fluoresced yellow in microscopic photographs (Supplementary Figs. 4D and 4E).

When “Quanxie” and “Chantui” powders were mixed 1:1 (w/w), they are distinguishable, since the brightness of fluorescence derived from “Quanxie” tissue was apparently higher than that from “Chantui” (Fig. 7C). In addition, the histogram pattern by the fluorescent luminance imaging analysis could provide the even origin of individual fragments as being from either “Quanxie” or “Chantui.”

DISCUSSION

Recent advances in molecular biological and phytochemical methods have provided new molecular phenotype markers. Molecular biological phenotypes using PCR and nucleotide sequences and phytochemical phenotypes determined by HPLC, TLC, and MS are useful to identify the constituent materials and origins of crude drugs. Microscopic examination methods have been traditionally used since they are convenient, fast, and require small amounts of materials to identify the origin of crude drugs. The specimens that require microscopic observation are usually chopped, broken, cut, fragmented, or powdered and then mounted on glass slides, after which the micromorphological characteristics can be difficult to use to distinguish between animals and plants, unless the observer knows individual characteristics. In microscopic observations of powdered crude drug preparation, many similar figures that were observed derived from completely different organisms including sometimes both insects and plants. In order to identify the ingredients found in a preparation of crude drugs containing plant and animal origins, detailed and accurate observation of the fragment characteristics is required and the standard reference photographs must be prepared.

The respiration systems of arachnida consist of trachea and/or book-lungs. Some arachnida have only trachea and others have both trachea and book-lungs, which they use depending on the environmental conditions.^{28,45,46} Scorpions have no trachea but respire using four pairs of book-lungs attached at spiracles on the third, fourth, fifth, and sixth sternites.^{27,28,45,46} Scorpions are known to have evolutionarily conserved relatively primitive organs such as book-lung. The microscopic characteristics of book-lung tissue observed here and in the standard reference photographs might be useful for the identification of scorpions in powdered crude drugs.

Scorpion cuticle is known to emit fluorescence. Fluorescence fingerprinting is advantageous over other analytical methods since that solid materials, such as whole bodies, exfoliated exoskeletons, and powdered materials, can be analyzed and recovered after the analysis. Fluorescence was also observed in the “Chantui,” “Sangpiaoxiao,” and “Jiangcan” samples, but their fluorescence fingerprint profiles differed from those of “Quanxie.” Since the fluorescence fingerprint profiles of separate classes might be expected to differ, the fluorescence fingerprint method was applied to identify crude drugs derived from arachnida. *Pandinus imperator* (emperor scorpion) fluoresced at 500 nm after irradiation at 365 nm and other scorpions showed similar species-specific fluorescence after species-specific excitation wavelengths.^{35,51} These facts added to our results presented here support the conclusion that fluorescence fingerprinting may be useful for the identification of Buthidae. The data presented here are insufficient for

perfect identification of individual Buthidae species. Significantly more fingerprint profile data are going to be measured to establish macroscale identification methods comparable to micro-morphological identification. In this study, we obtained preliminary results that a mixture of “Quanxie” and “Chantui” powders showed different emission values at specified emission wavelengths. This suggests that the fingerprint method may be useful to qualitatively and quantitatively identify crude drugs mixture with powder materials composed of different species origins.

While the fluorescence fingerprint method could play an effective role in identifying “Quanxie” at the macro-level when accompanied by macro-morphology data (Fig. 1), fluorescence microscopy could be a useful and powerful tool to survey the observed microscopic field and identify “Quanxie” using microscopic level data. Coupling fluorescence microscopy with a CCD camera followed by imaging analysis, the targeted regions of organs, tissues, and individual powdered fragments could be analyzed to determine their distinct fluorescences at three different fluorescence wavelengths. These data were then quantitatively presented as histograms. The merit of fluorescence microscopy observation was that fragments that fluoresced could be detected in a large number of objects under low-magnification. When one fragment in the powdered crude drug mixture was detected under the low-power field, its micro would be observed in a high-power field and then be compared with standard reference to identify its origin. When one fragment could be identified as originating from a certain “Quanxie” tissue or organ, further microscopic fluorescent luminance imaging analysis could then provide more reliable identification by comparing to reference histogram profiles, if they were available. Future detailed experiments to prepare references standard histogram profiles of all of individual tissues and organs of “Quanxie” should be conducted.

The fluorescence fingerprint and microscopic fluorescent luminance imaging analysis methods established here are an important breakthrough to have accurate, prompt, and convenient identification methodologies for crude drug identification. These methods will be able to identify crude drugs originated from many species, including “Quanxie,” when the necessary databases of the standard references of fluorescence fingerprint profiles and microscopic fluorescent luminance histograms are ready.

Acknowledgments We thank Mr. Kiyoshi Sugiyama and Dr. Takuro Maruyama for providing Vietnam and domestic market products and Dr. Naoko Sato for guidance and advice on measuring fluorescence fingerprints. We thank Dr. Nahoko Uchiyama for valuable experimental suggestions. We thank Mr. Hideki Nishikawa, Keyence Corporation, for cooperation in observation using Bz-X700 and for analytical advice. This work was partially supported by Health Labour Sciences Research Grant from the Ministry of Health, Labour, and Welfare.

Conflict of Interest The authors declare no conflict of interest.

Supplementary Materials The online version of this article contains supplementary materials.

REFERENCES

- 1) Liang YZ, Xie P, Chan K. Quality control of herbal medicines. *J. Chromatogr. B Analyt. Technol. Biomed. Life Sci.*, **812**, 53–70 (2004).
- 2) Montoro P, Piacente S, Pizza C. Quality issues of current herbal medicines. *Herbal Medicines. Development and Validation of Plant-Derived Medicines for Human Health*. (Bagetta G, Cosentino M, Corasaniti MT, Sakuraba S eds.) CRC Press, Boca Raton (2011). ISBN 978-1-4398-3769-6 (2016).
- 3) Shaw PC, Wang J, But PP-H. *Authentication of Chinese Medicinal Materials by DNA Technology*. World Scientific Publishing Co. Pye. Ltd. (2002). ISBN 978-981-02-4621-1.
- 4) Joshi K, Chavan P, Warude D, Patwardhan B. Molecular markers in herbal drug technology. *Curr. Sci.*, **87**, 159–165 (2004).
- 5) Jackson BP, Snowden DW. *Atlas of Microscopy of Medicinal Plants, Culinary Herbs and Spices*. CRC Press, Boca Raton (1990). ISBN 0-8493-7705-6.
- 6) Upton R, Graff A, Jolliffe G, Länger R. *Microscopic Characterization of Botanical Medicines (American Herbal Pharmacopoeia Botanical Pharmacognosy)*. CRC Press, Boca Raton (2011). ISBN 978-1-4200-7326-3.
- 7) Ministry of Health Labour and Welfare. *The Japanese Pharmacopoeia 17th ed. (Ministry Notification 64)*. Japan, p. 4 and pp. 120–121 (2016).
- 8) Chinese Pharmacopoeia Committee of Ministry of Public Health of the People's Republic of China. *Chinese Pharmacopoeia Vol. 1* The People's Health Publishing House, People's Republic of China, p. 143 (2015).
- 9) *Chinese Materia Medica*. (Jiangsu New Medical College ed.) Shanghai People's Publication House, People's Republic of China, pp. 1288–1291 (2006).
- 10) Xu G-J. *Chinese Materia Medica*, China Medical Science Press, People's Republic of China, pp. 1780–1782 (1996).
- 11) Namba T. *The Encyclopedia of Wakan-Yaku (Traditional Sino-Japanese Medicines) with Color Pictures Vol. II*. Hoikusha Publishing Co., Ltd., Japan, pp. 259–261 (1980). ISBN: 4586302046
- 12) Suzuki T. Studies of various editions of “*Heji Jufang*” and objective of compilations of “*Heji Jufang*” during the *Kyoho* era of the Edo period. *Jpn. J. History Pharm. Yakushigaku Zasshi*, **42**, 91–96 (2007).
- 13) Shimomura H, Tokumoto H, Sekita S, Satake M, Tokugawa M, Tokugawa N, Goda Y. Identification of components in “*Usaien*” preparation: contents of the heirloom gallipot of the Mito-Tokugawa family. *J. Nat. Med.*, **67**, 41–58 (2013).
- 14) Koch CL. Buthidae. “The Scorpion Files”: <https://www.ntnu.no/ub/scorpion-files/buthidae.php> Jan. 13, 2017.
- 15) Pocock RI. The Fauna of British India. “The Scorpion Files”: https://www.ntnu.no/ub/scorpion-files/pocock_fauna_india2.pdf, 1900. Dec. 19, 2017.
- 16) Vachon M. Etudes sur les Scorpions. “The Scorpion Files”: <https://www.ntnu.no/ub/scorpion-files/vachon2.pdf>, 1952. Dec. 19, 2017.
- 17) Pavlovsky EN. Studies on the organization and development of scorpions. *J. Cell Sci.*, **68**, 615–640 (1924) (<http://jcs.biologists.org/content/joces/s2-68/272/615.full.pdf>) Sep. 2016
- 18) Pavlovsky EN. Studies on the organization and development of scorpions. 5. The Lungs. *J. Cell Sci.*, **70**, 135–146 (1926) (<http://jcs.biologists.org/content/joces/s2-70/277/135.full.pdf>) Sep. 2016
- 19) Pavlovsky EN, Zarin EJ. On the structure and ferments of the digestive organs of scorpions, *J. Cell Sci.*, **70**, 221–261 (1926) (<http://jcs.biologists.org/content/joces/s2-70/278/221.full.pdf>) Sep. 2016
- 20) Takashima H. Nihon-san zenkatumoku oyobi kyakushumoku. *Acta Arachnologia*, **8**, 5–30 (1943).
- 21) Takashima H. Kyokuto-sasori. *Acta Arachnologia*, **9**, 51–53 (1944).
- 22) Takashima H. Scorpions of Shansi, North China. *Acta Arachnologia*, **10**, 112–116 (1948).
- 23) Isshiki O, Yonezawa A. A scorpion (*Buthus martensii* Karsch) found in Japan. *Med. Entomol. Zool.*, **11**, 117–123 (1960), Eisei Doubutu.
- 24) *Microscopical Identification of Powdered Crude Drugs* (Xu G-J. ed.), The People's Health Publication House, People's Republic of China, pp. 748–749 (1986).
- 25) Zhang GJ, Tanaka T, Zhang LH, Ohba K. Pharmacognostical studies on the Chinese crude drug “*Quanxie*.” *Nat. Med.*, **48**, 191–197 (1994).
- 26) Zhang GJ, Tanaka T, Xue-Qin L, Jie L, Xiu-Lian L, Kawamura T. Pharmacognostical studies on the Chinese crude drug “*Quanxie*.” *Nat. Med.*, **48**, 198–202 (1994).
- 27) Uchida T. *Systematic Zoology Vol. 7*, Nakayama-Shoten Co., Ltd., Japan (1966). ISBN: 9784521071152.
- 28) *New Illustrated Encyclopedia of the Fauna of Japan*. (Okada K, Uchida K, Uchida T eds.) Hokuryukan, Japan, pp. 339–341 (1988). ISBN: 9784832600218.
- 29) Clarke KU. *The Biology of the Arthropoda*, Baifukan Co., Ltd., Japan (1979). ISBN: 9784563037628.
- 30) Hjelle JT. Anatomy and morphology. *The Biology of Scorpions* (Polis GA. ed.) Stanford University Press, U.S.A., pp. 9–63 (1990). ISBN: 0804712492.
- 31) Pavan M. Presence and distribution of a fluorescent substance in scorpion tegument. *Boll. Soc. Ital. Biol. Sper.*, **30**, 801–803 (1954).
- 32) Pavan M. Preliminary data on characteristics of fluorescent substance of the tegument in scorpions. *Boll. Soc. Ital. Biol. Sper.*, **30**, 803–805 (1954).
- 33) Pavan M, Vachon M. Existence of a fluorescent substance in the skin of scorpions (Arachnida). *C. R. Hebd. Seances Acad. Sci.*, **239**, 1700–1702 (1954).
- 34) Lawrence RF. Fluorescence in Arthropoda. *J. Ent. Soc. S. Africa*, **17**, 167–170 (1954).
- 35) Stachel SJ, Stockwell SA, Vranken DLV. The fluorescence of scorpions and cataractogenesis. *Chem. Biol.*, **6**, 531–539 (1999).
- 36) Frost LM, Butler DR, XO'Dell B, Fet V. A coumarin as a fluorescent compound in scorpion cuticle. *Scorpions 2001: In Memoriam, Gary A. Polis* (Fet V, Selden PA eds.) British Arachnological Society, U.K., pp. 365–368 (2001).
- 37) Filshie BK, Hadley NF. Fine structure of the cuticle of the desert scorpion, *Hadrurus arizonensis*. *Tissue Cell*, **11**, 249–262 (1979).
- 38) Krishnan G. On the cuticle of the scorpion *Palamneus swammerdami*. *J. Cell Sci.*, **3**, 11–22 (1953).
- 39) Herraiz T. Relative exposure to β -carboline norharman and harman from foods and tobacco smoke. *Food Addit. Contam.*, **21**, 1041–1050 (2004).
- 40) Pfau W, Skog K. Exposure to β -carboline norharman and harman. *J. Chromatogr. B Analyt. Technol. Biomed. Life Sci.*, **802**, 115–126 (2004).
- 41) Nakamura Y, Fujita K, Sugiyama J, Tsuta M, Shibata M, Yoshimura M, Kokawa M, Nabetani H, Araki T. Discrimination of the geographic origin of mangoes using fluorescence fingerprint. *J. Jpn. Soc. Food Sci. Tech.*, **59**, 387–393 (2012).
- 42) Sugiyama J, Tsuta M. Discrimination and quantification technology for food using fluorescence fingerprint. *J. Jpn. Soc. Food Sci. Tech.*, **60**, 457–465 (2013).
- 43) Nguyễn CY. *Medicinal Plants and Traditional Medicines in Vietnam (Cẩm nang Cây thuốc và vị thuốc phương Đông và các bài thuốc ứng dụng)*, Nhà xuất bản Tổng hợp Tp. Hồ Chí Minh, Vietnam (2006). ISBN: 184906348.
- 44) Konoshima M. *Laboratory Manual of Botanical Morphology. Microscopic Experiments*. Hirokawa Publishing Co., Japan, pp. 280–281 (2005). ISBN: 4-567-44425-6.
- 45) Ono H. *Scorpions. Diversity and Evolution of Arthropoda* (Ishikawa R ed.) Shokabo Co., Ltd., Japan, pp. 123–126, 151–153 (2008). ISBN: 9784785358297.

- 46) Uchida T. *Fundamental Animal Taxonomy and Phylogeny*. Hokuryukan & New Science Co., Ltd., pp. 164–165 (1988). ISBN: 4-8326-0068-0.
- 47) *Biology of Insects, 2nd Ed.* (Matsuka M, Ohno M, Kitano H eds.) Tamagawa University Press, Japan (1984). ISBN: 9784472075421.
- 48) *Systematics of the Scorpion Family Vaejovidae, Glossary*. American Museum of Natural History, West Texas A & M University, California Academy of Sciences, U.S.A. <<http://www.vaejovidae.com/Glossary.htm>>. Sep. 2017
- 49) *Systematics of the Scorpion Family Vaejovidae, Interactive Tutorial on Scorpion Anatomy*. American Museum of Natural History, West Texas A & M University, California Academy of Sciences, U.S.A. <<http://www.vaejovidae.com/Anatomy.htm>>. Sep. 2017
- 50) Sugawara T. Mechanoreceptors of arthropods. *Comp. Physiol. Biochem*, **15**, 97–113 (1988).
- 51) Klock CT. A comparison of fluorescence in two sympatric scorpion species. *J. Photochem. Photobiol. B*, **91**, 132–136 (2008).

Regular Article

Eight *ent*-Kaurane Diterpenoid Glycosides Named Diosmariosides A–H from the Leaves of *Diospyros maritima* and Their Cytotoxic Activity

Susumu Kawakami,^a Shoko Nishida,^a Ayaka Nobe,^a Masanori Inagaki,^a Motohiro Nishimura,^a Katsuyoshi Matsunami,^b Hideaki Otsuka,^{*,a} Mitsunori Aramoto,^c Tadashi Hyodo,^d and Kentaro Yamaguchi^d

^aDepartment of Natural Product Chemistry, Faculty of Pharmacy, Yasuda Women's University; 6–13–1 Yasuhigashi, Asaminami-ku, Hiroshima 731–0153, Japan; ^bDepartment of Pharmacognosy, Graduate School of Biomedical and Health Sciences, Hiroshima University; 1–2–3 Kasumi, Minami-ku, Hiroshima 734–8553, Japan; ^cIriomote Station, Tropical Biosphere Research Center, University of the Ryukyus; 870 Aza Uehara Taketomi-cho, Yaeyama-gun, Okinawa 907–1541, Japan; and ^dFaculty of Pharmaceutical Sciences, Tokushima Bunri University, Kagawa Campus; 1314–1 Shido, Sanuki, Kagawa 769–2193, Japan.

Received July 12, 2018; accepted August 24, 2018

From the leaves of *Diospyros maritima*, collected from Okinawa Island, eight new glycosides based on *ent*-kaurane-type diterpenoids, entitled diosmariosides A–H, were isolated. The absolute structure of diosmarioside E (5) was determined by X-ray crystallographic analysis. The structure of diosmarioside H was elucidated to be a dimeric compound between diosmarioside A and a sugeroside through a ketal bond. An assay of cytotoxicity towards the lung adenocarcinoma (A549) cell line was performed. Among the compounds isolated, only diosmarioside D (4) and sugeroside 9 showed strong activity. The anti-microbial activity toward multi-drug resistant strains was also determined, but no activity was observed.

Key words *Diospyros maritima*; Ebenaceae; *ent*-kaurane; *ent*-kaurane glycoside; dimeric *ent*-kaurane glycoside

Diospyros maritima BLUME (Ebenaceae) is an evergreen tall tree with a height of ca. 10 m, distributed in Okinawa, Taiwan, Malaysia, Micronesia and Australia.¹⁾ In summer, it bears green sap fruits of 2 to 3 cm in diameter, which then turn to a dark orange color in autumn. It is known that the fruits contain a toxic naphthoquinone derivative, plumbagin, and their constituents were extensively investigated by Higa *et al.*^{2–4)} Recently, from the leaves and branches of a related Thai medicinal plant, *D. mollis*, the isolation of naphthoquinone glycosides was reported.⁵⁾ In our continuing work on Okinawan resource plants, the constituents of the leaves of *D. maritima* were investigated to give eight *ent*-kaurane diterpenoid glycosides, entitled diosmariosides A–H (1–8), along with a known *ent*-kaurane glucoside, sugeroside 9, isolated from *Ilex sugerokii* var. *brevipedunculata*⁶⁾ and *Rubus suaviusmus*,⁷⁾ and an *ent*-kaurane diterpenoid, (4*R*,16*R*)-16,17,19-trihydroxy-*ent*-kaur-3-one (10),⁸⁾ isolated from *Flickingeria fimbriata* (Fig. 1). The structure and stereochemistry of sugeroside 9, isolated from *R. suaviusmus*, was confirmed by X-ray crystallographic analysis.⁷⁾

Results and Discussion

Eight new compounds (1–8) and two known ones (9 and 10) were isolated from the MeOH extract of leaves of *D. maritima*, using various kinds of chromatographic techniques. The structures of the new compounds were elucidated by intensive one- and two-dimensional NMR spectroscopic analyses and chemical conversion. The absolute structure of diosmarioside E (5) was determined by X-ray crystallographic analysis. The structures of the known compounds were identified by the comparison of spectroscopic data with those reported in the literature.^{6,7)}

Diosmarioside A (1), $[\alpha]_D^{26}$ –63.8, was isolated as colorless

plates and its elemental composition was determined to be C₃₁H₅₀O₁₂ by the observation of a quasi-molecular ion peak [M+Na]⁺ using high-resolution (HR) electrospray ionization (ESI) MS. The IR spectrum exhibited strong absorption bands at 3460 and 3341, and 1693 cm⁻¹ ascribable to hydroxy groups and a carbonyl functional group, respectively. In the ¹H-NMR spectrum, signals for three singlet methyls, methylene protons on an isolated primary alcohol [δ_H 3.95 (1H, d, *J*=10.8 Hz, H-17b) and 4.47 (1H, d, *J*=10.8 Hz, H-17a)] and two anomeric protons (δ_H 4.99 and 5.80) were observed. Thus, 1 was expected to be a glycosidic compound and sugar analysis of its hydrolysate using a chiral detector revealed the presence of D-apiose and D-glucose. The ¹³C-NMR spectrum displayed 31 signals and eleven signals were expected to be the result of sugar moieties. The remaining 20 signals comprised of three methyls, nine methylenes, one of which carried an oxygen atom, three methines, and three quaternary, carbonyl and oxygenated tertiary carbons. These functionalities implied that diosmarioside A (1) was a diterpene with five degrees of unsaturation and the comparison of ¹³C-NMR data with those of sugeroside (9) indicated that 1 was an apiofuranosyl sugeroside (Table 1). The relative orientation of the C-17 primary carbinol group was expected to be the same as that of 9 from the phase sensitive (PS)-rotating frame nuclear Overhauser effect spectroscopy (ROESY) correlations between H₂-17 [δ_H 4.47 (d, *J*=10.8 Hz) and 3.95 (d, *J*=10.8 Hz)], and H-11a [δ_H 1.60 (m)]. The positions of the sugar linkage were determined by heteronuclear multiple-bond correlation spectroscopy (HMBC), in which the anomeric proton of D-apiofuranoside was correlated with the C-6 of glucopyranose and then that of glucopyranose with C-17 of the aglycone. The mode of linkage of D-glucopyranoside was determined to be β from the coupling constant of anomeric proton (*J*=7.6 Hz) and that

* To whom correspondence should be addressed. e-mail: otsuka-h@yasuda-u.ac.jp

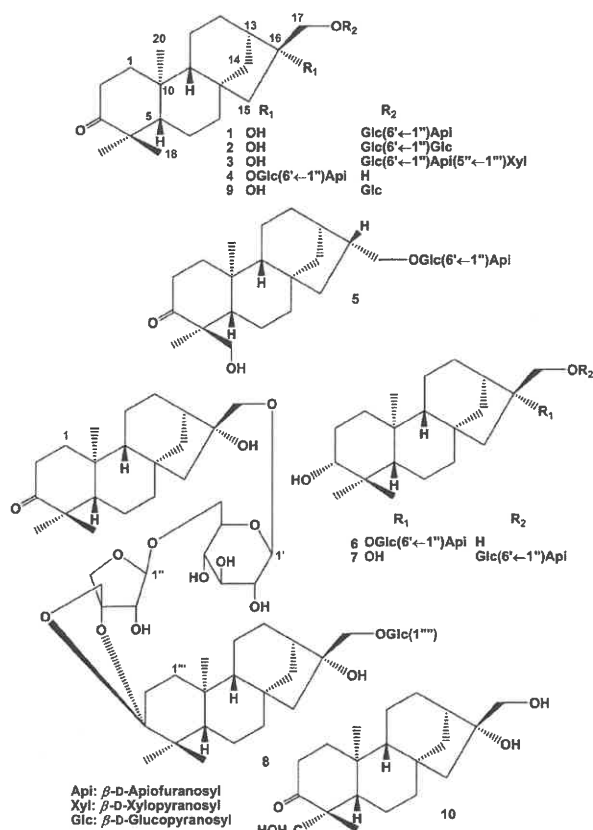


Fig. 1. New (1–8) and Known (9 and 10) Compounds Isolated

of β -D-apiofuranoside was also to be β by comparison of the ^{13}C -NMR data of authentic samples prepared in our laboratory [methyl β -D-apiofuranoside: δ_{C} 111.6 (C-1), 77.9 (C-2), 80.5 (C-3), 74.9 (C-4), 65.5 (C-5) and methyl α -D-apiofuranoside: δ_{C} 104.6 (C-1), 73.4 (C-2), 77.9 (C-3), 75.1 (C-4), 65.6 (C-5)]^{9,10} Diosmarioside A (**1**) was found to be in the *entio* series from the negative Cotton effect at 289 nm ($\Delta\epsilon$ -2.87) in the circular dichroism (CD) spectrum.^{11,12} Therefore, the structure of diosmarioside A (**1**) was elucidated, as shown in Fig. 1.

Diosmarioside B (**2**), $[\alpha]_{\text{D}}^{23} -65.4$, was isolated as an amorphous powder and its elemental composition was determined to be $\text{C}_{32}\text{H}_{52}\text{O}_{13}$. The physicochemical data for **2** were similar to those of **1**, and HPLC analysis of its hydrolysate showed only one peak for D-glucose, though NMR spectra indicated the presence of two anomeric signals [δ_{H} 4.97 (d, $J=7.8$ Hz) on δ_{C} 106.4 and δ_{H} 5.08 (d, $J=7.9$ Hz) on δ_{C} 105.4]. In the HMBC spectrum, one (δ_{H} 5.08) of the anomeric protons correlated with C-6' of the inner glucose unit and the other (δ_{H} 4.97) with C-17 of the aglycone. From a similar negative Cotton effect at 289 nm in the CD spectrum, **2** was also expected to be in the *ent*-series. Therefore, the structure of diosmarioside B (**2**) was elucidated to be 6'-*O*- β -D-glucopyranoside of the sугeroside, as shown in Fig. 1.

Diosmarioside C (**3**), $[\alpha]_{\text{D}}^{23} -92.6$, was isolated as an amorphous powder and its elemental composition was determined to be $\text{C}_{36}\text{H}_{58}\text{O}_{16}$. From the NMR spectroscopic data, diosmarioside C (**3**) was found to be an analogous compound to **1** and **2** with three sugar units. Sugar analysis of the hydrolysate of **3** revealed the presence of D-apiose, D-xylose and D-glucose. D-Xylose was expected to be the terminal sugar from typical five

^{13}C -NMR signals (δ_{C} 105.8, 74.7, 78.2, 71.1 and 67.2) and its anomeric proton (δ_{H} 4.82) was correlated with C-5'' (δ_{C} 72.8) of apiofuranoside in the HMBC spectrum. The anomeric proton of apiofuranoside was then correlated with C-6' (δ_{C} 69.0) of the inner glucose moiety. From a negative Cotton effect at 289 nm in the CD spectrum, **3** was also expected to be in the *ent*-series. Therefore, the structure of **3** was elucidated to be the 5''-*O*- β -D-xylopyranoside of diosmarioside A, as shown in Fig. 1.

Diosmarioside D (**4**), $[\alpha]_{\text{D}}^{25} -83.6$, was isolated as colorless needles and its elemental composition was determined to be $\text{C}_{31}\text{H}_{50}\text{O}_{12}$, which was the same as that of **1**. All the functionalities available from the NMR spectral data were also the same as those of **1** and sugar analysis showed the presence of D-apiose and D-glucose. However, the ^{13}C -NMR chemical shifts of oxymethylene (C-17) and oxygenated tertiary (C-16) carbons appeared at δ_{C} 63.0 and δ_{C} 90.2, respectively, which were shifted by -12.5 and $+9.6$ ppm, when compared with those of **1**. Thus, the sugar moiety must be attached to the hydroxy group at the C-16 position. HMBC correlation also supported this fact, with the anomeric proton of the glucose moiety showing a cross peak with C-16 carbon. The relative orientation of the C-17 primary carbinol group was expected to be the same as that of **9** from the PS-ROESY correlations between H-17a [4.12, (d, $J=13.0$ Hz)] and H-11a [(1.56, (m)]. From a negative Cotton effect at 290 nm in the CD spectrum, **4** was also expected to be in the *ent*-series. Therefore, the structure of **4** was elucidated, as shown in Fig. 1.

Diosmarioside E (**5**), $[\alpha]_{\text{D}}^{22} -96.0$, was isolated as colorless fine needles and its elemental composition was determined to be $\text{C}_{31}\text{H}_{50}\text{O}_{12}$, which was the same as that of **1**. Diosmarioside E (**5**) was also analogous to the aforementioned compounds, however, the oxygenated tertiary carbon disappeared, instead of which, an isolated primary alcohol [3.94 (1H, brd, $J=10.1$ Hz) and 3.64 (1H, brd, $J=10.1$ Hz)] was newly formed. Since these methylene protons showed a correlation cross peak with the carbonyl carbon, the newly formed oxymethylene was placed on either C-18 or C-19. The significant correlation signal between H₃-19 (δ_{H} 1.03) and H₃-20 (δ_{H} 0.91) in the ROESY enabled us to place the oxymethylene functional group at the 18-position (Fig. 2). Diosmarioside E (**5**) was found to be in the *entio* series from the negative Cotton effect at 294 nm ($\Delta\epsilon$ -0.71) in the CD spectrum^{11,12} and the geometry at the 16-position was explored by the PS-ROESY experiment. Significant ROESY correlations between H-17b (δ_{H} 3.47) and H-14b (δ_{H} 1.06), and H-16 (δ_{H} 2.18) and both of H-11a (δ_{H} 1.53) and H-12b (δ_{H} 1.32) suggested that the C-17 primary alcohol was in the α -face, namely, the absolute configuration of the 16-position to be *R* (Fig. 2). Enzymatic hydrolysis of **5** gave an aglycone (**5a**) and the correlations were found to be the same as those of glycosidic form, **5**. ^{13}C -NMR chemical shifts of C-16 and its neighboring carbons were reported for the 16*R* and 16*S* congeneric compounds in the literature.¹³ However, the data showed some discrepancy between those of **5a** and the 16*S* congener, as well as **5a** and the 16*R* one. Finally, the structure of **5a** was confirmed by the X-ray crystallographic analysis (Fig. 3) and the results obtained from the ROESY experiment were verified, namely, that C-16 had the 16*R* configuration. The Flack parameter [$\chi=-0.03(3)$] verified the absolute configuration of **5a**, as shown in Fig. 3, and the result from the CD experiment was also confirmed.

Table 1. ^{13}C -NMR Spectroscopic Data for Diosmariosides A–H (1–8), Sugeroside (9) and 5a (150 MHz, Pyridine- d_5)

C	1	9 ^{a)}	2	3	4	5	5a ^{b)}	6	7	8			
											Ca	Cb	
1	39.2	39.2	39.2	39.2	39.3	38.1	38.7	39.1	39.0	1	39.3	1'''	37.2
2	34.2	34.3	34.2	34.2	34.2	36.7	35.4	28.2	28.2	2	34.3	2'''	27.3
3	216.7	216.7	216.7	216.7	216.6	217.4	219.0	78.2	78.2	3	216.6	3'''	114.4
4	47.1	47.3	47.1	47.1	47.1	52.6	52.3	39.4	39.4	4	47.2	4'''	42.3
5	54.3	54.3	54.2	54.2	54.2	46.7	48.7	55.4	55.4	5	54.3	5'''	53.2
6	21.9	21.9	21.9	21.9	21.8	22.3	21.5	20.6	20.7	6	21.9	6'''	20.7
7	41.3	41.3	41.2	41.3	41.1	40.4	40.5	42.4	42.5	7	41.3	7'''	42.3
8	44.5	44.5	44.5	44.5	44.6	44.6	44.5	44.8	44.7	8	44.5	8'''	44.6
9	55.5	55.5	55.5	55.5	55.6	54.5	54.8	57.0	56.9	9	55.6	9'''	56.7
10	38.6	38.6	38.5	38.6	38.6	38.2	38.4	39.4	39.3	10	38.7	10'''	39.1
11	18.9	19.0	19.0	18.9	19.1	19.3	19.1	18.8	18.6	11	19.0	12'''	18.6
12	26.5	26.6	26.5	26.5	25.9	31.2	31.3	26.2	26.9	12	26.0	12'''	26.9
13	46.2	46.3	46.1	46.2	43.2	38.6	38.2	43.4	46.4	13	46.2	13'''	46.5
14	37.2	37.1	37.2	37.2	36.8	36.9	37.3	37.2	37.6	14	37.2	14'''	37.4
15	53.0	52.9	53.4	52.9	51.6	45.5	44.8	52.0	53.4	15	53.1	15'''	53.2
16	80.8	80.8	80.7	80.8	90.2	40.9	43.3	90.3	80.9	16	80.8	16'''	80.7
17	75.5	75.5	76.4	75.5	63.0	74.7	67.5	63.1	75.7	17	75.4	17'''	75.7
18	27.3	27.3	27.3	27.3	27.2	68.6	67.3	28.9	28.9	18	27.3	18'''	23.5
19	21.1	21.1	21.1	21.1	21.0	17.6	16.7	16.3	16.3	19	21.1	19'''	20.3
20	17.7	17.8	17.8	17.7	17.7	17.7	17.3	18.1	18.0	20	17.8	20'''	17.8
1'	106.3	106.6	106.4	106.3	98.4	104.9		98.5	106.4	1'	106.1	1'''	106.7
2'	75.4	75.5	75.2	75.4	75.3	75.1		75.3	75.4	2'	75.4	2'''	75.5
3'	78.6	78.8	78.5	78.6	78.9	78.6		78.9	78.6	3'	78.6	3'''	78.7
4'	71.9	71.7	71.7	71.7	72.1	71.9		72.1	71.9	4'	71.6	4'''	71.7
5'	77.3	78.7	77.2	77.3	77.1	77.2		77.1	77.3	5'	76.9	5'''	78.5
6'	69.0	62.9	70.2	69.0	69.1	69.0		69.2	68.9	6'	67.7	6'''	62.8
1''	111.2		105.4	110.9	111.1	111.2		111.2	111.2	1''	109.5		
2''	77.8		75.4	78.3	77.9	77.8		77.9	77.8	2''	79.0		
3''	80.5		78.3	79.3	80.5	80.5		80.5	80.5	3''	86.4		
4''	75.1		71.6	74.9	75.1	75.1		75.2	75.1	4''	74.5		
5''	65.7		78.5	72.8	65.8	65.6		65.9	65.7	5''	73.9		
6''			62.7										
1'''				105.8									
2'''				74.7									
3'''				78.2									
4'''				71.1									
5'''				67.2									

a) Data were taken from ref. 6 (100 MHz, pyridine- d_5). b) Data for CDCl_3 .

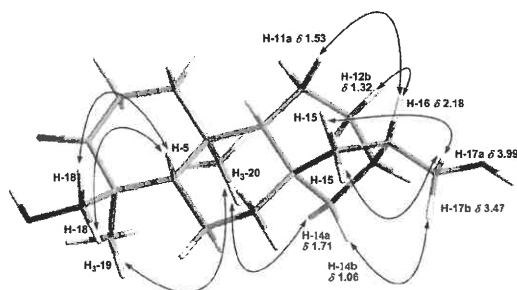


Fig. 2. ROESY Correlations of Diosmarioside E (5) Sugar Portion Was Omitted for Clearness

Diosmarioside F (6), $[\alpha]_D^{23} -57.8$, was isolated as colorless needles and its elemental composition was determined to be $\text{C}_{31}\text{H}_{52}\text{O}_{12}$. The ketone absorption band in the IR spectrum observed for compounds 1–5 disappeared, and oxygenated methine proton $[\delta_H 3.42$ (1H, dd, $J=10.7, 5.3$ Hz)] and carbon

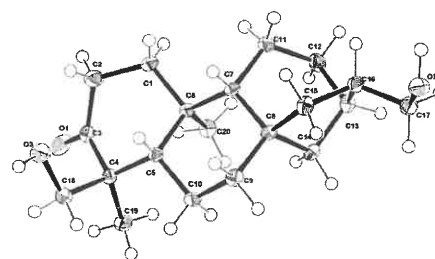


Fig. 3. An ORTEP Drawing of the Crystal Structure of the Aglycone of Diosmarioside E (5a)

($\delta_C 78.2$) signals were found in the NMR spectra. Since the HMBC correlations are between the *gem*-dimethyl protons ($\delta_H 0.96$ and 1.16) and the oxygenated methine carbon, this carbon must be at the 3-position. The ^{13}C -NMR data of the B, C and D rings were essentially the same as those of diosmarioside E (4) (Table 1). Therefore, to confirm the structure of 6, includ-

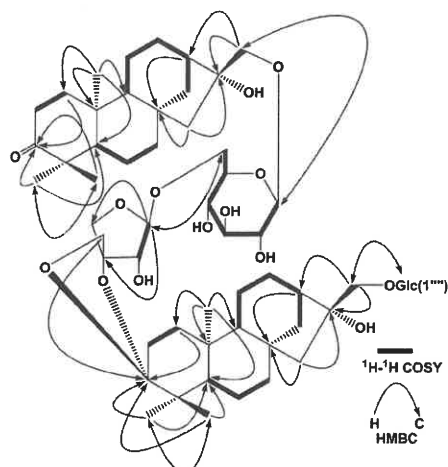


Fig. 4. ^1H - ^1H COSY and HMBC Correlations of Diosmarioside H (**8**)

Dual arrow curves denote that HMBC correlations were observed in both directions.

ing the absolute stereochemistry, diosmarioside E (**4**) was reduced with NaBH_4 . Hydride must be introduced from the less hindered *si*-face of the carbonyl carbon to give a sole product, **4a**, which was spectroscopically identical as diosmarioside F (**6**).

Diosmarioside G (**7**), $[\alpha]_D^{24} -42.2$, was isolated as an amorphous powder and its elemental composition was determined to be $\text{C}_{31}\text{H}_{52}\text{O}_{12}$. *D*-Apiose and *D*-glucose were analyzed to be present in the hydrolysate of **7** and their connectivity was confirmed from the data of HMBC spectrum. The ^{13}C -NMR chemical shifts of C-16 and C-17 suggested that the sugar moiety was attached at the hydroxy group of C-17. The secondary alcohol was at the C-3 position and then diosmarioside A (**1**) was reduced with NaBH_4 to give **1a** (=7) as a sole product. Therefore, the structure of **7** was elucidated, as shown in Fig. 1.

Diosmarioside H (**8**), $[\alpha]_D^{24} -49.4$, was isolated as an amorphous powder and its elemental composition was determined to be $\text{C}_{57}\text{H}_{90}\text{O}_{19}$. The IR spectrum exhibited a carbonyl absorption peak (1703 cm^{-1}) along with strong bands for hydroxy groups (3444 cm^{-1}). Three anomeric signals [δ_{H} 5.00 (d, $J=7.9\text{ Hz}$) on δ_{C} 106.1, δ_{H} 5.04 (d, $J=7.8\text{ Hz}$) on δ_{C} 106.7 and δ_{H} 5.61 (brs) on δ_{C} 109.5] were observed in the NMR spectra, while only two sugars, *D*-apiose and *D*-glucose, were detected in its hydrolysate. In the HMBC spectrum, one of the anomeric proton (δ_{H} 5.00) of *D*-glucopyranoside was correlated with one of the primary alcohol carbon, another anomeric proton (δ_{H} 5.04) of *D*-glucopyranoside with the other primary alcohol carbon and the anomeric proton (δ_{H} 5.61) of *D*-apiofuranoside with the 6'-position of *D*-glucopyranoside (Fig. 4). The remaining 40 carbon signals appeared as 19 sets of close peaks, except for carbonyl (δ_{C} 216.6) and ketal (δ_{C} 114.4) carbons. HMBC correlation of the methylene protons (δ_{H} 4.38 and 4.45) of the 5"-position of *D*-apiofuranoside with the ketal carbon suggested that diosmarioside H (**8**) was a dimeric compound of two kaurane units with 13 degrees of unsaturation. Upon inspection of the ^1H - ^1H correlation spectroscopy (COSY) and HMBC spectra (Fig. 4), the bond connectivity was trailed from C-5" of the *D*-apiofuranoside to establish that one of the kaurane units possessed diosmari-

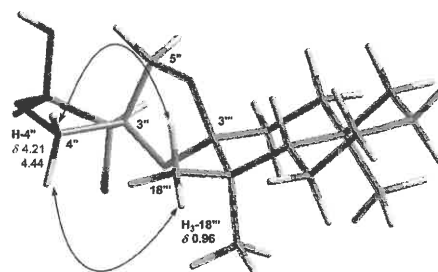


Fig. 5. ROESY Correlations of Diosmarioside H (**8**)

Table 2. Cytotoxicity toward A549 Cells (IC_{50} : μM)

1	>100
2	>100
3	>100
4	5.11 ± 0.23
5	>100
6	>100
7	>100
8	>100
9	2.39 ± 0.27
10	>100
Etoposide	36.5 ± 7.84

Etoposide: Positive control. Each value represents the mean \pm standard deviation (S.D.) with triplicate experiments.

oside A (**1**)-like (unit A) scaffold and that was followed from C-1" of the other *D*-glucopyranoside to the ketal carbon to conclude that the ketal derivative of sugeroside (**9**) (unit B) comprised of the rest of the structure (Fig. 1). Thus, the ketone of sugeroside (**9**) must form a cyclic ketal with hydroxy groups at C-3" and C-5" of *D*-apiofuranoside of the unit A. The ^{13}C -NMR chemical shifts of C-3" and C-5" in the unit A were apparently shifted downfield [C-3": δ_{C} 80.5 (**1**) \rightarrow δ_{C} 86.4 (**8**) and C-5": δ_{C} 65.7 (**1**) \rightarrow 73.9 (**8**)], when compared with those of **1**, proving that these groups were involved in the cyclic ketal formation. The negative Cotton effect ($\Delta\epsilon$: -0.73) at 289 nm in the CD spectrum confirmed that the unit A possessed an *ent*-series kaurane skeleton^{11,12} and the stereochemistry of the ketal region was substantiated using the PS-nuclear Overhauser effect spectrum. Significant cross peaks of H_3 -18" (δ_{H} 0.96) with H_2 -4" (δ_{H} 4.21 and 4.44) were able to assign the absolute configuration at the C-3" position to be *R* (Fig. 5), as well as. Since ^{13}C -NMR chemical shifts of C-13", C-14", C-15", C-16" and C-17" were indistinguishable from those of sugeroside (**9**) (Table 1), the unit B was also expected to have an *ent*-type framework. The structure of diosmarioside H (**8**) was elucidated to be a dimeric compound between diosmarioside A (**1**) and sugeroside (**9**).

A considerable amount of diosmarioside A (**1**) and sugeroside **9** were isolated as the mother compounds of **8** from the title plant. Although these compounds were treated with *d*-camphor sulfonic or *p*-toluene sulfonic acids in dehydrated dioxane, no reaction was observed.

Assay of cytotoxicity of compounds isolated toward adenocarcinomic human alveolar basal epithelial cell line, A549 was performed. Among them, only diosmarioside D (**4**) and sugeroside (**9**) showed strong activity at IC_{50} of $5.11\ \mu\text{M} \pm 0.23$ and $2.38\ \mu\text{M} \pm 0.26$, respectively (Table 2). At least, a ketonic functional group was required at the 3-position for the expres-

sion of activity, however, further structure–activity relationships are currently uncertain.

The anti-microbial activity toward the following strains, *Acinetobacter baumannii* NBRC 110492 (opportunisticly infectious), *Enterococcus faecalis* NBRC 100481 (opportunisticly infectious), *Klebsiella pneumoniae* NBRC 14441 (opportunisticly infectious), *Pseudomonas aeruginosa* MDRP610 (multi-drug resistant and opportunisticly infectious), *Serratia marcescens* NBRC 110513 (opportunisticly infectious), *Staphylococcus aureus* MS-29772 (methicillin resistant) and *Acinetobacter* sp. 160 (drug-resistant) was assayed. However, none of the compounds isolated were found to be active, suggesting that the cytotoxicity of compounds **4** and **9** might be specific to mammalian cells. In future work, we will comprehensively investigate the biological properties of these compounds, including the mode of action to the A549 tumor cells.

Experimental

General Experimental Procedures Melting points were measured on a Yanagimoto micro melting point apparatus and are uncorrected. Optical rotations were measured on a JASCO P-2200 digital polarimeter. IR spectra were measured on JASCO FT/IR-6100 spectrophotometers. ¹H- and ¹³C-NMR spectra were taken on a Bruker Avance III at 600 MHz and 150 MHz, respectively, with tetramethylsilane as an internal standard. CD spectra were obtained with a JASCO J-720 spectropolarimeter. Positive-ion HR-ESI-MS were measured with a Thermo Fisher Scientific LTQ Orbitrap XL. Silica gel column chromatography (CC) was performed on silica gel 60 (70–230 mesh) (E. Merck, Darmstadt, Germany) and reversed-phase octadecylsilanized (ODS) open CC on Cosmosil 75C₁₈-OPN (Nacalai Tesque, Kyoto, Japan) ($\phi=50$ mm, $L=25$ cm). HPLC was performed on an ODS column (Inertsil ODS-3; GL Science, Tokyo, Japan; $\phi=6$ mm, $L=25$ cm, 1.6 mL/min, Cosmosil Cholester; Nacalai Tesque; $\phi=6$ mm, $L=25$ cm, 1.6 mL/min, Cosmosil π NAP; Nacalai Tesque; $\phi=10$ mm, $L=25$ cm, 4.0 mL/min), and the eluate was monitored with photo diode array (200–400 nm) and refractive index monitors. β -Glucosidase was a generous gift from Shin Nihon Chemical Co., Ltd. (Anjo, Aichi, Japan).

Plant Material Leaves of *D. maritima* were collected in Taketomi-cho, Yaeyama-gun, Okinawa, Japan, in November, 2003 and a voucher specimen was deposited in the Herbarium of Pharmaceutical Sciences, Graduate School of Biomedical and Health Sciences, Hiroshima University (03-DM-Okina-1105).

Extraction and Isolation Air-dried leaves of *D. maritima* (7.80 kg) were extracted with methanol (MeOH) (45 L) three times. The MeOH extract was concentrated to 6 L and then washed with *n*-hexane (6 L, 245 g). The methanolic layer was concentrated to a viscous gum. The gummy mass was suspended in H₂O (6 L), and then partitioned with ethyl acetate (EtOAc) (6 L) and 1-BuOH (6 L), successively, to give 397 g and 216 g of EtOAc and 1-butanol (BuOH)-soluble fractions, respectively. The remaining water-layer was concentrated to give a H₂O-soluble-fraction (245 g). The 1-BuOH-soluble fraction was subjected to a Diaion HP-20 CC ($\phi=80$ mm, $L=50$ cm), and eluted with H₂O–MeOH (4:1, 5 L), (3:2, 5 L), (2:3, 5 L), and (1:4, 5 L), and MeOH (5 L), 1 L-fractions being collected. The residue (29.2 g) in fractions 11–14 of

Diaion HP-20 CC was subjected to silica gel CC ($\phi=50$ mm, $L=54.5$ cm), and eluted with CHCl₃ (3 L), CHCl₃–MeOH (99:1, 3 L), (49:1, 3 L), (97:3, 3 L), (19:1, 3 L), (37:3, 3 L), (9:1, 3 L), (7:1, 3 L), (17:3, 3 L), (33:7, 3 L), (4:1, 3 L), (3:1, 3 L), and (7:3, 3 L), 500 mL-fractions being collected. The residue (3.00 g out of 9.08 g) in fractions 50–56 was separated by ODS CC ($\phi=50$ mm, $L=25$ cm), and eluted with a linear solvent system from MeOH–H₂O (1:9, 2 L) to MeOH–H₂O (9:1, 2 L) linear gradient, 10 g-fractions being collected. Ninety three point two milligram of **7** was afforded as crystals in fraction 220–241.

The residue (64.5 g) in fractions 15–19 of Diaion HP-20 CC was subjected to silica gel CC ($\phi=80$ mm, $L=40$ cm), and eluted with CHCl₃ (6 L), CHCl₃–MeOH (99:1, 6 L), (49:1, 6 L), (97:3, 6 L), (19:1, 6 L), (37:3, 6 L), (9:1, 6 L), (7:1, 6 L), (17:3, 6 L), (33:7, 6 L), (4:1, 6 L), (3:1, 6 L), and (7:3, 6 L), 1 L-fractions being collected. Compounds **10** (56.4 mg), **9** (114 mg) and **4** (344 mg) were obtained as crystals in fractions 28, 42 and 44, respectively.

The residue (3.00 g out of 12.3 g) in fractions 53–62 was separated by ODS CC ($\phi=50$ mm, $L=25$ cm), and eluted with MeOH–H₂O (1:9, 2 L) to MeOH–H₂O (9:1, 2 L) linear gradient, 10 g-fractions being collected. The residue (524 mg) in fractions 216–226 was purified by HPLC (ODS-3, H₂O–MeOH, 2:3) and then the residue (111.0 mg) from the peak at 9.0 min was further purified by HPLC (Cholester, H₂O–MeOH, 11:9) to give 22.1 mg of **5** from the peak at 26.5 min. The residue (104 mg) from the peak at 10.2 min was further purified by HPLC (Cholester, H₂O–MeOH, 11:9) to give 37.9 mg of **2** and 12.4 mg of **3** from the peaks at 25.7 min and 33.2 min, respectively. ODS CC also afforded 9.7 mg of **6** and 449 mg of **1** as crystals in fractions 199–200 and 227–242, respectively. The residue (13.6 mg) in fractions 311–315 was purified by HPLC (ODS-3, H₂O–MeOH, 3:7) and then the residue (8.0 mg) from the peak at 31.0 min was further purified by HPLC (π NAP, H₂O–MeOH, 1:3) to give 5.4 mg of **8** from the peak at 35.4 min.

Diosmarioside A (**1**) Colorless plates, mp 203–204°C, $[\alpha]_D^{26} -63.8$ ($c=0.60$, MeOH); IR ν_{\max} (KBr) cm^{-1} : 3460, 3341, 2940, 2867, 1693, 1452, 1174, 1082; ¹H-NMR (pyridine-*d*₅, 600 MHz) δ : 5.80 (1H, d, $J=2.1$ Hz, H-1''), 4.99 (1H, $J=7.6$ Hz, H-1'), 4.78 (1H, $J=2.1$ Hz, H-2''), 4.77 (1H, brd, $J=11.3$ Hz, H-6'a), 4.61 (1H, d, $J=9.4$ Hz, H-4'a), 4.47 (1H, d, $J=10.8$ Hz, H-17a), 4.37 (1H, d, $J=9.4$ Hz, H-4'b), 4.21 (2H, m, H-3' and 6'b), 4.19 (2H, m, H₂-5''), 4.13 (1H, m, H-5'), 4.08 (1H, m, H-2'), 4.05 (1H, m, H-4'), 3.95 (1H, d, $J=10.8$ Hz, H-17b), 2.47 (2H, dd, $J=8.3$, 6.4 Hz, H₂-2), 2.42 (1H, brs, H-13), 1.94 (1H, brd, $J=11.7$ Hz, H-14a), 1.91 (1H, m, H-12a), 1.81 (1H, m, H-1a), 1.80 (1H, brd, $J=11.7$ Hz, H-14b), 1.76 (1H, d, $J=14.2$ Hz, H-15a), 1.61 (1H, m, H-7a), 1.61 (1H, d, $J=14.2$ Hz, H-15b), 1.60 (1H, m, H-11a), 1.44 (2H, m, H-11b and 12b), 1.40 (1H, m, H-7b), 1.30 (3H, m, H-5 and H₂-6), 1.24 (1H, ddd, $J=13.1$, 8.6, 8.6 Hz, H-1b), 1.08 (3H, s, H₃-18), 1.01 (3H, s, H₃-19), 0.96 (1H, brd, $J=8.4$ Hz, H-9), 0.92 (3H, s, H₃-20); ¹³C-NMR (pyridine-*d*₅, 150 MHz): Table 1; CD $\Delta\epsilon$ (nm): -2.87 (289) ($c=9.77 \times 10^{-5}$ M, MeOH); HR-ESI-MS (positive-ion mode) m/z : 637.3198 [M+Na]⁺ (Calcd C₃₁H₅₀O₁₂Na: 637.3194).

Diosmarioside B (**2**) Colorless amorphous powder, $[\alpha]_D^{23} -65.4$ ($c=0.50$, MeOH); IR ν_{\max} (film) cm^{-1} : 3368, 2933, 2869, 1702, 1456, 1162, 1045; ¹H-NMR (pyridine-*d*₅, 600 MHz) δ : 5.08 (1H, d, $J=7.9$ Hz, H-1''), 4.97 (1H, d, $J=7.8$ Hz, H-1'),

4.94 (1H, dd, $J=11.0, 1.6$ Hz, H-6'a), 4.78 (1H, dd, $J=8.6, 7.9$ Hz, H-2''), 4.54 (1H, dd, $J=11.6, 1.6$ Hz, H-6'a), 4.41 (1H, d, $J=11.0$ Hz, H-17a), 4.40 (1H, dd, $J=11.6, 5.1$ Hz, H-6''b), 4.27 (3H, m, H-6'b, 3'' and 4''), 4.22 (1H, dd, $J=8.8, 8.6$ Hz, H-3'), 4.15 (1H, m, H-5'), 4.12 (1H, dd, $J=9.5, 8.8$ Hz, H-4'), 4.08 (1H, dd, $J=8.6, 7.8$ Hz, H-2'), 4.05 (1H, d, $J=11.0$ Hz, H-17b), 3.95 (1H, m, H-5''), 2.48 (2H, dd, $J=8.6, 6.6$ Hz, H₂-2), 2.39 (1H, brs, H-13), 1.97 (1H, dd, $J=11.0, 3.6$ Hz, H-14a), 1.84 (1H, m, H-1a), 1.82 (1H, m, H-12a), 1.79 (1H, brd, $J=11.0$ Hz, H-14b), 1.78 (1H, d, $J=14.3$ Hz, H-15a), 1.71 (1H, d, $J=14.3$ Hz, H-15b), 1.64 (1H, m, H-7a), 1.61 (1H, m, H-11a), 1.45 (1H, m, H-12b), 1.44 (1H, m, H-11b), 1.38 (1H, m, H-7b), 1.30 (3H, m, H-5 and H₂-6), 1.26 (1H, ddd, $J=13.3, 8.6, 8.6$ Hz, H-1b), 1.08 (3H, s, H₃-18), 1.01 (3H, s, H₃-19), 0.96 (1H, brd, $J=8.6$ Hz, H-9), 0.92 (3H, s, H₃-20); ¹³C-NMR (pyridine-*d*₅, 150 MHz): Table 1; CD $\Delta\epsilon$ (nm): -1.01 (289) ($c=7.27\times 10^{-5}$ M, MeOH); HR-ESI-MS (positive-ion mode): m/z : 667.3305 [M+Na]⁺ (Calcd C₃₂H₅₂O₁₃Na: 667.3300).

Diosmarioside C (3) Colorless amorphous powder, $[\alpha]_D^{23}$ -92.6 ($c=0.31$, MeOH); IR ν_{\max} (film) cm⁻¹: 3369, 2932, 2869, 1698, 1457, 1159, 1049; ¹H-NMR (pyridine-*d*₅, 600 MHz) δ : 5.78 (1H, d, $J=2.8$ Hz, H-1''), 5.00 (1H, d, $J=7.9$ Hz, H-1'), 4.82 (1H, d, $J=7.6$ Hz, H-1'''), 4.80 (1H, d, $J=2.8$ Hz, H-2''), 4.75 (1H, dd, $J=11.2, 1.6$ Hz, H-6'a), 4.55 (1H, d, $J=9.5$ Hz, H-4''a), 4.49 (1H, d, $J=10.7$ Hz, H-17a), 4.45 (1H, d, $J=10.4$ Hz, H-5''a), 4.32 (1H, dd, $J=11.3, 5.2$ Hz, H-5''a), 4.31 (1H, d, $J=9.5$ Hz, H-4''b), 4.21 (1H, dd, $J=9.0, 8.9$ Hz, H-3'), 4.20 (1H, m, H-6'b), 4.19 (1H, m, H-4'''), 4.11 (1H, m, H-5'), 4.11 (1H, d, $J=10.4$ Hz, H-5''b), 4.11 (1H, dd, $J=8.6, 8.4$ Hz, H-3'''), 4.09 (1H, dd, $J=8.9, 7.9$ Hz, H-2'), 4.05 (1H, dd, $J=9.2, 9.0$ Hz, H-4'), 3.96 (1H, d, $J=10.7$ Hz, H-17b), 3.98 (1H, dd, $J=8.4, 7.6$ Hz, H-2'''), 3.65 (1H, dd, $J=11.3, 10.3$ Hz, H-5''b), 2.48 (2H, dd, $J=8.6, 6.2$ Hz, H₂-2), 2.43 (1H, brs, H-13), 1.94 (1H, dd, $J=11.3, 4.2$ Hz, H-14a), 1.90 (1H, m, H-12a), 1.82 (1H, ddd, $J=13.2, 13.0, 6.2$ Hz, H-1a), 1.80 (1H, brd, $J=11.3$ Hz, H-14b), 1.76 (1H, d, $J=14.2$ Hz, H-15a), 1.62 (1H, d, $J=14.2$ Hz, H-15b), 1.61 (2H, m, H-7a and 11a), 1.43 (2H, m, H-11b and 12b), 1.42 (1H, m, H-7b), 1.30 (3H, m, H-5 and H₂-6), 1.26 (1H, ddd, $J=13.2, 8.8, 8.6$ Hz, H-1b), 1.08 (3H, s, H₃-18), 1.01 (3H, s, H₃-19), 0.97 (1H, brd, $J=8.4$ Hz, H-9), 0.91 (3H, s, H₃-20); ¹³C-NMR (pyridine-*d*₅, 150 MHz): Table 1; CD $\Delta\epsilon$ (nm): -0.86 (289) ($c=5.16\times 10^{-5}$ M, MeOH); HR-ESI-MS (positive-ion mode): m/z : 769.3626 [M+Na]⁺ (Calcd C₃₆H₅₈O₁₆Na: 769.3617).

Diosmarioside D (4) Colorless needles, mp 238–239°C, $[\alpha]_D^{25}$ -83.6 ($c=0.25$, MeOH); IR ν_{\max} (KBr) cm⁻¹: 3341, 2936, 2876, 1704, 1458, 1360, 1160, 1056; ¹H-NMR (pyridine-*d*₅, 600 MHz) δ : 5.73 (1H, d, $J=1.9$ Hz, H-1''), 5.04 (1H, d, $J=7.8$ Hz, H-1'), 4.76 (1H, d, $J=1.9$ Hz, H-2''), 4.67 (1H, d, $J=9.1$ Hz, H-6'a), 4.61 (1H, d, $J=9.4$ Hz, H-4''a), 4.38 (1H, d, $J=9.4$ Hz, H-4''b), 4.24 (1H, dd, $J=8.9, 8.9$ Hz, H-3'), 4.22 (1H, d, $J=12.2$ Hz, H-5'a), 4.20 (1H, d, $J=12.2$ Hz, H-5'b), 4.12 (1H, d, $J=13.0$ Hz, H-17a), 4.08 (2H, m, H-5' and 6'b), 4.06 (1H, d, $J=13.0$ Hz, H-17b), 4.03 (1H, dd, $J=8.9, 7.8$ Hz, H-2'), 3.96 (1H, dd, $J=9.1, 8.9$ Hz, H-4'), 2.71 (1H, brs, H-13), 2.51 (2H, m, H₂-2), 2.15 (1H, brd, $J=11.3$ Hz, H-14a), 2.09 (1H, d, $J=14.4$ Hz, H-15a), 1.95 (1H, brd, $J=11.3$ Hz, H-14b), 1.81 (1H, ddd, $J=12.6, 6.4, 6.4$ Hz, H-1a), 1.72 (2H, m, H-7a and 12a), 1.70 (1H, d, $J=14.4$ Hz, H-15b), 1.56 (2H, m, H-11a and 12b), 1.42 (2H, m, H-7b and 11b), 1.30 (1H, m, H-5), 1.28 (2H, m, H₂-6), 1.25 (1H, m, H-1b), 1.06 (3H, s, H₃-18), 0.99 (1H, brd, $J=7.4$ Hz, H-9), 0.96 (3H, s, H₃-19), 0.96 (3H, s, H₃-20);

¹³C-NMR (pyridine-*d*₅, 150 MHz): Table 1; CD $\Delta\epsilon$ (nm): -2.14 (290) ($c=8.14\times 10^{-5}$ M, MeOH); HR-ESI-MS (positive-ion mode): m/z : 637.3198 [M+Na]⁺ (Calcd C₃₁H₅₀O₁₂Na: 637.3194).

Diosmarioside E (5) Colorless fine needles, mp 129–131°C, $[\alpha]_D^{22}$ -96.0 ($c=0.25$, MeOH); IR ν_{\max} (KBr) cm⁻¹: 3257, 2922, 2854, 1703, 1454, 1217, 1069; ¹H-NMR (pyridine-*d*₅, 600 MHz) δ : 5.84 (1H, d, $J=2.4$ Hz, H-1''), 4.83 (1H, d, $J=7.7$ Hz, H-1'), 4.80 (1H, m, H-2''), 4.80 (1H, brd, $J=11.3$ Hz, H-6'a), 4.62 (1H, d, $J=9.4$ Hz, H-4''a), 4.38 (1H, d, $J=9.4$ Hz, H-4''b), 4.25 (1H, dd, $J=9.1, 8.6$ Hz, H-3'), 4.25 (1H, dd, $J=11.3, 6.5$ Hz, H-6'b), 4.18 (2H, m, H₂-5''), 4.14 (1H, m, H-5'), 4.08 (1H, dd, $J=9.2, 9.1$ Hz, H-4'), 4.05 (1H, dd, $J=8.6, 7.7$ Hz, H-2'), 3.99 (1H, dd, $J=9.1, 7.0$ Hz, H-17a), 3.94 (1H, brd, $J=10.1$ Hz, H-18a), 3.64 (1H, brd, $J=10.1$ Hz, H-18b), 3.47 (1H, dd, $J=9.1, 8.9$ Hz, H-17b), 2.71 (1H, ddd, $J=17.2, 8.8, 3.7$ Hz, H-2a), 2.53 (1H, ddd, $J=17.2, 8.8, 8.6$ Hz, H-2b), 2.29 (1H, m, H-5), 2.28 (1H, m, H-13), 2.18 (1H, m, H-16), 1.84 (1H, ddd, $J=13.2, 8.6, 3.7$ Hz, H-1a), 1.71 (1H, brd, $J=11.6$ Hz, H-14a), 1.53 (1H, m, H-11a), 1.50 (1H, m, H-15a), 1.47 (1H, m, H-6a), 1.44 (1H, m, H-1b), 1.41 (1H, m, H-11b), 1.37 (3H, m, H₂-7 and 12a), 1.32 (1H, m, H-12b), 1.31 (1H, m, H-6b), 1.06 (1H, dd, $J=11.6, 3.8$ Hz, H-14b), 1.04 (1H, m, H-9), 1.03 (3H, s, H₃-19), 1.00 (1H, dd, $J=13.4, 5.2$ Hz, H-15b), 0.91 (3H, s, H₃-20); ¹³C-NMR (pyridine-*d*₅, 150 MHz): Table 1; CD $\Delta\epsilon$ (nm): -0.71 (294) ($c=3.26\times 10^{-5}$ M, MeOH); HR-ESI-MS (positive-ion mode): m/z : 637.3198 [M+Na]⁺ (Calcd C₃₁H₅₀O₁₂Na: 637.3194).

Diosmarioside F (6) Colorless needles, mp 272–273°C, $[\alpha]_D^{23}$ -57.8 ($c=0.32$, MeOH); IR ν_{\max} (KBr) cm⁻¹: 3412, 2930, 2869, 1169, 1047; ¹H-NMR (pyridine-*d*₅, 600 MHz) δ : 5.75 (1H, d, $J=2.1$ Hz, H-1''), 5.04 (1H, d, $J=7.9$ Hz, H-1'), 4.78 (1H, d, $J=2.1$ Hz, H-2''), 4.70 (1H, d, $J=8.6$ Hz, H-6'a), 4.62 (1H, d, $J=9.4$ Hz, H-4''a), 4.38 (1H, d, $J=9.4$ Hz, H-4''b), 4.23 (1H, d, $J=13.4$ Hz, H-5'a), 4.22 (1H, m, H-3'), 4.21 (1H, d, $J=13.4$ Hz, H-5'b), 4.15 (1H, d, $J=12.7$ Hz, H-17a), 4.10 (3H, m, H-17b, 5' and 6'b), 4.03 (1H, dd, $J=8.8, 7.9$ Hz, H-2'), 3.96 (1H, dd, $J=8.6, 8.3$ Hz, H-4'), 3.42 (1H, dd, $J=10.7, 5.3$ Hz, H-3), 2.74 (1H, brs, H-13), 2.16 (1H, brd, $J=11.2$ Hz, H-14a), 2.13 (1H, d, $J=14.8$ Hz, H-15a), 2.05 (1H, brd, $J=11.2$ Hz, H-14b), 1.87 (2H, m, H₂-2), 1.77 (1H, m, H-7a), 1.74 (3H, m, H-11a and H-15b), 1.65 (1H, m, H-12b), 1.54 (2H, m, H₂-11), 1.53 (1H, m, H-7b), 1.49 (1H, m, H-6a), 1.30 (1H, m, H-6b), 1.16 (3H, s, H₃-18), 1.01 (3H, s, H₃-20), 0.96 (1H, m, H-9), 0.96 (3H, s, H₃-19) 0.88 (1H, ddd, $J=12.7, 12.6, 4.3$ Hz, H-1b), 0.75 (1H, brd, $J=11.6$ Hz, H-5); ¹³C-NMR (pyridine-*d*₅, 150 MHz): Table 1; HR-ESI-MS (positive-ion mode): m/z : 639.3355 [M+Na]⁺ (Calcd C₃₁H₅₂O₁₂Na: 639.3351).

Diosmarioside G (7) Colorless amorphous powder, $[\alpha]_D^{24}$ -42.2 ($c=0.32$, MeOH); IR ν_{\max} (film) cm⁻¹: 3421, 2930, 2847, 1167, 1048; ¹H-NMR (pyridine-*d*₅, 600 MHz) δ : 5.80 (1H, d, $J=2.2$ Hz, H-1''), 4.99 (1H, d, $J=7.5$ Hz, H-1'), 4.79 (1H, d, $J=2.2$ Hz, H-2''), 4.70 (1H, d, $J=11.5$ Hz, H-6'a), 4.61 (1H, d, $J=9.3$ Hz, H-4''a), 4.48 (1H, d, $J=10.8$ Hz, H-17a), 4.37 (1H, d, $J=9.3$ Hz, H-4''b), 4.21 (2H, m, H-3' and 6'b), 4.20 (1H, d, $J=13.4$ Hz, H-5'a), 4.18 (1H, d, $J=13.4$ Hz, H-5'b), 4.13 (1H, m, H-5'), 4.08 (1H, dd, $J=8.2, 7.5$ Hz, H-2'), 4.04 (1H, dd, $J=9.3, 8.6$ Hz, H-4'), 3.95 (1H, d, $J=10.8$ Hz, H-17b), 3.42 (1H, dd, $J=11.1, 5.0$ Hz, H-3), 2.42 (1H, brs, H-13), 1.93 (1H, m, H-14a), 1.91 (2H, m, H-12a and 14b), 1.86 (2H, m, H₂-2), 1.78 (1H, d, $J=14.3$ Hz, H-15a), 1.74 (1H, brd, $J=13.3$ Hz, H-1a), 1.67 (1H, brd, $J=12.5$ Hz, H-7a), 1.64 (1H, d, $J=14.3$ Hz, H-15b), 1.56 (2H, m, H₂-11), 1.50 (2H, m, H-6a and 12b), 1.47

(1H, ddd, $J=12.5, 12.5, 3.4$ Hz, H-7b), 1.31 (1H, m, H-6b), 1.19 (3H, s, H₃-18), 1.00 (3H, s, H₃-19), 0.97 (3H, s, H₃-20), 0.92 (1H, brd, $J=7.5$ Hz, H-9), 0.86 (1H, ddd, $J=13.3, 12.7, 3.7$ Hz, H-1b), 0.75 (1H, brd, $J=11.5$ Hz, H-5); ¹³C-NMR (pyridine-*d*₅, 150 MHz): Table 1; HR-ESI-MS (positive-ion mode): m/z : 639.3355 [M+Na]⁺ (Calcd C₃₁H₅₂O₁₂Na: 639.3351).

Diosmarioside H (8) Colorless amorphous powder, $[\alpha]_D^{24}$ -49.4 ($c=0.36$, MeOH); IR ν_{\max} (KBr) cm⁻¹: 3444, 2932, 2869, 1703, 1456, 1054; ¹H-NMR (pyridine-*d*₅, 600 MHz) δ : 5.61 (1H, brs, H-1''), 5.04 (1H, d, $J=7.8$ Hz, H-1'''), 5.00 (1H, d, $J=7.9$ Hz, H-1'), 4.61 (1H, dd, $J=11.1, 1.7$ Hz, H-6'a), 4.59 (1H, dd, $J=11.7, 2.3$ Hz, H-6'''), 4.54 (1H, d, $J=10.3$ Hz, H-17a), 4.49 (1H, d, $J=10.7$ Hz, H-17'''), 4.45 (1H, d, $J=8.9$ Hz, H-5'a), 4.44 (1H, d, $J=8.6$ Hz, H-4'a), 4.43 (1H, dd, $J=11.7, 5.3$ Hz, H-6'''), 4.38 (1H, d, $J=8.9$ Hz, H-5'''), 4.33 (1H, brs, H-2''), 4.26 (1H, m, H-4'''), 4.25 (2H, m, H-3' and 3'''), 4.21 (1H, d, $J=8.6$ Hz, H-4'''), 4.16 (1H, dd, $J=11.1, 5.8$ Hz, H-6'b), 4.10 (2H, m, H-2' and 2'''), 4.09 (1H, m, H-4'), 4.05 (1H, m, H-5'), 4.00 (1H, d, $J=10.3$ Hz, H-17b), 4.00 (1H, m, H-5'''), 3.93 (1H, d, $J=10.7$ Hz, H-17'''), 2.52 (2H, dd, $J=8.6, 6.4$ Hz, H₂-2), 2.47 (1H, brs, H-13), 2.44 (1H, brs, H-13'''), 1.99 (1H, m, H-12a), 1.97 (1H, m, H-14a), 1.94 (1H, m, H-14'''), 1.89 (2H, m, H-1a and 14'''), 1.88 (1H, m, H-12'''), 1.86 (1H, m, H-14b), 1.84 (1H, m, H-2'''), 1.80 (1H, d, $J=14.3$ Hz, H-15a), 1.78 (1H, d, $J=14.3$ Hz, H-15'''), 1.77 (1H, m, H-2'''), 1.67 (1H, m, H-11a), 1.66 (2H, m, H-7a and 7'''), 1.66 (1H, d, $J=14.3$ Hz, H-15b), 1.61 (1H, d, $J=14.3$ Hz, H-15'''), 1.56 (1H, m, H-1'''), 1.53 (1H, m, H-12b), 1.52 (2H, m, H-11b and 11'''), 1.50 (2H, m, H-7''b and H-12''b), 1.47 (1H, m, H-11''b), 1.45 (1H, m, H-7b), 1.43 (1H, m, H-6''a), 1.35 (3H, m, H-5 and H₂-6), 1.33 (1H, m, H-5'''), 1.30 (1H, m, H-1b), 1.28 (1H, m, H-6''b), 1.16 (1H, ddd, $J=13.2, 13.2, 3.4$ Hz, H-1''b), 1.11 (3H, s, H₃-18), 1.03 (3H, s, H₃-19), 1.02 (1H, m, H-9), 1.00 (1H, m, H-9'''), 0.98 (3H, s, H₃-20''), 0.96 (3H, s, H₃-18'''), 0.95 (3H, s, H₃-19'''), 0.91 (3H, s, H₃-20); ¹³C-NMR (pyridine-*d*₅, 150 MHz): Table 1; CD $\Delta\epsilon$ (nm): -0.73 (289) ($c=1.86 \times 10^{-5}$ M, MeOH); HR-ESI-MS (positive-ion mode): m/z : 1101.5973 [M+Na]⁺ (Calcd C₅₇H₉₀O₁₉Na: 1101.5969).

Sugar Analysis About 500 μ g each of **1–8** was hydrolyzed with 1 M HCl (0.1 mL) at 90°C for 2 h. The reaction mixtures were partitioned with an equal amount of EtOAc (0.1 mL), and the water layers were analyzed by HPLC with a chiral detector (JASCO OR-4090) on an amino column [InertSustain NH₂, CH₃CN–H₂O (4:1), 1 mL/min]. A hydrolyzate of **2** gave a peak for D-glucose at 10.9 min, ones of **1, 4–8** gave peaks for D-apiose and D-glucose at 6.1 min and 10.9 min, respectively, and one of **3** gave peaks for D-apiose, D-xylose and D-glucose at 6.1, 7.3 and 10.9 min, respectively, with positive optical rotation signs. The peaks were identified by co-chromatography with authentic samples.

NaBH₄ Reduction of Diosmariosides D (4) and A (1) to Diosmariosides F (6) and G (7) To a solution of diosmarioside D (**4**) (20.3 mg) in 1.0 mL of MeOH was added 10.4 mg of CeCl₃·7H₂O and then 1.6 mg of NaBH₄, the reaction mixture being stirred for 5 min at 25°C. Excess NaBH₄ was quenched by the addition of 1 mL of (CH₃)₂CO and then the reaction mixture was evaporated to dryness. The residue was purified by preparative TLC (developed with CHCl₃–MeOH–H₂O, 15:6:1, and then eluted with CHCl₃–MeOH, 1:1) to afford 2.7 mg of **4a** (=6). Diosmarioside A (**1**) (20.0 mg) was similarly reduced to give 6.7 mg of **1a** (=7). **4a**: $[\alpha]_D^{22}$ -52.2

($c=0.27$, MeOH); NMR data were identical with those of **6**; HR-ESI-MS (positive-ion mode): m/z : 639.3351 [M+Na]⁺ (Calcd C₃₁H₅₂O₁₂Na: 639.3351). **1a**: $[\alpha]_D^{24}$ -37.3 ($c=0.34$, MeOH); NMR data were identical with those of **7**; HR-ESI-MS (positive-ion mode): m/z : 639.3352 [M+Na]⁺ (Calcd C₃₁H₅₂O₁₂Na: 639.3351).

Enzymatic Hydrolysis of Diosmarioside E (5) Diosmarioside E (**5**) (8.2 mg) was treated with β -glucosidase (4.0 mg) in 1 mL of H₂O at 37°C for 48 h. The reaction mixture was partitioned with 2 mL of EtOAc and the aglycone (**5a**) (2.0 mg) was recovered in the organic layer. Aglycone (**5a**): colorless crystals, mp 168–170°C, $[\alpha]_D^{26}$ -73.0 ($c=0.10$, CHCl₃); IR ν_{\max} (film) cm⁻¹: 3391, 2927, 2857, 1694, 1456, 1375, 1044; ¹H-NMR (CDCl₃, 600 MHz) δ : 3.94 (1H, d, $J=11.2$ Hz, H-18a), 3.42 (2H, m, H₂-17), 3.40 (1H, d, $J=11.2$ Hz, H-18b), 2.62 (1H, ddd, $J=16.6, 12.4, 7.2$ Hz, H-2a), 2.34 (1H, ddd, $J=16.6, 6.2, 2.9$ Hz, H-2b), 2.12 (1H, m, H-13), 2.10 (1H, ddd, $J=13.4, 7.2, 2.9$ Hz, H-1a), 1.97 (1H, dddd, $J=13.4, 7.9, 7.9, 7.9$ Hz, H-16), 1.87 (1H, brd, $J=11.7$ Hz, H-14a), 1.66 (1H, m, H-5), 1.64 (2H, m, H₂-11), 1.59 (2H, m, H-12a and 15a), 1.57 (1H, m, H-7a), 1.49 (1H, m, H-12b), 1.48 (1H, m, H-6a), 1.47 (1H, m, H-7b), 1.45 (1H, m, H-6b), 1.34 (1H, ddd, $J=13.4, 12.4, 6.2$ Hz, H-1b), 1.19 (3H, s, H₃-20), 1.14 (1H, brd, $J=7.6$ Hz, H-9), 0.96 (1H, brd, $J=11.7$ Hz, H-14b), 1.01 (3H, s, H₃-19), 0.95 (1H, dd, $J=13.5, 5.4$ Hz, H-15b); ¹³C-NMR (CDCl₃, 150 MHz): Table 1; CD $\Delta\epsilon$ (nm): -0.84 (290) ($c=3.16 \times 10^{-5}$ M, MeOH); HR-ESI-MS (positive-ion mode): m/z : 343.2245 [M+Na]⁺ (Calcd C₂₀H₃₂O₃Na: 343.2244).

X-Ray Crystallographic Analysis of 5a The colorless plate (0.200×0.150×0.010 mm³), obtained from methanol, was immersed in Paraton-N oil and placed in the N₂ cold stream at 100 K. The diffraction experiment was performed on a Bruker D8VENTURE system (PHOTON-100 CMOS detector, CuK α : $\lambda=1.54178$ Å). Absorption correction was performed by an empirical method implemented in SADABS.¹⁴ Structure solution and refinement were performed by using SHELXT-2014/5¹⁵ and SHELXL-2018/3.¹⁶

C₂₀H₃₂O₃, $M_r=320.45$; Orthorhombic, space group P2₁2₁2₁, $Z=4$, $D_{\text{calc}}=1.254$ g·cm⁻³, $a=7.2244(6)$, $b=11.0155(9)$, $c=21.3219(17)$ Å, $V=1696.8(2)$ Å³, 22546 observed and 3556 independent [$I>2\sigma(I)$] reflections, 335 parameters, final $R_1=0.0329$, $wR_2=0.0912$, $S=0.972$ [$I>2\sigma(I)$]. Flack parameter: $\chi=-0.03(3)$. All non-hydrogen atoms were refined anisotropically. The hydrogen atoms were refined isotropically on the calculated positions using a riding model except for hydroxy hydrogen. The largest difference peak and hole were 0.525 and -0.367 eÅ⁻³, respectively. Supplementary X-ray crystallographic data for **5a** (CCDC 1851583) can be obtained free of charge via www.ccdc.cam.ac.uk/conts/retrieving.html (or from the Cambridge Crystallographic Data Centre, 12 Union Road, Cambridge CB2 1EZ, UK; fax: (+44) 1223-336-033; or deposit@ccdc.cam.ac.uk).

Cytotoxic Activity toward Lung Adenocarcinoma, A549 Cells Cytotoxic activity toward lung adenocarcinoma cells was determined by colorimetric cell viability assay using 3-(4,5-dimethylthiazol-2-yl)-2,5-diphenyltetrazolium bromide (MTT). Lung adenocarcinoma cell line A549 was purchased from the JCRB Cell Bank, Japan. A549 cells were cultured in Dulbecco's modified Eagle's medium supplemented with 10% heat inactivated fetal calf serum, and kanamycin (100 μ g/mL) and amphotericin B (5.6 μ g/mL).

In a 96-well plate, 1 μ L aliquots of sample solutions and the cancer cells (5×10^3 cells/well) in 100 μ L medium were added to each well, and then the plate incubated at 37°C under a 5% CO₂ atmosphere for 72 h. A solution (100 μ L) of MTT (0.5 mg/mL) was then added to each well and the incubation was continued for a further 1 h. The absorbance of each well was measured at 540 nm using a Molecular Devices Versamax tunable microplate reader. Dimethyl sulfoxide (DMSO) was used as a negative control and etoposide as a positive control. The cytotoxic activity was calculated as:

$$\% \text{ inhibition} = [1 - (A_{\text{test}} - A_{\text{blank}}) / (A_{\text{control}} - A_{\text{blank}})] \times 100$$

where A_{control} is the absorbance of the control (DMSO) well, A_{test} the absorbance of the test wells, and A_{blank} the absorbance of the cell-free wells.

Anti-microbial Activity Anti-microbial activity toward bacteria was determined by the conventional paper disk (8 mm in diameter; ADVANTEC, Japan) diffusion method. Assay plates were prepared by pouring 25 mL of Müller–Hinton agar (Difco, U.S.A.) inoculated with a 250- μ L aliquot of an overnight broth culture of the test organisms into a culture dish. *Acinetobacter baumannii* NBRC 110492, *Enterococcus faecalis* NBRC 100481, *Klebsiella pneumoniae* NBRC 14441, *Serratia marcescens* NBRC 110513, *Pseudomonas aeruginosa* MDRP610, *Staphylococcus aureus* MS-29772, and *Acinetobacter* sp. 160 were used as test organisms. NBRC strains were obtained from the National Biological Resource Center, Japan. Other strains were provided by Laboratory of Bacterial Drug Resistance, Gunma University Graduate School of Medicine. Compounds 1–10 were dissolved in MeOH (1 mg/mL) and a paper disk containing each of the compounds (70 μ g) was placed on the assay plate seeded with each of the test organisms. Growth inhibition was examined after 24 h incubation at 37°C. Arbekacin, levofloxacin and piperacillin were used as positive controls.

Acknowledgments The measurements of HR-ESI-MS were performed with LTQ Orbitrap XL spectrometer at the Natural Science Center for Basic Research and Develop-

ment (N-BARD), Hiroshima University. We thank Dr. Koichi Tanimoto, Laboratory of Bacterial Drug Resistance, Gunma University Graduate School of Medicine, for providing clinical isolates (*P. aeruginosa* MDRP610, *S. aureus* MS-29772, and *Acinetobacter* sp. 160) to carry out this work. This work was supported in part by Grants-in-Aid from the Ministry of Education, Culture, Sports, Science and Technology of Japan, and the Japan Society for the Promotion of Science (Nos. 22590006, 23590130, 25860078, 15H04651 and 17K08336).


Conflict of Interest The authors declare no conflict of interest.

References

- 1) Hatushima S., "Flora of the Ryukyus. Added and Corrected," the Biological Society of Okinawa, Naha, Japan, 1975, p. 474.
- 2) Higa M., Ogihara K., Yogi S., *Chem. Pharm. Bull.*, **46**, 1189–1193 (1998).
- 3) Higa M., Noha N., Yokaryo H., Ogihara K., Yogi S., *Chem. Pharm. Bull.*, **50**, 590–593 (2002).
- 4) Higa M., Takashima Y., Yokaryo H., Harie Y., Suzuka T., Ogihara K., *Chem. Pharm. Bull.*, **65**, 739–745 (2017).
- 5) Suwama T., Watanabe K., Monthakantirat O., Luecha P., Noguchi H., Watanabe K., Umehara K., *J. Nat. Med.*, **72**, 220–229 (2018).
- 6) Hase T., Hagii H., Ishizu M., Ochi M., Ichikawa N., Kubota T., *Nippon Kagaku Kaishi*, 785–793 (1973).
- 7) Hirono S., Chou W.-H., Kasai R., Tanaka O., Tada T., *Chem. Pharm. Bull.*, **38**, 1743–1744 (1990).
- 8) Ding G., Fei J., Wang J., Xie Y., Li R., Gong N., Lv Y., Yu C., Zou Z., *Sci. Rep.*, **6**, 30560 (2016).
- 9) Kawakami S., Otsuka H., unpublished results.
- 10) Ishii T., Yanagisawa M., *Carbohydr. Res.*, **313**, 189–192 (1998).
- 11) Rüedi P., Wollenweber E., Marx D., Scheele C., *Z. Naturforsch.*, **44c**, 901–904 (1989).
- 12) Liu G., Müller R., Rüedi P., *Helv. Chim. Acta*, **86**, 420–438 (2003).
- 13) Borges-Argáez R., Medina-Balzábal L., May-Pat F., Peña-Rodoriges L. M., *Can. J. Chem.*, **75**, 801–804 (1997).
- 14) Sheldrick G. M., *SADABS*, University of Göttingen, Germany, (1996).
- 15) Sheldrick G. M., *Acta Crystallogr. A*, **71**, 3–8 (2015).
- 16) Sheldrick G. M., *Acta Crystallogr. C*, **71**, 3–8 (2015).

Article

Preliminary Quality Evaluation and Characterization of Phenolic Constituents in *Cynanchi Wilfordii Radix*

Takashi Uchikura ¹, Hiroaki Tanaka ¹, Hidemi Sugiwaki ¹, Morio Yoshimura ¹, Naoko Sato-Masumoto ² , Takashi Tsujimoto ², Nahoko Uchiyama ², Takashi Hakamatsuka ² and Yoshiaki Amakura ^{1,*}

¹ Department of Pharmacognosy, College of Pharmaceutical Sciences, Matsuyama University, 4-2 Bunkyo-cho, Matsuyama, Ehime 790-8578, Japan; 46150019@g.matsuyama-u.ac.jp (T.U.); 16130815@g.matsuyama-u.ac.jp (H.T.); h_sugiwa@g.matsuyama-u.ac.jp (H.S.); myoshimu@g.matsuyama-u.ac.jp (M.Y.)

² Division of Pharmacognosy, Phytochemistry and Narcotics, National Institute of Health Sciences, 3-25-26 Tonomachi, Kawasaki-ku, Kawasaki, Kanagawa 210-9501, Japan; nasato@nihs.go.jp (N.S.-M.); tsujimoto@nihs.go.jp (T.T.); nuchiyama@nihs.go.jp (N.U.); thakama@nihs.go.jp (T.H.)

* Correspondence: amakura@g.matsuyama-u.ac.jp; Tel.: +81-89-925-7111

Received: 5 February 2018; Accepted: 12 March 2018; Published: 14 March 2018

Abstract: A new phenolic compound, 2-*O*- β -laminaribiosyl-4-hydroxyacetophenone (**1**), was isolated from *Cynanchi Wilfordii Radix* (CWR, the root of *Cynanchum wilfordii* Hemsley), along with 10 known aromatic compounds, including cynandione A (**2**), bungeisides-C (**7**) and -D (**8**), *p*-hydroxyacetophenone (**9**), 2',5'-dihydroxyacetophenone (**10**), and 2',4'-dihydroxyacetophenone (**11**). The structure of the new compound (**1**) was elucidated using spectroscopic methods and chemical methods. The structure of cynandione A (**2**), including a linkage mode of the biphenyl parts that remained uncertain, was unambiguously confirmed using the 2D ¹³C–¹³C incredible natural abundance double quantum transfer experiment (INADEQUATE) spectrum. Additionally, health issues related to the use of *Cynanchi Auriculati Radix* (CAR, the root of *Cynanchum auriculatum* Royle ex Wight) instead of CWR have emerged. Therefore, constituents present in methanolic extracts of commercially available CWRs and CARs were examined using UV-sensitive high-performance liquid chromatography (HPLC), resulting in common detection of three major peaks ascribed to cynandione A (**2**), *p*-hydroxyacetophenone (**9**), and 2',4'-dihydroxyacetophenone (**11**). Thus, to distinguish between these ingredients, a thin-layer chromatography (TLC) method, combined with only UV irradiation detection, focusing on wilfosides C1N (**12**) and K1N (**13**) as marker compounds characteristic of CAR, was performed. Furthermore, we propose this method as a simple and convenient strategy for the preliminary distinction of CWR and CAR to ensure the quality and safety of their crude drugs.

Keywords: *Cynanchum wilfordii*; phenolic glycoside; 2-*O*- β -laminaribiosyl-4-hydroxyacetophenone; cynandione A; thin layer chromatography; *Cynanchum auriculatum*

1. Introduction

Cynanchi Wilfordii Radix (CWR), the dried root of *Cynanchum wilfordii* Hemsley (family Asclepiadaceae), is a crude drug listed in the Korean Herbal Pharmacopoeia [1]. CWR has been used in Korea as a substitute for *Polygoni Multiflori Radix*, the dried root of *Polygonum multiflorum* Thunberg (Polygonaceae), which is used for its restorative effects and is one of the important crude drugs listed in the Japanese, Korean, and Chinese Pharmacopoeias. Recently, the use of *Cynanchi Auriculati Radix* (CAR), the dried root of *Cynanchum auriculatum* Royke ex Wight, instead of CWR has led to health problems in Korea [2,3]. Although CAR resembles CWR closely in appearance,

CAR, a crude drug that differs from CWR in China, is currently treated as a toxic plant by the U.S. Food and Drug Administration (FDA) [4]. Therefore, standards and methods to distinguish CWR from CAR should be established to ensure the quality and safety of the crude drugs. We recently reported a survey on the original plant species of crude drugs widely distributed as CWR in the Korean and Chinese markets. This study revealed that CAR was incorrectly used in eight of the 13 products distributed as CWR, including possible confusion of CWR and CAR [5]. Previous phytochemical investigations of CWR identified the presence of pregnane glycosides, acetophenones, and humulanolides [6–11]. Although there are several reports on ingredient research using materials of CWA and CAR available on the market, they may not be of the precise species. Therefore, detailed phytochemical information on the raw material with defined origins is necessary to ensure the quality and safety of crude drugs.

Several studies have assessed the quality of CWR and CAR and have aimed to distinguish between them using high-performance liquid chromatography (HPLC) [12,13], and many methods used to identify crude drugs ensure reliability. However, in this study, the characterization of phenolic constituents in authentic original CWR plant species is identified using DNA sequences [5], and a simple and convenient thin-layer chromatography (TLC) method for the distinction of CWR and CAR to ensure the quality and safety of their crude drugs.

2. Results and Discussion

2.1. Isolation and Characterization

A homogenate of CWR in 80% methanol (MeOH) was concentrated and further extracted with *n*-hexane, ethyl acetate (EtOAc), and *n*-butanol (BuOH) to obtain the respective extracts and water (H₂O) extract. HPLC analysis was used to monitor the ultraviolet (UV)-sensitive compounds (phenols) in the EtOAc and *n*-BuOH extracts, which were separately chromatographed using a Diaion HP-20, YMC GEL ODS-AQ, and Chromatorex ODS with MeOH-H₂O in a stepwise gradient mode. The fractions showing similar HPLC or TLC patterns were combined and further purified using column chromatography to obtain compound **1**, cynandionene A (**2**) [14], uridine (**3**), guanosine (**4**), adenosine (**5**), tryptophan (**6**) [15], bungeiside-C (**7**), bungeiside-D (**8**), *p*-hydroxyacetophenone (**9**) [16], 2',5'-dihydroxyacetophenone (**10**) [13], and 2',4'-dihydroxyacetophenone (**11**) [16]. The known compounds **2–11** were identified by direct comparison with authentic specimens and by comparing their spectral data with those reported in the literature (Figure 1).

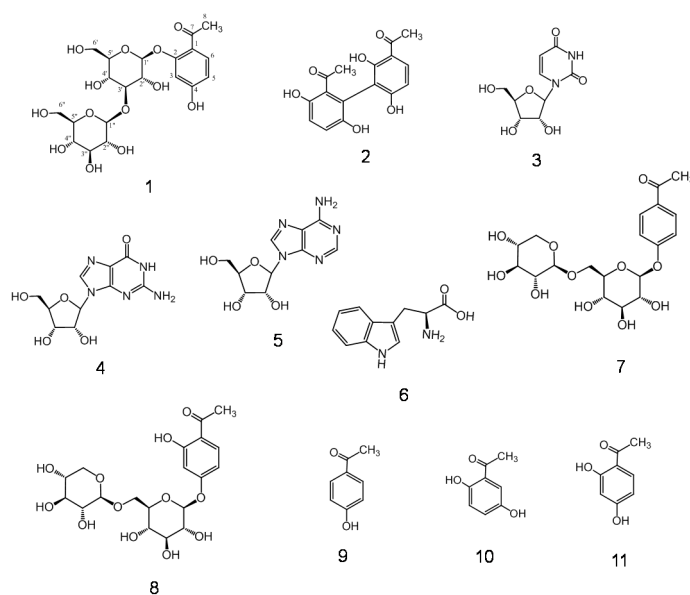


Figure 1. Structures of compounds 1–11.

Compound **1** was isolated as a light brown amorphous powder. Its molecular formula was assigned as $C_{20}H_{28}O_{13}$ based on its high resolution-electrospray ionization (HR-ESI)-mass spectrometry (MS, m/z 475.1473 $[M-H]^-$; calcd. for $C_{20}H_{28}O_{13}-H$: 475.1457) and ^{13}C -NMR (20 ^{13}C signals) spectra. The UV spectrum showed absorption maxima at 228, 269, and 301 nm. The proton (1H)- and ^{13}C -NMR spectra of compound **1** exhibited the following signal characteristics of the 2',4'-hydroxyacetophenone moiety. The 1H -NMR spectrum (Figure S1) assigned based on the 1H - 1H correlation spectroscopy (COSY) (Figure S2) exhibited signals due to an acetyl group (δ_H 2.62, 3H) and ABX-type proton signals due to a trisubstituted benzene proton, δ_H 6.69 (d, $J = 2.0$ Hz), 6.50 (dd, $J = 2.0, 8.5$ Hz), and 7.68 (d, $J = 8.5$ Hz), and two sets of sugar protons.

This acetophenone unit was also supported by eight carbon signals, δ_C 121.3, 160.9, 103.7, 164.9, 110.8, 133.3, 200.3, and 32.1 (C-1–8), in the ^{13}C -NMR spectrum (Figure S3) assigned based on heteronuclear single quantum coherence (HSQC) and heteronuclear multiple bond connectivity (HMBC) spectra (Figure 2, Figures S4 and S5). Additionally, an aglycone of compound **1** was chemically substantiated by acid hydrolysis followed by HPLC analysis, which showed the production of 2',4'-dihydroxyacetophenone. The presence of two sugar units in **1** was indicated by two anomeric proton signals at δ_H 5.05 (d, $J = 7.5$ Hz) and 4.58 (d, $J = 7.5$ Hz) and others assigned based on COSY, as shown in Table 1. Thus, the sugar residues were presumed to be hexoses, as revealed by 12 aliphatic carbon signals (δ_C 102.1, 110.8, 74.1, 75.5, 88.2, 77.9, 69.7, 71.6, 78.0, 78.2, 62.4, and 62.6) in the ^{13}C -NMR spectrum.

The sugar unit obtained following acid hydrolysis of compound **1** was identified as D-glucose by the HPLC analysis of derivatives prepared by the reaction with L-cysteine methyl ester and *o*-tolyl isothiocyanate according to the previously reported method [17]. The linking position of each unit was determined by correlations among the glucose H-1' (δ 5.05)/C-2 (δ 160.9) of the acetophenone moiety and glucose H-1'' (δ 4.95)/glucose C-3 (δ 88.2) in the HMBC spectrum. Moreover, the nuclear Overhauser effect spectroscopy (NOESY) results showed a correlation between the glucose H-1' (δ_H 5.05) and H-3 (δ_H 6.69) (Figure 2). β -Glycosidic linkages at each glucose core were assigned by a large coupling constant ($J = 7.5$ Hz). Therefore, compound **1** was established as 2-*O*- β -laminaribiosyl-4- hydroxyacetophenone.

Table 1. 1H - (500 MHz) and ^{13}C -NMR (126 MHz) data of compound **1** measured in MeOH- d_4 .

Positions	δ_C	δ_H (J in Hz)
1	121.3	
2	160.9	
3	103.7	6.69 (d, $J = 2.0$)
4	164.9	
5	110.8	6.50 (dd, $J = 2.0, 8.5$)
6	133.3	7.68 (d, $J = 8.5$)
7	200.3	
8	32.1	2.62 (3H, s)
Glucose-1'	102.1	5.05 (d, $J = 7.5$)
2'	74.1	3.74 (m) ^d
3'	88.2	3.67 (t, $J = 9.0$)
4'	69.7	3.54 (t, $J = 9.0$)
5'	78.0 ^a	3.52 (m) ^d
6'	62.4 ^b	3.94 (dd, $J = 1.5, 12.0$) ^c , 3.75 (m) ^{c,d}
Glucose-1''	105.3	4.58 (d, $J = 7.5$)
2''	75.5	3.30 (m) ^d
3''	77.9 ^a	3.39 (t, $J = 9.5$)
4''	71.6	3.30 (m) ^d
5''	78.2 ^a	3.35 (m) ^d
6''	62.6 ^b	3.89 (dd, $J = 2.0, 11.5$) ^c , 3.63 (m) ^{c,d}

^{a,b,c} Assignments may be interchanged. ^d Overlapped signals.

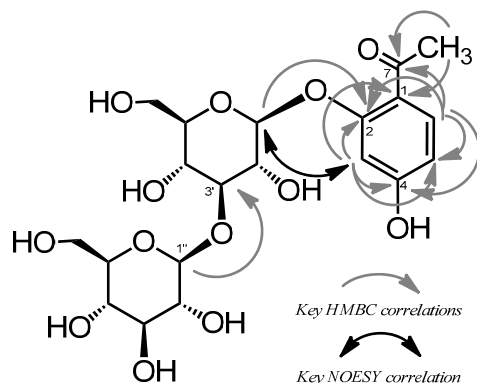


Figure 2. Key heteronuclear multiple bond connectivity (HMBC) correlations and nuclear Overhauser effect spectroscopy (NOESY) correlation of compound 1.

Cynandionene A (2) is a characteristic biacetophenone derivative with a biphenyl structure, which was revised from 4,3'-diacetyl-2,3,2',6'-tetrahydroxybiphenyl by 6,3'-diacetyl-2,5,2',6'-tetrahydroxybiphenyl after the structural elucidation [14]. It was difficult to confirm the present structure based only on the HMBC spectrum because a connection between C-1 and C-1' could not be confirmed. Therefore, in this study, we attempted to prove the connection of the biphenyl carbon-carbon bond using two-dimensional (2D) incredible natural abundance double quantum transfer experiment (INADEQUATE) for the first time. All C-C correlations were observed as shown in Figure 3. Compound 2 was shown to have C-C correlations between C-1 and C-1'. Therefore, the present biphenyl structure of compound 2 was supported by the 2D-INADEQUATE data. The positions of two acetyl groups were also confirmed using HMBC.

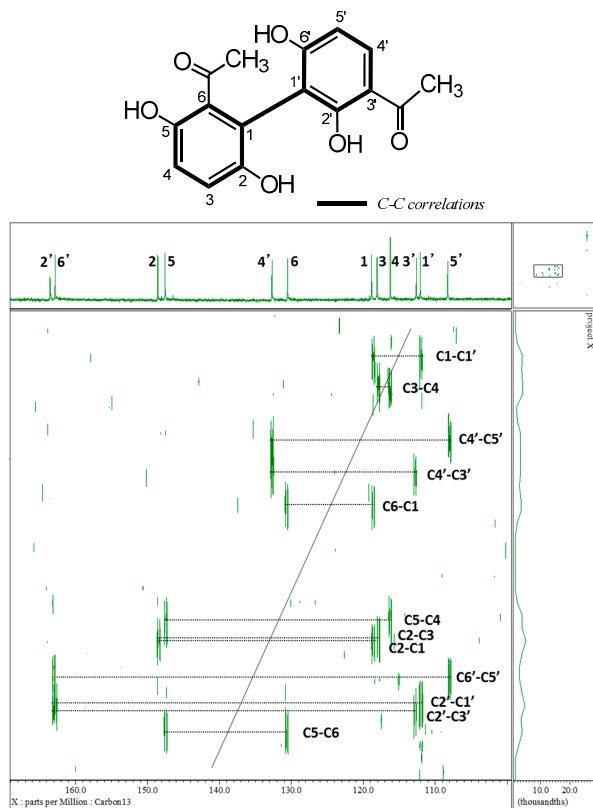


Figure 3. Two-dimensional incredible natural abundance double quantum transfer experiment (2D-INADEQUATE) spectrum of compound 2.

2.2. Preliminary Quality Evaluation of CWR and CAR Using TLC

CAR resembles CWR closely in appearance as shown in Figure 4. In this study, CWR and CAR (four and nine samples, respectively) identified using DNA sequences [5] were used as the test samples (Table 2 and Figure 4). HPLC chromatograms of MeOH extracts (CWR-Ex and CAR-Ex) obtained from these samples are shown in Figure 5.

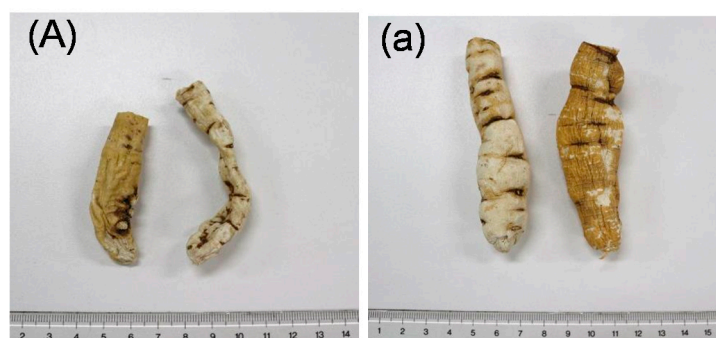


Figure 4. Crude drugs identified: (A) Cynanchi Wilfordii Radix (CWR, the root of *Cynanchum wilfordii* Hemsley) (Product C), and (a) Cynanchi Auriculati Radix (CAR, the root of *Cynanchum auriculatum* Royke ex Wight) (Product h).

Table 2. The Korean and Chinese market samples used in this study.

Products	Crude Drug	Locality	Market
A	Cynanchi Wilfordii Radix (CWR)	Korea	Korea
B	Cynanchi Wilfordii Radix (CWR)	Korea	Korea
C	Cynanchi Wilfordii Radix (CWR)	Yeongcheon	Korea
D	Cynanchi Wilfordii Radix (CWR)	Yeongcheon	Korea
a	Cynanchi Auriculati Radix (CAR)	Jiangsu	China
b	Cynanchi Auriculati Radix (CAR)	Jiangsu	China
c	Cynanchi Auriculati Radix (CAR)	Jiangsu	China
d	Cynanchi Auriculati Radix (CAR)	Jiangsu	China
e	Cynanchi Auriculati Radix (CAR)	Jiangsu	China
f	Cynanchi Auriculati Radix (CAR)	Jiangsu	China
g	Cynanchi Auriculati Radix (CAR)	Jiangsu	China
h	Cynanchi Auriculati Radix (CAR)	Korea	Korea
i	Cynanchi Auriculati Radix (CAR)	Korea	Korea

In all the HPLC analyses of CWR-Ex samples, three main peaks corresponding to cynandione A (**2**), *p*-hydroxyacetophenone (**9**), and 2',4'-dihydroxyacetophenone (**11**) were detected. In CAR-Ex, products **b–e** and **g–i**, but not **a** and **f**, were also mainly detected, suggesting that it would be difficult to distinguish these crude drugs by detecting these three compounds as reference compounds. On the other hand, CAR exhibited a peak corresponding to wilfosides K1N (**13**), which was not clearly detected in those of CWR. Because it was difficult to distinguish the species using HPLC analyses, a TLC method was developed. The TLC chromatogram of CAR-Ex with an EtOAc/water/MeOH/acetic acid (200:10:10:3, *v/v/v/v*) solvent mixture (A) as the mobile phase provided well-separated spots under UV light (254 nm) including a clear spot with approximately *R_f* 0.5 (Figure 6). This spot was revealed to be due to two compounds with almost the same *R_f*s. These two compounds were isolated by preparative TLC with the other solvent system, *n*-hexane-acetone (1:1), leading to clearly separated spots and were identified as wilfosides C1N (**12**) and K1N (**13**) [18].

Several previous studies have reported strategies for distinguishing CWR and CAR. For example, one method evaluated seven compounds in each sample, whereas another study used conduritol F as a marker compound, which is a characteristic constituent in CWR [12,13]. However, one method was complicated because it required the analysis of numerous constituents in samples using HPLC, and the other involved detection using a spray reagent using TLC. Additionally, the identification

of the type of samples is vague, although the appearances are similar. The method proposed in the present study is extremely simple because the sample was extracted with MeOH, followed only by a TLC method with UV irradiation detection. Thus, this method could be useful as a distinguishing tool among the preliminary TLC methods for comparison of CWR and CAR.

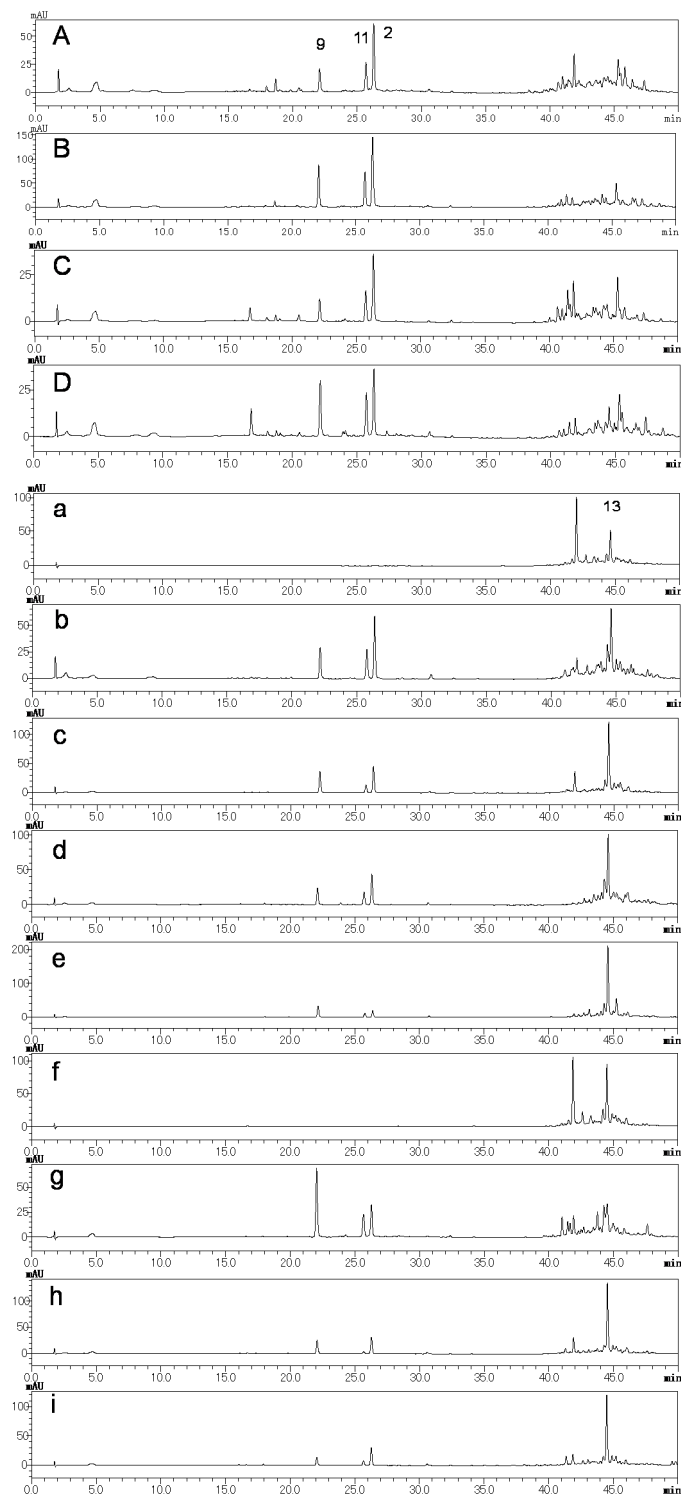


Figure 5. HPLC chromatograms of the crude drug extracts identified as *Cynanchi Wilfordii Radix* (CWR) (A–D) and *Cynanchi Auriculati Radix* (CAR) (a–i). The number on the chromatogram corresponds to the compound number. HPLC conditions are described in condition 1 of Section 3.

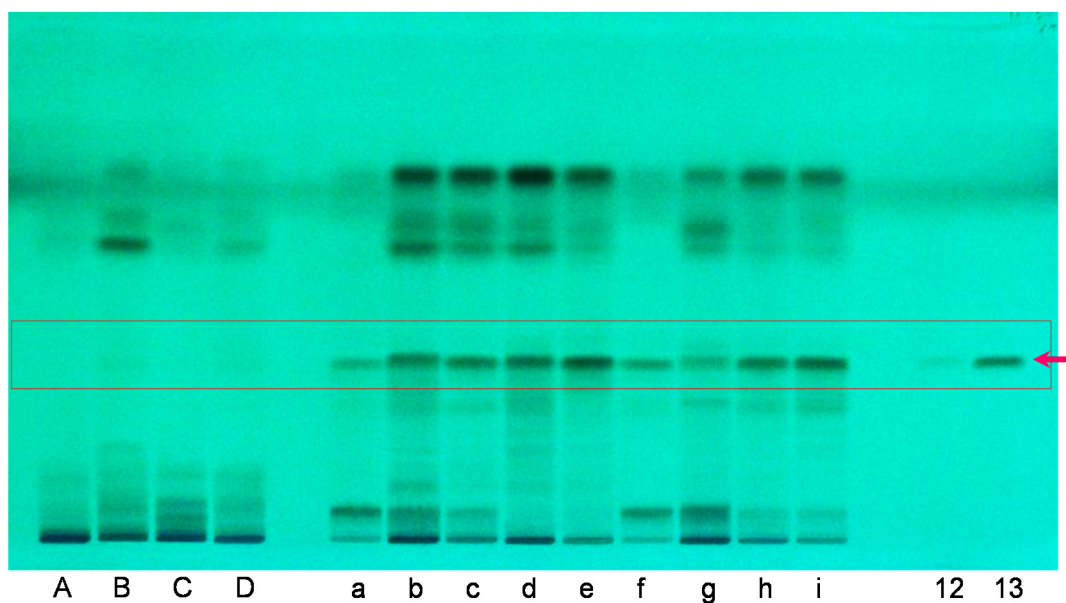
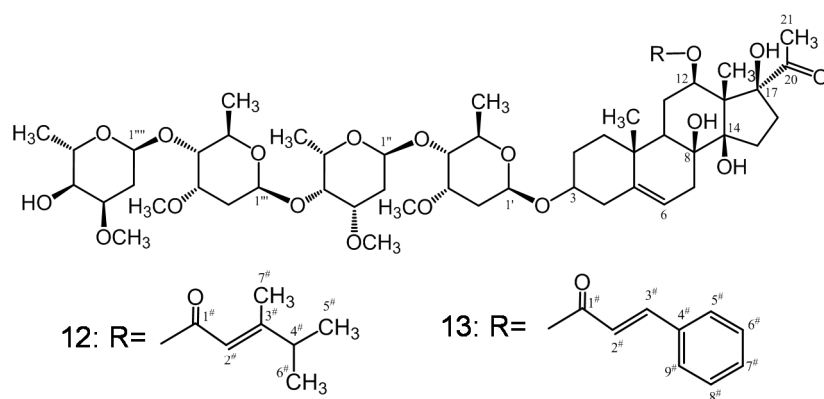


Figure 6. TLC chromatograms of the crude drugs *Cynanchi Wilfordii Radix* (CWR) (A–D) and *Cynanchi Auriculati Radix* (CAR) (a–i). TLC plate illuminated with UV 254 nm. 12: wilfoside C1N, 13: wilfoside K1N. Conditions are described in Section 3.

3. Experimental Section

3.1. General

Optical rotations were measured using a JASCO P-1020 digital polarimeter (JASCO Corporation, Tokyo, Japan). The UV spectra were recorded using a Shimadzu UVmini-1240 (Shimadzu Corporation, Kyoto, Japan). The HR-ESI-MS spectra were obtained using a micrOTOF-Q (Bruker Daltonics, Billerica, MA, USA) mass spectrometer with acetonitrile as the solvent. The NMR spectra were recorded using a Bruker AVANCE500 instrument (Bruker BioSpin, Billerica, MA, USA; 500 and 126 MHz for ^1H and ^{13}C , respectively) and chemical shifts were expressed as parts per million (ppm) relative to those of the solvents [MeOH- d_4 (δ_{H} 3.30; δ_{C} 49.0), and dimethyl sulfoxide (DMSO)- d_6 (δ_{H} 2.50; δ_{C} 39.5)] on a tetramethylsilane scale. The standard pulse sequences programmed for the instrument (AVANCE 500) were used for each 2D measurement (COSY, HSQC, and HMBC). The 2D-INADEQUATE spectrum was recorded using a JEOL ECA800 instrument (JEOL, Tokyo, Japan). Column chromatography was carried out using the Diaion HP-20, MCI-gel CHP-20P (Mitsubishi Chemical Co., Tokyo, Japan), Chromatorex ODS (Fuji Silysia Chemical Ltd., Aichi, Japan) and YMC GEL ODS (YMC Co. Ltd., Kyoto, Japan), respectively. Preparative TLC was carried out using TLC Silica gel 60 F₂₅₄ glass plates (Merck, Darmstadt, Germany). TLC was performed with CAMAG HPTLC equipment (CAMAG,

Muttenz, Switzerland) including a Linomat V applicator (CAMAG) and visualizer documentation system (CAMAG). The samples were spotted on HPTLC Silica gel 60 F₂₅₄ glass plates (20 × 10 cm, Merck), and the spots were detected using UV irradiation at 254 nm. The reversed-phase (RP) HPLC conditions were as follows. Condition 1: column, L-column ODS (5 μm, 150 × 2.1 mm i.d., Chemicals Evaluation and Research Institute, Tokyo, Japan); mobile phase, solvent A was 0.1% formic acid in water, and solvent B was 0.1% formic acid in acetonitrile (0–30 min, 0–50% B in A; 30–35 min, 50–85% B in A; 35–40 min, 85–85% B in A); injection volume, 2 μL; column temperature, 40 °C; flow-rate, 0.3 mL/min; and detection wavelength, 200–400 nm. Condition 2: column, YMC-pack ODS-AQ-3C2 (5 μm, 150 × 2.0 mm i.d., YMC Co. Ltd., Kyoto, Japan); mobile phase, 10 mmol/L phosphoric acid (H₃PO₄)-10 mmol/L monopotassium phosphate (KH₂PO₄)-acetonitrile (8:2); column temperature, 30 °C; flow-rate, 0.25 mL/min; and detection wavelength, 280 nm. Condition 3: column, YMC-pack ODS-AQ-3C2 (5 μm, 150 × 2.0 mm i.d., YMC Co. Ltd., Kyoto, Japan); mobile phase, 50 mmol/L phosphate buffer-acetonitrile (75:25); column temperature, 35 °C; flow-rate, 0.3 mL/min; and detection wavelength, 250 nm.

3.2. Materials

The CWR products used in the phytochemical investigation were purchased at a crude drug store at the Gyeongdong Market (Seoul, Korea). CWR and CAR for HPLC and TLC analyses were obtained from the Gyeongdong or Chinese markets and were provided by Japanese crude drug wholesalers. The identities of all the crude drugs were confirmed using DNA sequences [5]. All other reagents used were of analytical grade.

3.3. Extraction and Isolation

The CWR product (300 g) was homogenized in 3 L 80% MeOH [MeOH-H₂O (8:2)], the homogenate was filtered, concentrated to approximately 300 mL, and then extracted with 3 L each of *n*-hexane, EtOAc, and *n*-BuOH to obtain extracts at yields of *n*-hexane (492.9 mg), EtOAc (7.0 g), *n*-BuOH (13.2 g), and water (43.2 g), respectively. The EtOAc extract (500 mg) was chromatographed using the YMC GEL ODS with MeOH-H₂O (10:90→20:80→30:70→40:60→50:50→100:0) in stepwise gradient mode. The fractions showing similar HPLC patterns were combined and further purified using column chromatography with the Chromatorex ODS or preparative TLC with *n*-hexane-acetone (2:1 or 1:1), or both to obtain *p*-hydroxyacetophenone (**9**, 13.8 mg), 2',5'-dihydroxyacetophenone (**10**, 1.0 mg), 2',4'-dihydroxyacetophenone (**12**, 3.8 mg), and cynandionene A (**2**, 9.6 mg). The *n*-BuOH extract (12.5 g) was similarly separated using column chromatography over Diaion HP-20 with MeOH-H₂O (0:100→10:90→20:80→30:70→40:60→50:50→100:0) in stepwise gradient mode. The H₂O eluate (3.0 g) was separated using column chromatography using the Chromatorex ODS with aqueous MeOH to obtain uridine (**3**, 6.3 mg), and adenosine (**5**, 2.3 mg). The 10, 20, 30, and 40% MeOH eluates (120, 130, 89, and 52 mg, respectively) were purified using column chromatography with YMC GEL ODS using aqueous MeOH to obtain guanosine (**4**, 21.8 mg), tryptophan (**6**, 20.6 mg), bungeiside-C (**7**, 13.7 mg) plus compound **1** (2.4 mg), and bungeiside-D (**8**, 7.0 mg), respectively. These compounds were identified by direct comparison with authentic specimens or by comparing their spectral data with those reported in the literature. The physical spectral data of the new compound **1** are as follows.

2-O-β-Laminaribiosyl-4-hydroxyacetophenone (**1**): A light brown amorphous powder. UV λ_{max} (MeOH) nm (log ε): 228 (3.01), 269 (3.14), 301 (2.94). [α]_D²⁴ -14° (c 1.0, MeOH). ¹H-NMR (500 MHz, MeOH-*d*₄) and ¹³C-NMR (126 MHz, MeOH-*d*₄) data are shown in Table 1. HR-ESI-MS *m/z*: 475.1473 ([M-H]⁻, Calcd. for C₂₀H₂₈O₁₃-H: 475.1457).

Cynandione A (**2**): ¹H-NMR (DMSO-*d*₆, 800 MHz) δ 12.86 (1H, s, 2'-OH), 10.31 (1H, s, 6'-OH), 9.31 (1H, s, 2-OH), 8.49 (1H, s, 5-OH), 7.68 (1H, d, *J* = 2 Hz, H-4'), 6.72 (1H, d, *J* = 8 Hz, H-3), 6.67 (1H, d, *J* = 8 Hz, H-4), 6.43 (1H, d, *J* = 8 Hz, H-5'), 2.50 (3H, s, 8-CH₃), 2.19 (3H, s, 8'-CH₃). ¹³C-NMR (DMSO-*d*₆, 200 MHz) δ 203.7 (C-7'), 203.6 (C-7), 163.0 (C-2'), 162.8 (C-6'), 148.5 (C-2), 147.5 (C-5), 132.7 (C-4'),

130.7 (C-6), 118.7 (C-1), 117.9 (C-3), 116.3 (C-4), 112.8 (C-3'), 112.0 (C-1'), 108.0 (C-5'), 31.2 (C-8), 26.7 (C-8').

The CAR product (103 g) was homogenized in 80% MeOH (1 L), and the homogenate was filtered, concentrated to approximately 100 mL, and then extracted with *n*-hexane (300 mL), EtOAc (300 mL), *n*-BuOH (3 L), and water to obtain the solvent extracts at yields of 492.9 mg, 7.0 g, 13.2 g, and 43.2 g, respectively. The EtOAc extract (100 mg) was dissolved in MeOH and subjected to preparative TLC [*n*-hexane-acetone (1:1)] to yield wilfoside C1N (**12**, 8.0 mg) and wilfoside K1N (**13**, 10.5 mg). These compounds were identified by comparing their ¹H- and ¹³C-NMR data with those reported in literatures and were used as standard samples.

3.4. Partial Acid Hydrolysis of Compound 1

A solution of compound **1** (0.2 mg) in H₂O (0.2 mL) and 1 mol/L hydrochloric acid (HCl, 0.1 mL) was heated in a boiling water bath for 8 h. After removing the solvent, the residue was analyzed using HPLC (under Condition 2), and 2',4'-dihydroxyacetophenone was detected.

3.5. Determination of Sugar Configuration of Compound 1

The sugar configuration was determined using a previously described method [17]. Compound **1** (1.0 mg) was hydrolyzed by heating in 1 mol/L HCl (0.2 mL) and neutralized with Amberlite IRA400. After evaporation, the residue was dissolved in pyridine (0.2 mL) containing L-cysteine methyl ester hydrochloride (1.0 mg) and heated at 60 °C for 1 h. *o*-Tolyl isothiocyanate (1.0 mg) in pyridine (0.2 mL) was then added to the mixture and heated at 60 °C for 1 h. The reaction mixture was directly analyzed using RP-HPLC (under Condition 3). The peak coincided with that of the derivative of the authentic D-glucose sample.

3.6. Preparation of Test Solution of the Crude Drugs for HPLC and TLC

A sample of each product obtained from the open market was pulverized (0.2 and 1 g for the HPLC and TLC analyses, respectively), extracted with MeOH (1.0 mL) by sonication for 5 min, centrifuged, and the supernatant obtained was used as the test solution. The HPLC was performed under Condition 1 described in Section 3.1. For the TLC, aliquots (5 µL) of each test solution were applied to the HPTLC plates, which were developed in a TLC chamber saturated with EtOAc/water/MeOH/acetic acid (200:10:10:3, *v/v/v/v*) mixture as the mobile phase. The spots were detected under a UV lamp at 254 nm.

4. Conclusions

In the present study, a new phenolic compound, 2-*O*-β-lamaribiosyl-4-hydroxyacetophenone (**1**), was successfully isolated from CWR, in addition to 11 known compounds. Cynandione A (**2**), which is one of the main constituents of CWR with a biphenyl moiety, was identified using its 2D ¹³C-¹³C INADEQUATE spectrum; the carbon-carbon connection of the biphenyl moiety was clearly confirmed for the first time. The component distributions of MeOH extracts of CWR using a UV-sensitive HPLC analysis revealed three peaks of cynandione A (**2**), *p*-hydroxyacetophenone (**9**), and 2',4'-dihydroxyacetophenone (**11**), which were the main detected constituents. The emerging use of CAR in place of CWR has led to the need for a differentiating method, and therefore, we proposed and developed the present TLC method for the preliminary distinction between CWR and CAR.

Supplementary Materials: The following are available online at www.mdpi.com/1420-3049/23/3/656/link, Figures S1–S5.

Acknowledgments: The authors wish to thank Tochimoto Tenkaido Co., Ltd., Uchidawakanyaku Ltd., and Matsuura Yakugyo Co., Ltd. for providing crude drugs. We also thank Takuro Maruyama for supplying samples and his useful suggestions on our project. This work was supported by a Health Labour Sciences Research Grant provided by the Ministry of Health, Labour and Welfare of Japan.

Author Contributions: T.U., N.U., T.H. and Y.A. conceived and designed the experiments; T.U., H.T., H.S., M.Y., N.S.-M., T.T., N.U. and Y.A. performed the experiments; T.U. and Y.A. wrote the paper.

Conflicts of Interest: The authors declare no conflict of interest.

References

1. Korea Food and Drug Administration. *The Korean Herbal Pharmacopoeia*; Korea Food and Drug Administration: Seoul, Korea, 2002; p. 98.
2. Ministry of Food and Drug Safety, Korea. Available online: <http://www.mfds.go.kr/index.do?mid=676&seq=27270> (accessed on 25 January 2018).
3. Division of Safety Information on Drug and Food, National Institute of Health Sciences. Food Safety Information. Available online: <http://www.nihs.go.jp/hse/food-info/foodinfo/news/2015/foodinfo201509c.pdf> (accessed on 25 January 2018).
4. U.S. Food and Drug Administration (FDA). FDA Poisonous Plant Database. Available online: <https://www.accessdata.fda.gov/scripts/Plantox/Detail.CFM?ID=11513> (accessed on 25 January 2018).
5. Sato-Masumoto, N.; Uchikura, T.; Sugiwaki, H.; Yoshimura, M.; Masada, S.; Atsumi, T.; Watanabe, M.; Tanaka, N.; Uchiyama, N.; Amakura, Y.; et al. Survey on the original plant species of crude drugs distributed as *Cynanchi Wilfordii* radix and its related crude drugs in the Korean and Chinese markets. *Biol. Pharm. Bull.* **2017**, *40*, 1693–1699. [CrossRef] [PubMed]
6. Tsukamoto, S.; Hayashi, K.; Mistuhashi, H. Studies on the constituents of Asclepiadaceae plants. LX. Further studies on glycosides with a novel sugar chain containing a pair of optically isomeric sugars, D- and L-cymarose, from *Cynanchum wilfordii*. *Chem. Pharm. Bull.* **1985**, *33*, 2294–2304. [CrossRef]
7. Hwang, B.Y.; Kim, S.E.; Kim, Y.H.; Kim, H.S.; Hong, Y.-S.; Ro, J.S.; Lee, K.S.; Lee, J.J. Pregnane glycosides multidrug-resistance modulators from *Cynanchum wilfordii*. *J. Nat. Prod.* **1999**, *62*, 640–643. [CrossRef] [PubMed]
8. Yoon, M.-Y.; Choi, N.H.; Min, B.S.; Choi, G.J.; Choi, Y.H.; Jang, K.S.; Han, S.-S.; Cha, B.; Kim, J.-C. Potent in vivo antifungal activity against powdery mildews of pregnane glycosides from the roots of *Cynanchum wilfordii*. *J. Agric. Food Chem.* **2011**, *59*, 12210–12216. [CrossRef] [PubMed]
9. Li, J.-L.; Gao, Z.-B.; Zhao, W.-M. Identification and evaluation of antiepileptic activity of C₂₁ steroidal glycosides from the roots of *Cynanchum wilfordii*. *J. Nat. Prod.* **2016**, *79*, 89–97. [CrossRef] [PubMed]
10. Hwang, B.Y.; Kim, Y.H.; Ro, J.S.; Lee, K.S.; Lee, J.J. Acetophenones from roots of *Cynanchum wilfordii* HEMSLEY. *Arch. Pharm. Res.* **1999**, *22*, 72–74. [CrossRef] [PubMed]
11. Li, J.-L.; Fu, Y.F.; Zhang, H.-Y.; Zhao, W.-M. Two new humulanolides from the root of *Cynanchum wilfordii*. *Tetrahedron Lett.* **2015**, *56*, 6503–6505. [CrossRef]
12. Jiang, Y.F.; Choi, H.G.; Li, Y.; Park, Y.M.; Lee, J.H.; Kim, D.H.; Lee, J.-H.; Son, J.K.; Na, M.; Lee, S.H. Chemical constituents of *Cynanchum wilfordii* and the chemotaxonomy of two species of the family Asclepiadaceae, *C. wilfordii* and *C. auriculatum*. *Arch. Pharm. Res.* **2011**, *34*, 2021–2027. [CrossRef] [PubMed]
13. Li, Y.; Piao, D.; Zang, H.; Woo, M.-H.; Lee, J.-H.; Moon, D.-C.; Lee, S.-H.; Chang, H.W.; Son, J.K. Quality assessment and discrimination of the roots of *Cynanchum auriculatum* and *Cynanchum wilfordii* by HPLC-UV analysis. *Arch. Pharm. Res.* **2013**, *36*, 335–344. [CrossRef] [PubMed]
14. Lin, C.-N.; Huang, P.-L.; Lu, C.-M.; Yen, M.-H.; Wu, R.-R. Revised structure for five acetophenones from *Cynanchum taiwanianum*. *Phytochemistry* **1997**, *44*, 1359–1363.
15. SDBSWeb. National Institute of Advanced Industrial Science and Technology. Available online: <http://sdb.sdb.aist.go.jp> (accessed on 25 January 2018).
16. Li, J.; Kadota, S.; Kawata, Y.; Hattori, M.; Xu, G.-J.; Namba, T. Constituents of the roots of *Cynanchum bungei* DECNE. Isolation and structures of four new glucosides, bungeiside-A, -B, -C, and -D. *Chem. Pharm. Bull.* **1992**, *40*, 3133–3137. [CrossRef] [PubMed]


17. Tanaka, T.; Nakashima, T.; Ueda, T.; Tomii, K.; Kouno, I. Facile discrimination of aldose enantiomers by reversed-phase HPLC. *Chem. Pharm. Bull.* **2007**, *55*, 899–901. [[CrossRef](#)] [[PubMed](#)]
18. Liu, S.; Chen, Z.; Wu, J.; Wang, L.; Wang, H.; Zhao, W. Appetite suppressing pregnane glycosides from the roots of *Cynanchum auriculatum*. *Phytochemistry* **2013**, *93*, 144–153. [[CrossRef](#)] [[PubMed](#)]

Sample Availability: Samples of the compounds **1–13** are available from the authors.



© 2018 by the authors. Licensee MDPI, Basel, Switzerland. This article is an open access article distributed under the terms and conditions of the Creative Commons Attribution (CC BY) license (<http://creativecommons.org/licenses/by/4.0/>).

OPEN **Rapid and efficient high-performance liquid chromatography analysis of *N*-nitrosodimethylamine impurity in valsartan drug substance and its products**

Sayaka Masada, Genichiro Tsuji, Ryoko Arai, Nahoko Uchiyama, Yosuke Demizu, Tomoaki Tsutsumi, Yasuhiro Abe , Hiroshi Akiyama, Takashi Hakamatsuka, Ken-ichi Izutsu, Yukihiro Goda & Haruhiro Okuda

In July 2018, certain valsartan-containing drugs were voluntary recalled in Japan owing to contamination with *N*-nitrosodimethylamine (NDMA), a probable human carcinogen. In this study, an HPLC method was developed for the quantitative detection of NDMA simultaneously eluted with valsartan. Good linearity with a correlation coefficient (R^2) > 0.999 was achieved over the concentration range of 0.011–7.4 $\mu\text{g/mL}$. The limits of detection and quantification were 0.0085 $\mu\text{g/mL}$ and 0.0285 $\mu\text{g/mL}$, respectively. When the recalled valsartan samples were subjected to this method, the observed NDMA contents were in agreement with the reported values, indicating that our method achieved sufficient linearity, accuracy, and precision to detect NDMA in valsartan drug substances and products. Moreover, six samples (valsartan drug substances and tablet formulations), which had a possibility for NDMA contamination, were analyzed; none of the samples contained NDMA at detectable levels. Our method would be useful for the rapid screening and quantification of NDMA impurity in valsartan drug substances and products.

Valsartan-containing drugs contain the active pharmaceutical ingredient (API) valsartan. Valsartan [(2*S*)-3-Methyl-2-(*N*-{[2'-(1*H*-tetrazol-5-yl)biphenyl-4-yl]methyl}pentanamido)butanoic acid], an angiotensin II receptor antagonist, is mainly used for the treatment of hypertension and congestive heart failure. On 6th July 2018, the Ministry of Health, Labour and Welfare (MHLW) in Japan released that *N*-nitrosodimethylamine (NDMA) was detected as an impurity in valsartan-containing drugs whose API was supplied by Zhejiang Huahai Pharmaceutical in China. Simultaneously, ASKA Pharmaceutical Co., Ltd. in Japan announced a voluntary product recall of valsartan-containing drugs, because they found that there could be a risk of contamination of NDMA in the API purchased from Zhejiang Huahai Pharmaceutical¹. In addition, the MHLW recently notified that NDMA impurity in valsartan drug substances should not exceed 0.599 ppm².

NDMA is classified as a probable human carcinogen based on results from laboratory animal tests^{3–5} and is listed under WHO/IARC group 2A and EPA group B2^{6–8}. NDMA contamination was thought to be caused by the following changes in the production process of valsartan API^{9,10}: NDMA was generated during the tetrazole-formation step owing to the presence of dimethylamine as an impurity or a degradant in *N,N*-dimethylformamide (DMF) solvent and the presence of nitrous acid generated from sodium nitrite under acidic conditions (Fig. 1).

National Institute of Health Sciences, 3-25-26 Tonomachi, Kawasaki-ku, Kawasaki, Kanagawa, 210-9501, Japan. Sayaka Masada and Genichiro Tsuji contributed equally. Correspondence and requests for materials should be addressed to N.U. (email: nuchiyama@nihs.go.jp) or Y.D. (email: demizu@nihs.go.jp)

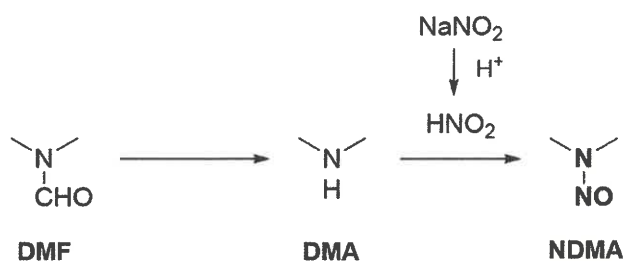


Figure 1. Prospective mechanism of NDMA production during the manufacturing process of valsartan (DMF: *N,N*-Dimethylformamide; DMA: Dimethylamine; NDMA: *N*-Nitrosodimethylamine).

As of September 2018, valsartan-containing products whose APIs were supplied from Zhejiang Huahai Pharmaceutical Co., Ltd., Zhejiang Tianyu Pharmaceutical Co., Ltd., Hetero Labs Ltd., and Zhuhai Rundu Pharmaceutical Co., Ltd. have been recalled in more than 20 countries, including the EU and USA^{11–16}. Regulatory bodies, European Medicines Agency (EMA), U.S. Food and Drug Administration (FDA), and the MHLW, cooperatively worked to handle the situation and take necessary measures to mitigate patient risk while estimating the risk of cancer due to NDMA-contaminated valsartan products^{17,18}. Government laboratories, including National Institute of Health Sciences in Japan, parallelly prepared methods to analyze NDMA in valsartan APIs and products in each market.

The API valsartan is listed in the Japanese Pharmacopoeia (JP)¹⁹ with methods for testing identity, purity, and assay; it is also listed in the US and European Pharmacopoeias^{20,21}. A purity test mainly focusses on expected impurities from synthesis and/or degradation. The purity test for valsartan focusses on heavy metals and related substances; however, these pharmacopoeias have never mentioned the need for testing NDMA as an impurity.

NDMA is mainly generated in foods and drinks after processing at an elevated temperature^{22–24}. It is also detected as a disinfection by-product in ground and drinking water^{25–27}. As the toxicity of NDMA is manifested even at $\mu\text{g}/\text{kg}$ levels^{28,29}, sensitive and specific methods were developed for the determination of NDMA at trace level. Gas chromatography–mass spectrometry (GC-MS) is the most frequently employed technique for NDMA analyses^{30–32}. In addition, several methods using liquid chromatography–mass spectrometry (LC-MS) or LC-MS/MS have been reported in scientific literature^{33–35}. However, only few studies have reported NDMA analysis using conventional high-performance liquid chromatography (HPLC)³⁶, especially in drugs. HPLC is the most popular technique for quality control of APIs and products in routine analysis, and it is preferable if NDMA impurity is simultaneously detected with drug substances by a single HPLC analysis. Thus, it is important to develop a fast and simple analytical method for NDMA in drugs by using HPLC.

In view of these situations, we tried to develop an HPLC method for the simultaneous detection of NDMA and valsartan. We analyzed valsartan drug substances and its products, including recalled samples, and confirmed the accuracy and precision of the method. This study provides a simple and accurate method for the quantification of NDMA impurity in valsartan products.

Results and Discussion

HPLC method development. To establish a practical method for the simultaneous detection of NDMA and valsartan, we first assayed each standard solution according to the HPLC condition for the quantitative assay for valsartan API and its tablet formulation defined in the JP¹⁹. When each standard solution of valsartan and NDMA was assayed following the modified JP method using isocratic mobile conditions, it was difficult to identify the peak of NDMA as it eluted during the void time (2.5 min) even with a flow rate of 0.80 mL/min, whereas the peak of valsartan was clearly detected at around 11 min (data not shown). Then, we developed a gradient elution program using a water-acetonitrile mobile phase containing 0.1% formic acid to detect NDMA and valsartan simultaneously within 30 min. Under this condition, peaks of NDMA and valsartan were successfully detected at 7.8 and 16.3 min, respectively (Fig. 2). Moreover, we confirmed the simultaneous detection of cilnidipine, another API in valsartan combination products, at 17.1 min under the same condition.

To assess the linearity of the developed method, we prepared a calibration plot using 10 concentration points of NDMA in the range of 0.0111–7.4 $\mu\text{g}/\text{mL}$ (0.15–100 μM) and constructed the calibration curve for quantification. The correlation coefficient (R^2) of the calibration curve was over 0.999. The limits of detection (LODs) and quantification (LOQs) were 0.0085 $\mu\text{g}/\text{mL}$ (at a S/N ratio of 3) and 0.0285 $\mu\text{g}/\text{mL}$ (at a S/N ratio of 10), respectively. The standardized limits of NDMA impurity in valsartan drug substances, which was set as 0.559 ppm by the MHLW², was equivalent to 0.02995 $\mu\text{g}/\text{mL}$ when 0.1 g of sample was extracted with 2 mL methanol. This concentration was almost equal to the LOQ. Recently, we reported a GC-MS method for the detection of NDMA in valsartan drug substance and products with much lower LOD (0.001 $\mu\text{g}/\text{mL}$ of NDMA corresponded to a S/N of 3)³⁷. However, this method needed the isotopic internal standard (NDMA- d_6) and multiple extraction steps as required for other MS-based methods. Generally, an HPLC method is low-cost and more suitable to routine analyses. Thus, the developed method would be useful for the rapid screening of NDMA contamination in valsartan drug substances with sufficient sensitivity.

Quantification of NDMA impurity in the recalled valsartan samples. Following the confirmation of linearity, we evaluated NDMA contents in the recalled valsartan samples using the developed HPLC

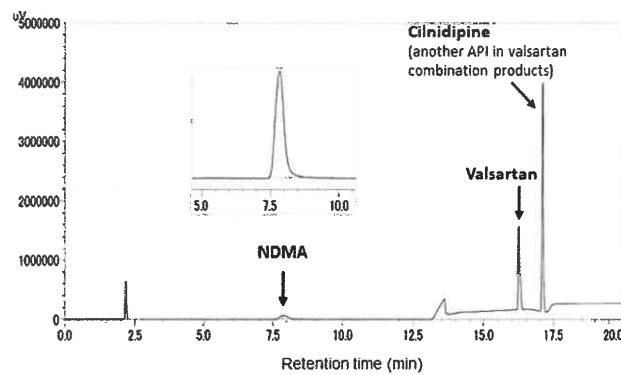


Figure 2. HPLC chromatograms of a mixture of reference standards.

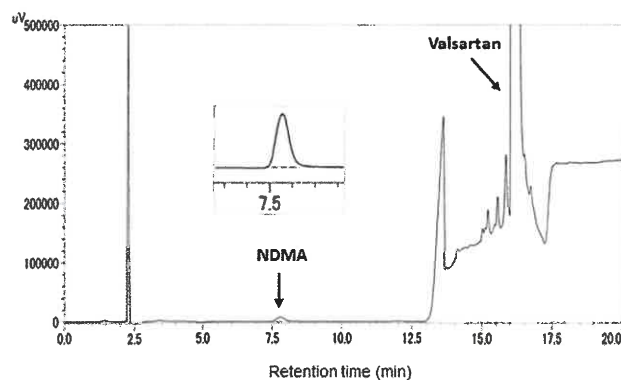


Figure 3. HPLC chromatograms of a sample solution of valsartan drug substances produced by Zhejiang Huahai Pharmaceutical Co., Ltd.

Product name	Manufacturer	Sample	Concentration of NDMA (µg/g)	NDMA contents (µg/tab)	Avg. ± SD	Reported NDMA value*
VALSARTAN TABLET 80mg [AA]	ASKA Pharmaceutical Co., Ltd.	Substance	51.4	—	54.7 ± 0.56	58 (µg/g)
			52.1	—		
			51.1	—		
		Tablets	15.7	3.91	4.25 ± 0.10	
			16.4	4.10		
			15.9	3.99		

Table 1. Comparison of NDMA contents observed by analysis of valsartan API and its tablets supplied by Zhejiang Huahai Pharmaceutical with previously reported values. *Previously determined values by GC-MS¹.

method. VALSARTAN TABLETS 80 mg [AA] and its substances were provided by ASKA Pharmaceutical Co., Ltd. through the MHLW. NDMA contents were estimated to be 36–74 ppm in the drug substances and 3.1–5.3 µg per tablet, respectively, based on GC-MS analysis according to the press release³. When a sample solution of drug substance (50 mg/mL in methanol) was analyzed using the developed method, the peak at 7.8 min was identified by comparing its retention time and UV spectrum with those of the NDMA reference standard (Fig. 3). NDMA content was calculated to be 54.7 µg/g, which was in agreement with the published value¹. A sample solution of the commercial product (150 mg/mL in methanol) provided a similar chromatogram, and its NDMA content was determined to be 17.0 µg/g. The corresponding NDMA content was estimated to be 4.25 µg per tablet (250 mg), which was in agreement with the published data (Table 1)¹.

Recovery test. Successively, a recovery test was carried out by analyzing spiked samples in the same way. Forty microliters of 10 mM NDMA (29.6 µg) was added to powdered VALSARTAN TABLETS [AA] (300 mg), and the spiked sample solution fortified at 98.67 µg/g was prepared. Five replicates of the spiked samples and triplicates of blanks (samples not spiked) were analyzed, and the recovery rate was determined to be 96.5% with 0.67% relative standard deviation (RSD). These results indicate that the developed method has sufficient linearity,

Product name	Manufacturer	Sample	Concentration of NDMA ($\mu\text{g/g}$)
VALSARTAN TABLETS 80 mg [SAWAI]	SAWAI Pharmaceutical Co., Ltd.	Substance	Not detected (<0.17)
VALSARTAN TABLET 80 mg [OHARA]	OHARA Pharmaceutical Co., Ltd.	Substance	Not detected (<0.17)
VALSARTAN TABLETS 80 mg [SANOFI]	Nihon Pharmaceutical Industry Co., Ltd.	Substance	Not detected (<0.17)
		Tablets	Not detected (<0.06)
ATEDIO [®] Combination Tab.	EA Pharma Co., Ltd.	Substance	Not detected (<0.17)
		Tablets	Not detected (<0.06)

Table 2. Concentration of NDMA impurity in valsartan API and commercial products supplied by Zhejiang Tianyu Pharmaceutical.

accuracy, and precision for the quantification of NDMA impurity in contaminated valsartan final products as well as its drug substances.

HPLC assay on APIs and commercial valsartan products. Finally, we investigated NDMA content in APIs and commercially available valsartan-containing products in the same way. Four valsartan APIs and two tablets, including an original drug ATEDIO[®] Combination Tab. (containing 80 mg valsartan and 10 mg cilnidipine), were supplied by Zhejiang Tianyu Pharmaceutical Co. Ltd. When their sample solutions (50 mg/mL and 150 mg/mL in methanol for API and tablets, respectively) were analyzed, no peak was detected for NDMA in the APIs of VALSARTAN TABLET 80 mg [SAWAI] and VALSARTAN TABLET 80 mg [OHARA]. Any peaks other than those for valsartan and cilnidipine were not detected in the API and tablets of ATEDIO[®] Combination Tab. Although a small peak was observed at around 8 min on the HPLC chromatogram of VALSARTAN TABLET 80 mg [SANOFI], it had a retention time different from that of NDMA and was not detected in the API. Thus, NDMA contents in all the samples were indicated to be below the LOD (<0.17 $\mu\text{g/g}$ for substances and <0.06 $\mu\text{g/g}$ for tablets) and below the acceptance limit for NDMA (0.599 ppm) (Table 2). The EMA reported that NDMA concentrations in valsartan API from Zhejiang Tianyu Pharmaceutical Co., Ltd. were considerably lower than those from Zhejiang Huahai Pharmaceutical¹⁴, and only one batch of valsartan-containing drugs distributed in Germany was recalled¹³. NDMA was not detectable in the tested samples probably because the manufacturing process of valsartan APIs for Japanese companies could be different from that for other foreign companies. Hence, we successfully developed a practical method for the rapid screening and quantification of NDMA impurity in valsartan-containing products.

Conclusion

A rapid and efficient HPLC method was developed for the quantitative detection of NDMA simultaneously eluted with valsartan. The method was found to have sufficient linearity, accuracy, and precision, and can be applied for the rapid screening and quantification of NDMA impurity in valsartan APIs and commercial products. This HPLC method would be useful for the quality control of APIs and products in routine analysis.

Methods

Reagents and materials. The commercial reagents of valsartan, cilnidipine, and NDMA with high purity (>98.0%, >98.0% and >99%, respectively) were purchased from Tokyo Chemical Industry Co., Ltd (Tokyo, Japan). APIs and its tablet formulations were provided by each company through the MHLW (Table 3).

Other reagents were of analytical grade.

Sample preparation. NDMA (14.8 μL , Mw: 74.08, density: 1.005) was transferred into a 2-mL volumetric flask, dissolved to volume with methanol (NDMA = 7.4 mg/mL, corresponding to 100 mM), and diluted 100-fold to obtain the stock solution at 1 mM. The standard solution of NDMA was prepared by 10-fold dilution of the stock solution for HPLC analysis (100 μM). Valsartan (8.7 mg, Mw: 435.53) and cilnidipine (9.9 mg, Mw: 492.53) reagents were accurately weighed, individually transferred into a 2-mL volumetric flask, and dissolved to volume with methanol to obtain the stock solutions at 10 mM. Each stock solution was diluted 100-fold to a final concentration of 100 μM as standard solutions and filtered through a 0.45- μm Ultrafree-MC centrifugal filter unit (Millipore, Billerica, MA) before HPLC analysis.

The drug substance (100 mg) or powdered tablet (300 mg) was dissolved with 2 mL methanol and centrifuged at 5,000 rpm for 5 min. The supernatant was filtered through a 0.45- μm Ultrafree-MC centrifugal filter unit. Triplicate test samples for each commercial product were prepared from every press-through sheet.

As NDMA is a carcinogenic substance, its handling was carried out in accordance with Safety Data Sheet, and the preparation of samples containing NDMA was performed in a fume hood.

HPLC analysis. HPLC method development and analyses were performed on a Shimadzu UFLC system comprising a binary gradient pump (LC-20AD), an autosampler (SIL-20AC), a column oven (CTO-20A), and a photodiode array detector (SPD-M20A) (Shimadzu, Tokyo, Japan). The first trial was carried out according to a modification of the method cited in the monographs of valsartan and its tablet in JP¹⁹. Briefly, 10 μL NDMA

Product name	Manufacturer	Tested sample	Supplier
VALSARTAN TABLET 80 mg [AA]	ASKA Pharmaceutical Co., Ltd.	Substance	Zhejiang Huahai Pharmaceutical Co., Ltd.
		Tablets	
VALSARTAN TABLETS 80 mg [SAWAI]	SAWAI Pharmaceutical Co., Ltd.	Substance	Zhejiang Tianyu Pharmaceutical Co., Ltd.
VALSARTAN TABLET 80 mg [OHARA]	OHARA Pharmaceutical Co., Ltd.	Substance	
VALSARTAN TABLETS 80 mg [SANOFI]	Nihon Pharmaceutical Industry Co., Ltd.	Substance	
		Tablets	
ATEDIO® Combination Tab.	EA Pharma Co., Ltd.	Substance	
		Tablets	

Table 3. Valsartan APIs and its products analyzed in this study.

standard solution was assayed by isocratic elution with a mixture of water, acetonitrile, and acetic acid (100) (500: 500: 1) on an HPLC system equipped with Unison UK-C18 column (250 × 4.6 mm, 3 μm, Imtakt, Kyoto, Japan) at a flow rate 0.8 mL/min and detected at 235 nm. Although the wavelength of maximum absorption of NDMA standard solution was 228 nm, we set the detection wavelength at 235 nm to achieve detection at lower noise and better baseline stability. In the finalized condition, HPLC analysis was carried out on Inertsil ODS-3 column (150 × 4.6 mm, 5 μm, GL Science, Tokyo, Japan) at 30 °C with a mobile phase comprising water containing 0.1% formic acid (A) and acetonitrile containing 0.1% formic acid (B) and detected at 235 nm. The gradient elution started at 0% B in 10 min and increased linearly to 100% in 5 min at a flow rate of 1.0 mL/min. A 10-μL aliquot of each sample was injected three times, and the reproducibility of the result was confirmed. Each peak obtained from the test samples was identified by comparing its retention time and UV spectrum with those of the reference standard for valsartan, cilnidipine, and NDMA. Peak areas were determined by the automatic integration method. The standard solution of NDMA was diluted for preparing calibration solutions at 0.15, 0.2, 0.3, 0.4, 0.5, 1, 5, 10, 50, 100 μM with methanol. The calibration solutions were analyzed to plot a calibration curve, and its slope, intercept, and coefficient of determination were calculated.

Recovery test. Forty microliters of 10 mM NDMA standard solution (740 μg/mL in methanol) was spiked to 300 mg of powdered VALSARTAN TABLETS [AA] and allowed to stand for 10 min. The spiked sample was dissolved with 1960 μL methanol and centrifuged at 5,000 rpm for 5 min. The supernatant was filtered through a 0.45-μm Ultrafree-MC centrifugal filter unit. The spiked sample was fortified to 98.67 μg/g with NDMA. Five replicates of spiked samples and three blanks (samples not spiked) were prepared and analyzed to determine the percentage of recovery.

Data Availability

The datasets generated during and/or analyzed during the current study are available from the corresponding authors on reasonable request.

References

- Ministry of Health, Labour and Welfare, Japan. Press release: Notice of voluntary collection of pharmaceutical products (Class I) (Valsartan Tablets 20 mg-40 mg-80 mg-160 mg AA, ASKA Pharmaceutical Co., Ltd.) (in Japanese), 6 July 2018, Available online, https://www.mhlw.go.jp/stf/newpage_00086.html (cited 26 September, 2018).
- Ministry of Health, Labour and Welfare, Japan. Notification: No. 1109-001, Document 3-1, Notice of the director of the Monitoring and guidance Narcotics Division (in Japanese), Available online, <https://www.pmda.go.jp/files/000226684.pdf> (cited 9 November, 2018).
- Ashley, L. M. & Halver, J. E. Dimethylnitrosamine-induced hepatic cell carcinoma in rainbow trout. *JNCI*. 41, 531–522 (1968).
- Barnes, J. M. & Magee, P. N. Some toxic properties of dimethylnitrosamine. *Br. J. Ind. Med.* 11, 167–174 (1954).
- Jakszyn, P. & González, C. A. Nitrosamine and related food intake and gastric and oesophageal cancer risk: a systematic review of the epidemiological evidence. *World J. Gastroenterol.* 12, 4296–4303 (2006).
- World Health Organization, Guidelines for Drinking-water Quality (2017).
- World Health Organization, *N-Nitrosodimethylamine In Drinking-water*. Background Document for Preparation of WHO Guidelines for Drinking-water Quality, in, Geneva (2008).
- International Agency for Research on Cancer, IARC Monographs on the Evaluation of the Carcinogenic Risk of Chemicals to Humans – Some *N*-Nitroso Compounds, Lyon, (1978).
- EMA CHMP List of questions. To be addressed by the API manufacturers for valsartan-containing medicinal products (16 July 2018), Available online, https://www.ema.europa.eu/documents/referral/valsartan-article-31-referral-chmp-list-questions-be-addressed-api-manufacturers-valsartan_en.pdf (cited 3 October, 2018).
- Pottgard, A. *et al.* Use of *N*-nitrosodimethylamine (NDMA) contaminated valsartan products and risk of cancer: Danish nationwide cohort study. *BMJ*. 362, k3851, <https://doi.org/10.1136/bmj.k3851> (2018).
- EMA reviewing medicines containing valsartan from Zhejiang Huahai following detection of an impurity. Some valsartan medicines being recalled across the EU, 05 July 2018, Available online, http://www.ema.europa.eu/docs/en_GB/document_library/Press_release/2018/07/WC500251498.pdf (cited 26 September, 2018).
- FDA announces voluntary recall of several medicines containing valsartan following detection of an impurity, 13 July 2018, Available online, <https://www.fda.gov/NewsEvents/Newsroom/PressAnnouncements/ucm613532.htm> (cited 26 September, 2018).
- Ministry of Health, Labour and Welfare, Japan. Notification: Notice of response to the detected cancer-causing substance in Valsartan medicines (in Japanese), 7 September 2018, Available online, <https://www.mhlw.go.jp/content/11121000/000360273.pdf>, (cited 6 October, 2018).
- EMA Update on medicines containing valsartan from Zhejiang Tianyu. Company no longer authorised to manufacture valsartan active substance for EU medicines due to presence of NDMA (20/August/2018), https://www.ema.europa.eu/documents/press-release/update-medicines-containing-valsartan-zhejiang-tianyu_en.pdf, (cited 21 November, 2018).

15. Valsartan: Slightly elevated NDMA levels were found in a batch of Valsartan HCT Aurobindo 320/25 mg (18/August/2018), <https://www.bfarm.de/SharedDocs/Pressemitteilungen/DE/2018/pm8-2018.html>.
16. Company Announcement (8/August/2018). Camber Pharmaceuticals, Inc. Issues Voluntary Nationwide Recall of Valsartan Tablets, USP, 40 mg, 80 mg, 160 mg and 320 mg Due to The Detection of Trace Amounts of *N*-Nitrosodimethylamine (NDMA) Impurity, Found in an Active Pharmaceutical Ingredient (API), https://www.fda.gov/Safety/Recalls/ucm616405.htm?utm_campaign=FDA%252.
17. EMA Update on review of recalled valsartan medicines. Preliminary assessment of possible risk to patients (2/August/2018), Available online, <https://www.ema.europa.eu/news/update-review-recalled-valsartan-medicines> (cited 26 September, 2018).
18. FDA updates recalled valsartan-containing product information and presents NDMA levels in some foods (20/August/2018), Available online, https://www.fda.gov/Drugs/DrugSafety/ucm613916.htm?utm_campaign=FDA%20updates%20recalled%20valsartancontaining%20product%20information%20to%20incorporate%20recalls%20of%20certain&utm_medium=email&utm_source=Eloqua, (cited 26 September, 2018).
19. The Ministry of Health, Labour and Welfare, Japan. Monographs for Valsartan and Valsartan Tablets referencing in *The Japanese Pharmacopoeia 17th Edition* 1248–1250 (2016).
20. The United States pharmacopoeial convention, United States Pharmacopoeia-USP 41 NF36, The United States pharmacopoeial convention, Inc., Rockville, (2018).
21. Council of Europe, European Pharmacopoeia, Council of Europe, Strasbourg (2018).
22. Rywotycki, R. Meat Nitrosamine Contamination Level Depending on Animal Breeding Factors. *Meat Sci.* **65**, 669–676 (2003).
23. US Food and Drug Administration, Dimethylnitrosamine in Malt Beverages, (2005).
24. Yurchenko, S. & Molder, U. The Occurrence of Volatile *N*-Nitrosamines in Estonian Meat Products. *Food Chem.* **100**, 1713–1721 (2007).
25. Najm, I. & Trussell, R. NDMA formation in water and wastewater. *J. Am. Water Works Assoc.* **93**, 92–99 (2001).
26. Mitch, W. *et al.* *N*-nitrosodimethylamine (NDMA) as a drinking water contaminant: a review. *Environ. Eng. Sci.* **20**, 389–404 (2003).
27. Richardson, S. D. & Postigo, C. Drinking water disinfection by-products, in: *Emerging Organic Contaminants and Human Health*, pp. 93–137 (Springer, 2011).
28. Issaq, H. J., McConnell, J. H., Weiss, D. E., Williams, D. J. & Saveedra, J. E. High performance liquid chromatography separations of nitrosamines. I. cyclic nitrosamines. *J. Liquid Chromatogr.* **9**, 1783 (1986).
29. USEPA *N*-nitrosodimethylamine, CASRN 62-75-9 (12/3/2002). Integrated Risk Information System, <http://www.epa.gov/IRIS/subst/0045.html>.
30. Raksit, A. & Johri, S. Determination of *N*-nitrosodimethylamine in environmental aqueous samples by isotope-dilution GC/MS-SIM. *J. AOAC Int.* **84**, 1413–1419 (2001).
31. Feng, D., Liu, L., Zhao, L., Zhou, Q. & Tan, T. Determination of volatile nitrosamines in latex products by HS-SPME-GC-MS. *Chromatographia* **74**, 817–825 (2011).
32. Qiang, M. *et al.* Determination of Ten Volatile Nitrosamines in Cosmetics by Gas Chromatography Tandem Mass Spectrometry. *Chin. J. Anal. Chem.* **39**, 1201–1207 (2011).
33. Zhao, Y. Y., Boyd, J., Hrudey, S. E. & Li, X. F. Characterization of new nitrosamines in drinking water using liquid chromatography tandem mass spectrometry. *Environ. Sci. Technol.* **40**, 7636–7641 (2006).
34. Herrmann, S. S., Duedahl-Olesen, L. & Granby, K. Simultaneous determination of volatile and non-volatile nitrosamines in processed meat products by liquid chromatography tandem mass spectrometry using atmospheric pressure chemical ionisation and electrospray ionisation. *J. Chromatogr. A.* **1330**, 20–29 (2014).
35. Ngongang, A. D., Duy, S. V. & Sauvé, S. Analysis of nine *N*-nitrosamines using liquid chromatography-accurate mass high resolution-mass spectrometry on a Q-Exactive instrument. *Anal. Methods* **7**, 5748–5759 (2015).
36. Cha, W., Fox, P. & Nalinakumari, B. High-performance liquid chromatography with fluorescence detection for aqueous analysis of nanogram-level *N*-nitrosodimethylamine. *Anal. Chim. Acta.* **566**, 109–116 (2006).
37. Tsutsumi, T. *et al.* Analysis of an impurity, *N*-nitrosodimethylamine, in valsartan drug substances and associated products using GC-MS. *Biol. Pharm. Bull.* **42**, 547–551 (2019).

Acknowledgements

This work was supported by a Health Labour Sciences Research Grant provided by the Ministry of Health, Labour and Welfare of Japan. This study was supported in part by grants from AMED under Grant Number JP19mk0101129j0101 (to Y.D.).

Author Contributions

Y.D., H.A., T.H., K.I., Y.G. and H.O. conceived and supervised the study. N.U. and Y.D. designed and conducted the experiments. S.M., G.T., R.A., T.T. and Y.A. performed the experiments. S.M., G.T., N.U. and Y.D. analyzed the results and wrote the manuscript. All authors reviewed and approved the final manuscript.

Additional Information

Competing Interests: The authors declare no competing interests.

Publisher's note: Springer Nature remains neutral with regard to jurisdictional claims in published maps and institutional affiliations.



Open Access This article is licensed under a Creative Commons Attribution 4.0 International License, which permits use, sharing, adaptation, distribution and reproduction in any medium or format, as long as you give appropriate credit to the original author(s) and the source, provide a link to the Creative Commons license, and indicate if changes were made. The images or other third party material in this article are included in the article's Creative Commons license, unless indicated otherwise in a credit line to the material. If material is not included in the article's Creative Commons license and your intended use is not permitted by statutory regulation or exceeds the permitted use, you will need to obtain permission directly from the copyright holder. To view a copy of this license, visit <http://creativecommons.org/licenses/by/4.0/>.

© The Author(s) 2019

Regular Article

Ebenamariosides A–D: Triterpene Glucosides and Megastigmanes from the Leaves of *Diospyros maritima*Susumu Kawakami,^a Erika Miura,^a Ayaka Nobe,^a Masanori Inagaki,^a Motohiro Nishimura,^a Katsuyoshi Matsunami,^b Hideaki Otsuka,^{*,a} and Mitsunori Aramoto^c^aDepartment of Natural Product Chemistry, Faculty of Pharmacy, Yasuda Women's University; 6–13–1 Yasuhigashi, Asaminami-ku, Hiroshima 731–0153, Japan; ^bDepartment of Pharmacognosy, Graduate School of Biomedical and Health Sciences, Hiroshima University; 1–2–3 Kasumi, Minami-ku, Hiroshima 734–8553, Japan; and ^cIriomote Station, Tropical Biosphere Research Center, University of the Ryukyus; 870 Aza Uehara, Taketomi-cho, Yaeyama-gun, Okinawa 907–1541, Japan.

Received September 18, 2019; accepted October 10, 2019

The 1-BuOH-soluble fraction of the methanol (MeOH) extract of *Diospyros maritima* was separated by chromatographic techniques to give three new oleanane-type and one new ursane-type triterpene glucoside, named ebenamariosides A–D (1–4); two megastigmanes were also isolated. The structures of triterpene glucosides was elucidated with extensive investigation by one and two dimensional NMR spectroscopy and the structures were confirmed by partial enzymatic hydrolyses to give the corresponding mono-glucosides and aglycones. The structures of the megastigmanes, including their absolute stereochemistries, were elucidated by spectroscopic evidence and by the modified Mosher's method. Two megastigmanes were chemically correlated and their absolute structures were unambiguously determined. The cytotoxicity of the triterpene glucosides and their degradation products were assayed. They did not show any significant activity.

Key words *Diospyros maritima*; Ebenaceae; ebenamarioside; triterpene glucoside; megastigmanane

Introduction

Diospyros maritima Blume (Ebenaceae) is a tall evergreen tree with a height of about 10m, distributed in Okinawa, Taiwan, Malaysia, Micronesia and Australia.¹⁾ In summer, it bears green sap fruits of 2 to 3 cm in diameter, which then turn to a dark orange colour in autumn. It is known that the fruits contain a toxic naphthoquinone derivative, plumbagin, and their constituents have been extensively investigated by Higa *et al.*^{2–4)} Recently, from the leaves and branches of a related Thai medicinal plant, *D. mollis*, the isolation of naphthoquinone glycosides was reported.⁵⁾ In our continuing work on Okinawan resource plants, the constituents of the leaves of *D. maritima* were investigated to give eight *ent*-kaurane-type diterpenoid glycosides, called diosmariosides A–H.⁶⁾ Further extensive work resulted in the isolation of four new triterpene saponins, named ebenamariosides A–D (1–4) and two megastigmanes (5, 6), along with two known flavonol glycosides, kaempferol 3-*O*-β-D-(2'',6''-di-*O*-α-L-rhamonopyranosyl)glucopyranoside (7)⁷⁾ and 3-*O*-β-D-(2'',6''-di-α-L-rhamonopyranosyl)galactopyranoside (8)⁸⁾ (Fig. 1). The cytotoxicity of the triterpenoids was assayed using the human lung adenocarcinoma cell line A549 and the parasitic protozoan *Leishmania major*.

Results and Discussion

The leaves of *D. maritima* extracted with MeOH and the MeOH extracts were separated by solvent partition according to the polarity of the constituents. The relatively polar 1-BuOH-soluble fraction was separated by various kinds of chromatography to afford four new triterpene saponins (1–4) and two new megastigmanes (5, 6), together with two known flavonol glycosides (7, 8). The structures of new triterpene derivatives were elucidated using one- and two-dimensional

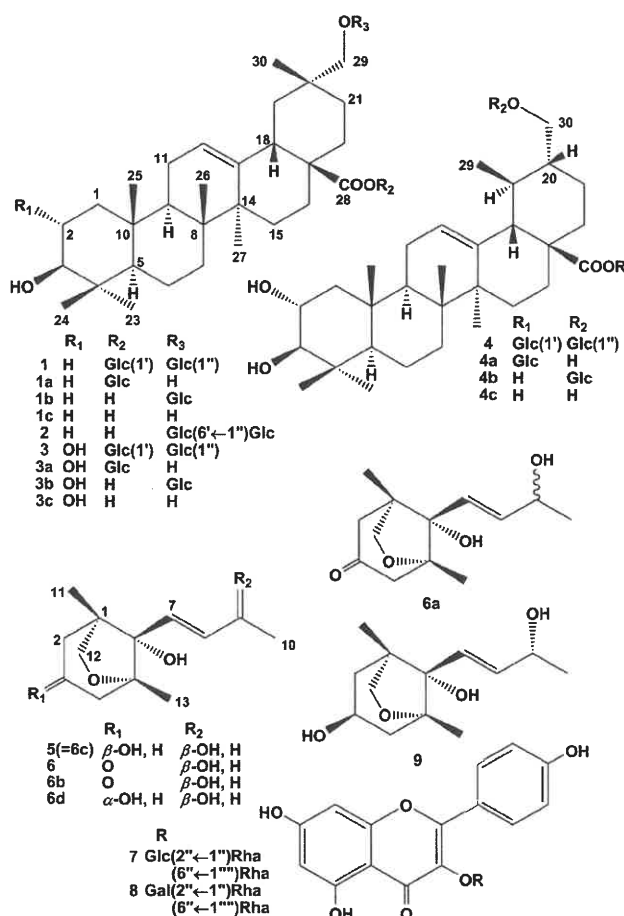


Fig. 1. Compounds Isolated and Related Ones

*To whom correspondence should be addressed. e-mail: otsuka-h@yasuda-u.ac.jp

spectroscopies. The structures of megastigmanes were elucidated by NMR and circular dichroism (CD) spectroscopies, and as well as by the modified Mosher method. The biological activity of four new triterpene saponins and their derivatives was assayed against the human lung adenocarcinoma cell line A549 and the parasitic protozoan *Leishmania major*.

Ebenamarioside A (**1**), $[\alpha]_D^{25} +15.1$, was isolated as a colorless amorphous powder and its molecular formula was determined to be $C_{42}H_{68}O_{14}$ by observation of a quasi-molecular ion peak ($[M + Na]^+$) in the high-resolution (HR) electrospray-ionisation (ESI) mass spectrometry. The IR spectrum showed strong absorption bands assignable to hydroxy (3439 cm^{-1}) and ester carbonyl (1745 cm^{-1}) functional groups. In the $^1\text{H-NMR}$ spectrum, signals assignable to six singlet methyls, oxymethylene protons (δ_{H} 3.40 and 3.91), oxymethine proton (δ_{H} 3.45), olefinic proton (δ_{H} 5.43) and two anomeric protons [δ_{H} 6.35 (d, $J=8.3\text{ Hz}$) and 4.85 (d, $J=7.8\text{ Hz}$)] were observed (Table 1). Since HPLC analysis of the hydrolysate of **1** revealed the presence of D-glucose as a sole sugar component, two D-glucose molecules were expected to be present in **1**. In the $^{13}\text{C-NMR}$ spectrum, other than 12 signals assignable to those of glucopyranose units, 30 signals observed comprised of six methyls, eleven methylenes including one oxymethylene, four methines with an oxygenated one, six quaternary carbons, one trisubstituted double bond and a carboxyl functional group. From the above evidence and the degrees of unsaturation ($\Delta=7$), ebenamarioside A (**1**) was assumed to be an oleanolic acid derivative with a primary hydroxy group. In the heteronuclear multiple bond connectivity (HMBC) spectrum, geminal oxymethylene protons showed correlation with a methyl carbon (C-30, δ_{C} 19.7), methylene carbons, C-19 (δ_{C} 41.1) and 21 (δ_{C} 29.2) as well as a quaternary carbon at δ_{C} 35.5 (Fig. 2). The significant correlation in the phase sensitive-nuclear Overhauser effect spectroscopy (PS-NOESY) spectrum between H-18 (δ_{H} 3.27) and H₃-30 (δ_{H} 1.10) on C-30 enabled us to place the oxymethylene carbon at the C-29 position (Fig. 2). Similarly, the oxymethine proton was placed at the 3-position from diagnostic HMBC between H-3 and C-4, C-23 and C-24 (Fig. 2). From the axial (10.2 Hz) and equatorial (4.6 Hz) coupling constants of H-3, the hydroxy group at the 3-position was in a β equatorial orientation. The positions of the sugar linkages were established to be on the carboxyl group at the C-28 and the hydroxy group at C-29 from HMBC correlations H-1' (δ_{H} 6.35) on δ_{C} 95.8 and C-28 (δ_{C} 176.4), and H-1'' (δ_{H} 4.85) on δ_{C} 105.5 and C-29 (δ_{C} 81.4), respectively. The mode of linkage was assigned to be β from the coupling constants of the anomeric protons. Therefore, the structure of ebenamarioside A (**1**) was elucidated to be 3 β ,29-dihydroxyolean-12-en-28-oic acid 28-*O*- β -D-glucopyranosyl ester 29-*O*- β -D-glucopyranoside, as shown in Fig. 1. Partial enzymatic hydrolysis of **1** using crude β -glucosidase liberated two monoglucosidic compounds (**1a** and **1b**) and an aglycone (**1c**). The structure of compound **1a** was elucidated to be mesembryantheneoidigenic acid 28-*O*- β -D-glucopyranosyl ester, isolated from *Salicornia europaea*,⁹ whereas that of **1b** mesembryantheneoidigenic acid 29-*O*- β -D-glucopyranoside, whose isolation have not yet been reported. The aglycone (**1c**) was spectroscopically identified with mesembryantheneoidigenic acid, isolated from a South American cactus, *Rhipsalis mesembryanthemoides*.^{10,11}

Ebenamarioside B (**2**), $[\alpha]_D^{27} -5.6$, was isolated as a color-

less amorphous powder and its elemental composition was the same as that of **1**. NMR spectra were similar to those of **1**. Two anomeric protons and carbons (δ_{H} 4.79 on δ_{C} 105.5 and δ_{H} 5.16 on δ_{C} 105.9) were also observed in the $^1\text{H-}$, $^{13}\text{C-}$ and heteronuclear single quantum correlation NMR spectra and D-glucose was a sole sugar unit. The distinct difference between **1** and **2** in the NMR signal was the carboxy carbons (C-28), such as δ_{C} 176.4 in **1** was shifted down to δ_{C} 180.2 in **2** and the anomeric carbon signal from an ester linkage (δ_{C} 95.8) appeared in **1** was not observed in **2**. While, in the HMBC spectrum, one of the anomeric proton at δ_{H} 5.16 was correlated with C-6' (δ_{C} 70.2) and then the other anomeric proton at δ_{H} 4.79 with C-29 (δ_{C} 81.4). Thus, the structure of **2** was 3 β ,20-dihydroxyolean-12-en-28-oic acid 29-*O*- β -D-(6'-*O*- β -D-glucopyranosyl)glucopyranoside, namely mesembryantheneoidigenic acid 29-*O*- β -gentiobioside, as shown in Fig. 1.

Ebenamarioside C (**3**), $[\alpha]_D^{27} +14.0$, was isolated as a colorless amorphous powder and its elemental composition was determined to be $C_{42}H_{68}O_{15}$, with one more oxygen atom than those of **1** and **2**. NMR spectroscopic data for the C, D and E-rings were essentially the same as those of **1** and **2**. In the $^1\text{H-NMR}$ spectrum, two oxymethine protons (δ_{H} 3.39 on δ_{C} 83.8 and δ_{H} 4.10 on δ_{C} 68.6) as well as oxymethylene protons (δ_{H} 3.39 and 3.89) were observed (Table 1). The position of the oxymethine protons were placed at the vicinal positions from the $^1\text{H-}^1\text{H}$ correlation spectroscopy correlation (COSY) (Fig. 3) and from the evidence of HMBC correlations, namely, H₃-23 (δ_{H} 1.25) and 24 (δ_{H} 1.08) and C-3 (δ_{C} 83.8) (Fig. 3). From the PS-NOESY correlations between H-2 (δ_{H} 4.10) and H₃-25 (axial) (δ_{H} 1.02), H-3 (δ_{H} 3.39) and H₃-23 (axial), and H₃-23 and H-5 (axial) (δ_{H} 1.00) (Fig. 3), the hydroxy groups at the 2- and 3-positions were placed in equatorial positions, which were further confirmed by the large coupling constant of the vicinal protons ($J=9.2\text{ Hz}$). Two oxymethines were found to be coupled each other from the $^1\text{H-}^1\text{H}$ -COSY spectroscopic evidence. The positions of the oxymethylene protons and sugar linkages were assigned by the similar manner used for ebenamarioside A (**1**). Therefore, the structure of **3** was elucidated to be 2 α ,3 β ,29-trihydroxyolean-12-en-28-oic acid 28-*O*- β -D-glucopyranosyl ester 29-*O*- β -D-glucopyranoside, as shown in Fig. 1. On enzymatic hydrolysis of **3** using crude naringinase, 28-*O*- β -D-glucopyranosyl ester (**3a**) was obtained. Glucoside **3a** is a known compound, isolated from the stem bark of *Terminalia superba* (= **3a'**)¹²; however, its $^{13}\text{C-NMR}$ data for MeOH-*d*₄ were slightly different from those of **3** to confirm the structure (Table 2). $^{13}\text{C-NMR}$ data of **3a** for pyridine-*d*₅ and dimethyl sulfoxide (DMSO)-*d*₆ were also slightly different from those of **3a'** (Table 2). Furthermore, the optical rotation value reported for **3a'** was $[\alpha]_D -18.1$ (*c* 0.1, MeOH) which showed an opposite sign to that of **3a**. In our report, the structure of **3a** was carefully elucidated with a highly detailed survey of the one- and two-dimensional NMR spectra. On the other hand, enzymatic hydrolysis of **3** using crude β -glucosidase gave 2 α ,3 β ,29-trihydroxyolean-12-en-28-oic acid 29-*O*- β -D-glucopyranoside (**3b**) and an aglycone (**3c**). Glucoside **3b** has not been isolated as a natural product and the aglycone (**3c**) was a known one, isolated from the pericarps of *Akebia trifoliata*.¹³

Ebenamarioside D (**4**), $[\alpha]_D^{26} -5.6$, was isolated as a colorless amorphous powder and its elemental composition was determined to be $C_{42}H_{68}O_{15}$, which was the same as that of

Table 1. ¹H-NMR Spectroscopic Data for Ebenamariosides A–D (1–4) (600 MHz, Pyridine-*d*₅)

H	1	2	3	4
1	0.99 ddd 12.7, 12.7, 4.1 1.55 m	1.04 m 1.57 m	1.28 m 2.24 dd 11.9, 4.2	1.25 m 2.24 dd 12.3, 4.0
2	1.85 2H m	1.85 m	4.10 ddd 11.9, 9.2, 4.2	4.10 ddd 12.3, 9.3, 4.0
3	3.45 dd 10.2, 4.6	3.47 dd 10.2, 5.7	3.39 d 9.2	3.38 d 9.3
5	0.85 brd 11.8	0.86 brd 12.0	1.00 m	0.99 m
6	1.37 m 1.55 m	1.37 m 1.57 m	1.40 m 1.54 m	1.38 m 1.52 m
7	1.37 m 1.49 ddd 12.8, 12.8, 3.4	1.32 m 1.50 m	1.38 m 1.49 m	1.38 m 1.54 m
9	1.64 dd 11.1, 6.7	1.66 dd 8.9, 8.9	1.74 dd 10.2, 7.3	1.70 m
11	1.95 2H m	1.95 m 2.17 m	1.95 m 2.09 brdd 13.4, 10.2	2.02 2H m
12	5.43 dd 3.5 3.5	5.48 brs	5.39 brs	5.42 brs
15	1.15 m 2.37 ddd 13.7, 13.7, 3.6	1.19 m 2.17 m	1.15 m 2.35 ddd 13.4, 13.4, 3.5	1.12 m 2.43 ddd 13.5, 13.5, 4.7
16	1.95 m 2.10 ddd 13.7, 13.7, 3.6	1.98 2Hm	1.98 2Hm	1.93 m 2.03 m
18	3.27 dd 13.8, 4.2	3.36 dd 13.7, 3.8	3.25 dd 13.6, 3.6	2.54 d 11.3
19	1.43 dd 13.6, 4.2 2.01 dd 13.8, 13.6	1.50 m 2.09 m	1.41 m 2.00 m	1.70 m —
20	—	—	—	1.26 m
21	1.35 m 1.67 ddd 13.7, 13.7, 4.1	1.43 m 1.79 m	1.33 m 1.65 ddd 13.9, 13.9, 3.6	1.56 m 1.93 m
22	1.82 m 1.87 m	1.85 m 2.06 m	1.79 brd 13.4 1.87 ddd 13.9, 13.9, 3.6	1.73 m 1.96 m
23	1.23 3H s	1.25 3H s	1.25 3H s	1.25 3H s
24	1.04 3H s	1.04 3H s	1.08 3H s	1.07 3H s
25	0.93 3H s	0.90 3H s	1.02 3H s	1.02 3H s
26	1.14 3H, s	1.03 3H s	1.12 3H s	1.15 3H s
27	1.21 3H s	1.27 3H s	1.19 3H s	1.12 3H s
29	3.40 d 9.2 3.91 d 9.2	3.41 d 9.2 4.04 d 9.2	3.39 d 9.0 3.89 d 9.0	0.93 3H d 6.3
30	1.10 3H s	1.22 3H s	1.09 3H s	3.84 dd 9.4, 3.1 4.00 m
1'	6.35 d 8.3	4.79 d 7.7	6.32 d 8.2	6.25 d 8.2
2'	4.22 dd 8.8, 8.3	4.02 dd 8.6, 7.7	4.20 dd 8.8, 8.2	4.19 dd 8.6, 8.2
3'	4.38 dd 9.0, 8.8	4.21 dd 8.9, 8.6	4.28 dd 8.9, 8.8	4.27 m
4'	4.25 dd 9.2, 9.0	4.16 dd 9.2, 8.9	4.36 dd 9.1, 8.9	4.34 dd 9.3, 9.1
5'	3.99 ddd 9.2, 4.6, 2.3	4.21 m	4.03 m	4.00 m
6'	4.43 dd 12.0, 4.6 4.48 dd 12.0, 2.3	4.37 dd 11.4, 5.8 4.88 brd 11.4	4.42 dd 11.0, 5.4 4.46 brd 11.0	4.38 dd 12.0, 4.3 4.44 dd 12.0, 2.1
1''	4.85 d 7.8	5.16 d 7.9	4.83 d 7.7	4.85 d 7.7
2''	4.07 dd 8.2, 7.8	4.07 m	4.05 m	4.04 dd 8.2, 7.7
3''	4.30 dd 8.6, 8.2	4.25 m	4.24 m	4.27 m
4''	4.42 dd 8.9, 8.6	4.26 m	4.24 m	4.23 dd 9.1, 8.9
5''	4.05 ddd 8.9, 5.4, 2.3	3.95 m	3.98 m	3.99 m
6''	4.43 dd 11.8, 5.4 4.59 dd 11.8, 2.3	4.39 dd 11.9, 5.2 4.53 brd 11.9	4.41 dd 11.4, 5.5 4.58 brd 11.4	4.41 dd 12.1, 5.7 4.58 dd 12.1, 2.2

3. The ¹H-NMR spectrum showed resonances for five singlet methyls and one doublet methyl, two oxygenated methines, two anomeric protons and one olefinic proton along with two oxymethylene protons coupled in a geminal system, but also coupled with one more proton [δ_{H} 3.84 (dd, $J=9.4$, 3.1 Hz) and 4.00 (m)]. Although six quaternary carbons were observed in the ¹³C-NMR spectra of aforementioned oleanane-type aglycones, only five quaternary ones were present in the molecule, and two more methine (C-19 and -20) and one less methylene carbons were observed in **4**, when the functional-

ity was compared with that of **3**. ¹³C-NMR chemical shifts of the A and B rings were essentially the same as those of **3** and the presence of a double bond between C-12 and C-13 was also similar to aforementioned triterpene aglycones. The proton spin-spin coupling sequences from the doublet methyl signal (δ_{H} 0.93) to oxymethylene protons *via* two methine signals (δ_{H} 1.70 and 1.26) were observed in the ¹H-¹H COSY spectrum (Fig. 4). The HMBC correlations between the doublet methyl proton and C-18 (δ_{C} 53.3), C-19 (δ_{C} 34.4) and C-20 (δ_{C} 44.6), and the oxymethylene protons and C-19,

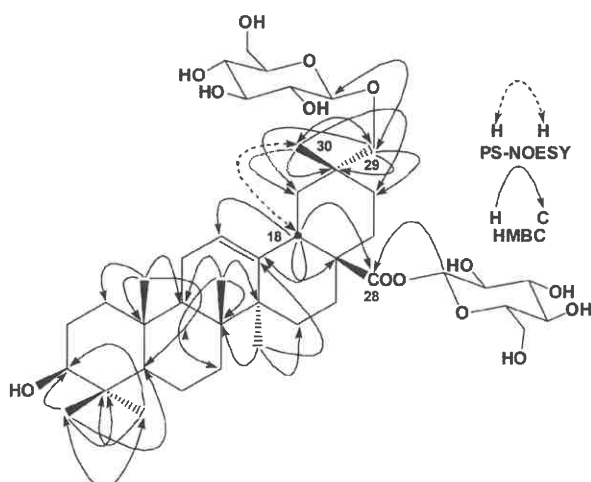


Fig. 2. Two Dimensional NMR Correlations of Ebenamarioside A (1)

C-20 and C-21 (δ_C 25.6) established the scaffold of the ring E to possess the ursane-type carbon framework (Fig. 4). This was also supported by the significant PS-NOESY correlations H-18 (δ_H 2.54) and H₃-29 (δ_H 0.93), and H-18 and H-20 (δ_H 1.26). The sugar linkages were assigned by the similar manner used for ebenamariosides A and C (1, 3). Therefore, the structure of ebenamarioside D (4) was elucidated to be 2 α ,3 β ,30-trihydroxyursan-12-en-28-oic acid 28-*O*- β -D-glucopyranosyl ester 30-*O*- β -D-glucopyranoside, as shown in Fig. 1. Enzymatic hydrolysis using crude β -glucosidase gave a mixture of monoglucosidic compounds (4a and 4b) and 2 α ,3 β ,30-trihydroxyurs-12-en-28-oic acid as an aglycone (4c), which is known as a microbial transformation product from corosolic acid by *Streptomyces asparaginoviolaceus*.¹⁴ The mixture of monoglucosidic compounds was separated by silica gel CC and HPLC to give 2 α ,3 β ,30-trihydroxyurs-12-en-28-oic acid 28-*O*- β -D-glucopyranosyl ester (4a) and 2 α ,3 β ,30-trihydroxyurs-12-en-28-oic acid 30-*O*- β -D-glucopyranoside (4b). These two monoglucosidic compounds were first described in this experiment.

Compound 5, $[\alpha]_D^{25} +10.2$, was isolated as a colorless powder and its elemental composition was determined to be C₁₃H₂₂O₄. In the ¹H-NMR spectrum, two singlet (δ_H 0.88 and 1.12) and one doublet (δ_H 1.28, $J = 6.4$ Hz) methyls, two olefinic protons [δ_H 6.03 (dd, $J = 15.5, 4.5$ Hz) and 6.06 (d, $J = 15.5$ Hz)] coupled in a trans geometry, two sets of methylene protons (δ_H 1.64 and 1.80, and 1.75 and 2.00), two oxygenated methylene protons (δ_H 3.68 and 3.77) and two oxygenated methine (δ_H 4.09 and 4.35) protons were found (Table 3). The ¹³C-NMR spectrum displayed 13 signals including three methyls, three methylenes, two methines with oxygen atoms, two olefinic carbons, two oxygenated tertiary and one quaternary carbon (Table 3). The number of carbons and degrees of unsaturation suggested that compound 5 was a megastigmane with a bicyclic scaffold. Two ¹H-¹H COSY correlations [-C(2)H₂-C(3)HOH-C(4)H₂- and -C(7)H=C(8)H-C(9)HOH-C(10)H₃] and HMBC correlations between H₂-11 (δ_H 3.68 and 3.77) and C-5 (δ_C 87.5) and other diagnostic correlations shown in Fig. 5a suggested 5 was 5,11-eopxy-3,6,9-trihydroxymegastigman-7-ene. The relative stereochemistry was established by the PS-NOESY spectrum. Correlations between H-7 (δ_H 6.06) and H-2ax (δ_H 1.64), H-4ax (δ_H 1.75), H₃-12 (δ_H 0.88) and H₃-13 (δ_H 1.12) sug-

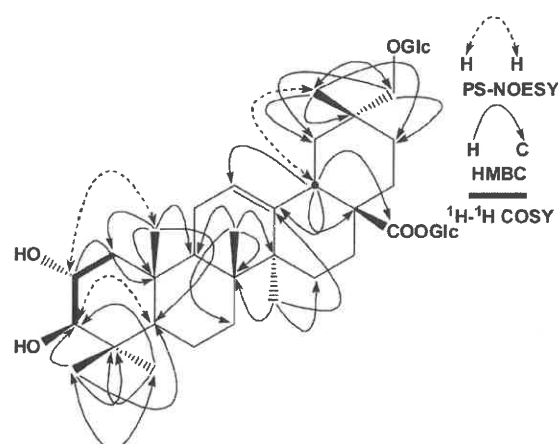


Fig. 3. Two Dimensional NMR Correlations of Ebenamarioside C (3)

gested these substituents were in the same face and those between H-11b (δ_H 3.68) and H-2eq (δ_H 1.80), H-3 (δ_H 4.09) and H-4eq (δ_H 2.00) these were in the same face and the opposite face to the side chain (Fig. 5b). A related compound (9) which showed superimposable NMR spectra with those of 5 was isolated from *Asclepias fruticosa* and the absolute structure of 9 was determined by the modified Mosher's method¹⁵ to have 1*R*,3*S*,5*R*,6*S*,9*R* configurations.¹⁶ Compound 5 was also subjected to the modified Mosher method and, as a result, 5 was found to have 1*R*,3*S*,5*R*,6*S*,9*S* configurations (Fig. 6). Therefore, 5 has the opposite configuration at the 9-position to that of 9 and thus it was found to be a new compound in nature.

Compound 6, $[\alpha]_D^{25} -0.74$, was isolated as a colorless syrup and its elemental composition was determined to be C₁₃H₂₀O₄ which was two hydrogen fewer than that of 5. ¹³C-NMR spectrum also displayed 13 signals including three methyls, three methylenes, one oxygenated methine, two oxygenated tertiary carbons, one quaternary carbon, one ketone, instead of oxygenated methine and one disubstituted double bond, whose NMR chemical shifts for CDCl₃ were almost superimposable to those of drummondol [6a, $[\alpha]_D^{23} -21.0$ (MeOH)] isolated from *Sesbania drummondii* by Powell and Smith, Jr.,¹⁷ whose geometry at the 9-position and the absolute configuration of bicyclo[3,2,1]octane region remains to be determined. Meanwhile, Çaliş et al. isolated drummondol 9-*O*- β -D-glucopyranoside from *Capparis spinosa* and the absolute configuration of the aglycone (6b) of the 9-position was determined to be 9*S* by the modified Mosher method.^{16,18} That of the ring region was discussed using the Cotton effects in the CD spectrum of 6b, compared with those of (+)-(*S*)-abscisic acid metabolites. Compound 6 showed similar Cotton effects [$\Delta\epsilon$ (nm): +0.64 (241), -0.30 (296)] to those of 6b¹⁸ and hence the absolute stereochemistries of 6 and 6b were expected to be the same at the 6-position. NaBH₄ reduction of 6 gave two products (6c and 6d). Hydride was introduced from the less hindered 3*si* face to form the major compound 6d and the minor compound 6c was obtained by the reduction of 6 from the 3*re* face. The ¹H-NMR signal of the H-3 proton of 6d was appeared as a doublet, $J = 5.7, 5.7$ Hz, indicating that the α -hydroxy group formed at the 3-position was in the pseudo axial orientation due to steric hindrance toward the epoxide ring.^{19,20} Meanwhile, the NMR spectroscopic data of the minor one (6c) were identical with those of 5 and similarly

Table 2. ¹³C-NMR Spectroscopic Data for Ebenamariosides A–D (1–4) and Their Derivatives (150 MHz, Pyridine-*d*₅)

C	1	1b	2	3	3a	3a ^{a)}	3a ^{b)}	3a ^{c)}	3b	4	4a	4b
1	39.0	39.0	39.0	47.8	47.9	48.2	47.0	46.8	47.8	48.1	48.1	48.0
2	28.1	28.1	28.1	68.6	68.6	69.5	66.8	67.0	68.6	68.6	68.6	68.6
3	78.1	78.1	78.5	83.8	83.8	84.5	81.9	82.1	83.8	83.8	83.8	83.8
4	39.4	39.4	39.4	40.0	40.0	40.4	39.1	38.9	39.9	39.8	39.8	39.9
5	55.8	55.8	55.8	55.9	55.9	56.7	55.1	54.7	55.9	55.9	55.9	55.9
6	18.8	18.8	18.8	18.8	18.9	19.6	18.2	17.9	18.9	18.8	18.9	18.8
7	33.2	33.3	33.3	33.1	33.1	32.4	32.2	32.1	33.2	33.5	33.5	33.5
8	40.0	39.8	39.8	39.8	39.9	40.5	39.0	38.8	39.8	40.2	40.3	40.0
9	48.1	48.1	48.1	48.1	48.2	49.1	47.4	47.0	48.1	48.1	48.1	48.1
10	37.4	37.4	37.4	38.5	38.6	39.3	36.9	37.5	38.5	38.4	38.5	38.5
11	23.8	23.8	23.8	23.5	23.5	24.0	23.5	22.4	23.8	23.8	23.9	23.7
12	123.0	122.7	122.6	122.9	122.8	123.7	122.7	121.4	122.5	126.4	126.2	125.9
13	144.1	144.8	144.8	144.0	144.4	145.0	143.8	143.5	144.8	138.1	138.5	139.0
14	42.1	42.2	42.2	42.1	42.2	42.9	41.5	41.2	42.2	42.5	42.6	42.5
15	28.3	28.4	28.3	28.2	28.3	28.9	28.0	27.1	28.3	28.6	28.7	28.6
16	23.5	23.8	23.8	23.9	24.0	24.7	23.2	22.9	23.9	24.7	24.7	25.0
17	47.4	47.1	47.1	47.2	47.5	48.3	46.4	46.2	47.0	48.2	48.4	47.9
18	41.0	41.2	41.2	40.9	41.2	41.9	42.2	39.9	41.2	53.3	53.4	53.6
19	41.1	41.3	41.2	41.0	41.0	41.4	41.7	39.9	41.3	34.4	33.7	34.6
20	35.5	35.8	35.7	35.5	36.4	36.9	35.3	35.3	35.7	44.6	47.2	45.0
21	29.2	29.4	29.3	29.2	28.9	29.3	31.8	27.8	29.4	25.6	25.5	25.9
22	31.8	32.5	32.5	31.7	32.1	33.9	33.7	30.9	32.5	36.5	36.8	37.2
23	28.8	28.8	28.8	29.3	29.3	29.3	28.8	28.7	29.3	29.4	29.4	29.4
24	16.6	16.6	16.6	17.6	17.7	17.8	17.3	17.0	17.7	17.7	17.8	17.7
25	15.7	15.6	15.6	16.9	17.0	17.2	16.0	16.3	16.9	17.1	17.1	17.0
26	17.6	17.5	17.5	17.5	17.6	17.7	16.9	16.6	17.5	17.7	17.7	17.5
27	26.1	26.2	26.2	26.0	26.1	26.3	25.7	25.5	26.2	23.7	23.8	23.9
28	176.4	180.2	180.2	176.4	176.5	178.0	175.9	175.1	180.3	176.2	176.3	179.9
29	81.4	81.6	81.4	81.3	73.7	74.3	74.7	72.1	81.6	17.1	17.1	17.3
30	19.7	19.8	19.8	19.7	19.7	19.6	19.9	19.0	19.8	73.2	65.0	73.5
1'	95.8		105.5	95.8	95.8	95.8	95.8	94.0		95.7	95.8	
2'	74.2		75.2	74.1	74.2	74.0	74.1	72.3		74.0	74.1	
3'	79.0		78.5	78.9	79.0	78.7	79.1	77.6		78.8	79.0	
4'	71.1		71.7	71.1	71.2	71.1	71.3	69.4		71.2	71.2	
5'	79.4		77.3	79.3	79.4	78.3	78.6	76.6		79.1	79.3	
6'	62.2		70.2	62.2	62.2	62.4	62.2	60.6		62.3	62.3	
1''	105.5	105.5	105.9	105.4					105.5	104.8		105.1
2''	75.3	75.4	75.2	75.2					75.4	75.2		75.3
3''	78.7	78.7	78.6	78.6					78.7	78.6		78.7
4''	71.7	71.8	71.7	71.7					71.8	71.7		71.8
5''	78.6	78.6	78.1	78.5					78.6	78.5		78.6
6''	62.9	62.9	62.7	62.9					62.9	62.9		63.0

a) Data for CD₃OD. b) Data were taken from ref. 12 (CD₃OD). c) Data for DMSO-*d*₆.

6c was subjected to the modified Mosher's method to give (*R*)- and (*S*)- α -methoxy- α -trifluoromethylphenylacetic acid (MTPA) esters of **6c**, which were the identical compounds with **5a** and **5b** from **5**. Therefore, the absolute configurations of drummondol (**6**) isolated in this experiment was confirmed to be 1*R*,5*R*,6*S*,9*S*, which was the same as the aglycone of (9*S*)-drummondol 9-*O*- β -D-glucopyranoside from *C. spinosa* (Fig. 1) and **6** is expected to be a new compound as a non-glucosidic form; however, a direct correlation with the original drummondol (**6a**) was precluded.

The cytotoxic activity of isolated ebenamariosides (**1–4**), their derivatives (**1a**, **1b**, **1c**, **3a**, **3b**, **3c**, **4a**, **4b** and **4c**), and compounds **5** and **6** was assayed using the human lung adenocarcinoma cell line A549. Compounds **1c** and **4c** showed slight activity with IC₅₀ values of 174 \pm 16 μ M and 107 \pm 8 μ M,

respectively, where that of the positive control etoposide was 23.3 \pm 4.3 μ M, while other compounds did not show any activity at 100 μ g/mL. Unfortunately, none of compounds were active toward *L. major* at 100 μ g/mL.

Closing Remarks From the leaves of *Diospyros maritima*, four triterpene saponins, named ebenamariosides A–D (**1–4**) and two megastigmanes (**5**, **6**) were isolated. The structures of ebenamariosides were carefully elucidated by interpretation of one- and two-dimensional NMR spectroscopies and enzymatic hydrolysis of **1**, **3** and **4** using crude β -glucosidase and naringinase gave corresponding monoglucosides and aglycones. The structures of megastigmanes were confirmed by the modified Mosher's method and the Cotton effect in the CD spectrum. Assays of inhibitory activities for triterpene derivatives toward human lung adenocarcinoma cell line, A549 and

Leishmania major did not show any significant activity.

Experimental

General Experimental Procedures Optical rotations were measured on a JASCO P-2200 digital polarimeter. IR spectra were measured on JASCO FT/IR-6100 spectrophotometers. ^1H - and ^{13}C -NMR spectra were taken on a Bruker Avance III at 600MHz and 150MHz, respectively, with tetramethylsilane as an internal standard. CD spectra were obtained with a JASCO J-720 spectropolarimeter. Positive and negative-ion HR-ESI-MS were performed with a Thermo Fisher Scientific LTQ Orbitrap XL. Silica gel column chromatography (CC) was performed on silica gel 60 (70–230 mesh) (E. Merck, Darmstadt, Germany) and reversed-phase octadecylsilylated (ODS) open CC on Cosmosil 75C₁₈-OPN (Nacalai Tesque, Kyoto, Japan) (Φ = 50 mm, L = 25 cm). HPLC was performed on an ODS column [Inertsil ODS-3 (GL Science Inc., Tokyo, Japan; Φ = 10 mm, L = 25 cm, 4.0 mL/min), Cosmosil

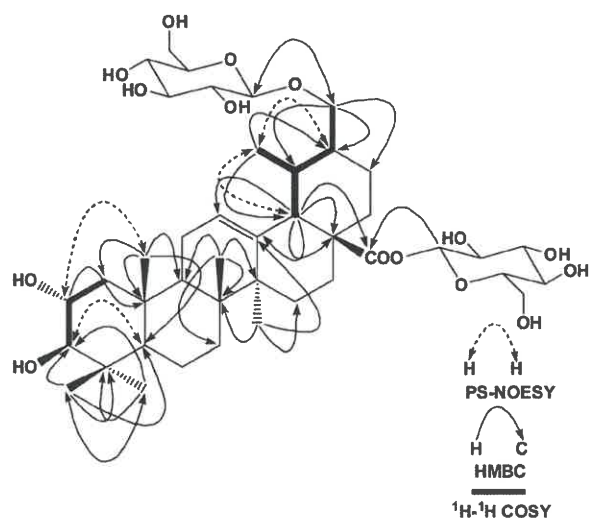


Fig. 4. Two Dimensional NMR Correlations of Ebenamarioside D (4)

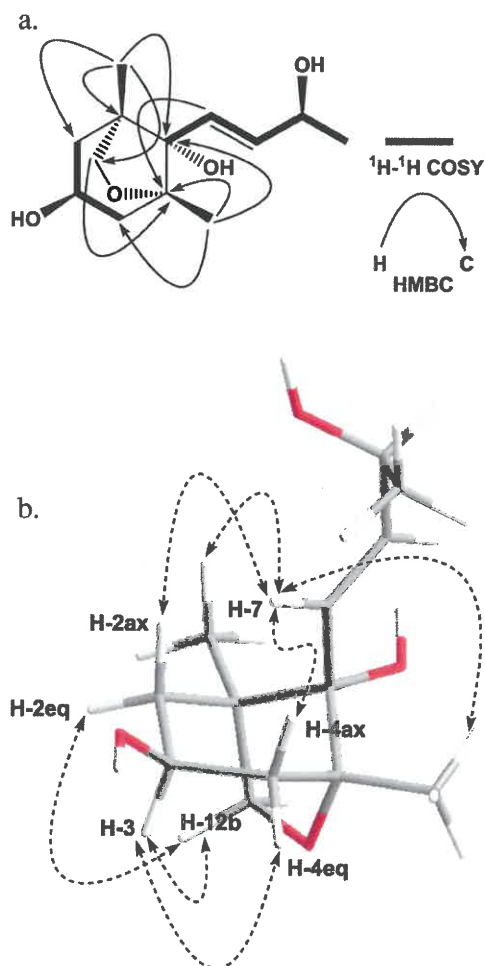


Fig. 5. a) ^1H - ^1H COSY and HMBC Correlations of **5**; b) PS-NOESY Correlations of **5**

a) Significant long range ^1H - ^1H correlations due to formation of W-figure were observed between H-2ax and H-12a and H-2 eq and H-4 eq.

Table 3. NMR Spectroscopic Data for Megastimane Derivatives (**5**, **6**) (C: 150MHz, H: 600MHz, CD₃OD)

	5		6	
	C	H	C	H
1	48.8	—	49.5	—
2	44.4	1.64 (ddd, 13.6, 10.5, 2.1) 1.80 (ddd, 13.6, 7.2, 1.4)	53.2	2.35 (dd, 18.1, 2.6) 2.65 (dd, 18.1, 2.9)
3	66.0	4.09 (dddd, 10.5, 10.5, 7.2, 7.2)	211.4	—
4	45.8	1.75 (dd, 13.6, 10.5) 2.00 (ddd, 13.6, 7.2, 1.4)	53.9	2.43 (dd, 18.1, 2.6) 2.78 (d, 18.1)
5	87.5	—	87.5	—
6	82.6	—	82.4	—
7	127.0	6.06 (d, 15.5)	125.7	6.02 (dd, 15.4, 1.5)
8	139.6	6.03 (d, 15.5, 4.5)	140.7	6.17 (dd, 15.4, 5.5)
9	69.2	4.35 (qd, 6.4, 4.5)	68.9	4.38 (dq, 6.4, 5.5, 1.5)
10	24.0	1.28 (d, 6.4)	24.0	1.28 (3H, d, 6.4)
11	16.3	0.88 (3H, s)	19.2	1.18 (3H, s)
12	77.1	3.68 (d, 7.4) 3.77 (dd, 7.4, 2.1)	78.4	3.65 (d, 7.5) 3.91 (dd, 7.5, 2.9)
13	19.5	1.12 (3H, s)	19.2	1.18 (3H, s)

Multiplicities and coupling constants in Hz are in the parentheses.

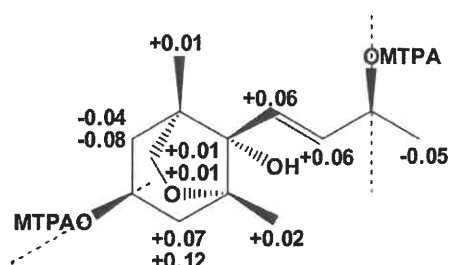


Fig. 6. Results of the Modified Mosher's Method of Compound 5
Figures are $\delta_{5b}-\delta_{5a}$ in ppm.

π NAP (Nacalai Tesque; $\Phi = 10$ mm, $L = 25$ cm, 4.0 mL/min) and Cosmosil PBr (Nacalai Tesque; $\Phi = 10$ mm, $L = 25$ cm, 4.0 mL/min)], and the eluate was monitored with photodiode array (200–400 nm) and refractive index monitors. Crude β -glucosidase (Sumizyme BGA) was a generous gift from Shin Nihon Chemical Co., Ltd. (Anjo, Aichi, Japan) (Lot No. 0930708-03). Crude naringinase was from Amano Enzyme Inc. (Nagoya, Aichi, Japan) as a gift (Lot No. NAG1252306). MTPAs were purchased from FUJIFILM Wako Pure Chemical Corporation (Osaka, Japan).

Plant Material Leaves of *D. maritima* were collected in Taketomi-cho, Yaeyama-gun, Okinawa, Japan, in November, 2003 and a voucher specimen was deposited in the Herbarium of Pharmaceutical Sciences, Graduate School of Biomedical and Health Sciences, Hiroshima University (03-DM-Okinawa-1105). The plant was identified by one of the authors (M.A.).

Extraction and Isolation Air-dried leaves of *D. maritima* (7.80 kg) were extracted with MeOH (45 L) three times. The MeOH extract was concentrated to 6 L and then washed with *n*-hexane (6 L, 245 g). The methanolic layer was concentrated to a viscous gum. The gummy mass was suspended in H₂O (6 L), and then partitioned with ethyl acetate (EtOAc) (6 L) and 1-butanol (1-BuOH) (6 L), successively, to give 397 g and 216 g of EtOAc and 1-BuOH-soluble fractions. The remaining water-layer was concentrated to give a H₂O-soluble fraction (245 g). The 1-BuOH-soluble fraction was subjected to a Diaion HP-20 CC ($\Phi = 80$ mm, $L = 50$ cm), and eluted with H₂O–MeOH (4:1, 5 L), (3:2, 5 L), (2:3, 5 L), and (1:4, 5 L), and MeOH (5 L), 1 L-fractions being collected.

The residue (17.5 g) in fractions 4–7 of a Diaion HP-20 CC was subjected to silica gel CC ($\Phi = 40$ mm, $L = 55$ cm), and eluted with CHCl₃ (3 L), CHCl₃–MeOH (99:1, 3 L), (49:1, 3 L), (97:3, 3 L), (19:1, 3 L), (37:3, 3 L), (9:1, 3 L), (7:1, 3 L), (17:3, 3 L), (33:7, 3 L), (4:1, 3 L), (3:1, 3 L), and (7:3, 3 L), 500 mL-fractions being collected. Compounds **6** (266 mg) and **5** (437 mg) were obtained in fractions 18–19 and 23–26, respectively.

The residue (29.2 g) in fractions 11–14 of a Diaion HP-20 CC was subjected to silica gel CC ($\Phi = 50$ mm, $L = 54.5$ cm), and eluted with CHCl₃ (3 L), CHCl₃–MeOH (99:1, 3 L), (49:1, 3 L), (97:3, 3 L), (19:1, 3 L), (37:3, 3 L), (9:1, 3 L), (7:1, 3 L), (17:3, 3 L), (33:7, 3 L), (4:1, 3 L), (3:1, 3 L), and (7:3, 3 L), 500 mL-fractions being collected. The residue (3.00 g out of 6.74 g) in fractions 57–65 of silica gel CC was separated by ODS CC ($\Phi = 50$ mm, $L = 25$ cm), and eluted with a linear gradient solvent system from MeOH–H₂O (1:9, 2 L) to MeOH–H₂O (9:1, 2 L), 10 g-fractions being collected. The residue

(160 mg) in fractions 223–234 was purified by HPLC (Inertsil ODS-3, H₂O–MeOH, 1:1) to give 36.4 mg of **3** from the peak at 10.2 min. The residue (88.1 mg) in fractions 240–249 was purified by HPLC (Cosmosil π NAP, H₂O–MeOH, 2:3) to give 32.8 mg of **4** from the peak at 10.2 min. The residue (2.81 g) in fractions 66–71 of silica gel CC was separated by ODS CC ($\Phi = 50$ mm, $L = 25$ cm), and eluted with a linear gradient solvent system from MeOH–H₂O (1:9, 2 L) to MeOH–H₂O (9:1, 2 L), 10 g-fractions being collected. The residue (136 mg) in fractions 106–129 was purified by HPLC (Cosmosil PBr, H₂O–MeOH, 3:2) to give 15.0 mg of **7** and 19.9 mg of **8** from the peaks at 25.0 min and 26.4 min, respectively.

The residue (64.5 g) in fractions 5–19 of a Diaion HP-20 CC was subjected to silica gel CC ($\Phi = 80$ mm, $L = 40$ cm), and eluted with CHCl₃ (6 L), CHCl₃–MeOH (99:1, 6 L), (49:1, 6 L), (97:3, 6 L), (19:1, 6 L), (37:3, 6 L), (9:1, 6 L), (7:1, 6 L), (17:3, 6 L), (33:7, 6 L), (4:1, 6 L), (3:1, 6 L), and (7:3, 6 L), 1 L-fractions being collected. The residue (3.00 g out of 12.3 g) in fractions 53–62 was separated by ODS CC ($\Phi = 50$ mm, $L = 25$ cm), and eluted with a linear gradient solvent system from MeOH–H₂O (1:9, 2 L) to MeOH–H₂O (9:1, 2 L), 10 g-fractions being collected. The residue (63.0 mg) in fractions 243–246 was purified by HPLC (Inertsil ODS-3, H₂O–MeOH, 3:7) to give 10.8 mg of **1** from the peak at 5.9 min. The residue (196 mg) in fractions 247–263 was purified by HPLC (Inertsil ODS-3, H₂O–MeOH–CH₃COOH, 7:13:0.1) to give 3.8 mg of **2** from the peak at 18.4 min.

Ebenamarioside A (1) Colorless amorphous powder, $[\alpha]_D^{25} +15.1$ ($c = 0.72$, MeOH); IR ν_{\max} (film) cm⁻¹: 3439, 2928, 2871, 1745, 1636, 1458, 1072; ¹H-NMR (600 MHz, pyridine-*d*₅): Table 1; ¹³C-NMR (150 MHz, pyridine-*d*₅): Table 2; HR-ESI-MS (positive-ion mode): m/z : 819.4499 [M + Na]⁺ (Calcd for C₄₂H₆₈O₁₄Na: 819.4501).

Ebenamarioside B (2) Colorless amorphous powder, $[\alpha]_D^{27} -5.6$ ($c = 0.43$, MeOH); IR ν_{\max} (film) cm⁻¹: 3393, 2936, 2872, 1686, 1043; ¹H-NMR (600 MHz, pyridine-*d*₅): Table 1; ¹³C-NMR (150 MHz, pyridine-*d*₅): Table 2; HR-ESI-MS (negative-ion mode): m/z : 795.4529 [M – H]⁻ (Calcd for C₄₂H₆₇O₁₄: 795.4525).

Ebenamarioside C (3) Colorless amorphous powder, $[\alpha]_D^{27} +14.0$ ($c = 0.10$, pyridine); IR ν_{\max} (film) cm⁻¹: 3353, 2927, 2876, 1705, 1045; ¹H-NMR (600 MHz, pyridine-*d*₅): Table 1; ¹³C-NMR (150 MHz, pyridine-*d*₅): Table 2; HR-ESI-MS (positive-ion mode): m/z : 835.4447 [M + Na]⁺ (Calcd for C₄₂H₆₈O₁₅Na: 835.4450).

Ebenamarioside D (4) Colorless amorphous powder, $[\alpha]_D^{26} -5.6$ ($c = 0.86$, MeOH); IR ν_{\max} (film) cm⁻¹: 3400, 2932, 2877, 1740, 1071; ¹H-NMR (600 MHz, pyridine-*d*₅): Table 1; ¹³C-NMR (150 MHz, pyridine-*d*₅): Table 2; HR-ESI-MS (positive-ion mode): m/z : 835.4449 [M + Na]⁺ (Calcd C₄₂H₆₈O₁₅Na: 835.4450).

Compound 5

Colorless amorphous powder, $[\alpha]_D^{26} +10.2$ ($c = 0.33$, MeOH); IR ν_{\max} (film) cm⁻¹: 3379, 2930, 2876, 1450, 1375, 1135, 1043; ¹H-NMR (600 MHz, CD₃OD): Table 3; ¹³C-NMR (150 MHz, CD₃OD): Table 3; HR-ESI-MS (positive-ion mode): m/z : 265.1411 [M + Na]⁺ (Calcd C₁₃H₂₂O₄Na: 265.1410).

Compound 6

Colorless syrup, $[\alpha]_D^{26}$ approx. 0.00 ($c = 0.81$, MeOH); IR ν_{\max} (film) cm⁻¹: 3414, 2932, 2877, 1715, 1455, 1242, 1042; ¹H-NMR (600 MHz, CD₃OD): Table 3; (CDCl₃) δ : 6.22 (1H,

dd, $J = 15.4, 5.4$ Hz, H-8), 5.91 (1H, dd, $J = 15.4, 1.2$ Hz, H-7), 4.45 (1H, qd, $J = 6.4, 5.4$ Hz, H-9), 3.91 (1H, dd, $J = 8.3, 3.0$ Hz, H-12a), 3.75 (1H, d, $J = 8.3$ Hz, H-12b), 2.65 (1H, d, $J = 18.3$ Hz, H-4a), 2.60 (1H, dd, $J = 18.3, 2.0$ Hz, H-4b), 2.55 (1H, dd, $J = 18.1, 3.0$ Hz, H-2a), 2.42 (1H, dd, $J = 18.1, 2.0$ Hz, H-2b), 1.33 (3H, d, $J = 6.4$ Hz, H₃-10), 1.21 (3H, s, H₃-13); 0.99 (3H, s, H₃-11); ¹³C-NMR (150 MHz, CD₃OD): Table 3; (CDCl₃) δ : 208.6 (C-3), 139.8 (C-8), 123.7 (C-7), 85.5 (C-5), 81.6 (C-6), 77.2 (C-12), 68.1 (C-9), 52.6 (C-4), 52.5 (C-2), 47.7 (C-1), 24.0 (C-10), 18.7 (C-13), 15.6 (C-11); CD ($c = 6.46 \times 10^{-5}$ M, MeOH) $\Delta\epsilon$ (nm): +0.64 (241), -0.30 (296); HR-ESI-MS (positive-ion mode): m/z : 263.1254 [M + Na]⁺ (Calcd C₁₃H₂₀O₄Na: 263.1254).

Sugar Analysis About 500 μ g each of 1–4 was hydrolyzed with 1 M HCl (0.1 mL) at 90°C for 2 h. The reaction mixtures were partitioned with an equal amount of EtOAc (0.1 mL), and the water layers were analyzed by HPLC with a chiral detector (JASCO OR-4090) on an amino column [InertSustain NH₂, 4.6 \times 250 mm (GL Science Inc.), CH₃CN–H₂O (4 : 1), flow rate: 1 mL/min]. All the hydrolyzates gave a peak for D-glucose at 10.9 min with positive optical rotation signs. The peaks were identified by co-chromatography with an authentic sample.

Enzymatic Hydrolysis of 1, 3 and 4 to 1a, 1b and 1c, 3a, 3b and 3c, and 4a, 4b and 4c, Respectively Ebenamari- oside A (1) (9.8 mg) in 1 mL of H₂O hydrolyzed with 15 mg of crude glucosidase at 37°C for 72 h. The reaction mixture was subjected to silica gel CC ($\Phi = 2$ cm, $L = 15$ cm) with increasing amounts of MeOH in CHCl₃ [CHCl₃–MeOH (9 : 1, 50 mL), (9 : 1, 100 mL to 7 : 3, 100 mL, linear gradient), (7 : 3, 50 mL) and (1 : 1, 100 mL)], 10-mL fractions being collected. An aglycone (1c) (2.8 mg) was obtained in fractions 5–6 and the monosaccharide mixture (1a and 1b) (5.5 mg) in fractions 9–12. The mixture fraction was purified by HPLC (ODS-3, H₂O–MeOH, 4 : 1) to give 1.9 mg of 1a and 3.0 mg of 1b from the peaks at 4.8 min and 8.7 min, respectively. Me- sembryanthenoidigenic acid 28-*O*- β -D-glucopyranosyl ester (1a): Amorphous powder, $[\alpha]_D^{25} +31.4$ ($c = 0.09$, MeOH), HR-ESI-MS (positive-ion mode) m/z : 657.3975 [M + Na]⁺ (Calcd for C₃₆H₅₈O₉Na: 657.3973)⁹; mesembryanthenoidigenic acid 30-*O*- β -D-glucopyranoside (1b): Amorphous powder, $[\alpha]_D^{25} +14.5$ ($c = 0.15$, MeOH), IR ν_{\max} (film) cm⁻¹: 3370, 2929, 2867, 1686, 1636, 1457, 1077; ¹H-NMR (600 MHz, pyridine-*d*₅) δ : 5.47 (1H, dd, $J = 3.3, 3.3$ Hz, H-12), 4.61 (1H, dd, $J = 11.7, 2.1$ Hz, H-6'a), 4.44 (1H, dd, $J = 11.7, 5.3$ Hz, H-6'b), 4.87 (1H, d, $J = 7.7$ Hz, H-1'), 4.28 (1H, dd, $J = 8.7, 8.4$ Hz, H-4''), 4.27 (1H, dd, $J = 8.4, 8.3$ Hz, H-3''), 4.10 (1H, dd, $J = 8.3, 7.7$ Hz, H-2''), 4.00 (1H, m, H-5''), 3.95 (1H, d, $J = 9.3$ Hz, H-29a), 3.46 (1H, dd, $J = 10.2, 5.6$ Hz, H-3), 3.44 (1H, d, $J = 9.3$ Hz, H-29b), 3.37 (1H, dd, $J = 13.6, 3.9$ Hz, H-18), 2.19 (1H, ddd, $J = 13.2, 13.0, 3.6$ Hz, H-15a), 2.12 (1H, ddd, $J = 13.0, 13.0, 3.0$ Hz, H-16a), 2.08 (1H, ddd, $J = 14.0, 14.0, 4.0$ Hz, H-22a), 2.04 (1H, dd, $J = 13.9, 13.8$ Hz, H-19a), 1.93 (3H, m, H₂-11 and H-16b), 1.84 (3H, m, H₂-2 and H-22b), 1.75 (1H, ddd, $J = 13.6, 13.3, 3.6$ Hz, H-21a), 1.66 (1H, dd, $J = 11.0, 6.7$ Hz, H-9), 1.57 (1H, m, H-6a), 1.56 (1H, m, H-1a), 1.51 (1H, ddd, $J = 12.6, 12.6, 3.5$ Hz, H-7a), 1.45 (1H, dd, $J = 13.6, 4.2$ Hz, H-19b), 1.43 (1H, m, H-21b), 1.38 (1H, m, H-6b), 1.33 (1H, m, H-7b), 1.26 (3H, s, H₃-27), 1.25 (3H, s, H₃-23), 1.21 (3H, s, H₃-30), 1.18 (1H, m, H-15b), 1.04 (3H, s, H₃-24), 1.03 (3H, s, H₃-26), 1.01 (1H, m, H-1b), 0.91 (3H, s, H₃-25), 0.87 (1H, brd, $J = 10.4$ Hz, H-5); ¹³C-NMR (150 MHz, pyridine-*d*₅): Table 2, HR-ESI-

MS (positive-ion mode) m/z : 633.4000 [M – H][–] (Calcd for C₃₆H₅₇O₉: 633.3997); mesembryanthenoidigenic acid (1c): $[\alpha]_D^{25} +24.9$ ($c = 0.14$, MeOH), HR-ESI-MS (positive-ion mode) m/z : 471.3473 [M – H][–] (Calcd for C₃₀H₄₇O₄: 471.3469)^{10,11}

Ebenamari- oside C (3) (9.5 mg) in 1 mL of H₂O was hydrolyzed with crude naringinase (15 mg) at 37°C for 72 h. The reaction mixture was subjected silica gel CC ($\Phi = 2$ cm, $L = 15$ cm) with increasing amounts of MeOH in CHCl₃ [CHCl₃–MeOH (9 : 1, 50 mL), (9 : 1, 100 mL to 7 : 3, 100 mL, linear gradient), (7 : 3, 50 mL) and (1 : 1, 100 mL)], 10-mL fractions being collected. 29-*O*- β -D-glucopyranosyl ester (3a) was obtained in fractions 11–13. Similarly ebenamari- oside C (3) (15 mg) in 1 mL of H₂O was hydrolyzed with crude β -glucosidase and silica gel CC with the same condition as above gave 5.2 mg of an aglycone (3c) and 5.6 mg of 29-*O*- β -D-glucopyranoside (3b) in fractions 5–8 and 11–13, respectively. 2 $\alpha,3\beta,29$ -Trihydroxyolean-12-en-28-oic acid 28-*O*- β -D-glucopyranosyl ester (3a): Amorphous powder, $[\alpha]_D^{24} +18.7$ ($c = 0.08$, MeOH), ¹³C-NMR (150 MHz, pyridine-*d*₅, MeOH-*d*₄ and DMSO-*d*₆): Table 1, HR-ESI-MS (positive-ion mode) m/z : 673.3922 [M + Na]⁺ (Calcd for C₃₆H₅₈O₁₀Na: 673.3922). 2 $\alpha,3\beta,29$ -Trihydroxyolean-12-en-28-oic acid 29-*O*- β -D-glucopyranoside (3b): Amorphous powder; $[\alpha]_D^{24} +9.6$ ($c = 0.28$, MeOH); IR ν_{\max} (film) cm⁻¹: 3379, 2934, 2872, 1687, 1459, 1050; ¹H-NMR (600 MHz, pyridine-*d*₅) δ : 5.43 (1H, dd, $J = 3.3, 3.3$ Hz, H-12), 4.87 (1H, d, $J = 7.7$ Hz, H-1'), 4.60 (1H, dd, $J = 11.8, 2.2$ Hz, H-6'a), 4.44 (1H, dd, $J = 11.8, 5.3$ Hz, H-6'b), 4.28 (2H, m, H-3'' and 4''), 4.10 (2H, m, H-2 and 2''), 4.00 (1H, m, H-5''), 3.94 (1H, d, $J = 9.1$ Hz, H-29a), 3.43 (1H, d, $J = 9.1$ Hz, H-29b), 3.40 (1H, d, $J = 9.6$ Hz, H-3), 3.35 (1H, dd, $J = 13.3, 3.1$ Hz, H-18), 2.25 (1H, dd, $J = 12.4, 4.2$ Hz, H-1a), 2.18 (1H, ddd, $J = 13.3, 13.0, 3.1$ Hz, H-15a), 2.10 (1H, m, H-11a), 2.05 (1H, m, H-22a), 2.01 (1H, m, H-19a), 1.98 (2H, m, H₂-16), 1.95 (1H, m, H-11b), 1.84 (1H, brd, $J = 13.6$ Hz, H-22b), 1.76 (1H, m, H-9), 1.75 (1H, m, H-21a), 1.56 (1H, m, H-6a), 1.51 (1H, m, H-7a), 1.43 (2H, m, H-19b and 21b), 1.38 (1H, m, H-6b), 1.31 (1H, m, H-7b), 1.28 (1H, m, H-1b), 1.27 (3H, s, H₃-23), 1.23 (3H, s, H₃-27), 1.21 (3H, s, H₃-30), 1.20 (1H, m, H-15b), 1.08 (3H, s, H₃-24), 1.02 (3H, s, H₃-26), 1.01 (1H, m, H-5), 0.99 (3H, s, H₃-25), ¹³C-NMR (150 MHz, pyridine-*d*₅): Table 2; HR-ESI-MS (positive-ion mode) m/z : 649.3951 [M – H][–] (Calcd for C₃₆H₅₇O₁₀: 649.3946). 2 $\alpha,3\beta,29$ -Trihydroxyolean-12-en-28-oic acid (3c): Amorphous powder; $[\alpha]_D^{24} +34.6$ ($c = 0.26$, MeOH); HR-ESI-MS (positive-ion mode) m/z : 487.3422 [M – H][–] (Calcd for C₃₀H₄₇O₅: 487.3418).

Ebenamari- oside C (4) (16.6 mg) in 1 mL of H₂O was hydrolyzed with crude β -glucosidase 37°C for 72 h. The reaction mixture was separated by silica gel CC with the same condition as above to give 4.1 mg of an aglycone (4c) and 9.4 mg of a mixture of two monoglucosidic compounds (4a and 4b) in fractions 5–8 and 10–15, respectively. The mixture was purified by HPLC (ODS-3, H₂O–MeOH, 4 : 1) to afford 6.3 mg of 28-*O*- β -D-glucopyranosyl ester (4a) and 1.9 mg of 30-*O*- β -D-glucopyranoside (4b) from the peaks at 3.9 min and 9.2 min, respectively. 2 $\alpha,3\beta,30$ -Trihydroxyurs-12-en-28-oic acid 28-*O*- β -D-glucopyranosyl ester (4a): Amorphous powder; $[\alpha]_D^{24} +17.9$ ($c = 0.31$, MeOH); IR ν_{\max} (film) cm⁻¹: 3373, 2925, 2877, 1732, 1456, 1073; ¹H-NMR (600 MHz, pyridine-*d*₅) δ : 6.31 (1H, d, $J = 8.1$ Hz, H-1'), 5.48 (1H, dd, $J = 3.4, 3.4$ Hz, H-12), 4.47 (1H, dd, $J = 11.8, 2.4$ Hz, H-6'a), 4.41 (1H, dd, $J = 11.8, 4.4$ Hz, H-6'b), 4.39 (1H, dd, $J = 9.5, 8.9$ Hz, H-4'),

4.31 (1H, dd, $J=8.9, 8.7$ Hz, H-3'), 4.23 (1H, dd, $J=8.7, 8.1$ Hz, H-2'), 4.11 (1H, ddd, $J=11.1, 9.6, 4.3$ Hz, H-2), 4.04 (1H, ddd, $J=9.5, 4.4, 2.4$ Hz, H-5'), 3.93 (1H, dd, $J=10.7, 2.9$ Hz, H-30a), 3.88 (1H, dd, $J=10.7, 5.6$ Hz, H-30b), 3.39 (1H, d, $J=9.4$ Hz, H-3), 2.65 (1H, d, $J=11.5$ Hz, H-18), 2.49 (1H, ddd, $J=13.8, 13.7, 4.4$ Hz, H-15a), 2.26 (1H, dd, $J=12.5, 4.4$ Hz, H-1a), 2.21 (1H, ddd, $J=13.5, 13.4, 4.2$ Hz, H-16a), 2.07 (1H, m, H-22a), 2.06 (1H, m, H-16b), 2.05 (2H, m, H₂-11), 2.01 (1H, m, H-19), 1.86 (2H, m, H₂-21), 1.84 (1H, m, H-22b), 1.74 (1H, dd, $J=10.0, 7.4$ Hz, H-9), 1.54 (1H, m, H-7a), 1.52 (1H, m, H-6a), 1.40 (1H, m, H-7b), 1.38 (1H, m, H-6b), 1.27 (1H, m, H-1b), 1.26 (3H, s, H₃-23), 1.20 (3H, s, H₃-27), 1.19 (3H, s, H₃-26), 1.18 (1H, m, H-15b), 1.16 (1H, m, H-20), 1.11 (3H, d, $J=6.4$ Hz, H₃-29), 1.09 (3H, s, H₃-24), 1.04 (3H, s, H₃-25), 1.01 (1H, d, $J=12.1$ Hz, H-5); ¹³C-NMR (150MHz, pyridine-*d*₅): Table 2; HR-ESI-MS (positive-ion mode) m/z : 673.3925 [M + Na]⁺ (Calcd for C₃₆H₅₈O₁₀Na: 673.3922).

2 α ,3 β ,30-Trihydroxyurs-12-en-28-oic acid 30-*O*- β -D-glucopyranoside (**4b**): Amorphous powder; $[\alpha]_D^{25} +5.5$ ($c=0.10$, MeOH); IR ν_{\max} (film) cm⁻¹: 3370, 2930, 2871, 1686, 1457, 1050; ¹H-NMR (600MHz, pyridine-*d*₅) δ : 5.45 (1H, dd, $J=3.1, 3.1$ Hz, H-12), 4.90 (1H, d, $J=7.8$ Hz, H-1'), 4.62 (1H, dd, $J=11.7, 2.2$ Hz, H-6'a), 4.45 (1H, dd, $J=11.7, 5.3$ Hz, H-6'b), 4.30 (1H, dd, $J=8.8, 8.9$ Hz, H-3''), 4.27 (1H, dd, $J=8.9, 8.9$ Hz, H-4''), 4.10 (1H, m, H-2), 4.09 (1H, m, H-2''), 4.07 (1H, m, H-30a), 4.03 (1H, m, H-5''), 3.89 (1H, dd, $J=9.5, 3.5$ Hz, H-30b), 3.40 (1H, d, $J=9.4$ Hz, H-3), 2.65 (1H, d, $J=11.3$ Hz, H-18), 2.32 (1H, ddd, $J=13.8, 13.8, 4.4$ Hz, H-15a), 2.24 (1H, dd, $J=12.5, 4.4$ Hz, H-1a), 2.07 (1H, m, H-16a), 2.04 (1H, m, H-21a), 2.03 (1H, m, H-22a), 2.02 (2H, m, H₂-11), 1.96 (1H, m, H-16b), 1.94 (1H, m, H-22b), 1.75 (2H, m, H-9 and 19), 1.66 (1H, m, H-21b), 1.55 (1H, m, H-6a), 1.54 (1H, m, H-7a), 1.39 (1H, m, H-20), 1.38 (1H, m, H-6b), 1.37 (1H, m, H-7b), 1.28 (3H, s, H₃-23), 1.28 (1H, m, H-1b), 1.17 (3H, s, H₃-27), 1.16 (1H, m, H-15b), 1.08 (3H, s, H₃-24), 1.04 (3H, s, H₃-26), 1.03 (1H, m, H-5), 1.01 (3H, d, $J=6.4$ Hz, H₃-29), 0.98 (3H, s, H₃-25); ¹³C-NMR (150MHz, pyridine-*d*₅): Table 2; HR-ESI-MS (positive-ion mode) m/z : 649.3948 [M - Na]⁻ (Calcd for C₃₀H₅₅O₁₀: 649.3946).

2 α ,3 β ,30-Trihydroxyurs-12-en-28-oic acid (**4c**): Amorphous powder; $[\alpha]_D^{25} +17.7$ ($c=0.13$, EtOH); HR-ESI-MS (positive-ion mode) m/z : 487.3423 [M - H]⁻ (Calcd for C₃₀H₄₇O₅: 487.3418).

Preparation of (R)- and (S)-MTPA Esters (5a and 5b) from 5 A solution of **5** (1.0mg) in 0.5mL of dry CH₂Cl₂ were reacted with (*R*)-MTPA (21.5mg) in the presence of 1-ethyl-3-(3-dimethylaminopropyl)carbodiimide hydrochloride (EDC) (13.4mg) and *N,N*-dimethyl-4-aminopyridine (4-DMAP) (16.1mg). The mixture was then occasionally stirred at 37°C for 24h. After the addition of CHCl₃ (1.5mL), the reaction mixture was successively washed with H₂O (1mL), 1M HCl (1mL), NaHCO₃-saturated H₂O (1mL), and brine (1mL). The organic layer was dried with Na₂SO₄ and evaporated under reduced pressure. The residue was purified by preparative TLC [silica gel (0.25mm thickness), being applied for 8cm width, with development with CHCl₃-MeOH (19:1) for 9cm and then eluting with CHCl₃-MeOH (1:1)] to furnish an ester **5a** (0.5mg) from the band at $R_f=0.67$. Through the same procedure, **5b** (0.6mg, $R_f=0.59$) were prepared from **5** (1.0mg) using (*S*)-MTPA (25.4mg), EDC (15.8mg), and 4-DMAP (15.5mg), respectively.

(*R*)-MTPA ester of **5** (**5a**): amorphous powder; ¹H-NMR (600MHz, CDCl₃) δ : 7.35–7.55 (5H, m, aromatic protons), 6.05 (1H, d, $J=15.2$ Hz, H-7), 6.02 (1H, dd, $J=15.2, 4.9$ Hz, H-8), 5.66 (1H, qd, $J=6.5, 4.9$ Hz, H-9), 5.44 (1H, dddd, $J=10.5, 10.5, 7.2, 7.2$ Hz, H-3), 3.87 (1H, d, $J=8.2$ Hz, H-12a), 3.77 (1H, dd, $J=8.2, 2.0$ Hz, H-12b), 3.53 (3H, s, -OMe), 3.51 (3H, s, -OMe), 2.18 (1H, ddd, $J=13.6, 7.2, 1.5$ Hz, H-4), 2.03 (1H, ddd, $J=13.6, 7.2, 1.5$ Hz, H-2), 1.73 (1H, dd, $J=13.6, 10.5$ Hz, H-4), 1.70 (1H, ddd, $J=13.6, 10.5, 2.0$ Hz, H-2), 1.45 (3H, d, $J=6.5$ Hz, H₃-10), 1.08 (3H, s, H₃-13), 0.90 (3H, s, H₃-11); HR-ESI-MS (positive-ion mode) m/z : 697.2206 [M + Na]⁺ (Calcd for C₃₃H₃₆O₈F₆Na: 697.2207).

(*S*)-MTPA ester of **5** (**5b**): amorphous powder; ¹H-NMR (600MHz, CDCl₃) δ : 7.35–7.55 (10H, m, aromatic protons), 6.11 (1H, d, $J=15.5$ Hz, H-7), 6.08 (1H, dd, $J=15.5, 5.5$ Hz, H-8), 5.63 (1H, qd, $J=6.5, 5.5$ Hz, H-9), 5.44 (1H, dddd, $J=10.7, 10.7, 7.1, 7.1$ Hz, H-3), 3.88 (1H, d, $J=8.3$ Hz, H-12a), 3.78 (1H, dd, $J=8.3, 2.1$ Hz, H-11b), 3.52 (3H, s, -OMe), 3.49 (3H, s, -OMe), 2.25 (1H, ddd, $J=13.6, 7.1, 1.5$ Hz, H-4), 1.99 (1H, ddd, $J=13.6, 7.1, 1.5$ Hz, H-2), 1.85 (1H, ddd, $J=13.6, 10.7$ Hz, H-4), 1.62 (1H, ddd, $J=13.6, 10.7, 2.1$ Hz, H-2), 1.40 (3H, d, $J=6.5$ Hz, H₃-10), 1.10 (3H, s, H₃-13), 0.91 (3H, s, H₃-11); HR-ESI-MS (positive-ion mode) m/z : 697.2206 [M + Na]⁺ (Calcd for C₃₃H₃₆O₈F₆Na: 697.2207).

NaBH₄ Reduction of 6 To a solution of **6** (11.0mg) in MeOH (1mL) was added 8.2mg of NaBH₄ and the reaction mixture was stirred for 5min at 25°C. Excess NaBH₄ was quenched by the addition of 1mL of acetone and then the reaction mixture was evaporated to dryness. The resultant residue was purified by HPLC [Inertsil ODS-3, 6×250mm, H₂O–MeOH (1:4), flow rate: 1.6mL/min] to give 3.1mg of **6c** (=5) and 5.8mg of **6d** from the peaks at 10.9min and 13.3min, respectively.

Compound **6c**: amorphous powder; $[\alpha]_D^{24} +7.1$ ($c=0.31$, MeOH); HR-ESI-MS (positive-ion mode) m/z : 265.1409 [M + Na]⁺ (Calcd for C₁₃H₂₂O₄Na: 265.1410).

Compound **6d**: amorphous powder; $[\alpha]_D^{24} -5.5$ ($c=0.29$, MeOH); IR ν_{\max} (film) cm⁻¹: 3402, 2929, 2889, 1604, 1453, 1381, 1101, 1053; ¹H-NMR (600MHz, CD₃OD) δ : 6.02 (1H, dd, $J=15.5, 5.6$ Hz, H-8), 5.82 (1H, dd, $J=15.5, 1.0$ Hz, H-7), 4.33 (1H, qd, $J=6.4, 5.6$ Hz, H-9), 4.12 (1H, d, $J=6.9$ Hz, H-12a), 4.02 (1H, dd, $J=5.7, 5.7$ Hz, H-3), 3.76 (1H, dd, $J=6.9, 2.3$ Hz, H-12b), 2.13 (1H, dd, $J=15.5, 5.7$ Hz, H-4a), 2.02 (1H, ddd, $J=15.3, 5.7, 2.2$ Hz, H-2a), 1.84 (1H, dd, $J=15.5, 2.2$ Hz, H-4b), 1.73 (1H, dd, $J=15.3, 2.3$ Hz, H-2b), 1.25 (3H, d, $J=6.4$ Hz, H₃-10), 1.13 (3H, s, H₃-13), 0.86 (3H, s, H₃-11); ¹³C-NMR (150MHz, CD₃OD) δ : 139.4 (C-8), 126.8 (C-7), 87.2 (C-5), 82.5 (C-6), 76.3 (C-12), 69.1 (C-9), 66.0 (C-3), 48.0 (C-1), 45.1 (C-4), 44.9 (C-2), 24.1 (C-10), 19.7 (C-13), 16.3 (C-11); HR-ESI-MS (positive-ion mode) m/z : 265.1408 [M + Na]⁺ (Calcd for C₁₃H₂₂O₄Na: 265.1410).

Cytotoxic Activity toward Human Lung Adenocarcinoma, A549 Cells Cytotoxic activity toward lung adenocarcinoma cells was determined by colorimetric cell viability assay using 3-(4,5-dimethylthiazol-2-yl)-2,5-diphenyltetrazolium bromide (MTT). Lung adenocarcinoma cell line A549 was purchased from the JCRB Cell Bank, Japan. A549 cells were cultured in Dulbecco's modified Eagle's medium supplemented with 10% heat inactivated FCS, and kanamycin (100 μ g/mL) and amphotericin B (5.6 μ g/mL). In a 96-well plate, 1 μ L aliquots of sample solutions and the cancer cells

(5×10^3 cells/well) in $100 \mu\text{L}$ medium were added to each well, and then the plate incubated at 37°C under a 5% CO_2 atmosphere for 72 h. A solution ($100 \mu\text{L}$) of MTT (0.5 mg/mL) was then added to each well and the incubation was continued for a further 1 h. The absorbance of each well was measured at 540 nm using a Molecular Devices Versamax tunable microplate reader. DMSO was used as a negative control and doxorubicin as a positive control. The cytotoxic activity was calculated as:

$$\% \text{ inhibition} = [1 - (A_{\text{test}} - A_{\text{blank}}) / (A_{\text{control}} - A_{\text{blank}})] \times 100$$

where A_{control} is the absorbance of the control DMSO well, A_{test} the absorbance of the test wells, and A_{blank} the absorbance of the cell-free wells.

Anti-Leishmania Activity The anti-*Leishmania major* activity toward promastigotes was determined by the colorimetric cell viability MTT assay. The promastigotes at the logarithmic growth phase were cultured in M199 medium supplemented with 10% heat-inactivated fetal bovine serum and $100 \mu\text{g/mL}$ of kanamycin. In a 96-well plate, $1 \mu\text{L}$ aliquot of sample solutions and *L. major* cells (1×10^5 cells/well) in $100 \mu\text{L}$ medium were added to each well, and then the plate was incubated at 27°C under an ambient atmosphere for 72 h. A solution of MTT ($100 \mu\text{L}$) was then added to each well and the incubation was continued overnight. The formazan product of MTT reduction was then dissolved in DMSO and then the absorbance was measured using a Molecular Devices Versamax tunable microplate reader. DMSO was used as a negative control and amphotericin B as a positive control. The experiment was performed in triplicate. The anti-*Leishmania major* activity was quantified as the percentage of the control absorbance of reduced dye at 540 nm. The inhibitory activity was calculated as:

$$\% \text{ inhibition} = [1 - (A_{\text{test}} - A_{\text{blank}}) / (A_{\text{control}} - A_{\text{blank}})] \times 100$$

where A_{control} is the absorbance of the control (DMSO) well, A_{test} the absorbance of the test wells, and A_{blank} the absorbance of the cell-free wells.

Acknowledgments The measurements of HR-ESI-MS were performed with LTQ Orbitrap XL spectrometer at the Natural Science Center for Basic Research and Development (N-BARD), Hiroshima University. This work was supported in part by Grants-in-Aid from the Ministry of Education, Culture, Sports, Science and Technology of Japan, and the

Japan Society for the Promotion of Science (Nos. 22590006, 23590130, 25860078, 15H04651, 17K08336 and 18K06740).

Conflict of Interest The authors declare no conflict of interest.

Supplementary Materials The online version of this article contains supplementary materials.

References

- Hatusima S., "Flora of the Ryukyus. Added and Corrected," The Biological Society of Okinawa, Naha, 1975 p. 474.
- Higa M., Ogihara K., Yogi S., *Chem. Pharm. Bull.*, **46**, 1189–1193 (1998).
- Higa M., Noha N., Yokaryo H., Ogihara K., Yogi S., *Chem. Pharm. Bull.*, **50**, 590–593 (2002).
- Higa M., Takashima Y., Yokaryo H., Harie Y., Suzuka T., Ogihara K., *Chem. Pharm. Bull.*, **65**, 739–745 (2017).
- Suwama T., Watanabe K., Monthakantirat O., Luecha P., Noguchi H., Watanabe K., Umehara K., *J. Nat. Med.*, **72**, 220–229 (2018).
- Kawakami S., Nishida S., Nobe A., Inagaki M., Nishimura M., Matsunami K., Otsuka H., Aramoto M., Hyodo T., Yamaguchi K., *Chem. Pharm. Bull.*, **66**, 1057–1064 (2018).
- Kazuma K., Noda N., Suzuki M., *Phytochemistry*, **62**, 229–237 (2003).
- Dini I., Tenore G. C., Dini A., *Food Chem.*, **84**, 163–168 (2004).
- Yin M., Wang X., Wang M., Chen Y., Dong Y., Zhao Y., Feng X., *Chem. Nat. Compd.*, **48**, 258–261 (2012).
- Tursch R., Leclercq J., Chiurdoglu G., *Tetrahedron Lett.*, **6**, 4161–4166 (1965).
- Magina M. D. A., Dalmarco E. M., Dalmarco J. B., Colla G., Pizzolatti M. G., Brighente I. M. C., *Quim. Nova*, **35**, 1184–1188 (2012).
- Tabopda T. K., Ngoupayo J., Tanoli S. A. K., Mitaine-Offer A.-C., Ngadjui B. T., Ali M. S., Luu B., Lacaille-Duboi M.-A., *Planta Med.*, **75**, 522–527 (2009).
- Wang J., Ren H., Xu Q.-L., Zhou Z.-Y., Wu P., Wei X.-Y., Cao Y., Chen X.-X., Tan J.-W., *Food Chem.*, **168**, 623–629 (2015).
- Feng X., Li D.-P., Zhang Z.-S., Chu Z.-Y., Luan J., *Nat. Prod. Res.*, **28**, 1879–1886 (2014).
- Ohtani I., Kusumi T., Kashman Y., Kakisawa H., *J. Am. Chem. Soc.*, **113**, 4092–4096 (1991).
- Abe F., Yamauchi T., *Chem. Pharm. Bull.*, **48**, 1908–1911 (2000).
- Powell R. G., Smith, Jr. C. R., *J. Nat. Prod.*, **44**, 86–90 (1981).
- Çalış İ., Kuruüzüm-Uz A., Lorenzetto P. A., Rüedi P., *Phytochemistry*, **59**, 451–457 (2002).
- Milborrow B. V., *Phytochemistry*, **14**, 1045–1053 (1975).
- Cheng Y.-X., Zhou J., Deng S.-M., Tan N.-H., *Planta Med.*, **68**, 91–94 (2002).

Note

Temperature-Dependent Formation of *N*-Nitrosodimethylamine during the Storage of Ranitidine Reagent Powders and Tablets

Yasuhiro Abe,[#] Eiichi Yamamoto,[#] Hiroyuki Yoshida, Akiko Usui, Naomi Tomita, Hitomi Kanno, Sayaka Masada, Hidetomo Yokoo, Genichiro Tsuji, Nahoko Uchiyama, Takashi Hakamatsuka, Yosuke Demizu, Ken-ichi Izutsu,* Yukihiko Goda, and Haruhiro Okuda

National Institute of Health Sciences; 3–25–26 Tonomachi, Kawasaki-ku, Kawasaki 210–9501, Japan.

Received May 19, 2020; accepted July 22, 2020; advance publication released online August 8, 2020

The purpose of this study was to elucidate the effect of high-temperature storage on the stability of ranitidine, specifically with respect to the potential formation of *N*-nitrosodimethylamine (NDMA), which is classified as a probable human carcinogen. Commercially available ranitidine reagent powders and formulations were stored under various conditions, and subjected to LC-MS/MS analysis. When ranitidine tablets from two different brands (designated as tablet A and tablet B) were stored under accelerated condition (40 °C with 75% relative humidity), following the drug stability guidelines issued by the International Conference on Harmonisation (ICH-Q1A), for up to 8 weeks, the amount of NDMA in them substantially increased from 0.19 to 116 ppm and from 2.89 to 18 ppm, respectively. The formation of NDMA that exceeded the acceptable daily intake limit (0.32 ppm) at the temperature used under accelerated storage conditions clearly highlights the risk of NDMA formation in ranitidine formulations when extrapolated to storage under ambient conditions. A forced-degradation study under the stress condition (60 °C for 1 week) strongly suggested that environmental factors such as moisture and oxygen are involved in the formation of NDMA in ranitidine formulations. Storage of ranitidine tablets and reagent powders at the high temperatures also increased the amount of nitrite, which is considered one of the factors influencing NDMA formation. These data indicate the necessity of controlling/monitoring stability-related factors, in addition to controlling impurities during the manufacturing process, in order to mitigate nitrosamine-related health risks of certain pharmaceuticals.

Key words *N*-nitrosodimethylamine (NDMA); ranitidine; forced degradation; storage; impurity

Introduction

In 2018, the finding of *N*-nitrosodimethylamine (NDMA) and other nitrosamines in multiple valsartan and angiotensin II receptor blocker (ARB) formulations triggered concern about trace impurities of probable human carcinogens in these widely used pharmaceutical products.¹⁾ Regulatory agencies collaborated to analyze impurities in the products, investigate the cause, and enact several measures, including establishment of interim criteria for distribution, in order to mitigate the potential risk. Analysis by HPLC, GC-MS, and/or LC-MS/MS indicated unacceptable amounts of NDMA in some active pharmaceutical ingredients (APIs) and their drug products.^{2–5)} Interim criteria to control the levels of mutagenic impurities (*e.g.*, NDMA and *N*-nitrosodiethylamine (NDEA)) were established on the basis of acceptable daily exposure limits to the particular compound and the drug's maximum daily dose, following the International Conference on Harmonisation (ICH) M7 guideline.^{1,6–8)}

Ranitidine and other H₂-receptor antagonists (*e.g.*, nizatidine) represent another group of pharmaceuticals with similar nitrosamine contamination issue.⁹⁾ In 2019, multiple products were recalled from the market after varying amounts of NDMA were found in some APIs and tablets.^{9–12)} The intrinsically unstable nature and ternary amine structure of ranitidine raised some questions regarding the cause of impurity found in the products; it is of particular interest whether the NDMA

is formed during storage of solid formulations of ranitidine HCl (Fig. 1). Ranitidine HCl readily degrades during the storage of the solids at elevated temperature and humidity.^{13–16)} The stability of ranitidine APIs and formulations had been assessed using accelerated stress tests during drug development in the 1980s, but the risk of formation of NDMA impurities at sub-ppm levels was not explored. The potential of NDMA formation during storage was suggested in an Australian regulatory report in 2019. The report showed that some products that were nearing their expiration dates had higher levels of NDMA than products that were newer.¹⁰⁾ The observation of elevated NDMA level by GC-based analysis of ranitidine products in another study also suggested degradation-related NDMA formation from ranitidine.¹⁷⁾ Forced degradation studies, especially those profiling degradation products, performed under relevant stress conditions are expected to provide valuable information for predicting potential drug changes during storage at ambient temperatures.¹⁸⁾ However, to the best of our knowledge, no experimental data have been reported on possible NDMA formation during the storage of ranitidine formulations.

Several theories have been proposed regarding factors affecting NDMA formation. The European Medicines Agency (EMA) reported that NDMA could be generated when dimethylamine released from ranitidine is exposed to a source of nitrite (*e.g.*, sodium nitrite).¹⁹⁾ Environmental health studies have reported that chloramination of water leads to the production of NDMA from ranitidine and other tertiary amine

[#]These authors contributed equally to this work.

*To whom correspondence should be addressed. e-mail: izutsu@nihs.go.jp

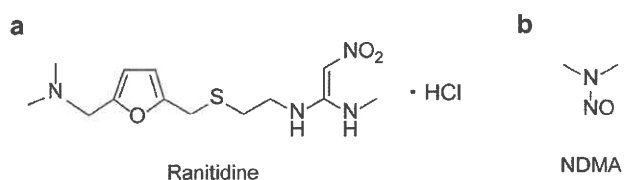


Fig. 1. Chemical Structure of (a) Ranitidine HCl and (b) *N*-Nitrosodimethylamine (NDMA)

compounds.^{20–23} There are also conflicting reports regarding possible NDMA formation due to the reaction of ranitidine with nitrite in the gastrointestinal tract after oral ingestion.^{9,24}

In the present study, forced degradation of ranitidine HCl-containing reagent powders and ethical tablet formulations, which were commercially available in Japan, was performed for short durations under high-temperature storage conditions to assess possible NDMA formation.

Experimental

Chemicals and Reagents The NDMA standard (>99.0% purity) was purchased from FUJIFILM Wako Pure Chemical Corporation (Osaka, Japan), and deuterium-labeled NDMA (NDMA-*d*₆), the internal standard (IS), was purchased from AccuStandard (New Haven, CT, U.S.A.). Ranitidine HCl reagent powders were obtained from Cayman Chemical (Ann Arbor, MI, U.S.A.) and Toronto Research Chemicals (Toronto, Ontario, Canada). Two pharmaceutical formulations of ranitidine tablet 150 mg, which are commercially available in Japan, were also used in this study. Methanol and dimethyl sulphoxide (DMSO) were purchased from Kanto Chemical Corporation (Tokyo, Japan). Acetonitrile, formic acid, ammonium acetate, and the nitrite reference standard were purchased from FUJIFILM Wako Pure Chemical Corporation.

Storage of Samples at High Temperatures Ranitidine tablets in push-through packages and ranitidine reagent powders (approximately 250 mg) in glass vials with hermetic caps were stored in a storage chamber (CSH-112, Espec Corp., Osaka, Japan) controlled at 40 or 50 °C with 75% relative humidity (RH) for up to 8 weeks. For a subset of ranitidine reagent powders (vacuumed sample), the headspace air in the vial was removed by using a freeze dryer (FreeZZone 6; Lab-conco, Kansas City, MO, U.S.A.). Ranitidine reagent powders kept in open, hermetically sealed (closed), and vacuum vials were then subjected to a forced-degradation study under high-temperature conditions (60 °C/50% RH) for 1 week.

Headspace-GC-MS (HS-GC-MS) Analysis Ranitidine tablets were ground to a fine powder using an agate mortar and 250 mg of the tablet powder was weighed into a 10-mL headspace vial. One hundred and twenty-five microliters of NDMA-*d*₆ solution (10 µg/mL in DMSO) and DMSO was added to vial to make a total volume of 2.5 mL and the vial was immediately capped and crimped. The vial was shaken for 30 min using a mechanical shaker, and then subjected to HS-GC/MS analysis.

NDMA was analyzed using a GC-MS system (7890B/5977B; Agilent Technologies, Palo Alto, CA, U.S.A.) operated in the electron ionization mode (70 eV). The headspace oven temperature was operated isothermally within the range of 80–110 °C for 10 min. The vial equilibration and injection times were set at 10 and 1 min, respectively. The GC injector was operated at

Table 1. Multiple Reaction Monitoring Transition for NDMA and NDMA-*d*₆

Analyte	Precursor ion (<i>m/z</i>)	Product ion (<i>m/z</i>)	Q1 Pre bias	Collision energy	Q3 Pre bias
NDMA	75.09	43.10	–15.0	–18.0	–15.0
NDMA- <i>d</i> ₆ (IS)	81.09	46.15	–15.0	–16.0	–16.0

220 °C with a 5:1 split ratio. Helium was used as the carrier gas at a constant flow rate of 3 mL/min. A DB-WAX capillary column (30 m × 0.25 mm, film thickness: 0.25 µm; Agilent Technologies) was used with the following oven program: hold at 70 °C for 4 min, ramp from 70 to 110 °C at 10 °C/min, ramp from 110 to 240 °C at 20 °C/min, and then held at 240 °C for 2 min. The MS transfer line temperature was maintained at 250 °C. The mass spectrometer was operated in the selected ion monitoring (SIM) mode. For NDMA detection, *m/z* 42 and 74 were used for confirmation and quantification, respectively. For NDMA-*d*₆ detection, *m/z* 46 and 80 were used for confirmation and quantification, respectively.

LC-MS/MS Analysis Approximately 75 mg of ranitidine reagent powder was weighed into a polypropylene tube and 0.25 mL of NDMA-*d*₆ solution (25 µg/mL in 20% methanol) and 1.0 mL of 20% methanol were added. Two ranitidine tablets (150 mg each) were placed in a polypropylene tube and 1.0 mL of NDMA-*d*₆ solution (25 µg/mL in 20% methanol) and 4.0 mL of 20% methanol were added. After vigorous shaking followed by centrifuge filtration using a 0.22-µm centrifugal filter unit (Ultrafree-MC-GV polyvinylidene difluoride (PVDF); Merck Millipore, Billerica, MA, U.S.A.), the amount of NDMA present in the filtrate was determined by LC-MS/MS.

LC separations were performed on a Nexera LC-40 ultra-high performance liquid chromatography system (Shimadzu, Kyoto, Japan) with a Shimpack ARATA C18 column (3.0 × 75 mm, 2.2-µm particle size, 12-nm pore size). Mobile phase A consisted of water–acetonitrile–formic acid (990:10:1, v/v/v) and mobile phase B consisted of water–acetonitrile–formic acid (100:900:1, v/v/v). The flow rate and column temperature were 450 µL/min and 40 °C, respectively, and the injection volume was 5 µL. A linear gradient was used for elution, consisting of mobile phase B from 0 to 1% in 1 min, 1 to 30% in 0.25 min, and 30% for 1.25 min. The column was then equilibrated for 4 min with mobile phase A. Mass spectrometric detection was performed on a Shimadzu LCMS8060 tandem mass spectrometer with an electrospray ionization source in the positive ion mode. The nebulizer gas flow rate was 3 L/min. The interface, desolvation tube, and heating block temperatures were 300, 250, and 400 °C, respectively, and the drying gas flow rate was 10 L/min. Multiple reaction monitoring transitions for the analytes are shown in Table 1.

The method was linear ($R^2 > 0.999$) in the range of 1–50000 ng/mL. The limit of quantification (LOQ) was 1 ng/mL (0.03 ppm) with a signal-to-noise (*S/N*) ratio of ≥10. The recovery rate of NDMA spiked at three concentrations (3.5, 10, and 50 ng/mL) was 93–102%, with a relative standard deviation of 0.26–0.99% ($n = 3$).

Ion Chromatography Analysis Ranitidine tablets and powders dissolved in purified water (3 mg/mL) were dechlorinated using a MetaSep Ag SPE column (GL Sciences, Tokyo,

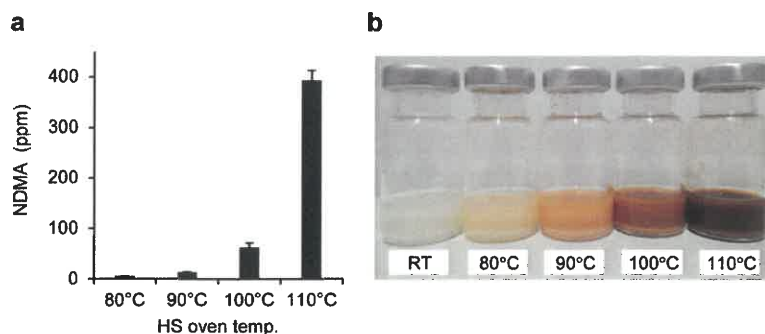


Fig. 2. Effect of Headspace Oven Temperature on HS-GC-MS Analysis of NDMA in Ranitidine Tablets

(a) Amount of NDMA produced under various heating conditions in the headspace (HS) oven. Each result represents the mean \pm standard deviation (S.D.) ($n = 3$). (b) Changes in visual appearance after 10 min of HS oven equilibration at various temperatures. (Color figure can be accessed in the online version.)

Japan), and then centrifuged with a 0.22- μm centrifugal filter unit (Ultrafree-MC-GV PVDF). Nitrite ion levels in the filtrates were determined by ion chromatography using a Dionex Integriion HPLC System (Thermo Scientific, San Jose, CA, U.S.A.) equipped with an IonPac AG19-4 μm guard column (4 \times 50 mm), an IonPac AS19-4 μm anion exchange column (4 \times 250 mm), an anion dynamically regenerated suppressor (4 mm), and a UV detector (214 nm). Ten microliters of sample was used for all injections. The mobile phase was produced using an electrochemical potassium hydroxide (KOH) eluent generator. For KOH gradient elution, the concentration was maintained at 20 mM for the first 12 min, increased to 80 mM over 4 min, and then maintained for 14 min. The flow rate and column temperature were 0.8 mL/min and 30 °C, respectively. A six-point calibration curve of nitrite ion standard was prepared from 0.005 to 1.0 ppm for which the R^2 values were >0.999 . The LOQ of this method was estimated to be 1.67 ppm with an S/N ratio of ≥ 10 .

Results and Discussion

Rapid Forced-Degradation Study by HS-GC-MS The HS-GC-MS analysis was initially used to clarify the cause for a high amount of NDMA being found on GC-MS analysis of ranitidine tablets in previous report.¹⁷⁾ Figure 2a shows the amount of NDMA detected under various heating conditions (80–110 °C) in the headspace oven for 10 min. The amount of NDMA sharply increased upon exposure to temperatures above 100 °C. Browning of the formulation was also observed in a temperature dependent manner (Fig. 2b). These data indicate that ranitidine decomposes on heating and that NDMA is generated during headspace equilibration. The results confirmed that HS-GC-MS is not suitable for the accurate quantification of NDMA because sample heating generates NDMA in the extremely high-temperature headspace and/or other part of the systems. However, HS-GC-MS may provide a simple method for rapid screening of other drugs that has potential risk of NDMA formation. For example, the HS-GC-MS analysis of nizatidine, which is structurally similar to ranitidine, showed an apparent formation of NDMA by heating at 130 °C (Fig. S1). Nizatidine may be more thermostable than ranitidine, as the amount of NDMA generated by heating of nizatidine tablet was much lower than that obtained with ranitidine. In the subsequent experiments, we performed LC-MS/MS analysis to avoid heat treatment-induced sample decomposition during the measurement.

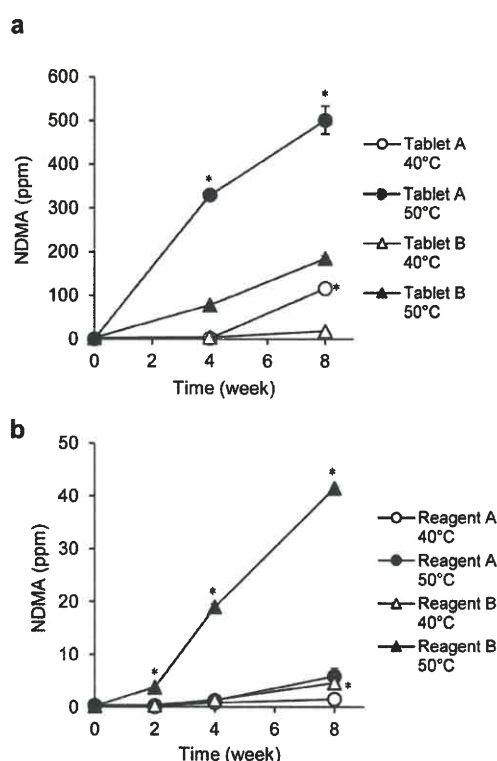


Fig. 3. NDMA Formation in Ranitidine Samples during 8 Weeks of Storage under Accelerated and Stress Conditions

The amount of NDMA in (a) ranitidine tablets and (b) ranitidine reagent powders stored at 40 °C/75% RH or 50 °C/75% RH were measured by LC-MS/MS. Each result represents the mean \pm S.D. ($n = 3$). * $p < 0.005$; (a) vs. tablet B, (b) vs. reagent A compared at the same storage conditions by Student's t -test.

NDMA Formation from Ranitidine under Accelerated Stress Conditions The potential formation of NDMA during the storage of ranitidine tablets and reagent powders was evaluated under accelerated stress conditions following the guidelines issued by the ICH. According to the notifications from the Ministry of Health, Labour and Welfare of Japan and the U.S. Food and Drug Administration (FDA), the accepted daily intake limit for NDMA in ranitidine drug substance was set to be 0.32 ppm (0.32 μg of NDMA in 1 g of ranitidine) based on the maximum daily dose of ranitidine (300 mg/d).^{12,25)} Two ranitidine tablet formulations found to have NDMA levels below (tablet A) and above (tablet B) the limit in preliminary

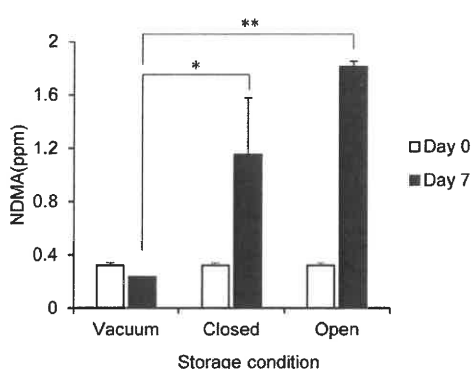


Fig. 4. Forced-Degradation Study of Ranitidine Reagent Powder A Stored under Various Environmental Conditions at 60 °C

Ranitidine reagent powders were stored in glass vials with (closed) or without (open) caps at 60 °C/50% RH and was then subjected to NDMA measurement by LC-MS/MS. Samples devoid of moisture/oxygen (vacuum) were also used in this study. Each result represents the mean \pm S.D. ($n = 3$). * $p < 0.05$; ** $p < 0.001$; compared with the vacuum sample on each day by Student's *t*-test.

studies were used in the storage study. The NDMA level in ranitidine tablet A was below the acceptable limit (0.32 ppm) on day 0, but increased to 1.42 and 116 ppm after 4 and 8 weeks, respectively, when stored at 40 °C/75% RH (Fig. 3a). In addition, more NDMA was produced under storage conditions of 50 °C/75% RH and exceeded 500 ppm after 8 weeks. Ranitidine tablet B contained a higher amount of NDMA (2.89 ppm) at the beginning of the study than tablet A. However, the level of NDMA generated from tablet B after 8 weeks storage at 40 and 50 °C was less than that from tablet A (Fig. 3a). Storage of the two ranitidine reagent powders at 40 and 50 °C for 8 weeks induced the production of smaller and different amounts of NDMA (Fig. 3b). We also observed browning of the ranitidine tablets and reagent powders after 8 weeks of storage at 40–50 °C (data not shown).

The formation of NDMA at levels above the official limit even in the samples stored for 4 or 8 weeks under the ICH-recommended accelerated stability testing conditions clearly indicates the risk of its formation during storage of the products at ambient temperatures. The preliminary result of the storage study was shared by regulatory bodies. The FDA recently requested the removal of all ranitidine products from the market because of the increasing amounts of NDMA noted in some ranitidine products over time and when stored at temperatures higher than room temperature, which may result in consumer exposure to NDMA levels above acceptable limits.²⁶⁾ These findings also indicate the relevance of the regulatory decisions to stop the distribution of ranitidine products.

Factors Affecting the Formation of NDMA Various factors including differences in storage conditions (*e.g.*, humidity, oxygen, and temperature), solid-state forms (*e.g.*, crystal form) and their physicochemical properties, and drug formulations (*e.g.*, excipients, impurities, residual water, tablet/powder form, and coatings), may affect NDMA formation. In order to clarify the impact of these potential factors, the effect of storage conditions (humidity and oxygen) on NDMA formation was studied by storing ranitidine reagent powder A in open/closed/vacuum vials at 60 °C/75% RH for 1 week. The amount of NDMA newly formed during storage in the vacuum vial, in which the air has been removed and hermetically sealed with a lid to prevent moisture/oxygen infiltration, was much

Table 2. Amount of Nitrite Ion in Ranitidine after High-temperature Storage for 8 Weeks

Storage conditions	Nitrite ion (ppm)		
	Day 0	8 weeks 40 °C/75% RH	8 weeks 50 °C/75% RH
Ranitidine tablet A	11.1 \pm 1.0	300.3 \pm 5.1	155.3 \pm 0.7
Ranitidine tablet B	25.9 \pm 0.6	186.3 \pm 10.8	177.7 \pm 2.0
Ranitidine reagent A	9.2 \pm 1.3	16.0 \pm 1.4	42.2 \pm 1.4
Ranitidine reagent B	25.4 \pm 0.9	58.5*	117.9*

Each result represents the mean \pm S.D. ($n = 3$), * $n = 1$

less than that in the closed and open vials (Fig. 4). These data suggest that the formation of NDMA in ranitidine is triggered by exposure to the atmosphere (*e.g.*, moisture and oxygen), as well as by high-temperature conditions. The variation in the rates of NDMA formation observed on storage of tablet A and B (Fig. 3a) can be partially explained by their different coatings and/or packaging, which determined the exposure to moisture and oxygen. For example, both tablets were film-coated, but different excipients were used.

Ranitidine HCl has been reported to exist in two crystalline forms, namely Form 1 and Form 2,²⁷⁾ and differences in stability of polymorphic crystals may be another factor influencing NDMA formation. Hence, the crystal form of the samples was evaluated with X-ray diffraction (XRD) (Fig. S2). The XRD patterns of the reagent powder A and B indicated identical ranitidine crystalline form and that they are Form 2 (stable form) from the characteristic diffraction peak at near $2\theta = 20^\circ$.²⁸⁾ Therefore, the differences in the profiles of NDMA formation observed for reagents A and B (Fig. 3b) were not due to the difference in the crystal form but were attributable to other factors. Scanning electron microscopy observations suggested some differences in particle morphology between ranitidine reagent powder A and B (Fig. S3). Reagent A formed dense clumps with a diameter of approximately 300 μm , whereas sparse agglomeration was observed in reagent B. The relevance of the morphological differences on the NDMA formation should be intriguing topic for further study.

The amount of nitrite, which is considered one of the factors influencing NDMA formation,¹⁹⁾ in ranitidine used in this study was analyzed by ion chromatography. Table 2 clearly shows that the storage of each ranitidine tablet/reagent for 8 weeks under high-temperature conditions led to an increase in nitrite from Day 0. It suggested contribution of nitrite produced by the self-decomposition of ranitidine to the formation of NDMA in the ranitidine formulations, while clear relationship between the amounts of nitrite and NDMA was not observed.

Conclusion

In this study, we examined the effect of high-temperature storage of ranitidine on the formation of NDMA and then assessed factors affecting NDMA formation. The current findings clearly indicate that temperature-dependent formation of NDMA occurred during the storage of ranitidine tablets and reagent powders. Exposure of the atmosphere and nitrite produced by the self-decomposition of ranitidine may have contributed to NDMA formation during storage. Although it is not fully understood what/how the self-decomposing products

of ranitidine (including nitrite) contribute to the formation of NDMA in the chemical reaction, NDMA formation observed during the storage of ranitidine tablets necessitates the use of additional measures to control stability-related nitrosamine impurities in order to mitigate the safety risk of these products throughout their lifecycle. As many factors and complexities are involved in the generation of NDMA, further research is required to understand the process completely. Currently, we are performing an in-depth analysis of the mechanism of NDMA formation by focusing on the self-decomposition of ranitidine.

Acknowledgment This study was partially supported by AMED under Grant Number JP20mk0101130.

Conflict of Interest The authors declare no conflict of interest.

Supplementary Materials The online version of this article contains supplementary materials.

References

- 1) U.S. Food and Drug Administration. "Statement on the agency's ongoing efforts to resolve safety issue with ARB medications." : <https://www.fda.gov/news-events/press-announcements/statement-agencys-ongoing-efforts-resolve-safety-issue-arb-medications>, cited 31 March, 2020.
- 2) Masada S., Tsuji G., Arai R., Uchiyama N., Demizu Y., Tsutsumi T., Abe Y., Akiyama H., Hakamatsuka T., Izutsu K. I., Goda Y., Okuda H., *Sci. Rep.*, **14**, 11852 (2019).
- 3) Parr M. K., Joseph J. F., *J. Pharm. Biomed. Anal.*, **164**, 536–549 (2019).
- 4) Sörgel F., Kinzig M., Abdel-Tawab M., Bidmon C., Schreiber A., Ermel S., Wohlfart J., Besa A., Scherf-Clavel O., Holzgrabe U., *J. Pharm. Biomed. Anal.*, **172**, 395–405 (2019).
- 5) Tsutsumi T., Akiyama H., Demizu Y., Uchiyama N., Masada S., Tsuji G., Arai R., Abe Y., Hakamatsuka T., Izutsu K. I., Goda Y., Okuda H., *Biol. Pharm. Bull.*, **42**, 547–551 (2019).
- 6) International Council for Harmonisation of Technical Requirements for Pharmaceuticals for Human Use, "ICH Harmonised Guideline: Assessment and Control of DNA Reactive (Mutagenic) Impurities in Pharmaceuticals to Limit Potential Carcinogenic Risk," M7 (R1) 2017.
- 7) European Medicines Agency. "Sartan medicines: companies to review manufacturing processes to avoid presence of nitrosamine impurities." : <https://www.ema.europa.eu/en/documents/referral/valsartan-article-31-referral-sartan-medicines-companies-review-manufacturing-processes-avoid_en.pdf>, cited 31 March, 2020.
- 8) Ministry of Health Labour and Welfare of Japan. "Notification: setting of interim limits for NDMA and NDEA in Sartan drugs (in Japanese)." : <https://www.pmda.go.jp/files/000226684.pdf>, cited 31 March, 2020.
- 9) U.S. Food and Drug Administration. "Statement on new testing results, including low levels of impurities in ranitidine drugs. (Nov. 01, 2019)." : <https://www.fda.gov/news-events/press-announcements/statement-new-testing-results-including-low-levels-impurities-ranitidine-drugs>, cited 3 March, 2020.
- 10) Therapeutic Goods Administration (TGA) Australian Government Department of Health. "Contamination of ranitidine medicines with the nitrosamine NDMA TGA laboratory testing. Version 1.0." : <https://www.tga.gov.au/sites/default/files/tga-laboratories-testing-ranitidine-medicines.pdf>, cited 31 March, 2020.
- 11) European Medicines Agency. "EMA to review ranitidine medicines following detection of NDMA EMA/503622/2019." : <https://www.ema.europa.eu/en/documents/referral/ranitidine-article-31-referral-ema-review-ranitidine-medicines-following-detection-ndma_en.pdf>, cited 31 March, 2020.
- 12) Ministry of Health Labour and Welfare of Japan. "Notification: analysis of carcinogenic substances in ranitidine hydrochloride (in Japanese)." : <https://www.pmda.go.jp/files/000231528.pdf>, cited 31 March, 2020.
- 13) Teraoka R., Otsuka M., Matsuda Y., *J. Pharm. Sci.*, **82**, 601–604 (1993).
- 14) Guerrieri P., Salameh A. K., Taylor L. S., *Pharm. Res.*, **24**, 147–156 (2007).
- 15) Guerrieri P. P., Smith D. T., Taylor L. S., *Langmuir*, **24**, 3850–3856 (2008).
- 16) Jamrógiewicz M., Wielgomas B., *J. Pharm. Biomed. Anal.*, **76**, 177–182 (2013).
- 17) U.S. Food and Drug Administration. "10/2/19: UPDATE—FDA provides update on testing of ranitidine for NDMA impurities." : <https://www.fda.gov/drugs/drug-safety-and-availability/fda-updates-and-press-announcements-ndma-zantac-ranitidine>, cited 31 March, 2020.
- 18) Blessy M., Patel R. D., Prajapati P. N., Agrawal Y. K., *J. Pharm. Anal.*, **4**, 159–166 (2014).
- 19) European Medicines Agency. "To be addressed by the marketing authorisation holders for ranitidine-containing medicinal products." : <https://www.ema.europa.eu/en/documents/referral/ranitidine-article-31-referral-chmp-list-questions_en.pdf>, cited 31 March, 2020.
- 20) Liu Y. D., Selbes M., Zeng C., Zhong R., Karanfil T., *Environ. Sci. Technol.*, **48**, 8653–8663 (2014).
- 21) Shen R., Andrews S. A., *Water Res.*, **47**, 802–810 (2013).
- 22) Roux J. L., Gallard H., Croué J. P., Papot S., Deborde M., *Environ. Sci. Technol.*, **46**, 11095–11110 (2012).
- 23) Shen R., Andrews S. A., *Water Res.*, **45**, 5687–5694 (2011).
- 24) Zeng T., Mitch W. A., *Carcinogenesis*, **37**, 625–634 (2016).
- 25) U.S. Food and Drug Administration. "Laboratory analysis of ranitidine and nizatidine products." : <https://www.fda.gov/drugs/drug-safety-and-availability/laboratory-tests-ranitidine>, cited March, 2020.
- 26) U.S. Food and Drug Administration. "FDA requests removal of all ranitidine products (zantac) from the market." : <https://www.fda.gov/news-events/press-announcements/fda-requests-removal-all-ranitidine-products-zantac-market>, cited 6 April, 2020.
- 27) Wu V., Rades T., Saville D. J., *Pharmazie*, **55**, 508–512 (2000).
- 28) Agatonovic-Kustrin S., Wu V., Rades T., Saville D., Tucker I. G. P., *Int. J. Pharm.*, **184**, 107–114 (1999).



ISSN (E): 2320-3862

ISSN (P): 2394-0530

NAAS Rating: 3.53

www.plantsjournal.com

JMPS 2021; 9(1): 29-32

© 2021 JMPS

Received: 08-11-2020

Accepted: 17-12-2020

Hideaki Otsuka

^a Graduate School of Biomedical and Health Sciences, Hiroshima University, 1-2-3 Kasumi, Minami-ku, Hiroshima, Japan
^b Department of Natural Product Chemistry, Faculty of Pharmacy, Yasuda Women's University, 6-13-1 Yasuhigashi, Asaminami-ku, Hiroshima, Japan

Junko Shitamoto

Graduate School of Biomedical and Health Sciences, Hiroshima University, 1-2-3 Kasumi, Minami-ku, Hiroshima, Japan

Etsuko Sueyoshi

Graduate School of Biomedical and Health Sciences, Hiroshima University, 1-2-3 Kasumi, Minami-ku, Hiroshima, Japan

Katsuyoshi Matsunami

Department of Natural Product Chemistry, Faculty of Pharmacy, Yasuda Women's University, 6-13-1 Yasuhigashi, Asaminami-ku, Hiroshima, Japan

Yoshio Takeda

Department of Natural Product Chemistry, Faculty of Pharmacy, Yasuda Women's University, 6-13-1 Yasuhigashi, Asaminami-ku, Hiroshima, Japan

Corresponding Author:**Hideaki Otsuka**

^a Graduate School of Biomedical and Health Sciences, Hiroshima University, 1-2-3 Kasumi, Minami-ku, Hiroshima, Japan
^b Department of Natural Product Chemistry, Faculty of Pharmacy, Yasuda Women's University, 6-13-1 Yasuhigashi, Asaminami-ku, Hiroshima, Japan

A megastigmane glucoside from *Sambucus chinensis*

Hideaki Otsuka, Junko Shitamoto, Etsuko Sueyoshi, Katsuyoshi Matsunami and Yoshio Takeda

Abstract

From the aerial part of *Sambucus chinensis*, a new megastigmane glucoside (1) was isolated, together with seven known compounds. The structure of compound 1 was elucidated by spectroscopic analysis together with the application of the modified Mosher's method to be (3*S*,5*R*,6*S*,9*R*)-megastigman-5,6-epoxy-3,9-diol 9-*O*- β -D-glucopyranoside. The structure of a closely related compound, sammangaoside B, has been reinvestigated, and it was assigned as (3*S*, 5*R*, 6*S*, 9*S*)-megastigman-5,6-epoxy-3,9-diol 9-*O*- β -D-glucopyranoside. Therefore, compound 1 is a new compound from nature.

Keywords: *Sambucus chinensis*, Adoxaceae, megastigmane, absolute structure

Introduction

Sambucus chinensis (Adoxaceae) is a perennial herb of 1 m to 2 m in height that grows in Japan, Taiwan, and China [1]. It is a component of a Chinese traditional formula that is expected to cure wounds and throbbing pain. However, its phytochemical investigation is quite limited. The aerial part of *S. chinensis* was collected on Okinawa Island, and the constituents in the 1-BuOH-soluble fraction were investigated. A new compound, megastigman-5,6-epoxy-3,9-diol 9-*O*- β -D-glucopyranoside (1), was isolated, along with seven known compounds (Fig. 1), and this paper deals with the structure elucidation of 1, including its absolute stereochemistry. Known compounds were spectroscopically identified as (6*R*,7*E*,9*R*)-megastigma-4,7-dien-9-ol *O*- β -D-glucopyranoside (2) [2], (6*R*,7*E*,9*R*)-megastigman-3-on-9-ol *O*- α -L-arabinopyranosyl (1" \rightarrow 6')- β -D-glucopyranoside (3) [3], citroside B (4) [4], actindioionoside (5) [5], prunasin (6) [6], lucumin (7) [7], and demethylalangsidi (8) [8].

Results and Discussion

From the 1-BuOH-soluble fraction of the MeOH extract of the aerial part of *Sambucus chinensis*, a new megastigmane glucoside (1), together with seven known compounds (2–8), was isolated using various kinds of chromatographic techniques. This paper deals with the structural elucidation of compound 1.

Compound 1, $[\alpha]_{\text{D}}^{25} -37.6$, was isolated as an amorphous powder, and its elemental composition was determined to C₁₉H₃₄O₈ by HR-ESI MS. A broad band at 3395 cm⁻¹ shown in the IR spectrum indicated that 1 is a glycosidic compound. A set of six typical signals attributable to those of glucopyranose was observed in the ¹³C-NMR spectrum, and the remaining 13 signals comprised four methyls, four methylenes, two methines bearing an oxygen atom, two oxygenated tertiary carbons and one quaternary carbon. The numbers of carbon atoms and these functionalities were suggestive that 1 was a megastigmane derivative. The three degrees of unsaturation demanded one more cyclic system besides a six-membered ring and a sugar moiety. The third cyclic system was assumed to be an epoxide ring from two oxygenated tertiary carbons that are frequently found in the megastigmane skeleton, and the ¹H-¹H COSY and HMBC correlations shown in Fig. 2 supported the assumption. Enzymatic hydrolysis of 1 gave a rearranged aglycone (1a) and D-glucose. The aglycone must have two ring systems from the results of HR-MS (C₁₃H₂₄O₃), and the ¹³C-NMR chemical shifts of C-5 (δ_{C} 67.7) and C-6 (δ_{C} 71.3) were drastically shifted downfield at δ_{C} 78.9 and 90.9 (Table 1). A closely related megastigmane glucoside was isolated from *Scorodocarpus bornensis* as scorospiroside [9].

^{13}C -NMR chemical shifts of scorospiroside at C-5 and C-6 were reported as δ_{C} 77.4 and 90.2, which are close to those of 1a, although NMR was run in a different solvent (pyridine- d_5). Two-dimensional NMR diagnosis in Fig. 3 (^1H - ^1H COSY and HMBC) confirmed the structure, and the modified Mosher's method (Fig. 4) revealed 1a had the 3S configuration^[10]. By the phase-sensitive NOESY correlation between H-9 and H₃-13, the configuration at the 9-position was determined to be R (Fig. 5). Therefore, the structure of 1 was elucidated to be as shown in Fig. 1. The same structure was proposed as sammangaoside B (9), isolated from *Clerodendrum inerme*^[11]. The structure of sammangaoside B was determined by comparison of NMR with reported data^[13, 14]. The same compound (9) was also isolated from *Tricalysia dubia*^[12], and the configuration at the 9-position was revised to be S, as shown 10 in Fig. 1. NMR data of 1 and 9 showed some discrepancy, especially at C-6 through C-10 and C-1' (Table 1). Compound 1 must have a different structure from sammangaoside B, as shown in Fig. 1.

Botanical safety handbook says that American and European elders, *S. canadensis* and *S. nigra*, respectively, contain cyanogenic glycosides, ingestion of which may cause vomiting or severe diarrhea^[15]. Since more than 2 g of a cyanogenic glucoside, purnasin, was isolated from 5.45 kg of the title plant, the actual content of cyanogenic glycosides must be much higher than the amount isolated, and usage of this plant is recommended with care.

The monoterpene indole alkaloid glucoside $\delta\delta$ alangsoside is a characteristic compound of Alangiaceae plants^[16, 17]. Isolation of demethylalangsoside (8) implies that Adoxaceae and Alangiaceae have some genetic relationship.

Table 1: NMR Spectroscopic Data for Compounds 1 and 1a, and Sammangaoside B (10) (C: 100 Hz; H: 400 MHz, CD₃OD).

	1		1a		10 ^a
	C	H	C	H	
1	36.7	-	40.2	-	36.6
2	49.3	1.17 o	47.0	1.39 ddd 12, 4, 2	49.3
		1.47 ddd 13, 3, 2		1.55 dd 12, 12	
3	64.5	3.63 m	65.3	3.98 ddd 12, 5, 3	64.4
4	42.6	1.60 dd 14, 9	46.9	1.71 dd 12, 11	42.6
		2.22 ddd 14, 5, 2		1.80 ddd 12, 5, 2	
5	67.7	-	78.9	-	67.4
6	71.3	-	90.9	-	70.8
7	27.8	1.75 m	28.1	1.91 dt 12, 2	27.9
		1.85 m		2.11 m	
8	35.2	1.72 2H m	36.4	1.47 dt 10, 2	34.4
				2.02 m	
9	76.5	3.83 m	78.0	4.10 dq 10, 6	77.8
10	20.0	1.20 3H d 6	21.2	1.19 3H d 6	21.8
11	29.6	1.17 3H s	26.3	1.19 3H s	29.5
12	25.9	1.04 3H s	29.1	0.98 3H s	25.9
13	21.3	1.37 3H s	27.9	1.17 3H s	21.3
1'	102.7	4.30 d 8			103.8
2'	75.3	3.12 dd 9, 8			75.3
3'	78.3	3.24 m			78.2
4'	72.0	3.24 m			71.7
5'	77.9	3.24 m			77.8
6'	63.0	3.64 dd 12, 6			62.8
		3.84 dd 12, 2			

o: overlapped signal.

^aData were taken from Ref. 11 and 12.

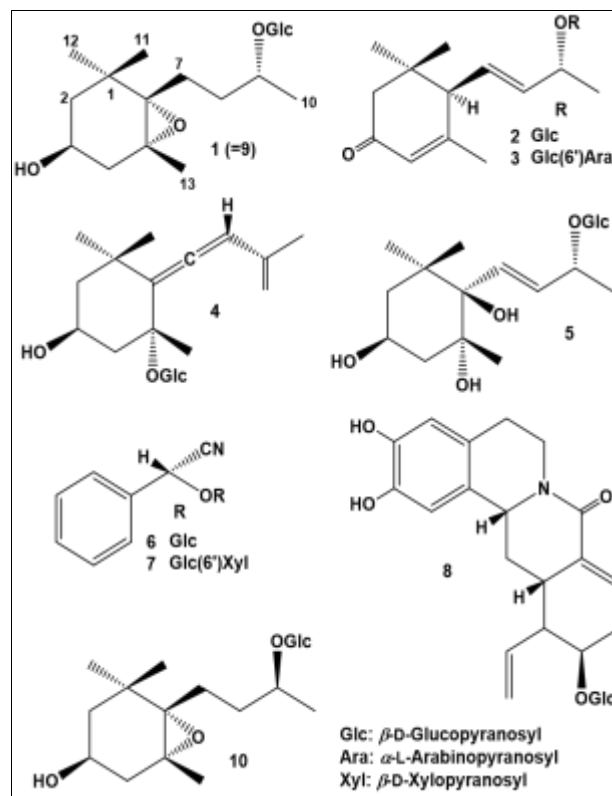


Fig 1: The structures of compounds isolated and sammangaoside b.

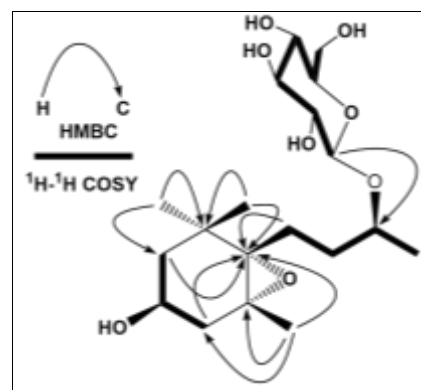


Fig 2: Diagnostic ^1H - ^1H COSY and HMBC correlations of 1

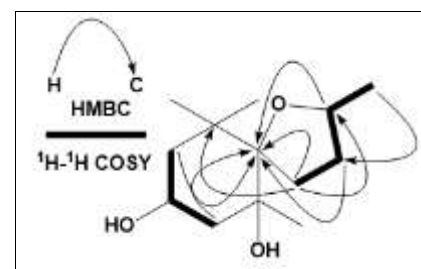


Fig 3: ^1H - ^1H COSY and HMBC correlations of 1a

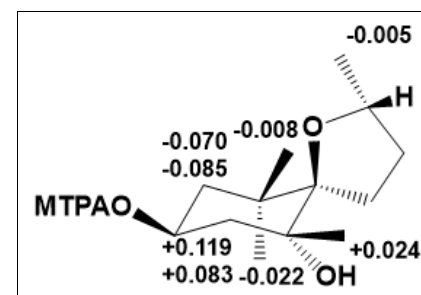


Fig 4: The results of the modified Mosher's method of 1a ($\Delta\delta_{\text{S}} - \delta_{\text{R}}$)

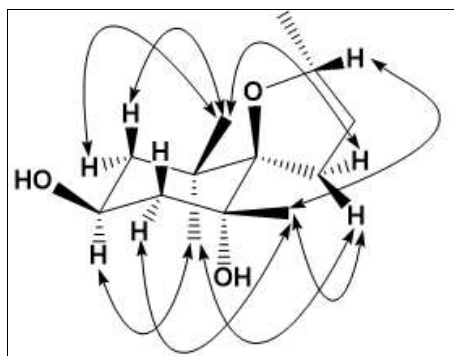


Fig 5: Phase-sensitive NOESY correlations of 1a

Experimental

General experimental procedure

Optical rotations were measured on a JASCO P-1030 digital polarimeter. IR spectrum was measured on Horiba FT-710. ^1H - and ^{13}C -NMR spectra were taken on a JEOL JNM α -400 spectrometer at 400 MHz and 100 MHz with tetramethylsilane as an internal standard. Positive-ion HR-ESI-MS was performed with an Applied Biosystems QSTAR XL NanoSpray TM System.

A highly-porous synthetic resin (Diaion HP-20) was purchased from Mitsubishi Chemical Corporation (Tokyo, Japan). Silica gel column chromatography (CC) was performed on silica gel 60 (E. Merck, Darmstadt, Germany), and ODS open CC on Cosmosil 75C₁₈-OPN (Nacalai Tesque, Kyoto) [$\Phi = 50$ mm, $L = 20$ cm, linear gradient: MeOH-H₂O (1:9, 1 L) \rightarrow (1:1, 500 mL) \rightarrow (7:1, 500 mL), fractions of 10 g being collected]. The DCCC (Tokyo Rikakikai, Tokyo, Japan) was equipped with 500 glass columns ($\Phi = 2$ mm, $L = 40$ cm), the lower and upper layers of a solvent mixture of CHCl₃-MeOH-H₂O-1-PrOH (9:12:8:2) being used as the stationary and mobile phases, respectively. Five-gram fractions were collected and numbered according to their order of elution with the mobile phase. HPLC was performed on an ODS column (Inertsil; GL Science, Tokyo, Japan; $\Phi = 6$ mm, $L = 25$ cm, 1.6 mL/min), and the eluate was monitored with UV (254 nm) and refractive index monitors. *B-Glucosidase* from almond was purchased from Wako Pure Chemical Industries, Ltd (Osaka, Japan) and crude hesperidinase was a generous gift from Tanabe Pharmaceutical Co., Ltd. (Osaka, Japan).

Plant material

Aerial parts of *S. chinensis* were collected in Motobu-cho, Kunigami-gun Okinawa and a voucher specimen was deposited in the Herbarium of Faculty of Pharmaceutical Sciences, Graduate School of Biomedical and Health Sciences, Hiroshima University (03-SC-Okinawa-0701).

Extraction and isolation

Aerial parts of *S. chinensis* (5.45 kg) were extracted three times with MeOH (30 L \times 3) at room temperature for one week and then concentrated to 3 L *in vacuo*. The concentrated extract was washed with *n*-hexane (3 L, 77.1 g), and then, the MeOH layer was concentrated to a gummy mass. The latter was suspended in H₂O (3 L) and extracted with EtOAc (3 L) to give 172 g of an EtOAc-soluble fraction. The aqueous layer was extracted with 1-BuOH (3 L) to give a 1-BuOH-soluble fraction (114 g), and the remaining H₂O-layer was concentrated to furnish 582 g of a H₂O-soluble fraction. The 1-BuOH-soluble fraction (119 g) was subjected to a Diaion HP-20 CC ($\Phi = 60$ mm, $L = 55$ cm), using H₂O-MeOH (4:1, 2 L), (3:2, 4 L), (2:3, 4 L), and (1:4, 4 L), and MeOH (4 L), with 1 L fractions being collected. The residue (26.0 g) in fractions 4–7 of the 20–40 % MeOH eluent was subjected to

silica gel ($\Phi = 60$ mm, $L = 46$ cm) CC and elution with CHCl₃ (2 L), CHCl₃-MeOH [(99:1, 4 L), (97:3, 4 L), (19:1, 4 L), (37:3, 4 L), (9:1, 4 L), (7:1, 4 L), (4:1, 4 L), and (7:3, 3 L)], and MeOH (2 L), with 500 mL fractions being collected. The residue (2.04 g out of 4.07) in fractions 39–45 of the 10–12.5 % MeOH eluate was separated by ODS open CC. From fractions 68–95, 1.17 g of 6 was obtained. The residue (63.5 mg) in fractions 96–112 was purified by HPLC (MeOH-H₂O, 3:7) to give 3.5 mg of 1 from the peak at 20 min. The residue (2.51 g) in fractions 46–51, obtained on silica gel CC, was subjected ODS open CC and the residue (370 mg) in fractions 95–113 was purified by DCCC to give a residue (16.9 mg) in fractions 51–57, which was finally purified by HPLC (MeOH-H₂O, 3:7) to afford further amount of 1 (2.8 mg) from the peak at 20 min. The residue (2.49 g out of 4.12 g) in fractions 52–63, obtained on silica gel CC, was applied to ODS open CC to give a residue (107 mg) in fractions 148–159, which was then purified by DCCC to yield 52.0 mg of 8 and 24.7 mg of 3 in fractions 33–42 and 43–51, respectively. The residue (2.00 g) in fractions 64–76, obtained on silica gel CC was subjected ODS open CC. The residue (256 mg) in fractions 59–68 was applied to DCCC to give a residue (45.9 mg) in fractions 13–16 which was purified by HPLC (MeOH-H₂O, 3:7) to give 18.9 mg of 5 from the peak at 10 min. The residue (222 mg) fractions 69–78 was subjected to DCCC to give a residue (48.2 mg) in fractions 21–26 which was finally purified by HPLC (MeOH-H₂O, 3:7) to give 3.2 mg of 7 from the peak at 23 min.

The residue (21.0 g) in fractions 8–12 of the 40–60 % MeOH eluent, obtained on Diaion HP-20 CC was separated by silica gel CC ($\Phi = 60$ mm, $L = 46$ cm) CC and elution with CHCl₃ (2 L), CHCl₃-MeOH [(99:1, 4 L), (97:3, 4 L), (19:1, 4 L), (37:3, 4 L), (9:1, 4 L), (7:1, 4 L), (4:1, 4 L), and (7:3, 3 L)], and MeOH (2 L), with 500 mL fractions being collected. The residue (2.60 g) in fractions 38–45 was applied to ODS open CC and the residue (227 mg) thus obtained in fractions 141–151 was purified by DCCC to give 5.5 mg of 2 in fractions 94–96. The residue (2.62 g) in fractions 46–52 was similarly subjected to ODS open CC and the residue (311 mg) in fractions 127–139 was purified by DCCC to give 139 mg of 4 in fractions 30–40.

Compound 1 Amorphous powder, $[\alpha]_D^{25} -37.6$ (c 0.17, MeOH); IR ν_{max} (film) cm^{-1} : 3395, 2929, 1455, 1385, 1078, 1036, 896; ^1H -NMR (400 MHz, CD₃OD): Table 1; ^{13}C -NMR (100 MHz, CD₃OD): Table 1; NMR: HR-ESI-MS (positive-ion mode) m/z : 413.2150 [M+Na]⁺ (Calcd for C₁₉H₃₄O₈Na: 413.2145).

Enzymatic hydrolysis of 1

Compound 1 (5.3 mg) was hydrolyzed with 7.2 mg of *β -Glucosidase* in 2 mL of H₂O at 37 °C for 2 h and then 5 mg of crude hesperidinase was added. After 18 h, the reaction mixture was evaporated and subjected column CC (silica gel, 20 g) with CHCl₃ (100 mL), CHCl₃-MeOH (19:1, 100 mL), CHCl₃-MeOH (9:1, 100 mL), CHCl₃-MeOH (17:3, 100 mL) and CHCl₃-MeOH (7:3, 100 mL), 12-mL fractions being corrected. Aglycone 1a (1.8 mg) and D-glucose (4.3 mg) were recovered in fractions 17–22 and 33–42, respectively.

Aglycone 1a: Amorphous powder, $[\alpha]_D^{28} -15.6$ (c 0.12, MeOH); ^1H -NMR (400 MHz, CD₃OD): δ 0.89 (3H, s, H₃-12), 1.17 (3H, s, H₃-13), 1.187 (3H, d, $J = 6$ Hz, H₃-10), 1.191 (3H, s, H₃-11), 1.39 (1H, ddd, $J = 2, 4, 12$ Hz, H-2eq), 1.47 (1H, ddd, $J = 2, 10, 10$ Hz, H-8a), 1.55 (1H, dd, $J = 12, 12$ Hz, H-2ax), 1.71 (1H, dd, $J = 11, 12$ Hz, H-4ax), 1.80 (1H, ddd, $J = 2, 5, 12$ Hz, H-4eq), 1.91 (1H, ddd, $J = 2, 12, 12$ Hz, H-7a), 2.02 (1H, m, H-8b), 2.11 (1H, m, H-7b), 3.98 (1H,

ddd, $J = 3, 5, 12$ Hz, H-3), 4.10 (1H, qd, $J = 6, 10$ Hz, H-9); $^{13}\text{C-NMR}$ (100 MHz, CD_3OD): δ 21.2 (C-10), 26.3 (C-11), 27.9 (C-13), 28.1 (C-7), 29.1 (C-12), 36.4 (C-8), 40.2 (C-1), 46.9 (C-4), 47.0 (C-2), 65.3 (C-3), 78.0 (C-9), 78.9 (C-5), 90.9 (C-6); HR-ESI-MS (positive-ion mode) m/z : 251.1627 $[\text{M}+\text{Na}]^+$ (Calcd for $\text{C}_{13}\text{H}_{24}\text{O}_3\text{Na}$: 251.1617).

D-glucose: $[\alpha]_{\text{D}}^{25} +35.7$ (c 0.29, H_2O , after being dissolved in the solvent).

Preparation of (R)- and (S)-MTPA esters (1b and 1c) from 1a

A solution of 1a (0.8 mg) in 1 mL of dry CH_2Cl_2 were reacted with (*R*)- α -methoxy- α -trifluoromethylphenylacetic acid (MTPA) (27 mg) in the presence of 1-ethyl-3-(3-dimethylaminopropyl) carbodiimide hydrochloride (EDC) (18 mg) and *N,N*-dimethyl-4-aminopyridine (4-DMAP) (12 mg). The mixture was then occasionally stirred at room temperature for 45 min. After the addition of CHCl_3 (1.5 mL), the reaction mixture was successively washed with H_2O (1 mL), 4 M HCl (1 mL), NaHCO_3 -saturated H_2O (1 mL), and brine (1 mL). The organic layer was dried with Na_2SO_4 and evaporated under reduced pressure. The residue was purified by preparative TLC [silica gel (0.25 mm thickness), being applied for 8 cm width, with development with CHCl_3 -MeOH (9: 1) for 9 cm and then eluting with CHCl_3 -MeOH (1: 1)] to furnish an ester 1b (0.5 mg) from the band at $R_f = 0.67$. Through the same procedure, 1c (0.1 mg, $R_f = 0.59$) were prepared from 1a (1.0 mg) using (*S*)-MTPA (42 mg), EDC (18 mg), and 4-DMAP (12 mg), respectively.

(*R*)-MTPA ester of 1a (1b): Amorphous powder, $^1\text{H-NMR}$ (400 MHz, CDCl_3): δ 0.92 (3H, s, H₃-12), 1.19 (3H, d, $J = 6$ Hz, H₃-10), 1.21 (3H, s, H₃-13), 1.27 (3H, s, H₃-11), 1.60 (1H, ddd, $J = 2, 4, 12$ Hz, H-2eq), 1.81 (1H, dd, $J = 12, 12$ Hz, H-2ax), 1.85 (1H, ddd, $J = 2, 5, 12$ Hz, H-4eq), 1.93 (1H, dd, $J = 12, 12$ Hz, H-4ax), 3.56 (3H, q, $J = 1$ Hz, $-\text{OCH}_3$), 4.09 (1H, m, H-9), 5.44 (1H, m, H-3), 7.39-7.41 (3H, m, aromatic protons), 7.51-7.55 (2H, m, aromatic protons); HR-ESI-MS (positive-ion mode) m/z : 467.2011 $[\text{M}+\text{Na}]^+$ (Calcd for $\text{C}_{23}\text{H}_{31}\text{O}_5\text{F}_3\text{Na}$: 467.2015).

(*S*)-MTPA ester of 1a (1c): Amorphous powder. $^1\text{H-NMR}$ (400 MHz, CDCl_3): δ 0.90 (3H, s, H₃-13), 1.20 (3H, d, $J = 6$ Hz, H₃-10), 1.23 (3H, s, H₃-13), 1.26 (3H, s, H₃-11), 1.53 (1H, ddd, $J = 2, 4, 12$ Hz, H-2eq), 1.73 (1H, dd, $J = 12, 12$ Hz, H-2ax), 1.93 (1H, ddd, $J = 2, 5, 12$ Hz, H-4eq), 2.05 (1H, dd, $J = 12, 12$ Hz, H-4ax), 3.55 (3H, q, $J = 1$ Hz, $-\text{OCH}_3$), 4.09 (1H, m, H-9), 5.43 (1H, m, H-3), 7.39-7.41 (3H, m, aromatic protons), 7.52-7.55 (2H, m, aromatic protons); HR-ESI-MS (positive-ion mode) m/z : 467.2023 $[\text{M}+\text{Na}]^+$ (Calcd for $\text{C}_{23}\text{H}_{31}\text{O}_5\text{F}_3\text{Na}$: 467.2015).

Acknowledgements

The authors are grateful for access to the superconducting NMR instrument (JEOL JNM α -400) at the Analytical Center of Molecular Medicine of the Hiroshima University Faculty of Medicine, and an Applied Biosystem QSTAR XL system ESI (Nano Spray)-MS at the Analysis Center of Life Science of the Graduate School of Biomedical Sciences, Hiroshima University. This work was supported in part by Grants-in-Aid from the Ministry of Education, Science, Sports, Culture and Technology of Japan, the Japan Society for the Promotion of Science (Nos. 22590006, 23590130 and 25860078). Thanks are also due to the Research Foundation for Pharmaceutical Sciences and the Takeda Science Foundation for the financial support.

Conflict of interest

We declare that we have no conflict of interest.

References

- Hatusima S. Flora of The Ryukyus (Including Amami Islands, Okinawa Islands and Sakishima Archipelago) (Added and Corrected) Biological Society of Okinawa, Naha, Japan, 1975, 586-589.
- Pabst A, Barron D, Semon E, Schreier P. Two diastereomeric 3-oxo- α -ionol β -D-glucosides from Raspberry fruit. *Phytochemistry* 1992; 31(5):1649-1652.
- Matsuda N, Isawa K, Kikuchi M. Megastigmane glycosides from *Lonicera gracilipes* var. *glandulosa*. *Phytochemistry* 1997;45(4):777-779.
- Umehara K, Hattori I, Miyase T, Ueno A, Hara S, Kageyama C. Studies on the constituents of leaves of *Citrus unshiu* Marcov. *Chemical and Pharmaceutical Bulletin* 1988;36(12):5004-5008.
- Otsuka H, Hirata E, Shinzato T, Takeda Y. Stereochemistry of megastigmane glucoside from *Glochidion zeylanicum* and *Alangium premnifolium*. *Phytochemistry* 2003;62(5):763-768.
- Nahrstedt A, Rothenbach J. Occurrence of the cyanogenic glucoside prunasin and its corresponding mandelic acid amide glucoside in *Olinia* species (Oliniaceae). *Phytochemistry* 1993;34(2):433-436.
- Takeda T, Gonda R, Hatano K. Constitution of lucumin and its related glycosides from *Calocarpum sapota* Merrill. *Chemical and Pharmaceutical Bulletin* 1997;45(4):697-699.
- Itoh A, Tanahashi T, Nagakura N. 6'-*O*-Feruloyl- and 6'-*O*-sinapoyldemethylalangisides tetrahydroisoquinoline-monoterpene glucoside from *Alangium platanifolium*. *Phytochemistry* 1992;31(3):1037-1040.
- Abe F, Yamauchi T. Megastigmane and flavonoids from the leaves of *Scorodocarpus bornensis*. *Phytochemistry* 1993;33(6):1499-1501.
- Ohtani I, Kusumi T, Kashman Y, Kakisawa H. High-field FT NMR application of Mosher's method. The absolute configurations of marine terpenoids. *Journal of the American Chemical Society* 1991;113(11):4092-4096.
- Kanchanapoom T, Kasai R, Chumsri P, Hiraga Y, Yamasaki K. Magastigmane and iridoid glucosides from *Clerodendrum inerme*. *Phytochemistry* 2001;58(1):333-336.
- Otsuka H, Shitamoto J, He DH, Matsunami K, Shinzato T, Aramoto M *et al.* Tricalysiosides P-U: *Ent*-kaurane glucosides and a labdane glucoside from leaves of *Tricalysia dubia* Ohwi. *Chemical and Pharmaceutical Bulletin* 2007;55(11):16605-16605.
- Pabst A, Barron D, Semon E, Schreier P. Two diastereomeric 3-oxo- α -ionol β -D-glucosides from raspberry fruit. *Phytochemistry* 1992;31(5):1649-1652.
- Takeda Y., Zhang H, Matsumoto T, Otsuka H, Oiso Y *et al.* Megastigmasne glycosides from *Salvia nemorosa*. *Phytochemistry* 1997;44(1):117-120.
- McGuffin M, Hobbs C, Upton R, Goldberg A, eds. Botanical safety handbook. American Herbal Products Association. CRC Press, New York, USA, 1997, 102.
- Shoeb A, Raj K, Kapil RS, Popli SP. Alangiside, the monoterpenoid alkaloid glycoside from *Alangium lamarckii* Thw. *Journal of the Chemical Society, Perkin Transactions 1* 1975; (13):1245-1248.
- Tanahashi T, Kobayashi C, Itoh A, Nagakura N, Inoue K *et al.* A tetrahydroisoquinoline-monoterpene glucoside and an iridoid glucosides from *Alangium kurzii*. *Chemical and Pharmaceutical Bulletin* 2000;48(3):415-419.

成分本質(原材料)の分類にかかる照会様式(植物・動物等由来)

照会年月日 _____ 年 _____ 月 _____ 日

【申請番号】: 厚労省が記入

照会者: 名称 _____ (担当者 _____)
TEL _____ e-mail _____

下記の成分本質(原材料)につき、別添資料に基づき照会します。

1. 成分本質(原材料)の概要: 植物・動物等由来

項目		資料番号
一般的名称		
他名等		
英名・現地名		
学名(科・属)		
使用部位		
同じ属又は科の既判断 成分本質の分類	品目及び判断: 流通実態:	

その他の情報*	資料番号

* 水, エタノール以外の抽出の場合は, 判断しようとする成分本質(原材料)が何であることを明らかにすること.
例) ●●のアセトン抽出物→原則不可(物質が特定できない場合は, 2. 含有成分等に関する情報に記載すること)
△△△(物質名)→可

所管の地方自治体(提出先) _____ 担当部局 _____ (担当者 _____)
TEL _____ e-mail _____

2. 含有成分等に関する情報

項目 (調べたものにチェックを入れること)		資料番号
検索元	<input type="checkbox"/> SciFinder <input type="checkbox"/> 化合物大辞典(CCD) <input type="checkbox"/> KNApSAcK <input type="checkbox"/> Google Scholar <input type="checkbox"/> PubMed <input type="checkbox"/> その他(_____)	

No.	化合物名	組成式	構造式	CAS 登録番号	成分本質中の 含有量	文献書誌情報	資料番号
1							
2							
3							
4							
5							

含有成分等についての知見	資料番号
(特に、部位や抽出溶媒の違いによる含有量の差など)	

3. 成分本質の医薬品としての使用実態に関する情報

項目(調べたものにチェックを入れること)		資料番号
検索元	<input type="checkbox"/> 「日本薬局方」 <input type="checkbox"/> 「欧州薬局方」 <input type="checkbox"/> 「米国薬局方」 <input type="checkbox"/> 「英国薬局方」 <input type="checkbox"/> 「中国薬典」 <input type="checkbox"/> 「香港中薬材標準」 <input type="checkbox"/> その他各国医薬品公定書() <input type="checkbox"/> 「中薬大辞典」 <input type="checkbox"/> 「和漢薬」 <input type="checkbox"/> 「The Complete German Commission E Monographs」 <input type="checkbox"/> 「WHO Monographs on Selected Medicinal Plants」 <input type="checkbox"/> KEGG MEDICUS 医薬品検索 <input type="checkbox"/> FDA承認薬データベース <input type="checkbox"/> EU EMA <input type="checkbox"/> PMDA 医薬品検索 <input type="checkbox"/> JAPIC 医薬品情報データベース <input type="checkbox"/> 「保健薬辞典」 <input type="checkbox"/> その他()	

項目			資料番号		
国内での承認前例	<input type="checkbox"/> 有 (品目)	<input type="checkbox"/> 無			
海外での承認実態	<input type="checkbox"/> 有 (品目)	<input type="checkbox"/> 無			
(有の場合)					
医薬品名	承認国	効能効果	使用部位	用法用量	資料番号

民間薬的な使用の有無	<input type="checkbox"/> 有 <input type="checkbox"/> 無	
(有の場合)		資料番号
使用される国・地域や使用部位、用法等の知見		

4. 含有成分等の医薬品としての使用実態に関する情報

項目 (調べたものにチェックを入れること)		資料番号
検索元	<input type="checkbox"/> 「日本薬局方」 <input type="checkbox"/> 「欧州薬局方」 <input type="checkbox"/> 「米国薬局方」 <input type="checkbox"/> 「英国薬局方」 <input type="checkbox"/> 「中国薬典」 <input type="checkbox"/> その他各国医薬品公定書() <input type="checkbox"/> KEGG MEDICUS 医薬品検索 <input type="checkbox"/> FDA承認薬データベース <input type="checkbox"/> EU EMA <input type="checkbox"/> PMDA 医薬品検索 <input type="checkbox"/> JAPIC 医薬品情報データベース <input type="checkbox"/> 「保険薬辞典」 <input type="checkbox"/> その他()	

項目			資料番号
国内での承認前例	<input type="checkbox"/> 有 ()品目	<input type="checkbox"/> 無	
海外での承認実態	<input type="checkbox"/> 有 ()品目	<input type="checkbox"/> 無	

(有の場合)

化合物No.	医薬品名	承認国	効能効果	用法用量	資料番号

民間薬的な使用の有無	<input type="checkbox"/> 有 <input type="checkbox"/> 無
------------	---

(有の場合)

		資料番号
使用される国・地域や用法等の知見		

5. 食経験に関する情報

項目					資料番号
国内での食経験	<input type="checkbox"/> 有	<input type="checkbox"/> 無			
(有の場合)					
流通形態(該当にチェックを入れること)		喫食部位	喫食実績	喫食量	
<input type="checkbox"/> 生食 <input type="checkbox"/> 料理 <input type="checkbox"/> その他()			年以上	トン/年	
<input type="checkbox"/> 生食 <input type="checkbox"/> 料理 <input type="checkbox"/> その他()			年以上	トン/年	
海外での食経験	<input type="checkbox"/> 有	<input type="checkbox"/> 無			
(有の場合)					
国・地域	流通形態(該当にチェックを入れること)	喫食部位	喫食実績	喫食量	資料番号
	<input type="checkbox"/> 生食 <input type="checkbox"/> 料理 <input type="checkbox"/> サプリメント <input type="checkbox"/> その他()		年以上	トン/年	
	<input type="checkbox"/> 生食 <input type="checkbox"/> 料理 <input type="checkbox"/> サプリメント <input type="checkbox"/> その他()		年以上	トン/年	
	<input type="checkbox"/> 生食 <input type="checkbox"/> 料理 <input type="checkbox"/> サプリメント <input type="checkbox"/> その他()		年以上	トン/年	
今後想定される商品形態	<input type="checkbox"/> 有	<input type="checkbox"/> 無			
(有の場合)					

食経験と有害事象についての知見	資料番号

6. 成分本質の安全性に関する情報

項目 (調べたものにチェックを入れること)		資料番号
検索元	<input type="checkbox"/> RTECS (Registry of Toxic Effects of Chemical Substances) <input type="checkbox"/> 「Dictionary of Plant Toxins」 <input type="checkbox"/> ChemIDplus Advanced <input type="checkbox"/> 「Poisonous Plants」 <input type="checkbox"/> Google Scholar <input type="checkbox"/> 「健康食品」の安全性・有効性情報 <input type="checkbox"/> 「Botanical Safety Handbook (メディカルハーブ安全性ハンドブック)」 <input type="checkbox"/> 「The Botany and Chemistry of Hallucinogens」 <input type="checkbox"/> EFSA (European Food Safety Authority) <input type="checkbox"/> ADMEデータベース <input type="checkbox"/> PubMed <input type="checkbox"/> その他(_____)	

項目			資料番号				
成分本質の急性毒性データ	<input type="checkbox"/> 有	<input type="checkbox"/> 無					
成分本質の急性以外の毒性データ	<input type="checkbox"/> 有 (亜急性・慢性・発がん性・遺伝毒性・感作性 等)	<input type="checkbox"/> 無					
麻薬・覚醒剤様作用	<input type="checkbox"/> 有	<input type="checkbox"/> 無					
(有の場合)							
毒性試験の種類	OECDガイドライン番号	成分本質の投与形態(エキス, 粉末等*)	対象動物	投与経路	毒性値	文献書誌情報	資料番号

* 毒性試験に使用した試料の製造方法についても示すこと。

体内動態や薬理作用についての知見	資料番号

7. 含有成分等の安全性に関する情報

項目 (調べたものにチェックを入れること)		資料番号
検索元	<input type="checkbox"/> RTECS (Registry of Toxic Effects of Chemical Substances) <input type="checkbox"/> 「Dictionary of Plant Toxins」 <input type="checkbox"/> ChemIDplus Advanced <input type="checkbox"/> INCHEM <input type="checkbox"/> Google Scholar <input type="checkbox"/> 「健康食品」の安全性・有効性情報 <input type="checkbox"/> 「Botanical Safety Handbook (メディカルハーブ安全性ハンドブック)」 <input type="checkbox"/> 「The Botany and Chemistry of Hallucinogens」 <input type="checkbox"/> EFSA (European Food Safety Authority) <input type="checkbox"/> ADMEデータベース <input type="checkbox"/> PubMed <input type="checkbox"/> その他(_____)	

項目							資料番号
7-1. 含有成分の急性毒性データ	<input type="checkbox"/> 有				<input type="checkbox"/> 無		
7-2. 含有成分の急性以外の毒性データ	<input type="checkbox"/> 有 (亜急性・慢性・発がん性・遺伝毒性・感作性 等)				<input type="checkbox"/> 無		
7-3. 麻薬・覚醒剤様作用	<input type="checkbox"/> 有				<input type="checkbox"/> 無		
(上記で検索対象とした各含有成分のデータ)							
7-1. 含有成分の急性毒性データ							
化合物No.	毒性試験の種類	OECDガイドライン番号	対象動物	投与経路	毒性値(有(数値記入)・データ無)	文献書誌情報	資料番号
7-2. 含有成分の急性以外の毒性データ							
化合物No.	毒性試験の種類	OECDガイドライン番号	対象動物	投与経路	毒性値(有(数値記入)・データ無)	文献書誌情報	資料番号
7-3. 麻薬・覚醒剤様作用							
化合物No.	毒性試験の種類	OECDガイドライン番号	対象動物	投与経路	毒性値(有(数値記入)・データ無)	文献書誌情報	資料番号

体内動態や薬理作用についての知見	資料番号

8. 諸外国における評価と規制に関する情報

項目(調べたものにチェックを入れること)			資料番号
米国ハーブ製品協会 (AHPA) による安全性 クラス分類	<input type="checkbox"/> 有 クラス: _____	<input type="checkbox"/> 無	
ドイツ薬用植物評価委員会(Commission E) による認定ハーブ	<input type="checkbox"/> 該当	<input type="checkbox"/> 非該当	
米国食品医薬品庁 (FDA) のGRAS物質	<input type="checkbox"/> 該当	<input type="checkbox"/> 非該当	
欧州食品安全機関(EFSA)による分類 (新規食品・伝統食品など)	<input type="checkbox"/> 該当	<input type="checkbox"/> 非該当	
その他機関による評価	<input type="checkbox"/> 有	<input type="checkbox"/> 無	

9. 資料リスト

検索元情報

2. 含有成分等に関する情報

- SciFinder <https://www.jaici.or.jp/SCIFINDER/>
- 化合物大辞典 (CCD) https://www.jaici.or.jp/wcas/wcas_chapman2.htm
- KNApSAcK <http://www.knapsackfamily.com/KNApSAcK/>
- Google Scholar <https://scholar.google.co.jp/>
- PubMed <https://www.ncbi.nlm.nih.gov/pubmed/>

3. 成分本質の医薬品としての使用実態に関する情報

4. 含有成分等の医薬品としての使用実態に関する情報

- 「第17改正日本薬局方」 <https://www.pmda.go.jp/rs-std-jp/standards-development/jp/0013.html>
- 「欧州薬局方 (European Pharmacopoeia, EP)」
- 「米国薬局方 (United States Pharmacopoeia, USP)」
- 「英国薬局方 (British Pharmacopoeia, BP)」
- 「中華人民共和国薬典 (Pharmacopoeia of the People's Republic of China, CP)」
- 「香港中薬材標準 (HongKong Chinese Materia Medica Standard, HKCMMS)」
<https://www.cmro.gov.hk/html/eng/GCMTI/hkcmms/volumes.html>
- 「The Complete German Commission E Monographs」
<http://cms.herbalgram.org/commissione/index.html>
- 「WHO Monographs on Selected Medicinal Plants」
 - vol.1 <https://apps.who.int/medicinedocs/en/d/Js2200e/>
 - vol.2 <https://apps.who.int/medicinedocs/en/d/Js4927e/>
 - vol.3 <https://apps.who.int/medicinedocs/en/m/abstract/Js14213e/>
 - vol.4 <https://apps.who.int/medicinedocs/en/m/abstract/Js16713e/>

※海外の薬局方の調べ方

- 国立国会図書館「海外の薬局方」
https://rnavi.ndl.go.jp/research_guide/entry/theme-honbun-400059.php

※海外の薬局方の出版元など

- 日本医薬情報センター「世界の公定書」 https://www.japic.or.jp/service/library/cou_official.html
- 「中薬大辞典」 上海化学技術出版社、小学館編 小学館、1985.12
<https://ci.nii.ac.jp/ncid/BN01241405>
- 「和漢薬」 赤末金芳著 医歯薬出版、1980.3 <https://ci.nii.ac.jp/ncid/BN15896592>

- KEGG MEDICUS (医薬品検索) https://www.kegg.jp/medicus-bin/search_drug
- Drugs@FDA (承認薬データベース) <https://www.accessdata.fda.gov/scripts/cder/daf/index.cfm>
- European Medicines Agency (EMA) <https://www.ema.europa.eu/en/medicines>
- PMDA 医療用医薬品検索 <https://www.pmda.go.jp/PmdaSearch/iyakuSearch/>
- PMDA一般用医薬品検索 <https://www.pmda.go.jp/PmdaSearch/otcSearch/>
- JAPIC 日本の新薬データベース
https://www.shinsahoukokusho.jp/dar_us/dar/search/usDarSearch.jsp

- 「JAPIC医療用・一般用医薬品集」 <https://www.japic.or.jp/service/cd/iyakuhinsyuu.html>

□ 「保険薬辞典」

<https://www.jiho.co.jp/shop/list/detail/tabid/272/pdid/51926/Default.aspx#Relevanceltem>

6. 成分本質の安全性に関する情報

7. 含有成分等の安全性に関する情報

□ RTECS (Registry of toxic Effects of Chemical Substances) https://www.jaici.or.jp/stn_web/index.html

□ ChemIDplus Advanced <https://chem.nlm.nih.gov/chemidplus/chemidlite.jsp>

□ Internationally Peer Reviewed Chemical Safety Information (INCHEM) <http://www.inchem.org/#/search>

□ Google Scholar <https://scholar.google.co.jp/>

□ 医薬基盤健康栄養研 「健康食品」の安全性・有効性情報 <https://hfnet.nibiohn.go.jp/contents/indiv.html>

□ 「Dictionary of Plant Toxins」Edited by Jeffrey B. Harborne and Herbert Baxter; Associate Editor Gerard P. Moss. John Wiley & Sons, Chichester. 1996. <https://pubs.acs.org/doi/abs/10.1021/jm9703202>

□ 「Poisonous Plants: a color field guide」 Lucia Woodward. David & Charles, 1985

□ 「Botanical Safety Handbook」 Edited by Zoe Gardner and Michael McGuffin, CRC Press, 2013

<http://www.ahpa.org/Resources/BotanicalSafetyHandbook.aspx>

□ 「メディカルハーブ安全性ハンドブック」 ゴーイ・ガードナー、マイケル・アクガフィン 編著、今知美 訳、林真一郎、渡辺肇子 日本語監訳、小池一男 日本語版監修、東京堂出版、2016.3

<https://ci.nii.ac.jp/ncid/BB21006436>

□ 「The Botany and Chemistry of Hallucinogens」 Richard E. Schultes and Albert Hofmann. Charles C. Thomas, 1981

□ EFSA (European Food Safety Authority)

Compendium of Botanicals <http://www.efsa.europa.eu/en/data/compendium-botanicals>

<https://dwh.efsa.europa.eu/bi/asp/Main.aspx?rwtrep=301>

<https://www.efsa.europa.eu/en/efsajournal/pub/2663>

□ ADME Database (薬物動態データベース)

<https://www.fujitsu.com/jp/group/kyushu/solutions/industry/lifescience/asp/adme-database/>

□ PubMed <https://www.ncbi.nlm.nih.gov/pubmed/>

□ OECD毒性試験ガイドライン (翻訳版) <http://www.nihs.go.jp/hse/chem-info/oecdindex.html>

8. 諸外国における評価と規制に関する情報

【米国ハーブ製品協会 (AHPA) による安全性クラス分類】

□ 「Botanical Safety Handbook」 Edited by Zoe Gardner and Michael McGuffin, CRC Press, 2013

<http://www.ahpa.org/Resources/BotanicalSafetyHandbook.aspx>

□ 「メディカルハーブ安全性ハンドブック」 ゴーイ・ガードナー、マイケル・アクガフィン 編著、今知美 訳、林真一郎、渡辺肇子 日本語監訳、小池一男 日本語版監修、東京堂出版、2016.3

【ドイツ薬用植物評価委員会 (Commission E) による認定ハーブ】

□ 「The Complete German Commission E Monographs」

<http://cms.herbalgram.org/commissione/index.html>

【米国食品医薬品庁 (FDA) のGRAS物質】

□ FDA「SCOGS Database」 <https://www.accessdata.fda.gov/scripts/fdcc/?set=SCOGS>

【欧州食品安全機関 (EFSA) による分類】

EU Novel Food Catalogue

http://ec.europa.eu/food/safety/novel_food/catalogue/search/public/index.cfm

Food Additives

https://webgate.ec.europa.eu/foods_system/main/index.cfm

成分本質(原材料)の分類にかかる照会様式(その他(化学物質等))

照会年月日 _____ 年 _____ 月 _____ 日

【申請番号】: 厚労省が記入

照会者: 名称 _____ (担当者 _____)
TEL _____ e-mail _____

下記の化学物質等につき、別添資料に基づき照会します。

1. 成分本質(原材料): その他(化学物質等)の概要

項目		資料番号
<input type="checkbox"/> 単一化合物 <input type="checkbox"/> 化合物群 <input type="checkbox"/> 酵素 <input type="checkbox"/> その他		
一般的名称		
他名等		
組成式・構造式		
CAS番号・EC番号		
由来となる主な動植物等と部位等		
由来となる主な動植物等の含有量		
同じ化合物群又は酵素群の既判断 成分本質の分類	品目及び判断: 流通実態:	

その他の情報 *	資料番号

* 水, エタノール以外の抽出の場合は, 判断しようとする成分本質(原材料)が何であることを明らかにすること。
例) ●●のアセトン抽出物→原則不可(物質が特定できない場合は, 2. 含有成分等に関する情報に記載すること)
△△△(物質名)→可

所管の地方自治体(提出先) _____ 担当部局 _____ (担当者 _____)
TEL _____ e-mail _____

2. 個別化合物に関する情報

項目 (調べたものにチェックを入れること)		資料番号
検索元	<input type="checkbox"/> SciFinder <input type="checkbox"/> 化合物大辞典(CCD) <input type="checkbox"/> KNApSAcK <input type="checkbox"/> Google Scholar <input type="checkbox"/> PubMed <input type="checkbox"/> その他(_____)	

No.	化合物名	組成式	構造式	CAS 登録番号	文献書誌情報	資料番号
1						
2						
3						
4						
5						

個別化合物についての知見	資料番号
(特に、化合物群中の個別化合物の含有量(比率)など)	

3. 化学物質等の医薬品としての使用実態に関する情報

項目(調べたものにチェックを入れること)		資料番号
検索元	<input type="checkbox"/> 「日本薬局方」 <input type="checkbox"/> 「欧州薬局方」 <input type="checkbox"/> 「米国薬局方」 <input type="checkbox"/> 「英国薬局方」 <input type="checkbox"/> 「中国薬典」 <input type="checkbox"/> その他各国医薬品公定書() <input type="checkbox"/> KEGG MEDICUS 医薬品検索 <input type="checkbox"/> FDA承認薬データベース <input type="checkbox"/> EU EMA <input type="checkbox"/> PMDA 医薬品検索 <input type="checkbox"/> JAPIC 医薬品情報データベース <input type="checkbox"/> 「保険薬辞典」 <input type="checkbox"/> その他()	

項目			資料番号
国内での承認前例	<input type="checkbox"/> 有 ()品目	<input type="checkbox"/> 無	
海外での承認実態	<input type="checkbox"/> 有 ()品目	<input type="checkbox"/> 無	

(有の場合)

医薬品名	承認国	効能効果	用法用量	資料番号

民間薬的な使用の有無	<input type="checkbox"/> 有 <input type="checkbox"/> 無
------------	---

(有の場合)

		資料番号
使用される国・地域や用法等の知見		

4. 化学物質等の食経験に関する情報

項目			資料番号	
国内での食経験	<input type="checkbox"/> 有	<input type="checkbox"/> 無		
(有の場合)				
流通形態(該当にチェックを入れること)		喫食実績	喫食量	
<input type="checkbox"/> 調味料 <input type="checkbox"/> 食品添加物 <input type="checkbox"/> その他()		年以上	トン/年	
<input type="checkbox"/> 調味料 <input type="checkbox"/> 食品添加物 <input type="checkbox"/> その他()		年以上	トン/年	
海外での食経験	<input type="checkbox"/> 有	<input type="checkbox"/> 無		
(有の場合)				
国・地域	流通形態(該当にチェックを入れること)	喫食実績	喫食量	資料番号
	<input type="checkbox"/> 調味料 <input type="checkbox"/> 食品添加物 <input type="checkbox"/> サプリメント <input type="checkbox"/> その他()	年以上	トン/年	
	<input type="checkbox"/> 調味料 <input type="checkbox"/> 食品添加物 <input type="checkbox"/> サプリメント <input type="checkbox"/> その他()	年以上	トン/年	
	<input type="checkbox"/> 調味料 <input type="checkbox"/> 食品添加物 <input type="checkbox"/> サプリメント <input type="checkbox"/> その他()	年以上	トン/年	
今後想定される商品形態	<input type="checkbox"/> 有	<input type="checkbox"/> 無		
(有の場合)				

食経験と有害事象についての知見	資料番号
(アグリコン(非糖部)の情報がなくとも、配糖体としての食経験がある場合は追記すること)	

5. 由来となる動植物の食経験に関する情報

項目					資料番号
国内での食経験	<input type="checkbox"/> 有	<input type="checkbox"/> 無			
(有の場合) 由来となる動植物等の名称:					
流通形態(該当にチェックを入れること)		喫食部位	喫煙実績	喫食量	
<input type="checkbox"/> 生食 <input type="checkbox"/> 料理 <input type="checkbox"/> その他()			年以上	トン/年	
<input type="checkbox"/> 生食 <input type="checkbox"/> 料理 <input type="checkbox"/> その他()			年以上	トン/年	
海外での食経験	<input type="checkbox"/> 有	<input type="checkbox"/> 無			
(有の場合) 由来となる動植物等の名称:					
国・地域	流通形態(該当にチェックを入れること)	喫食部位	喫煙実績	喫食量	資料番号
	<input type="checkbox"/> 生食 <input type="checkbox"/> 料理 <input type="checkbox"/> サプリメント <input type="checkbox"/> その他()		年以上	トン/年	
	<input type="checkbox"/> 生食 <input type="checkbox"/> 料理 <input type="checkbox"/> サプリメント <input type="checkbox"/> その他()		年以上	トン/年	
	<input type="checkbox"/> 生食 <input type="checkbox"/> 料理 <input type="checkbox"/> サプリメント <input type="checkbox"/> その他()		年以上	トン/年	

食経験と有害事象についての知見	資料番号

6. 化学物質等の安全性に関する情報

項目 (調べたものにチェックを入れること)		資料番号
検索元	<input type="checkbox"/> RTECS (Registry of Toxic Effects of Chemical Substances) <input type="checkbox"/> 「Dictionary of Plant Toxins」 <input type="checkbox"/> ChemIDplus Advanced <input type="checkbox"/> 「Poisonous Plants」 <input type="checkbox"/> Google Scholar <input type="checkbox"/> 「健康食品」の安全性・有効性情報 <input type="checkbox"/> 「Botanical Safety Handbook (メディカルハーブ安全性ハンドブック)」 <input type="checkbox"/> 「The Botany and Chemistry of Hallucinogens」 <input type="checkbox"/> EFSA (European Food Safety Authority) <input type="checkbox"/> ADMEデータベース <input type="checkbox"/> PubMed <input type="checkbox"/> その他(_____)	

項目			資料番号
化学物質等の急性毒性データ	<input type="checkbox"/> 有	<input type="checkbox"/> 無	
化学物質等の急性以外の毒性データ	<input type="checkbox"/> 有 (亜急性・慢性・発がん性・遺伝毒性・アレルギー 等)	<input type="checkbox"/> 無	
麻薬・覚醒剤様作用	<input type="checkbox"/> 有	<input type="checkbox"/> 無	

(有の場合)

化合物名*	毒性試験の種類	OECDガイドライン番号	投与形態	対象動物	投与経路	毒性値	文献書誌情報	資料番号

*化合物群等の場合、その名称を記載し、個別化合物についての毒性情報がある場合、個別に記載すること。また、毒性試験に使用した試料の製造方法についても示すこと。

体内動態や薬理作用についての知見	資料番号

7. 諸外国における評価と規制に関する情報

項目(調べたものにチェックを入れること)			資料番号
米国食品医薬品庁 (FDA) のGRAS物質	<input type="checkbox"/> 該当	<input type="checkbox"/> 非該当	
欧州食品安全機関(EFSA)による分類 (新規食品・伝統食品など)	<input type="checkbox"/> 該当	<input type="checkbox"/> 非該当	
その他機関による評価	<input type="checkbox"/> 有	<input type="checkbox"/> 無	

8. 資料リスト

検索元情報

2. 個別化合物に関する情報

- SciFinder <https://www.jaici.or.jp/SCIFINDER/>
- 化合物大辞典 (CCD) https://www.jaici.or.jp/wcas/wcas_chapman2.htm
- KNApSAcK <http://www.knapsackfamily.com/KNApSAcK/>
- Google Scholar <https://scholar.google.co.jp/>
- PubMed <https://www.ncbi.nlm.nih.gov/pubmed/>

3. 化学物質等の医薬品としての使用実態に関する情報

- 「第17改正日本薬局方」 <https://www.pmda.go.jp/rs-std-jp/standards-development/jp/0013.html>
- 「欧州薬局方 (European Pharmacopoeia, EP)」
- 「米国薬局方 (United States Pharmacopoeia, USP)」
- 「英国薬局方 (British Pharmacopoeia, BP)」
- 「中華人民共和国薬典 (Pharmacopoeia of the People's Republic of China, CP)」

※海外の薬局方の調べ方

- 国立国会図書館「海外の薬局方」
https://rnavi.ndl.go.jp/research_guide/entry/theme-honbun-400059.php

※海外の薬局方の出版元など

- 日本医薬情報センター「世界の公定書」 https://www.japic.or.jp/service/library/cou_official.html
- KEGG MEDICUS (医薬品検索) https://www.kegg.jp/medicus-bin/search_drug
- Drugs@FDA (承認薬データベース) <https://www.accessdata.fda.gov/scripts/cder/daf/index.cfm>
- European Medicines Agency (EMA) <https://www.ema.europa.eu/en/medicines>
- PMDA 医療用医薬品検索 <https://www.pmda.go.jp/PmdaSearch/iyakuSearch/>
- PMDA一般用医薬品検索 <https://www.pmda.go.jp/PmdaSearch/otcSearch/>
- JAPIC 日本の新薬データベース
https://www.shinsahoukokusho.jp/dar_us/dar/search/usDarSearch.jsp
- 「JAPIC医療用・一般用医薬品集」 <https://www.japic.or.jp/service/cd/iyakuhinsyuu.html>
- 「保険薬辞典」
<https://www.jiho.co.jp/shop/list/detail/tabid/272/pdid/51926/Default.aspx#Relevanceltem>

6. 安全性に関する情報

- RTECS (Registry of toxic Effects of Chemical Substances) https://www.jaici.or.jp/stn_web/index.html
- ChemIDplus Advanced <https://chem.nlm.nih.gov/chemidplus/chemidlite.jsp>
- Internationally Peer Reviewed Chemical Safety Information (INCHEM) <http://www.inchem.org/#/search>
- Google Scholar <https://scholar.google.co.jp/>
- 医薬基盤健康栄養研「健康食品」の安全性・有効性情報 <https://hfnet.nibiohn.go.jp/contents/indiv.html>
- 「Dictionary of Plant Toxins」Edited by Jeffrey B. Harborne and Herbert Baxter; Associate Editor Gerard P. Moss. John Wiley & Sons, Chichester. 1996. <https://pubs.acs.org/doi/abs/10.1021/jm9703202>

- 「Poisonous Plants: a color field guide」 Lucia Woodward. David & Charles, 1985
- 「Botanical Safety Handbook」 Edited by Zoe Gardner and Michael McGuffin, CRC Press, 2013
<http://www.ahpa.org/Resources/BotanicalSafetyHandbook.aspx>
- 「メディカルハーブ安全性ハンドブック」 ゴーイ・ガードナー、マイケル・アクガフィン 編著、今知美 訳、林真一郎、渡辺肇子 日本語監訳、小池一男 日本語版監修、東京堂出版、2016.3
<https://ci.nii.ac.jp/ncid/BB21006436>
- 「The Botany and Chemistry of Hallucinogens」 Richard E. Schultes and Albert Hofmann. Charles C. Thomas, 1981
- EFSA (European Food Safety Authority)
Compendium of Botanicals <http://www.efsa.europa.eu/en/data/compendium-botanicals>
<https://dwh.efsa.europa.eu/bi/asp/Main.aspx?rwtrep=301>
<https://www.efsa.europa.eu/en/efsajournal/pub/2663>
- ADME Database (薬物動態データベース)
<https://www.fujitsu.com/jp/group/kyushu/solutions/industry/lifescience/asp/adme-database/>
- PubMed <https://www.ncbi.nlm.nih.gov/pubmed/>
- OECD毒性試験ガイドライン (翻訳版) <http://www.nihs.go.jp/hse/chem-info/oecdindex.html>

7. 諸外国における評価と規制に関する情報

【米国食品医薬品庁 (FDA) のGRAS物質】

- FDA「SCOGS Database」 <https://www.accessdata.fda.gov/scripts/fdcc/?set=SCOGS>

【欧州食品安全機関 (EFSA) による分類】

- EU Novel Food Catalogue
http://ec.europa.eu/food/safety/novel_food/catalogue/search/public/index.cfm
- Food Additives https://webgate.ec.europa.eu/foods_system/main/index.cfm

研究成果の刊行に関する一覧表

雑誌

発表者氏名	論文タイトル名	発表誌名	巻号	ページ	出版年
Tokumoto, H., Shimomura, H., Hakamatsuka, T., Ozeki, Y. and Goda, Y.	Fluorescence coupled with macro and microscopic examinations of morphological phenotype give key characteristics for identification of crude drugs derived from scorpions.	<i>Biol. Pharm. Bull.</i>	41	510-523	2018
Kawakami, S., Nishida, S., Nobe, A., Inagaki, M., Nishimura, M., Matsunami, K., Otsuka, H., Aramoto, M., Hyodo, T. and Yamaguchi, K.	Eight ent-kaurane diterpenoid glycosides named diosmariosides A- H from the leaves of <i>Diospyros maritima</i> and their cytotoxic activity.	<i>Chem. Pharm. Bull.</i>	66	1057- 1064	2018
Uchikura, T., Tanaka, H., Sugiwaki, H., Yoshimura, M., Sato-Masumoto, N., Tsujimoto, T., Uchiyama, N., Hakamatsuka, T. and Amakura, Y.	Preliminary quality evaluation and characterization of phenolic constituents in <i>Cynanchi Wilfordii Radix.</i> , doi:10.3390/molecules23030656	<i>Molecules</i>	23	656	2018
Masada, S., Tuji, G., Arai, R., Uchiyama, N., Demizu, Y., Tsutsumi, T., Abe, Y., Akiyama, H., Hakamatsuka, T., Izutsu, K.-i., Goda, Y. and Okuda, H.	Rapid and efficient high-performance liquid chromatography analysis of N-nitrosodimethylamine impurity in valsartan drug substance and its medicines., doi:https://doi.org/10.1038/s41598-019-48344-5 1	<i>Sci. Rep.</i>	9	11852	2019
Kawakami, S., Miura, E., Nobe, A., Inagaki, M., Nishimura, M., Matsunami, K., Otsuka, H. and Aramoto, M.	Ebenamariosides A-D: Triterpene glucosides and megastigmanes from the leaves of <i>Diospyros maritima</i> .	<i>Chem. Pharm. Bull.</i>	67	1337- 1346	2019

<p>Abe Y., Yamamoto E., Yoshida H., Usui A., Tomita N., Kanno H., Masada S., Yokoo H., Tsuji G., Uchiyama N., Hakamatsuka T., Demizu Y., Izutsu KI., Goda Y., Okuda H.</p>	<p>Temperature-dependent formation of N-nitrosodimethylamine during the storage of ranitidine reagent powders and tablets.</p>	<p><i>Chem. Pharm. Bull.</i></p>	<p>68</p>	<p>1008-1012</p>	<p>2020</p>
<p>Otsuka, H., Shitamoto, J., Sueyoshi, E., Matsunami, K., Takeda, Y.</p>	<p>A megastigmane glucoside from <i>Sambucus chinensis</i>.</p>	<p><i>J. Med. Plants Stud.</i></p>	<p>9</p>	<p>29-32</p>	<p>2021</p>